UNIVERSITÉ DE NEUCHÂTEL

CHYN
Centre d'hydrogéologie et de géothermie

Evaluating the effect of climate change on groundwater resources: From local to catchment scale

Thèse présentée à la Faculté Science
Centre d'hydrogéologie et géothermie (CHYN)
Université de Neuchâtel

Pour l'obtention du grade de docteur ès Science

Par

Christian Möck

Acceptée sur proposition du jury :

Prof. Daniel Hunkeler, University of Neuchâtel, Switzerland, directeur de thèse
Prof. Philip Brunner, University of Neuchâtel, Switzerland, co- directeur de thèse
Prof. Alain Dassargues, University of Liège, Belgium, rapporteur
Prof. Richard Taylor, University College London, England, rapporteur

Soutenue le 11.11.2013

Université de Neuchâtel
2014

UNIVERSITÉ DE NEUCHÂTEL

Faculté des sciences
Secrétariat-décanat de Faculté
Rue Emile-Argand 11
2000 Neuchâtel - Suisse
Tél: + 41 (0)32 718 2100
E-mail: secretariat.sciences@unine.ch

IMPRIMATUR POUR THESE DE DOCTORAT

La Faculté des sciences de l'Université de Neuchâtel autorise l'impression de la présente thèse soutenue par

Monsieur Christian MOECK

Titre:

Evaluating the effect of climate change on groundwater resources : From local to catchment scale

sur le rapport des membres du jury composé comme suit:

- Prof. Daniel Hunkeler, Université de Neuchâtel, directeur de thèse
- Prof. Philip Brunner, Université de Neuchâtel, co-directeur de thèse
- Prof. Alain Dassargues, Université de Liège, Belgique
- Prof. Richard Taylor, University College London, UK

Neuchâtel, le 20 mars 2014

Le Doyen, Prof. P. Kropf

Mots clés en français : Changement climatique, renouvellement de la nappe phréatique, simplification de modèle, fréquence des sécheresses, effets des plantes

Mots clés en anglais : Climate change, groundwater recharge, model simplification, crop effect, drought frequency

Abstract

There is strong evidence that climate is changing and will affect the water resources. A major question arising from the evaluation of climate change (CC) impacts on groundwater resources is to what extent groundwater recharge will change. Given that for Switzerland, climate models predict more frequent hot and dry summers in the future while precipitation will tend to increase in winter, a special attention was given to possible changes in the seasonal distribution of recharge. However, to provide robust predictions, uncertainty has to be considered in all simulations. Three uncertainty sources can be distinguished: the latter can originate from climate models uncertainty, the unknown evolution of land use and society in general, and the hydrological models themselves. The role of these three types of uncertainty has received a major attention in this study. Three studies were carried out to evaluate the effect of CC on the hydrological system. Two of these studies were dedicated to the topic of groundwater recharge whereas the third was focused on the CC response of an aquifer system.

The first recharge related study deals with the question of how uncertainty due to climate models interacts with uncertainty associated with different hydrological models. Although different models were used to simulate groundwater recharge in numerous climate impact studies, it is not yet clear whether models of different complexity give similar recharge predictions for a given climate scenario. Therefore, five different commonly used approaches to simulate groundwater recharge were compared under CC.
In this analysis models with different complexity were applied over a time span of several years and predictive model bias occurs. Using CC data with more extreme weather conditions increases the resulting bias. The potential for model predictive error increases with the difference between the climatic forcing function used in the CC predictions and the climatic forcing function used in calibration period. The difference between the reference recharge and simulated recharge from physical based but homogenous model as well as semi-mechanistic model are smallest whereas the differences increase with the simple models. The differences are due to structural model deficits such as the limitation of reproducing preferential flow. Thus, results of CC impact studies using the soil water balance approach to estimate recharge need to be interpreted with caution, although the majority of CC impact assessment studies are using this approach. Comparison of both uncertainties, i.e. CC and model simplification, indicate that the highest uncertainty is related to CC, but a model simplification can also introduce a significant predictive error.

The second recharge related study explores how different crops and crop rotations influence CC effects on groundwater recharge. The predicted temperature increase will doubtlessly lead to an increase in evaporation and can be intensified by the

presence of crops. To address this question, we relied on lysimeter data to ensure that the models represent previously measured crop specific effects on groundwater recharge appropriately before attempting to simulate future trends. In addition to effects of crop types, effects of soils types were considered. To study the effect of soil types on recharge was possible thanks to the presence of three Swiss dominant soil types in the lysimeter facility. This study attempts to explore the combined effect of CC and changes in land use on groundwater recharge. We address these questions by combining numerical modeling techniques with high quality lysimeter data. The simulated results of the 1D numerical model indicate that for most crops a decreasing trend occurs (between -5 to -60%) due to higher evapotranspiration rates. However, for catch crops (fast-growing crop that is grown between successive plantings of a main crop) such as Phacelia and Temporary grassland, an increasing recharge trend can also be observed (up to 15%). Using these catch crops in a crop sequence can buffer the decreasing trend in future recharge rates, but the buffer capacity depends strongly on the growing season.

It is very likely that crop parameters such as leaf area index (LAI) and root depth (RD) will change in future due to increasing water stress (reduced water content in the lysimeter). Therefore, an analysis of the sensitivity of LAI and RD on recharge was carried out. It was found that simulated recharge is inversely related to LAI and RD where recharge is more sensitive to a decrease in LAI than to RD. Therefore, recharge estimates based on literature LAI and RD values probably represent an upper boundary on recharge rate changes for the future. However, in all simulations a high predictive uncertainty in results is given due to the variability originating from general circulation model (GCM) and regional climate model (RCM) combinations and stochastic realisations of the future climatic conditions.

The final study explored how changes in groundwater recharge might influence groundwater levels for a small aquifer used for water supply. The soil-unsaturated zone-groundwater system was considered as a whole using the physically based model HydroGeoSphere (HGS). The model was based on a wide range of field data. The main objective of this part was to evaluate if seasonal shifts of groundwater recharge can lead to lower groundwater levels in late summer and a potential water shortage. Such effects are mainly expected for highly transmissive systems with a low storage capacity that are expected to react rapidly to seasonal variations in recharge. Therefore, a small aquifer consisting of highly permeable glacio-fluvial deposits and used for water supply for a small town was selected.

The physically based model HydroGeoSphere (HGS) was used to simulate changes in recharge rates and groundwater levels based on 10 GCM (Global Circulation Model) - RCM (Regional Climate Model) combinations for the A1B emission scenario. Future recharge rates were compared to rates observed during historical drought periods. The recharge drought frequency was quantified using a threshold approach. The flow simulations indicate that the strongest effect of CC on recharge occurs in autumn and not in summer, when the temperature changes are the highest. For the winter season, recharge rates increase for almost all climate model chains and

periods. In summer and autumn, temporal water stress, which is defined as reduced drinking water supply, can occur but the intensity depends on the chosen climate model chain. The uncertainty which comes from the variability among different model chains is large although all climate model chains show the same trend in the recharge seasonality. An estimation of drought frequency for a "worst-case" scenario indicates an increase in frequency and intensity under predicted CC. For the water supply in Wohlenschwil, water shortage will most likely more frequently occur in summer and autumn whereas no water stress is predicted for all other seasons.

All studies demonstrated that the uncertainty surrounding projected recharge rates and groundwater levels are relatively large. Some model chains indicate decreasing recharge and groundwater levels until the end of century, while other show increasing trends. For instance for the Wohlenschwil aquifer a change in annual recharge between -16% and 12% was simulated, while the mean of all climate model chains indicate no changes. Therefore, it is quite difficult to state on the magnitude of the change with high confidence. However, not the mean is important, but rather the seasonality. Almost all climate model chains lead to a change in seasonality but with a different magnitude. In addition, the uncertainty linked to the interannual variability of the climate is highly uncertain and can lead to strongly different results and conclusions depending on analyzed equiprobable stochastic realisations. However, the main uncertainty is linked to GCM-RCM combinations. This uncertainty is followed by the uncertainty originated by natural variability of the climate and model simplification. The calibration of the hydrological model is a further uncertainty, but could be reduced by improving the model calibration, if needed.
Although uncertainty in all predictions makes it difficult to state on the magnitude of the change with high confidence, it becomes obviously that a proper consideration of possible effects of CC on groundwater are needed. Results indicate that groundwater is only slightly effected in northern Switzerland on an annual basis but temporal changes can lead to periods with low recharge rates and groundwater tables and therefore to limit water supply.

Acknowledgments

I have been very happy and proud to perform this research at the Centre of Hydrogeology and Geothermics (CHYN), a very inspiring research environment with great colleagues. Of course, there were a lot of people supporting me during my study and I would like to thank all them gratefully.

A special thanks to Daniel Hunkeler and Philip Brunner who supervised this thesis. I would like to thank for support, mentoring and openness to discussion. Thanks for raising new ideas after each discussion.
Thank you to Richard Taylor and Alain Dassargues who have accepted to join the jury of this thesis and to take time to read this report.
I wish to thank Volker Prasuhn for his guidance and patience, while introducing me into the world of lysimeters. I also would like to thank Mario Schirmer for taken always time for meetings about the project and providing support of various issues. I wish to thank John Doherty for his support in using his code PEST. His support at the initial state of my study prevent a lot of frustrations and headache about PEST.

Special thanks to Daniel Käser, we shared the office for 3 years, Oliver Schilling and Daniel Partington for discussions about hydrological modeling and private issues. You guys were being such a pleasant office mates.

The fieldwork would not have been possible without the guidance of Roberto Costa. Thanks for helping me in the field and solving all technical problems. I would like to thank also Antoine Baillieux, who was working with me at the Wohlenschwil catchment. I really enjoyed the fieldwork and discussion with you. I want to thank my colleagues at the CHYN for a good balance between work and pleasure, making my PhD years to such a pleasurable experience. A special thanks to Alice, Philip, Jessica, Yuexia, Oliver, Daniel K., Daniel P., Daniel B., Jordi, Simon, Florian, Bibiane, and Fabio.

Thanks to Swiss National Foundation NFP61 “Sustainable water resources”, which allowed me to carried out this research.

I am very grateful to my friends for their support and for making life outside the office so appreciated. Last but not least I wish to thank my family. I am very grateful to my family for their love and support. Thanks for everything. Particular thank to Katrina and my daughter Nele. Your daily smiles makes every day so worthwhile.

Neuchâtel, October 2013
Christian Möck

Table of Contents

Acknowledgments

Table of Figures

Table of Figures

Table of Figures

Table of Figures

List of Tables

Chapter 1

1.1 Introduction

As highlighted in the Fourth Assessment Report of the Intergovernmental Panel on Climate change (IPCC, 2007) the recently measured increase in global average air and ocean temperatures, the widespread melting of ice and the global average sea level rise are many factors that point towards climate warming. Numerous studies argue that these changes are mostly related to human activities, particularly to the emission of greenhouse gases and aerosols into the atmosphere. An increase in temperature is predicted for most areas in the world. On a global scale, wet climates are becoming wetter and dry climates are becoming drier. Not only the mean climate is expected to change but also extremes such as strong precipitation events and dry spells.

However, these future climate predictions are associated with a large spatial and temporal variation as well as uncertainties. Local climate systems, which can react differently to external forces compared to global systems, are difficult to predict. These climate predictions are affected by several sources of uncertainties. These uncertainties can be due to site-specific reactions caused by topography for example, or the difficulty to predict anthropogenic factors such as greenhouse gas emission trends and land use changes. In addition, the climate system is very intricate as it contains many nonlinear feedback mechanisms such as atmosphere-ocean or atmospheric-dynamic vegetation feedbacks. Some of these relationships are well understood whereas many other are still doubtful. For instance, many small-scale processes such as cloud formation are too small to be represented on the computational grid. However, Stephens (2002) shows how clouds can strongly affect climate change (CC) predictions. This complexity of the climate system makes it very difficult to predict the effect of greenhouse gases and aerosols on the future climate.

Furthermore, when comparing climate model data to observed values, often-systematic errors can be found in variables such as precipitation and temperature, making it necessary to scale and apply correction methods on the data. This bias correction is needed to use the data for hydrological impact studies. In addition to bias correction, there is also a need to downscale results from general climate models (GCM) to regional climate models (RCM) for the investigated catchments to archive the necessary spatial resolution.

However, apart from uncertainties in the predictions and downscaling, observed changes and simulations provide evidence that water resources are potentially affected by CC (IPCC, 2008). CC can modify water availability and water demand.

The combination of decreasing water availability and increasing demand can lead to water shortage. These changes can have consequences for societal, political, economic and ecologic conditions. The United Nations Environment Program about groundwater (UNEP - Morris et al., 2003) mentioned that the contribution from groundwater is vital for water supply. Around two billion people depend directly on aquifers used for drinking water supply. In addition, groundwater is largely used for food production and drinking water supply for almost the half of the largest megacities in the world. In this context of CC, groundwater will likely become more important due to increasing water shortage. This key water source is already under pressure in many regions of the world with a high conflict potential but the conflict potential will certainly still increase due to CC.
Therefore, evaluating the effect of CC on groundwater resources is crucial. Impact studies can indicate how hydrological systems react under CC and are therefore needed and important. A good system understanding and uncertainty projection of CC is always required to make prediction with a high degree of confidence. Only then, policymakers and water managers can develop a sustainable water management strategy.

1.2 Aim and objectives

The project was carried out in the framework of the Swiss national research program on sustainable water management (NRP 61).
The general aim of this PhD study is to increase the understanding of how and to what extent CC affects groundwater systems in Switzerland and influences groundwater availability for water supply. The project focuses on aquifers that are mainly renewed by direct recharge i.e. by infiltration of precipitation through the soil zone. These groundwater systems provide around 40% of drinking water in Switzerland while another 40% originates from aquifers in interaction with rivers. CC effects on alluvial aquifers were investigated in a companion project.

Evaluating CC impacts on groundwater resources raises the question to what extent groundwater recharge will change. Therefore, a major part of this PhD thesis focuses on this topic. Given that for Switzerland, climate models predict more frequent hot and dry summers, while precipitation tends to increase in winter, a special attention was given to possible changes in the seasonal distribution of recharge. The studies mainly considers conditions typically for the Swiss plateau, where most of the population, industrial and agricultural activities are located. In this region, precipitation in form of snow plays only a minor role. Hence, the question of how snow-melt water influences groundwater recharge is not considered in detail in this PhD.

In addition to groundwater recharge, the effect of CC on groundwater levels was explored based on a case study. The main objective of this part was to evaluate if seasonal shifts of groundwater recharge can lead to lower groundwater levels in late

summer and a potential water shortage. Such effects are mainly expected for highly transmissive systems with a low storage capacity that are expected to react rapidly to seasonal variations in recharge. Therefore, a small aquifer consisting of highly permeable glacio-fluvial deposits was selected that is used for water supply for a small town.

When evaluating CC effects on any system, uncertainty is a major challenge due to the strong impact on all predictions. In CC impact studies in hydrology, mainly three sources of uncertainty can be distinguished, uncertainty due to the uncertainty of climate models, the uncertainty due to unknown evolution of land use and society in general, and the uncertainty related to the hydrological models themselves. In this PhD, the role of these three types of uncertainty has received a major attention.

Before outlining the research approach in more detail, methods that have previously been used to simulate CC effects on groundwater resources will be reviewed. First, common approaches to simulate future climate conditions will be briefly summarized and downscaling methods (from the global to the local scale), which are relevant for groundwater models, are discussed (Chapter 2.1). Then, a brief overview of expected climate change trends for Switzerland will be given (Chapter 2.2.). A major part of the review (Chapter 2.3) will be dedicated to the analysis of modeling approaches used in previous studies to predict future groundwater recharge and impacts on aquifers. Finally, the role of different types of uncertainties in CC impact studies will be discussed (Chapter 2.4).

Chapter 2

2.1 General circulation model

GCMs are tools to simulate the climate response to an increase in both greenhouse gas and aerosol concentrations (McGuffie and Henderson- Sellers, 1997). These 3D numerical mathematical models are based on the Navier-Stokes equation. GCMs can cover processes and interplay between the atmosphere, ocean, land surface, snow and ice (Le Treut et al., 2007).

Although GCMs provide geographically distributed and physically consistent predictions of CC, the mesh resolution is frequently around 100-300 km and therefore too coarse for many impact studies. The regional feedback mechanisms are poorly represented for catchment impact studies (Stoll et al., 2011). Downscaling of the GCMs to local/regional scale is therefore required.

Although the GCMs are sophisticated tools for CC studies, any physical process that occurs on scales smaller than the grid of a GCM such as radiation, turbulence or cloud formation must be represented using effective parameters. Distinct parts of the model which describe for instance clouds, cumulus convection, turbulence and surface albedo must be represented with semi-empirical mathematical expressions (McGuffie and Henderson-Sellers, 1997). However, this parameterisation contributes to the model uncertainty (IPCC-TGICA, 2007). Feedback processes such as cloud formation, radiation and snow albedo are another type of uncertainty in the simulations of future climate. For these reasons, GCMs can give different responses to the same forcing depending on how certain processes and feedback are represented (IPCC-TGICA, 2007). Another type of uncertainty originates from the socio-economic scenario. These scenarios are based on a large number of assumptions about global demographics and societal development, energy demand, technologic and economic trends, and corresponding decisions and choices that our world is taking now and may take in the future (IPCC, 2000). In total four storylines, also referred to as pathways, are created to describe the future anthropogenic greenhouse gas emissions (A1, B1, A2 and B2).

In this PhD thesis, only the scenario A1B, which is moderate in terms of CO_2 emission increase compared to other scenarios, is used. Only one scenario, the A1B was chosen to lower the computational demand but still representing a reasonable future developing within both extremes, strong increase as well as constant to decrease of greenhouse gas emission (Nakicenovic 2000). The A1B emission scenario is characterized by a balance across technological emphasis between fossil intensive and no fossil energy sources, where balanced is defined as the point where one does not rely too heavily on one particular energy sources. Balance is defined as the point where one does not rely too heavily on one particular energy source. It is assumed that similar improvement rates of all energy supply and end-use technologies arise. The A1B scenario belongs to the A1 scenario family describing a

future world of very rapid economic growth, global population that peaks in mid-century and declines thereafter, and the rapid introduction of new and more efficient technologies (CH2011, 2011).
A temperature increase of 2.1 to 4.5°C with a mean of 3.1 °C is predicted for Switzerland compared to the reference periods 1980-2009 due to the increase in emissions of both gas and aerosol, (Figure 2.1). For comparison, the A2 scenario is described as a "high" radiative forcing scenario with a mean temperature increase of 3.8°C. High radiative forcing scenarios enclose a very heterogeneous world, where a continuous population growth is assumed and technological changes are more fragmented and slower than other storylines. All these assumptions lead to the largest increase in greenhouse gas concentrations of all possible pathways.

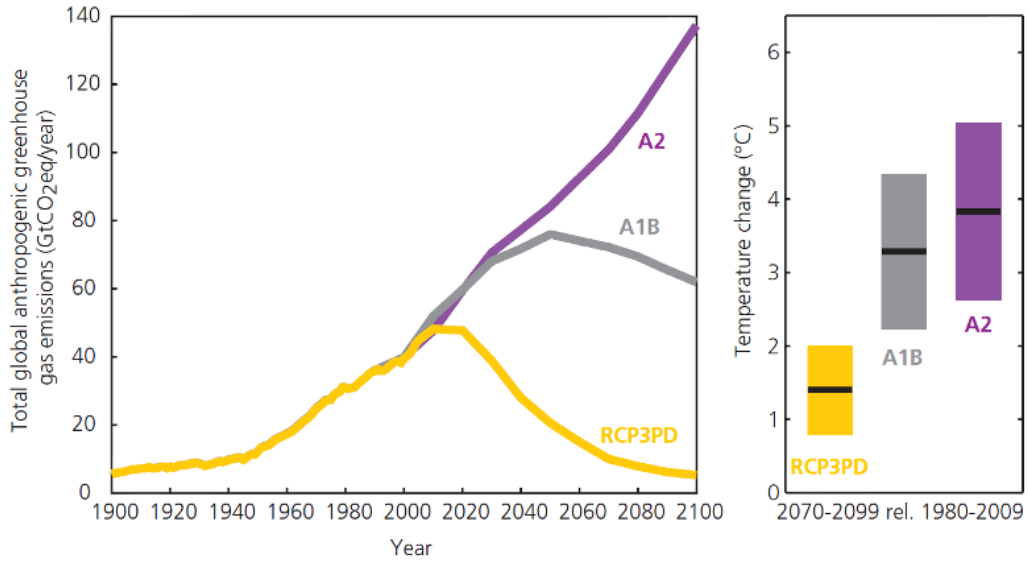

Figure 2. 1: The three pathways of anthropogenic greenhouse gas emissions, along with projected annual mean warming for Switzerland for the 30-year average centered at 2085 (aggregated from the four seasons and three representative regions). These pathways are based on assumptions about global demographics and societal development, energy demand, technologic and economic trends, and corresponding decisions and choices that our world is taking now and may take in the future. The unit «CO_2eq» is a reference unit by which other greenhouse gases (e.g. CH_4) can be expressed in units of CO_2. (Figure taken from CH2011 (2011)).

The inter-model spread between the three pathways of anthropogenic greenhouse gas emissions (Figure 2.1, left panel) as well as the variability in the predictions originated by different climate models (right panel; 10 GCM-RCM combinations) in the predicted temperature ranges is shown. All scenarios follow a similar trend between 2011-2020, whereas they deviate increasingly from each other later on. As mentioned earlier, GCMs model runs are time consuming. GCMs are therefore often not run over a complete time series in transient mode but for certain time intervals denoted as time slices or periods.

2.2 Spatial downscaling

Downscaling results from GCMs is needed to obtain the spatial resolution for the investigated catchment scale on a more regional scale. Two downscaling methods are available. (1) statistical-empirical methods such as "Prefect Prog" can be used, which establish relationships between synoptic-scale predictors and local weather conditions, based on observed evidence and transfer relations into the future. (2) "MOS" (Model Output Statics) also known as "weather generators" approach, applies transfer functions to relate simulations to observations. It involves stochastic modeling of (mostly daily) local weather sequences. The advantages of these methods are their cheapness and their efficiency (Stoll et al., 2011). The disadvantages lie in the assumption of a stationary state and in the lack of account for feedback mechanisms. Dynamical downscaling, which implies the use of regional climate models (RCMs), is frequently performed. This methodology implies that a RCM is nested at a higher resolution into a coarse resolution GCM. This is very attractive due to the physically consistent responses. However, limited spatial resolution is given by the RCM, and simulations are computationally expensive.
In this process, time-varying large-scale atmospheric fields like wind, temperature and moisture are supplied as lateral boundary conditions. These boundary conditions provide consistent solutions compared to the GCM, but on a sub-grid scale with a more detailed physical description of the orography and land use (CH2011). This process gives the opportunity to generate different GCM-RCM combinations based on different GCM or RCM model parameterisation or structure (CH2011). RCMs can simulate changes in a finer mesh resolution and can take complex topography features, lakes and land cover differences into account. These physically based simulations can improve in respect to GCM output predictions on regional scales (Wang et al. 2004). This is important because land surface feature regulates the regional distribution of climate variables in many regions. However, RCMs are still computationally time expensive and therefore only data for specific scenario periods are available. More comprehensive information about the different approaches and methods can be found in many reviews and research papers (e.g. Wilby and Wigley 1997, Nakicenovic 2000, Fowler et al. 2007, Buser, Kuensch et al. 2009, Buser et al. 2010, Buser, Kuensch et al. 2010, Bosshard et al. 2011, Fischer et al. 2012).

Different model chains were used in this study (stars in Figure 2.2). The chosen GCM and RCM combinations represent a wide range of model structures and assumptions in the model parameterisation. These most reliable model chains are given by the ENSEMBLE project, a project supported by the European commission to develop an ensemble prediction for CC.

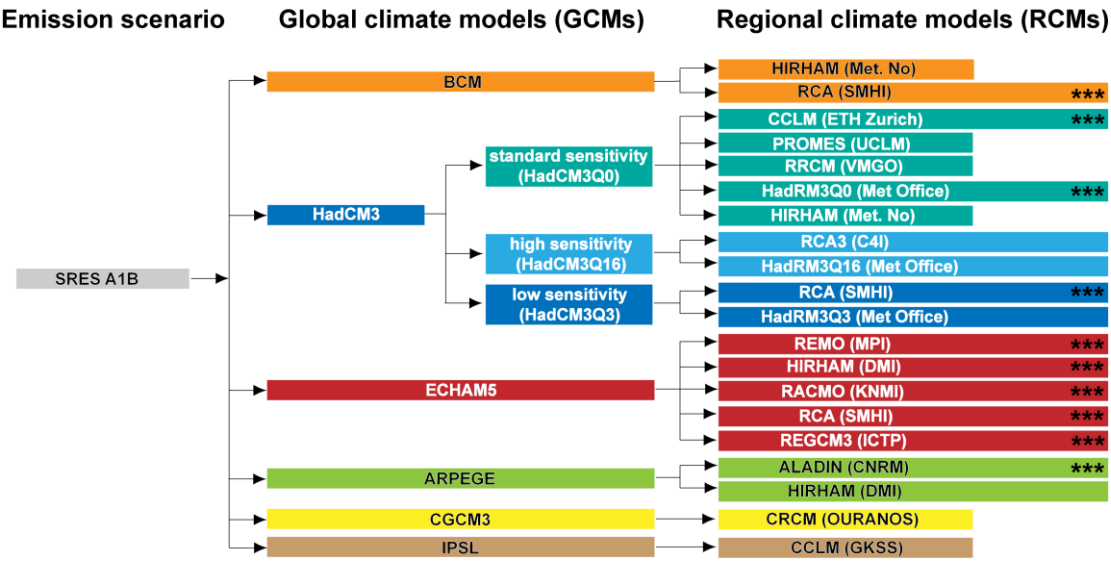

Figure 2. 2: Schematic illustration of the utilized model chains of the ENSEMBLE project, all using the A1B emission scenario. Short and long RCM-bars represent simulations that cover the periods 1951–2050 and 1951–2100, respectively. All model chains marked by stars (***) have been used in this PhD. (Figure taken from CH2011 (2011)).

The spatial resolution of the RCMs is, however, still too coarse for the CC impact studies carried out in this PhD thesis. Therefore, additional downscaled data were required, which were provided by the Center for Climate Systems Modeling (C2SM; http://www.c2sm.ethz.ch/). In this study the following two methodologies were used:

(1) The so-called delta change approach (Hay et al. 2000, Xu et al. 2005) was used. This method shifts an observed time series by a climate change induced value (Hay et al. 2000). Future weather periods are thus a function of the past climate conditions with added (temperature) or multiplied (precipitation) delta change values (factors). These delta change values are provided for many weather stations in Switzerland for mean temperatures and precipitations (C2SM). Observed time series of both parameters are scaled on a daily basis according to the climate change signal derived from individual GCM-RCM chains. The daily time series of delta change factors for precipitation and temperature covers three periods (2035, 2060 and 2085) relative to the reference period 1980-2009. Details of the methodology are described in Bosshard et al. (2011). This method, however, assumes that the model bias remains constant through time. Furthermore, future interannual variability is not taken into account. The length and numbers of dry or wet spells hence remains unchanged.

(2) In addition to the delta change approach, a stochastic weather generator was used (LARS-WG, Racsko et al. 1991, Semenov and Barrow 1997, Semenov et al. 1998) which generates long, synthetic, daily time series of climatic forcing functions. These

simulations are highly related to properties of the observed weather records (Wilby and Wigley 1997). Relationships between daily weather generator parameters and climatic averages for the present period combined with CC signals were established to generate future time series

A combination of the delta change approach with the stochastic weather generator is described in the following. The model chains (GCM-RCM combinations, Figure 2.2) provide a daily time series of delta change factors for precipitation and temperature for three periods (2035, 2060 and 2085) relative to the reference period 1980-2009. In this PhD, these values were combined with the stochastic ‘‘weather generator’’ approach to generate transient climate change scenarios. Linear interpolation was carried out between the three periods with delta change values in order to obtain a continuous time series for each day and each year between 2011 and 2085. These continuous time series of delta change values were subsequently used in a stochastic weather generator (LARS-WG, Racsko et al. 1991, Semenov and Barrow 1997, Semenov et al. 1998) to create possible different realisations of future precipitation and mean temperature values for each of the model chains used for the CC impact studies in this PhD. The different realisations were needed to cover in the most realistic way future possible weather patterns. Using this stochastic approach, it is possible to simulate climate variability. Another advantage of the transient climate change scenarios is that it is possible to analyze in detail the occurrence of expected change. Whereas for the delta change method a recharge increase or decrease can only be predicted for stationary time periods.

The conceptual approach is shown as an example in figure 2.3 for the climate model chain “ETHZ_HadCM3Q0”. The linear interpolation between the years 2011, 2035, 2060 and 2085 for temperature and precipitation for each year from 2011 to 2085 and day during the year is presented.

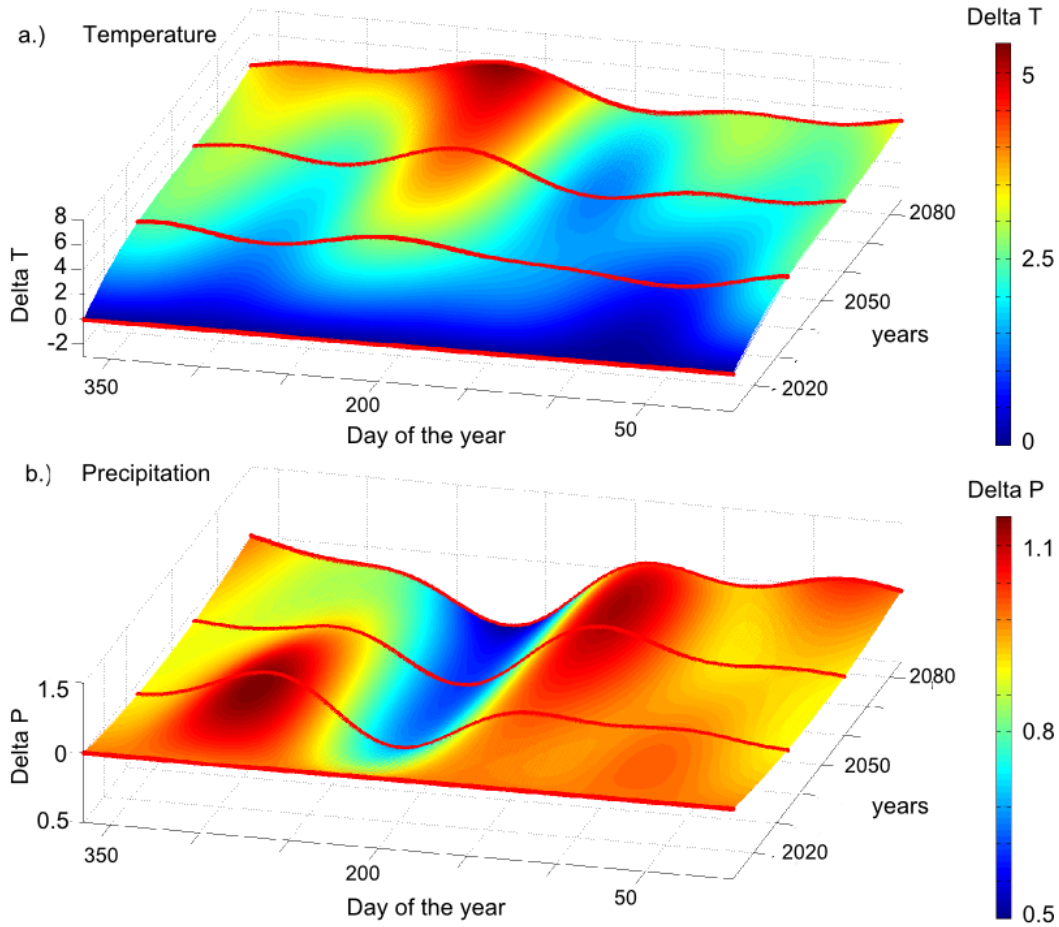

Figure 2. 3: Linear delta change factor interpolation between the year 2011 and the three time periods 2035, 2060 and 2085 (red lines) for a.) temperature and b.) precipitation for each year from 2011 to 2085 and each day is shown. Red and blue colors indicate increase and decrease trends, respectively.

2.3 Projected climate change for Switzerland

There is strong evidence that climate is changing, as reported in the CH2011 report. The projected increase in temperature for Switzerland follows a similar trend as the trend predicted for Europe (CH2011, 2011). Generally, for southern Europe, a stronger warming is predicted compared to the northern part. For the winter period, a decrease in snow cover is expected for many regions, which intensifies the warming due to lower albedo. In Europe wet climates are becoming wetter and dry climates are becoming drier, which is consistent with the global trend. The climate models indicate that summer temperatures increase more strongly than winter temperatures, and that the warming is slightly more pronounced south of the Alps than in the north. For precipitation amounts, no clear trend between north and south can be shown. Especially for the alpine region, precipitation could either increase or decrease. In this region, predictions of precipitation are quite difficult due to a broad range of mechanisms and microclimates. Due to the fact that studied areas in this project are located in the northern part of Switzerland, changes in precipitation and temperature

of this region will be described in more detail and only a brief description about the changes in the southern part will be given.

Observed and predicted temperatures and precipitations for summer and winter seasons for northern Switzerland show an increasing trend (Figure 2.4) with the three different emission scenarios and selected time periods. For the A1B scenario, the seasonal mean temperature will increase by 2.7-4.1°C until 2100 compared to the reference periods (1980-2009) while the increase is slightly higher (3.2-4.8°C) for the A2 scenario. For the three scenario periods of A1B, an increase in temperature of 0.9–1.4°C by 2035, 2.0–2.9°C by 2060, and 2.7–4.1°C by 2085 is expected (Fischer et al., 2011). Regional and seasonal differences in temperature are relatively small for the first two scenario periods but become more important towards the end of the time series (2100, scenario period 2085). Also, the chosen emission scenario has a weak impact on the predicted changes for the scenario period 2035. However, with increasing time, differences between the emission scenarios in predicted temperature rise.

Trends for precipitation show differences between the summer and the winter. Projected summer precipitation will decrease by 18-24% for the A1B scenario, whereas a 21-28% decrease is predicted for the A1 scenario. Winter precipitation will probably increase, especially in southern Switzerland. However, these predictions are highly uncertain compared to projected changes in temperature. Simulations indicate that an increase in the northern part of Europe is very likely, whereas a decrease in the southern part is predicted. Switzerland is, however, located close to the so-called "transition zone" between these two regimes (CH2011, 2011), implying that uncertainties on the sign of future precipitation changes are large.

No clear trend is seen for all emission scenarios for 2035, but for the subsequent scenario periods, summer precipitation decreases. For the A1B scenario, a decrease in mean precipitation of 10-17% by 2060 and 18-24% by 2085 is predicted (Fischer, Weigel et al. 2012). For the winter period, a small increase is very likely. The decrease in summer precipitation and increase in winter precipitation partly compensate each other with a net decrease of only 10% or less. For southern Switzerland, a bigger change is predicted (an increase of 20% in winter), but the net effect is likely to be more negative compared to the northern part.

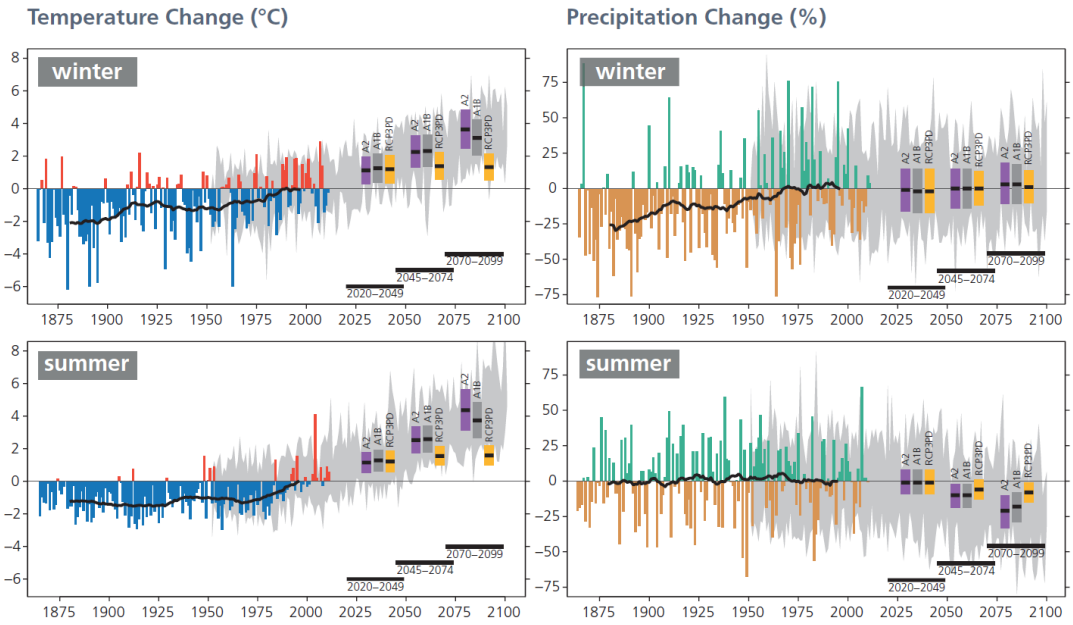

Figure 2. 4: Past and future changes in seasonal temperature (°C) and precipitation (%) over northern Switzerland. The changes are relative to the reference period 1980–2009. The thin colored bars display the year-to-year differences with respect to the average of observations over the reference period; the heavy black lines are the corresponding smoothed 30-year averages. The grey shading indicates the range of year-to-year differences as projected by climate models for the A1B scenario (5–95 percentile range for the available model set). The thick colored bars show best estimates of the future projections, and the associated uncertainty ranges, for selected 30-year time-periods and for three greenhouse gas emission scenarios. (Figure taken from CH2011 (2011)).

Together with changes in precipitation and mean temperature, extreme events are also likely to be affected by CC. More frequent and longer warm spells and heat waves are expected. The length of dry spells will also probably increase (BUWAL 2004). During the last decades, the frequency and duration of heat waves have already substantially increased over central Europe including Switzerland (Frich et al. 2002, Della-Marta et al. 2007, Anagnostopoulou and Tolika 2012, Fernandez-Montes and Rodrigo 2012, Kostopoulou et al. 2012, Long et al. 2012, Buishand et al. 2013, Nemec et al. 2013). Schär et al. (2004) point out that by the end of 2100, every second summer could be as warm as the well acknowledged European summer heatwave of 2003 (Stott et al. 2004, Orsolini and Nikulin 2006, Olita et al. 2007, Schiaparelli et al. 2007, Wegner et al. 2008, Trigo et al. 2009, Munari 2011). Many other studies confirm this finding (e.g. Beniston 2007, Beniston 2007, Beniston and Goyette 2007, Beniston et al. 2007, Beniston 2009, Beniston 2013, Fischer et al. 2007, Vidale et al. 2003, Lenderink et al. 2007).

The prediction of frequency and intensity of heavy precipitation events is quite difficult and highly uncertain. However, in the past, an increase in heavy precipitation events was observed in Switzerland (Beniston 2006, Hohenegger et al.

2008, Jaun et al. 2008). Once again it is very likely that the frequency, duration and intensity of both wet and dry extremes changes under CC.
A conceptual scheme, which tries to merge the aforementioned findings for extreme events for the past, together with the actual weather and future predictions is illustrated in figure 2.5. Potential changes in frequency and intensity of temperature and precipitation extremes in a changing climate are shown (dashed lines are used to present the future distribution). Changes in the distribution of temperature and precipitation (mean, variability and shape) might lead to changes in the frequency and intensity of hot, cold, wet and dry extremes.

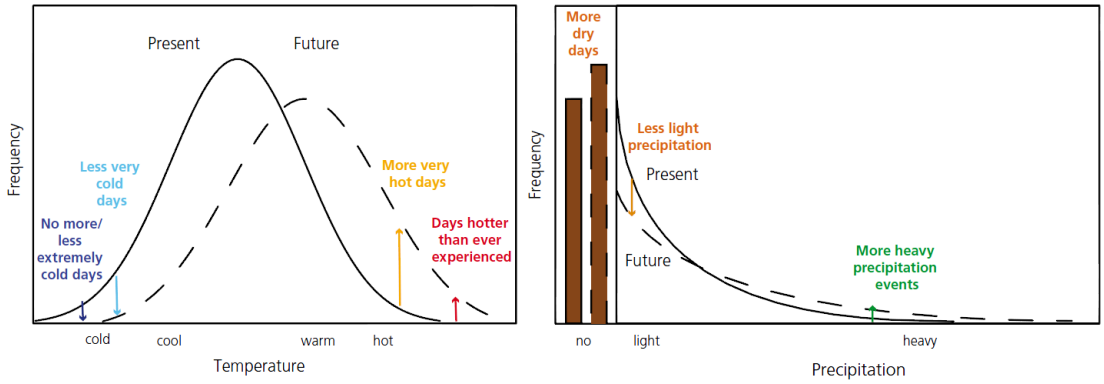

Figure 2. 5: Illustration of potential changes in frequency and intensity of temperature and precipitation extremes in a changing climate. Current and potential future distributions are depicted with full and dashed lines, respectively. Changes in the distribution of temperature and precipitation (mean, variability and shape) potentially lead to changes in the frequency and intensity of hot, cold, wet and dry extremes. (Figure modified from CCSP 2008).

2.4 Climate Change and Hydrology

The aim of this section is not to provide a complete picture about CC and hydrology but rather to summarise the main aspects of this wide research field.
It is indisputable that the evaluation of the effect of climate change on water resources is essential for a successful water management under future climate conditions. Changes in precipitation patterns and amounts as well as increases in mean temperatures can have a significant impact on all components of the hydrological cycle. Changes in

- river discharge (Eckhardt and Ulbrich 2003, Scibek 2007, Serrat-Capdevila and Valdes et al., 2007, van Roosmalen et al., 2007, Woldeamlak et al., 2007, Goderniaux et al., 2009, Mileham et al., 2009, van Roosmalen et al., 2009, Kingston and Taylor 2010, van Roosmalen et al., 2010, Gosling et al., 2011, Kingston et al., 2011, Velázquez et al., 2013, Barthel 2011, Barthel 2011, Barthel et al., 2011, Barthel et al., 2011, Todd et al., 2011, van Roosmalen et

al., 2011, Barthel et al., 2012, Gosling et al., 2012, Sonnenborg et al., 2012, Thompson et al., 2013),

- surface runoff (Woldeamlak et al.. 2007, Mileham et al., 2008, Mileham et al., 2009, Gosling et al., 2011, Barthel et al., 2012, Gosling et al., 2012, Bush et al., 2010, Gosling 2013, Seidel and Martinec 2004, Furher et al,. 2013, Alaoui et al., 2013, Chiew et al., 1995),
- groundwater recharge (Holman 2006, Holman 2006, Scibek 2006, Serrat-Capdevila et al., 2007, van Roosmalen et al., 2007, Woldeamlak et al., 2007, Barthel et al., 2008, Mileham et al., 2008, Goderniaux et al., 2009, van Roosmalen et al., 2009, Barthel et al., 2010, Kingston and Taylor 2010, van Roosmalen et al., 2010, Barthel 2011, Barthel 2011, Barthel et al., 2011, Barthel et al., 2011, Stoll et al., 2011, van Roosmalen et al., 2011, Barthel et al., 2012, McCallum et al., 2010, Crosbie et al., 2011, Crosbie et al., 2012, Thampi and Raneesh 2012, Crosbie et al., 2013),
- snowpack (Graham et al., 2007, Seidel and Martinec 2004, Andréasson et al., 2004, Wilby et al., 2008, Benistion 1997, Benistion et al., 2003, Furher et al., 2013, Alaoui et al., 2013),
- and soil moisture content (Asiedu et al., 2013, Rodriguez-Iturbe 2000, Laio et al., 2001, Chiew et al., 1995, Seneviratne et al., 2010, Fischer et al., 2007)

can occur. An excellent review can be found in Green et al. (2011) and a summary of recommendations on how to deal with CC and groundwater is presented in Holman et al. (2012).

The majority of CC impact studies focus on surface water. Although groundwater has received more attention in the past years (Green et al., 2011), there is still little known about the sensitivity of groundwater to CC compared to surface water. The often slow response of groundwater to changes in the climatic forcing functions due to CC compared to surface water can be an explanation. The significance of impact studies dealing with CC and groundwater is perhaps less noticed.

A major requirement in CC impact studies is a good knowledge about groundwater recharge. Quantification is needed because for any robust model prediction, groundwater recharge is one of the main drivers of the hydrological system. This applies not only to groundwater studies but also to surface water as baseflow directly depends on the renewal of groundwater resources.

Further trends in groundwater recharge are directly related to the predicted changes in temperature and precipitation due to an increase in greenhouse gas concentrations. However, it is unlikely to assume that societal, political and economic conditions will remain unchanged in the future and that only climate change will be the driving force for changes in recharge rate (Holman et al., 2012). Land use will likely change which has a direct impact on the water balance (e.g. Holman 2006, Keese et al., 2005, Eitzinger et al., 2003).

For predictions of CC impacts on water resources, mathematical models are essential. These models provide insight into the response of groundwater systems to CC (Green

et al., 2011). In past studies, a wide range of models evaluating the effect of climate change on recharge and groundwater were used. The degree of complexity in the subsurface and surface system influenced the model choice to a major extent. The scale and data required for driving or validate the model can also restrict the application of certain type of models. Green et al. (2011) point out that the assessment of the advantages and disadvantages of these various approaches for climate impact modeling require further investigation.

2.5 Groundwater and Recharge Modeling

The following studies dealing with groundwater and recharge modeling are sorted according to four categories of model complexity for recharge estimation (Table 2.1). Some studies have used simple empirical relationships between precipitation and recharge (category 1). A more common approach is to use soil water balances to calculate recharge. A soil water balance is calculated with a dedicated code (category 2) and sometimes the output is then sequentially used as input for a groundwater flow model. Alternatively, a soil water balance may be calculated in the framework of an integrated hydrological model (e.g. MIKE SHE (Refsgaard and Storm 1995)), which makes it possible to calibrate the soil water model to some extent (category 3). Finally fully coupled physical-based models are increasingly used that usually model soil water behavior based on the Richards equation (category 4).

Only a few studies have used empirical relationships between precipitation and recharge (Category 1). Serrat-Capdevilla et al. (2007) used an empirical relationship between recharge and precipitation to estimate recharge in Arizona. It was assumed that soil moisture changes are small over a long period and precipitation minus evapotranspiration lead to the available water for recharge. In this approach evapotranspiration was expressed as factors estimated from experiments under historical climatic conditions. This empirical relationship is therefore highly uncertain because it is unknown if the applied factors stay constant in time under changing climatic conditions due to CC. Nevertheless, the calculated recharge was used subsequently in a 3D MODFLOW model to estimate the CC impact on groundwater. Results suggest that recharge will decrease, which affects the dynamics of the investigated riparian area, for instance baseflow dynamics in the long term.

The most common approach to quantify groundwater recharge is the use of water balance models (Category 2). This approach is particularly appealing for large scale models as only a small number of parameters is required. Water balances can be applied at different scales. Usually a water balance is made for the soil zone only to calculate the “excess” water that is available for recharge. Several studies have used such an approach. Yusoff et al. (2002) generated recharge with a more conventional soil water balance method and used the simulated recharge as input for the MODFLOW (Harbaugh 2005). For the Chalk aquifer in eastern England a decrease in recharge, especially during autumn is predicted. Longer and drier summers are

expected. In the study of Brouyère et al. (2004) recharge fluxes were computed by a soil model, which is applied at the top of the groundwater model as prescribed fluxes in a relatively small watershed in Belgium. They found that future climate changes could result in a decrease in groundwater levels, whereas the seasonal variation did not change. Effects of CC were simulated with a soil-water balance model for a study site in Uganda (Mileham et al., 2008, Mileham et al., 2009). The authors of this study point out that spatial interactions between the interpolated rainfall and model parameter distributions had significant effects on the average model outcomes. However, an increase in recharge of 53% and runoff 137% is simulated by additionally transforming the rainfall distribution to account for changes in rainfall intensity. In the study of Jyrkama et al. (2007), groundwater recharge was simulated based on a water balance approach. An increase due to CC for the studied catchment in Ontario was found. A strong spatial variation in groundwater recharge which strongly depended on landscape characteristics such as soil types and land use could be shown. Woldeamlak et al. (2007) analyzed the sensitivity of water balance components to CC for a sandy aquifer in Belgium using a water balance module to compute seasonal and annual recharge, evapotranspiration and runoff. A steady state groundwater model (MODFLOW) was used to predict the effect of CC. An increase in surface runoff and groundwater recharge was found for all seasons, expect for the summer recharge. Spatial distribution of groundwater recharge rates was simulated with the model WetSpass (Batelaan and De Smedt, 2001).

Other studies have used larger scale water balances to quantify recharge e.g. by relating stream flow to groundwater recharge. Loaiciga et al. (2000) calculated the recharge from a water balance of the streamflow and used in a two-dimensional model (“GWSIM) to evaluate the effect of CC for a karst aquifer in Texas. Water shortage is predicted even if water abstraction does not increase. In the studies of Allen et al. (2004), Scibek and Allen (2006a), Scibek et al. (2007), the effect of CC on the unconfined alluvial aquifer, which is influenced by river stages, was simulated in the framework of a combined modeling approach. Simulated recharge values was based in the HELP model (Schroeder et al., 1994), whereas groundwater flow was simulated with a 3D MODFLOW groundwater model (Harbaugh 2005). In addition, the BRANCH model (Schaffranek et al., 1981) is used in this framework to simulate the river stages. Both, increase and decrease in recharge compared to historical recharge was simulated depending on time period and model chain.

Fully integrated hydrological models (Category 3) are increasingly used in CC impact studies like MIKE SHE (Refsgaard and Storm 1995). Surface water and groundwater flows are simultaneously modeled with water exchanges between both domains. However, a relatively simple water balance method to compute water flows in the partially saturated zone is applied to estimate recharge. While this kind of simplification could be used in areas where the influence of the partially saturated zone is limited (for instance arid regions) and recharge occur mainly due to the interaction with rivers, it creates serious limitation in humid regions where direct

recharge mainly occur. Even though these models have limitations they still can simulate the entire hydrologic cycle. For instance, van Roosmalen et al. (2007, 2009) developed a coupled model based on "MIKE SHE" that simulates surface water and groundwater flows simultaneously for a CC impact study in Denmark. Simulated annual recharge increased significantly which results in increasing groundwater levels and discharge rates. In the work of Stoll et al. (2011), the integrated "MIKE SHE" model was used for a peri-alpine catchment in Switzerland. The effect of CC was investigated through the application of eight GCMs-RCMS combinations used with three different downscaling methods. No further groundwater stress was found for this region, but an increase in the piezometric head was found between 0.3 to 1.1m depending on the downscaling method. An increase in mean annual recharge of 5 to 165mm for the period 2071-2100 is simulated. In this study it was found that the weaknesses and differences of three downscaling methods influenced highly the predictions of all hydrological fluxes.

In the past years, a range of fully coupled, physically based models such as PARFLOW (Ashby and Falgout, 1996), InHM (Vanderkwaak and Loague, 2001) and HydroGeoSphere (HGS) (Therrien et al., 2007) have been developed (Category 4). These types of models simulate simultaneously processes between the surface and subsurface for each node and time step. These models are the most powerful tools for simulating hydrological processes at the moment. Although the model methodology is very attractive for CC impact studies due to the fact that interconnected flow processes, such as groundwater recharge, are physical based represented, they have only been applied in a few CC impact studies so far. Sulis et al. (2012) studied the effect of differences in the downscaling approach for a study area in Canada with the model CATCHY, a coupled, physically based, spatially distributed model for surface–subsurface simulations. The results indicate that river discharge, groundwater recharge and soil moisture respond differently to downscaling anomalies in the climate output with greater variability for annual discharge compared to recharge and soil moisture storage. Goderniaux et al. (2009) simulate the recharge process from the surface to the subsurface domain between each node at each time step. This fully coupled approach was carried out with the HGS code for a catchment of 465km^2 in Belgium. They found a decrease in groundwater levels by up to 8m. In addition, a decrease in surface water flow rate from 9 to 33 % until 2080 was predicted.

Table 2. 1: Summary of the different modeling approaches to estimate groundwater recharge in CC impact studies.

Modeling approach to estimate recharge rates	References
Empirical relationship between recharge and precipitation	Serrat-Capdevilla et al., 2007
Water balance	Loaiciga et al., 2000 Yusoff et al., 2002 Brouyère et al., 2004 Mileham et al., 2008 Mileham et al., 2009 Jyrkama et al., 2007 Woldeamlak et al., 2007 Allen et al., 2004 Scibek and Allen 2006 Scibek et al., 2007
Integrated hydrological model	van Roosmalen et al., 2007 van Roosmalen et al., 2009 Stoll et al., 2011
Integrated fully coupled physically based model	Goderniaux et al., 2009 Sulis et al., 2012

Most of the referred studies in the literature review investigated the effect of CC with simple recharge estimation methods. However, models like HGS has the advantage that the inter-connected flow processes, such as groundwater recharge, are represented physically based and all flow equations are simultaneously solved in all domains. These types of models are powerful to predict effects of CC on recharge rates and patterns in the most realistic way currently available. The holistic modeling approach using integrated fully coupled physically based models allowed studying recharge and groundwater droughts at the same time and to identify the key processes leading to water shortage.

2.6 Uncertainty in hydrological impact studies

Uncertainty in hydrological CC impact studies has different sources. Schematically, it can be described as a cascade of uncertainties involving the chosen emission scenario with different greenhouse gas and aerosol concentrations, the choice of GCMs, GCMs imperfection, natural variability, the downscaling method, the model structure and the parameterisation of the hydrological model (Figure 2.6). In addition, differences in predictions under CC can differ due to multiple GCM-RCM combinations. Furthermore, natural variability is often comparable to the trend

caused by CC. Therefore, even if models agree on a trend, it may take several decades for the CC trend to be detectable.

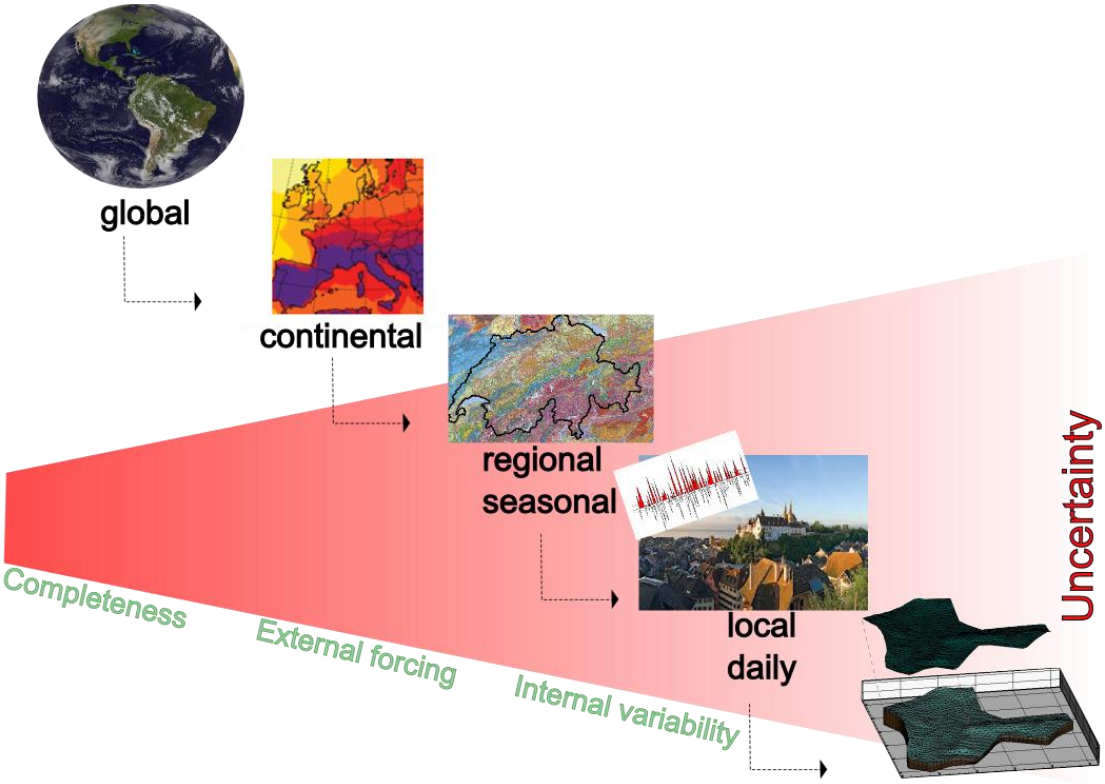

Figure 2. 6: Cascade of uncertainty for CC impact studies in hydrology. Uncertainty is a function of the chosen emission scenario, the choice of GCM, GCMs imperfection and natural variability, the downscaling method, the transfer or bias-correction method, the model structure and parameterisation of the hydrological model.

In the following, a brief summary of uncertainties is given. A more comprehensive discussion of uncertainties in CC projections can be found in Tebaldi and Knutti 2007, Mueller 2010, IPCC 2007, Green et al., 2011.

The uncertainty regarding future greenhouse gas emissions, parameterisation of the GCMs, semi-empirical mathematical expressions, missing feedback process such as clouds, and issues with boundary conditions for GCMs and RCMs are already discussed in Chapter 1.1, 2.1.1 and 2.1.2. Here, the focus is in hydrological models and how the mentioned different types of uncertainties interact.

One type of uncertainty was reported by e.g. Stoll et al. (2011). They showed in a multi-model CC approach including different downscaling methods that downscaling is an important source of uncertainty, which is often not taken into account. However, new statistical methods have been recently developed enabling a better quantification of uncertainties in climate projections (e.g. Buser et al., 2009, Buser et al., 2010, Fischer et al., 2012) and an improved downscaling of climate variables to specific sites (Bosshard et al., 2011). Another type of uncertainty is the combination of

multiple GCMs and RCMs, which shows a high variability in future predictions. Predictions based on the same scenario but with different climate model chains can give large differences. For instance, Jackson et al (2011) predicted, a change in groundwater recharge between -26 to 31% for a Chalk aquifer in the UK based on 13 GCMs.

Hydrological model parameterisation as well as model simplification is another type of uncertainty. Some studies (e.g. Moore and Doherty 2006, Hunt et al., 2007, Doherty et al., 2011) show how model simplification can introduce predictive bias, diverging of the simulation output due to choosing simpler model structures. Model parameters from simpler models must take a compensatory role during the calibration process to achieve satisfactory results but may introduce bias for future predictions (Doherty et al., 2011). Additionally, structural noise, or the imperfect nature of models or model parameters to reproduce reality, is often the dominant contributor to model-to-measurement misfit and can increase the uncertainty in predictions (Doherty et al., 2010). These model structural errors that are often the main source of predictive uncertainty and bias are typically ignored (Refsgaard et al., 2006, Rojas et al., 2008), especially for climate change studies. Cuthbert and Tindimugaya (2010) show that different groundwater recharge models give similar long-term historic recharge rates but still respond very differently to changes in precipitation intensity. The different model structures with different sensitivity to changes in the precipitation intensity leads to the diverging results. Jiang et al. (2007) observed differences in predicated recharge rates using 6 different water balance models although historical recharge rates were reproduced well with all models. Velazques et al. (2013) show that the chosen hydrological model can affect the climate change response of different hydrological performance indicators, especially for low flow periods for surface water. However, Crosbie et al. (2011) pointed out that the uncertainty originating from GCMs and downscaling is larger than the uncertainty from different model structures thanks to the use of three different hydrological models.

2.7 Research approach

A series of three studies is carried out, two of them dedicated to the topic of groundwater recharge, and a third one to the CC response of a complete aquifer. These studies are complemented by new methodological developments documented in the annex. In the following, the specific objectives and research approach of different parts of the PhD are outlined.

The first recharge related study (Chapter 3) deals with the question on how uncertainty due to climate models interacts with uncertainty associated with different hydrological models. The need to consider uncertainty in climate models in CC impact studies has already been highlighted by numerous studies (see chapter 2.6). However, although different models to simulate groundwater recharge have been used before (see chapter 2.5), it is not clear yet whether models of different

complexity give similar recharge predictions for a given climate scenario. Therefore, five different approaches to simulate groundwater recharge were compared. To consider uncertainty in climate models, future climate patterns were simulated using 10 model chains for each recharge model. In the climate models, three stationary future periods were considered, 2035, 2060 and 2085, using a fairly classical delta change approach. We were particularly interested to see if the direction and magnitude of change in recharge was the same for all models or whether some models predict a decrease and other an increase in recharge due to differences in model structure. When simulating recharge, a major challenge is that recharge cannot directly be measured. Therefore, it is often not even clear if the chosen models can correctly simulate the past recharge, which raises doubts about the reliability of predictions. To reduce this uncertainty, we made use of data from a lysimeter facility in Switzerland to evaluate if the models relate meteorological data to recharge in a realistic way. Thereby, we assumed that lysimeter outflow is a good indicator for groundwater recharge.

The second study (Chapter 4) explores how different crops and crop rotations influence CC effects on groundwater recharge. The predicted temperature increase will doubtlessly lead to an increase in evapotranspiration. It is well known that evapotranspiration can strongly vary among crops. Accordingly, CC effects on recharge might be crop dependant. To address this question, we again relied on lysimeter data from the same facility to ensure that the models represent crop specific effects on groundwater recharge appropriately in the past before attempting to simulate future trends. In addition to effects of crop types, effects of soils types were considered as in the lysimeter facility the three dominant soil types of Switzerland are represented. For simulating future climate conditions, a more sophisticated approach was used which consists of a transient simulation of climate trends using time varying delta change factors and a stochastic weather generator (see chapter 4).

The final study (Chapter 5) explored how changes in groundwater recharge might influence groundwater levels for a small aquifer used for water supply. The study was carried out by considering the soil-unsaturated zone-groundwater system as a whole using the physically-based model Hydrogeosphere (HGS). The model layer distribution and model parameter calibrated was based on a large range of field data including extensive geophysical data, piezometers installed with the direct Push technology, information from drill logs, pumping tests as well as tracer tests in both, the saturated and unsaturated zone. A procedure to couple HGS to PEST was developed (Annex) including the pilot point calibration approach. In first step, model outputs for groundwater recharge were analysed. In contrast to the lysimeter-inspired recharge studies above, here recharge reflected the effect of the entire unsaturated zone, which reached to up 10m at some locations. Future recharge rates were compared to rates observed during historical drought periods and the recharge drought frequency was quantified using a threshold approach. Finally, the effect on groundwater levels was explored.

2.5 References

Allen, D. M., D. C. Mackie (2004). "Groundwater and climate change: a sensitivity analysis for the Grand Forks aquifer, southern British Columbia, Canada." Hydrogeology Journal 12(3): 270-290.

Allen, M. R. and W. J. Ingram (2002). "Constraints on future changes in climate and the hydrologic cycle." Nature 419(6903): 224.

Anagnostopoulou, C. and K. Tolika (2012). "Extreme precipitation in Europe: statistical threshold selection based on climatological criteria." Theoretical and Applied Climatology 107(3-4): 479-489.

Andréasson, J., Bergström, S., Carlsson, B., Graham, L. P., & Lindström, G. (2004). Hydrological change-climate change impact simulations for Sweden. AMBIO: A Journal of the Human Environment, 33(4), 228-234.

Ashby, S. F. and Falgout R. D.: A parallel multigrid preconditioned conjugate gradient algorithm for groundwater flow simulations, Nuclear Science and Engineering, 124(1), 145-159 pp., 1996.

Alaoui, A., Willimann, E., Jasper, K., Felder, G., Herger, F., Magnusson, J., & Weingartner, R. (2013). Modeling the effects of land use and climate changes on hydrology in the Ursern valley, Switzerland. Hydrological Processes.

Asiedu, E. K., Ampadu, B., Bonsu, M., & Abunyewa, A. A. (2013). Hydrological and Physical Changes of Soils Under Cocoa Plantations of Different Ages During the Dry Season in the Transition Zone of Ghana. Journal of Natural Sciences Research, 3(7), 52-58.

Barthel, R. (2011). "An indicator approach to assessing and predicting the quantitative state of groundwater bodies on the regional scale with a special focus on the impacts of climate change." Hydrogeology Journal 19(3): 525-546.

Barthel, R., S. Janisch, et al. (2010). "Using the Multiactor-Approach in Glowa-Danube to Simulate Decisions for the Water Supply Sector Under Conditions of Global Climate Change." Water Resources Management 24(2): 239-275.

Barthel, R., S. Janisch, et al. (2008). "An integrated modeling framework for simulating regional-scale actor responses to global change in the water domain." Environmental Modeling & Software 23(9): 1095-1121.

Barthel, R., T. Krimly, et al. (2011). "Global change impacts on groundwater in Southern Germany-Part 2: Socioeconomic aspects." Grundwasser 16(4): 259-268.

Barthel, R., T. G. Reichenau (2012). "Integrated Modeling of Global Change Impacts on Agriculture and Groundwater Resources." Water Resources Management 26(7): 1929-1951.

Barthel, R., T. G. Reichenau (2011). "Global change impacts on groundwater in Southern Germany-Part 1: Natural aspects." Grundwasser 16(4): 247-257.

Batelaan, O., and De Smedt. F. (2001). "WetSpass: a flexible, GIS based, distributed recharge methodology for regional groundwater modeling." IAHS Publications: 11-18.

Beniston, M. (2006). "August 2005 intense rainfall event in Switzerland: Not necessarily an analog for strong convective events in a greenhouse climate." Geophysical Research Letters 33(5): L05701.

Beniston, M. (2007). "Entering into the "greenhouse century": Recent record temperatures in Switzerland are comparable to the upper temperature quantiles in a greenhouse climate." Geophysical Research Letters 34(16).

Beniston, M. (1997). Variations of snow depth and duration in the Swiss Alps over the last 50 years: links to changes in large-scale climatic forcings. Climatic Change, 36(3-4), 281-300.

Beniston, M., Keller, F., & Goyette, S. (2003). Snow pack in the Swiss Alps under changing climatic conditions: an empirical approach for climate impacts studies. Theoretical and Applied Climatology, 74(1-2), 19-31.

Beniston, M. (2007). "Linking extreme climate events and economic impacts: Examples from the Swiss Alps." Energy Policy 35(11): 5384-5392.

Beniston, M. (2009). "Trends in joint quantiles of temperature and precipitation in Europe since 1901 and projected for 2100." Geophysical Research Letters 36.

Beniston, M. (2013). "Exploring the behaviour of atmospheric temperatures under dry conditions in Europe: evolution since the mid-20th century and projections for the end of the 21st century." International Journal of Climatology 33(2): 457-462.

Beniston, M. and S. Goyette (2007). "Changes in variability and persistence of climate in Switzerland: Exploring 20th century observations and 21st century simulations." Global and Planetary Change 57(1-2): 1-15.

Beniston, M., D. B. Stephenson (2007). "Future extreme events in European climate: an exploration of regional climate model projections." Climatic Change 81: 71-95.

Bosshard, T., S. Kotlarski (2011). "Spectral representation of the annual cycle in the climate change signal." Hydrology and Earth System Sciences 15(9): 2777-2788.

Brouyere, S., G. Carabin (2004). "Climate change impacts on groundwater resources: modelled deficits in a chalky aquifer, Geer basin, Belgium." Hydrogeology Journal 12(2): 123-134.

Buishand, T. A., G. De Martino, (2013). "Homogeneity of precipitation series in the Netherlands and their trends in the past century." International Journal of Climatology 33(4): 815-833.

Buser, C. M., H. R. Kuensch (2009). "Bayesian multi-model projection of climate: bias assumptions and interannual variability." Climate Dynamics 33(6): 849-868.

Buser, C. M., H. R. Kuensch (2010). "Bayesian multi-model projections of climate: generalization and application to ENSEMBLE results." Climate Research 44(2-3): 227-241.

Buser, C. M., H. R. Kuensch (2010). "Biases and Uncertainty in Climate Projections." Scandinavian Journal of Statistics 37(2): 179-199.

Bush, M. B., J. A. Hanselman (2010). "Nonlinear climate change and Andean feedbacks: an imminent turning point?" Global Change Biology 16(12): 3223-3232.

BUWAL, BWG, MeteoSchweiz, 2004: Auswirkungen des Hitzesommers 2003 auf die Gewässer. Bundesamt für Umwelt, Wald und Landschaft, Berne, 174 pp.

CCSP, 2008: Climate Models: An Assessment of Strengths and Limitations. A Report by the U.S. Climate Change Science Program and the Subcommittee on Global Change Research, Department of Energy, Office of Biological and Environmental Research, Washington, D. C., USA, 124 pp.

CH2011 (2011). Swiss Climate Change Scenarios CH2011, published by C2SM, MeteoSwiss, ETH, NCCR Climate, and OcCC, Zurich, Switzerland, 88 pp. ISBN: 978-3-033-03065-7.

Chiew, F. H. S., Whetton, P. H., McMahon, T. A., & Pittock, A. B. (1995). Simulation of the impacts of climate change on runoff and soil moisture in Australian catchments. Journal of Hydrology, 167(1), 121-147.

Crosbie, R. S., W. R. Dawes, et al. (2011). "Differences in future recharge estimates due to GCMs, downscaling methods and hydrological models." Geophysical Research Letters 38.

Crosbie, R. S., T. Pickett (2013). "An assessment of the climate change impacts on groundwater recharge at a continental scale using a probabilistic approach with an ensemble of GCMs." Climatic Change 117(1-2): 41-53.

Crosbie, R. S., D. W. Pollock (2012). "Changes in Koppen-Geiger climate types under a future climate for Australia: hydrological implications." Hydrology and Earth System Sciences 16(9): 3341-3349.

Cuthbert, M. O. and C. Tindimugaya (2010). "The importance of preferential flow in controlling groundwater recharge in tropical Africa and implications for modeling the impact of climate change on groundwater resources." Journal of Water and Climate Change 1(4): 234-245.

Della-Marta, P. M., M. R. Haylock (2007). "Doubled length of western European summer heat waves since 1880." Journal of Geophysical Research-Atmospheres 112(D15).

Doherty, J., and Welter, D. (2010). A short exploration of structural noise. Water Resources Research, 46(5).

Doherty, J., Christensen, S. (2011). Use of paired simple and complex models to reduce predictive bias and quantify uncertainty. Water Resources Research, 47(12).

Eckhardt, K. and U. Ulbrich (2003). "Potential impacts of climate change on groundwater recharge and streamflow in a central European low mountain range." Journal of Hydrology 284(1-4): 244-252.

Eitzinger, J., M. Stastna (2003). "A simulation study of the effect of soil water balance and water stress on winter wheat production under different climate change scenarios." Agricultural Water Management 61(3): 195-217.

Fernandez-Montes, S. and F. S. Rodrigo (2012). "Trends in seasonal indices of daily temperature extremes in the Iberian Peninsula, 1929-2005." International Journal of Climatology 32(15): 2320-2332.

Fischer, A. M., A. P. Weigel (2012). "Climate change projections for Switzerland based on a Bayesian multi-model approach." International Journal of Climatology 32(15): 2348-2371.

Fischer, E. M., S. I. Seneviratne (2007). "Contribution of land-atmosphere coupling to recent European summer heat waves." Geophysical Research Letters 34(6).

Fischer, E. M., S. I. Seneviratne (2007). "Soil moisture - Atmosphere interactions during the 2003 European summer heat wave." Journal of Climate 20(20): 5081-5099.

Fowler, H. J., S. Blenkinsop (2007). "Linking climate change modeling to impacts studies: recent advances in downscaling techniques for hydrological modeling." International Journal of Climatology 27(12): 1547-1578.

Frich, P., L. V. Alexander (2002). "Observed coherent changes in climatic extremes during the second half of the twentieth century." Climate Research 19(3): 193-212.

Fuhrer, J., Smith, P., & Gobiet, A. (2013). Implications of climate change scenarios for agriculture in alpine regions—A case study in the Swiss Rhone catchment. Science of The Total Environment.

Goderniaux, P., S. Brouyere (2009). How can large scale integrated surface - subsurface hydrological model be used to evaluate long term climate change impact on groundwater reserves. Calibration and Reliability in Groundwater Modeling: Managing Groundwater and the Environment 137-140.

Goderniaux, P., S. Brouyere (2009). "Large scale surface-subsurface hydrological model to assess climate change impacts on groundwater reserves." Journal of Hydrology 373(1-2): 122-138.

Gosling, S. N. (2013). "The likelihood and potential impact of future change in the large-scale climate-earth system on ecosystem services." Environmental Science & Policy 27: S15-S31.

Gosling, S. N., G. R. McGregor (2012). "The benefits of quantifying climate model uncertainty in climate change impacts assessment: an example with heat-related mortality change estimates." Climatic Change 112(2): 217-231.

Gosling, S. N., R. G. Taylor (2011). "A comparative analysis of projected impacts of climate change on river runoff from global and catchment-scale hydrological models." Hydrology and Earth System Sciences 15(1): 279-294.

Graham, L. P., Hagemann, S., Jaun, S., Beniston, M. (2007). On interpreting hydrological change from regional climate models. Climatic Change, 81(1), 97-122.

Green (2011). "Beneath the surface of global change: Impacts of climate change on groundwater." Journal of Hydrology 405.3, 532-560.

Harbaugh, A.W.: MODFLOW-2005—The U.S. Geological Survey modular ground-water model—The ground-water flow process: U.S. Geological Survey Techniques and Methods book 6, chap. A-16, 2005.

Hay, L. E., R. J. L. Wilby (2000). "A comparison of delta change and downscaled GCM scenarios for three mountainous basins in the United States." Journal of the American Water Resources Association 36(2): 387-397.

Hohenegger, C., A. Walser (2008). "Cloud-resolving ensemble simulations of the August 2005 Alpine flood." Quarterly Journal of the Royal Meteorological Society 134(633): 889-904.

Holman, I. P. (2006). "Climate change impacts on groundwater recharge-uncertainty, shortcomings, and the way forward?" Hydrogeology Journal 14(5): 637-647.

Holman, I. P., D. M. Allen (2012). "Towards best practice for assessing the impacts of climate change on groundwater." Hydrogeology Journal 20(1): 1-4.

Hunt, R. J., J. Doherty (2007). "Are models too simple? Arguments for increased parameterisation." Ground Water 45(3): 254-262.

Intergovernmental Panel on Climate Change (IPCC) (2000), Special report on emissions scenarios (SRES): a special report of working group III of the intergovernmental panel on climate change, pp. 570, Cambridge Univ. Press, Cambridge.

Intergovernmental Panel on Climate Change (IPCC) (2007a), Climate models and their evaluation, in Climate Change 2007: The Physical Science Basis. Contribution of Working Group I to the Fourth Assessment Report of the IPCC, edited by D.A. Randall et al., pp. 73, Cambridge Univ. Press, New York.

Intergovernmental Panel on Climate Change (IPCC) (2007b), Global climate projections, in Climate Change 2007: The Physical Science Basis. Contribution of Working Group I to the Fourth Assessment Report of the IPCC, edited by G.A. Meehl et al., pp. 98, Cambridge Univ. Press, New York.

Intergovernmental Panel on Climate Change (IPCC) (2007c), Regional climate projections, in Climate Change 2007: The Physical Science Basis. Contribution of Working Group I to the Fourth Assessment Report of the IPCC, edited by J.H. Christensen et al., pp. 93, Cambridge Univ. Press, New York.

Intergovernmental Panel on Climate Change (IPCC) (2008), Climate change and water, edited by B.C. Bates et al., Tech. paper of the IPCC, pp. 210, IPCC Secretariat, Geneva.

IPCC-TGICA (2003), Guidelines for use of climate scenarios developed from regional climate model experiments, Prepared by T.R. Carter on behalf of the IPCC, Task Group on Data and Scenario Support for Impact and Climate Asesment, pp. 66, Available at www.ipcc-data.org/guidelines.

IPCC-TGICA (2004), Guidelines for use of climate scenarios developed from statistical downscaling methods, Prepared by R.L. Wilby on behalf of the IPCC, Task Group on Data and Scenario Support for Impact and Climate Asesment, pp. 27, Available at www.ipcc-data.org/guidelines.

IPCC-TGICA (2007), General guidelines on the use of scenario data for climate impact and adaptation assessment, Version 2, Prepared by T.R. Carter on behalf of the IPCC, Task Group on Data and Scenario Support for Impact and

Climate Asessment, pp. 66, Available at www.ipcc-data.org/guidelines.

Jackson, C. R., R. Meister (2011). "Modeling the effects of climate change and its uncertainty on UK Chalk groundwater resources from an ensemble of global climate model projections." Journal of Hydrology 399(1-2): 12-28.

Jaun, S., B. Ahrens (2008). "A probabilistic view on the August 2005 floods in the upper Rhine catchment." Natural Hazards and Earth System Sciences 8(2): 281-291.

Jiang, T., Y. D. Chen (2007). "Comparison of hydrological impacts of climate change simulated by six hydrological models in the Dongjiang Basin, South China." Journal of Hydrology 336(3-4): 316-333.

Jyrkama, M. I., & Sykes, J. F. (2007). "The impact of climate change on spatially varying groundwater recharge in the grand river watershed (Ontario)." Journal of Hydrology 338.3 (2007): 237-250.

Jyrkama, M. I., J. F. Sykes (2002). "Recharge estimation for transient ground water modeling." Ground Water 40(6): 638-648.

Keese, K. E., B. R. Scanlon (2005). "Assessing controls on diffuse groundwater recharge using unsaturated flow modeling." Water Resources Research 41(6).

Kingston, D. G. and R. G. Taylor (2010). "Sources of uncertainty in climate change impacts on river discharge and groundwater in a headwater catchment of the Upper Nile Basin, Uganda." Hydrology and Earth System Sciences 14(7): 1297-1308.

Kingston, D. G., J. R. Thompson (2011). "Uncertainty in climate change projections of discharge for the Mekong River Basin." Hydrology and Earth System Sciences 15(5): 1459-1471.

Kostopoulou, E., C. Giannakopoulos (2012). "Climate extremes in the NE Mediterranean: assessing the E-OBS dataset and regional climate simulations." Climate Research 54(3): 249.

Laio, F., Porporato, A., Ridolfi, L., & Rodriguez-Iturbe, I. (2001). Plants in water-controlled ecosystems: Active role in hydrologic processes and response to water stress: II. Probabilistic soil moisture dynamics. Advances in Water Resources, 24(7), 707-723.

Lenderink, G. and E. Van Meijgaard (2008). "Increase in hourly precipitation extremes beyond expectations from temperature changes." Nature Geoscience 1(8): 511-514.

Lenderink, G., A. van Ulden, et al. (2007). "Summertime inter-annual temperature variability in an ensemble of regional model simulations: analysis of the surface energy budget." Climatic Change 81: 233-247.

Le Treut, H., Somerville, R., Cubasch, U., Ding, Y., Mauritzen, C., Mokssit, A., Peterson, T., Prather, M., 2007. Historical overview of climate change. In: Solomon, S., Qin, D., Manning, M., Chen, Z., Marquis, M., Averyt, K.B., Tignor, M., Miller, H.L. (Eds.), Climate Change 2007: The Physical Science Basis. Contribution of Working Group I to the Fourth Assessment Report of The Intergovernmental Panel on Climate Change. Cambridge University Press, Cambridge, United Kingdom, and New York, NY, USA.

Loaiciga, H. A., D. R. Maidment (2000). "Climate-change impacts in a regional karst aquifer, Texas, USA." Journal of Hydrology 227(1-4): 173-194.

Loáciga, H.A., (2003). Climate change and ground water. Annals of the Association of American Geographers 93 (1), 30–41.

Long, D., B. R. Scanlon (2012). "Are Temperature and Precipitation Extremes Increasing over the U.S. High Plains?" Earth Interactions 16.

McCallum, J. L., R. S. Crosbie (2010). "Impacts of climate change on groundwater in Australia: a sensitivity analysis of recharge." Hydrogeology Journal 18(7): 1625-1638.

McGuffie, K., and A. Henderson-Sellers (1997), A climate modeling primer, 253 pp., John Wiley & Sons Ltd, Chichester.

Mearns, L., and NARCCAP Team (2009), The North American Regional Climate Change Assessment Program (NARCCAP): overview of Phase II results, IOP Conf. Series: Earth and Environmental Science, 6, 022007, doi:10.1088/1755-1307/6/2/022007

Mileham, L., R. Taylor (2008). "Impact of rainfall distribution on the parameterisation of a soil-moisture balance model of groundwater recharge in equatorial Africa." Journal of Hydrology 359(1-2): 46-58.

Mileham, L., R. G. Taylor (2009). "The impact of climate change on groundwater recharge and runoff in a humid, equatorial catchment: sensitivity of projections to rainfall intensity." Hydrological Sciences Journal-Journal Des Sciences Hydrologiques 54(4): 727-738.

Moore, C. and J. Doherty (2006). "The cost of uniqueness in groundwater model calibration." Advances in Water Resources 29(4): 605-623.

Mueller, P. (2010). "Constructing climate knowledge with computer models." Wiley Interdisciplinary Reviews-Climate Change 1(4): 565-580.

Munari, C. (2011). "Effects of the 2003 European heatwave on the benthic community of a severe transitional ecosystem (Comacchio Saltworks, Italy)." Marine Pollution Bulletin 62(12): 2761-2770.

Nakicenovic, N. (2000). "Greenhouse gas emissions scenarios." Technological Forecasting and Social Change 65(2): 149-166.

Nemec, J., C. Gruber (2013). "Trends in extreme temperature indices in Austria based on a new homogenised dataset." International Journal of Climatology 33(6): 1538-1550.

Olita, A., R. Sorgente (2007). "Effects of the 2003 European heatwave on the Central Mediterranean Sea: surface fluxes and the dynamical response." Ocean Science 3(2): 273-289.

Orsolini, Y. J. and G. Nikulin (2006). "A low-ozone episode during the European heatwave of August 2003." Quarterly Journal of the Royal Meteorological Society 132(615): 667-680.

Racsko, P., L. Szeidl (1991). "A Serial Approach To Local Stochastic Weather Models." Ecological Modeling 57(1-2): 27-41.

Refsgaard, J. C., J. P. van der Sluijs (2006). "A framework for dealing with uncertainty due to model structure error." Advances in Water Resources 29(11): 1586-1597.

Refsgaard, J. C., and B. Storm (1995). MIKE SHE, in Computer Models of Watershed Hydrology, edited by V. J. Singh, pp. 809–846, Water Resour. Publ., Littleton, Colo.

Rodriguez-Iturbe, I. (2000). Ecohydrology: A hydrologic perspective of climate-soil-vegetation dynamies. Water Resources Research, 36(1), 3-9.

Rojas, R., L. Feyen (2008). "Conceptual model uncertainty in groundwater modeling: Combining generalized likelihood uncertainty estimation and Bayesian model averaging." Water Resources Research 44(12).

Schar, C. and G. Jendritzky (2004). "Climate change: Hot news from summer 2003." Nature 432(7017): 559-560.

Schaffranek, Raymond W., R. A. Baltzer, and D. E. Goldberg. A model for simulation of flow in singular and interconnected channels. US Government Printing Office, 1981.

Schiaparelli, S., M. Castellano (2007). "A benthic mucilage event in North-Western Mediterranean Sea and its possible relationships with the summer 2003 European heatwave: short term effects on littoral rocky assemblages." Marine Ecology-an Evolutionary Perspective 28(3): 341-353.

Schroeder, Paul R. (1994). "The hydrologic evaluation of landfill performance (HELP) model: Engineering documentation for version 3.": 9-94.

Scibek, J. and Allen , D.M. (2006). "Modeled impacts of predicted climate change on recharge and groundwater levels." Water Resources Research 42.11 (2006)

Scibek, J., Allen, D. M., Cannon, A. J., & Whitfield, P. H (2007). Journal of Hydrology, 333(2), 165-181. Groundwater–surface water interaction under scenarios of climate change using a high-resolution transient groundwater model. Journal of Hydrology, 333(2), 165-181.

Seidel, K., & Martinec, J. (2004). Remote sensing in snow hydrology: runoff modeling, effect of climate change. Springer.

Semenov, M. A. and E. M. Barrow (1997). "Use of a stochastic weather generator in the development of climate change scenarios." Climatic Change 35(4): 397-414.

Semenov, M. A., R. J. Brooks (1998). "Comparison of the WGEN and LARS-WG stochastic weather generators for diverse climates." Climate Research 10(2): 95-107.

Seneviratne, S. I., Corti, T., Davin, E. L., Hirschi, M., Jaeger, E. B., Lehner, I., & Teuling, A. J. (2010). Investigating soil moisture–climate interactions in a changing climate: a review. Earth-Science Reviews, 99(3), 125-161.

Serrat-Capdevila, A., J. B. Valdes, et al. (2007). "Modeling climate change impacts and uncertainty on the hydrology of a riparian system: The San Pedro Basin (Arizona/Sonora)." Journal of Hydrology 347(1-2): 48-66.

Soboll, A., M. Elbers (2011). "Integrated regional modeling and scenario development to evaluate future water demand under global change

conditions." Mitigation and Adaptation Strategies for Global Change 16(4): 477-498.

Sonnenborg, T. O., K. Hinsby (2012). Assessment of climate change impacts on the quantity and quality of a coastal catchment using a coupled groundwater-surface water model. Climatic Change 113(3-4): 1025-1048.

Stephens, G. L., D. G. Vane, (2002). The cloudsat mission and the a-train - A new dimension of space-based observations of clouds and precipitation. Bulletin of the American Meteorological Society 83(12): 1771-1790.

Stocker, T. F. (2003). Global change - South dials north. Nature 424(6948): 496.

Stoll, S., H. J. H. Franssen (2011). "Analysis of the impact of climate change on groundwater related hydrological fluxes: a multi-model approach including different downscaling methods." Hydrology and Earth System Sciences 15(1): 21-38.

Stott, P., Stone, D (2004). Human contribution to the European heatwave of 2003. Nature 432(7017): 610-614.

Sulis M., C. Paniconi, M. Marrocu, D. Huard, D. Chaumont (2012). Hydrologic response to multimodel climate output using a physically based model of groundwater/surface water interactions, Water Resour. Res., 48, W12510, doi:10.1029/2012WR012304.

Tebaldi, C. and R. Knutti (2007). The use of the multi-model ensemble in probabilistic climate projections. Philosophical Transactions of the Royal Society A: Mathematical, Physical and Engineering Sciences 365(1857): 2053-2075.

Thampi, S. G. and K. Y. Raneesh (2012). Impact of anticipated climate change on direct groundwater recharge in a humid tropical basin based on a simple conceptual model. Hydrological Processes 26(11): 1655-1671.

Therrien, R. McLaren, R.G., Sudicky, E.A.: HydroGeoSphre-a three dimensional numerical model describing fully integrated subsurface and surface flow and solute transport, Groundwater Simulations Group, University of Waterloo, 2007.

Thompson, J. R., A. J. Green (2013). Assessment of uncertainty in river flow projections for the Mekong River using multiple GCMs and hydrological models. Journal of Hydrology 486: 1-30.

Todd, M. C., R. G. Taylor (2011). Uncertainty in climate change impacts on basin-scale freshwater resources - preface to the special issue: the QUEST-GSI methodology and synthesis of results. Hydrology and Earth System Sciences 15(3): 1035-1046.

Trigo, R. M., A. M. Ramos (2009). Evaluating the impact of extreme temperature based indices in the 2003 heatwave excessive mortality in Portugal. Environmental Science & Policy 12(7): 844-854.

Vaccaro, J. J. (1992). Sensitivity of Groundwater Recharge Eestimates to Climate Variabilty and Change, Columbia Plateau, Washington. Journal of Geophysical Research-Atmospheres 97(D3): 2821-2833.

van Roosmalen, L., B. S. B. Christensen (2007). Regional differences in climate change impacts on groundwater and stream discharge in Denmark. Vadose Zone Journal 6(3): 554-571.

van Roosmalen, L., J. H. Christensen (2010). An intercomparison of regional climate model data for hydrological impact studies in Denmark. Journal of Hydrology 380(3-4): 406-419.

van Roosmalen, L., T. O. Sonnenborg (2009). Impact of climate and land use change on the hydrology of a large-scale agricultural catchment. Water Resources Research 45(7): W00A15.

van Roosmalen, L., T. O. Sonnenborg (2009). Impact of climate and land use change on the hydrology of a large-scale agricultural catchment. Water Resources Research 45.

van Roosmalen, L., T. O. Sonnenborg (2011). Comparison of Hydrological Simulations of Climate Change Using Perturbation of Observations and Distribution-Based Scaling. Vadose Zone Journal 10(1): 136-150.

Velázquez, J. A., J. Schmid (2013). An ensemble approach to assess hydrological models' contribution to uncertainties in the analysis of climate change impact on water resources. Hydrol. Earth Syst. Sci. 17(2): 565-578.

Vidale, P. L., D. Luthi (2003). Predictability and uncertainty in a regional climate model." Journal of Geophysical Research-Atmospheres 108(D18).

Viner, D. (2002), A qualitative assessment of the sources of uncertainty in climate change impacts assessment studies, in Climatic Change: implications for the hydrological cycle and for water management, edited by M. Beniston, Springer Netherlands, 139–149.

Wang, Y. Q., L. R. Leung (2004). Regional climate modeling: Progress, challenges, and prospects. Journal of the Meteorological Society of Japan 82(6): 1599-1628.

Wegner, K. M., M. Kalbe (2008). Mortality selection during the 2003 European heat wave in three-spined sticklebacks: effects of parasites and MHC genotype. Bmc Evolutionary Biology 8.

Wilby, R. L. and T. M. L. Wigley (1997). Downscaling general circulation model output: a review of methods and limitations. Progress in Physical Geography 21(4): 530-548.

Wilby, R. L., Beven, K. J., & Reynard, N. S. (2008). Climate change and fluvial flood risk in the UK: more of the same?. Hydrological Processes, 22(14), 2511-2523.

Woldeamlak, S. T., O. Batelaan (2007). Effects of climate change on the groundwater system in the Grote-Nete catchment, Belgium. Hydrogeology Journal 15(5): 891-901.

Yusoff, I., Hiscock, K.M., Conway, D., 2002. Simulation of the impacts of climate change on groundwater resources in eastern England. Geological Society, London Special Publications 193 (1), 325–344.

Xu, C. Y., E. Widen (2005). Modeling hydrological consequences of climate change - Progress and challenges. Advances in Atmospheric Sciences 22(6): 789-797.

Zektser, I. S. and H. A. Loaiciga (1993). Groundwater Flues in the Global Hydrologic Cycle – Past, Present and Future. Journal of Hydrology 144(1-4): 405-427.

Chapter 3

3. Predictive uncertainty of groundwater recharge rates caused by climate model chain variability and model simplification[1]

3.1 Abstract

Accurate knowledge of groundwater recharge is essential for sustainable water resources management, especially under expected climate change (CC). However, to quantify the influence of CC, models with different levels of complexity are commonly used, which can lead to inconsistent results. These inconsistencies are related to the varying degree of process simplification between physically based and lumped models. Another source of uncertainty is the variability among different combinations of general circulation models (GCM) and regional climate models (RCM). The relative importance of both uncertainties was so far not systematically investigated. Therefore, we evaluate how models with various degrees of complexity influence the prediction of groundwater recharge and secondly how this uncertainty compares to the uncertainty originating from the variability among different GCM-RCM combinations. Model complexity is subdivided into structural complexity (i.e. physically based and lumped models) and model discretization (i.e. spatial heterogeneous or homogenous model parameter discretization). We used a highly heterogeneous, physically based 2D synthetic reference model to generate daily reference recharge data for actual and predicted future weather conditions, based on climate prediction from 10 GCM-RCM combinations. Models of simpler conceptual structure were calibrated against groundwater recharge outputs of the complex reference model. Different calibration periods were used to assess the significance of different inputs for the calibration. Forward runs with best-calibrated parameters were carried out and corresponding results for each model and climate model chain were compared based on model scenario ratios to the reference model outputs. Good fits based on performance criteria are achieved through model calibration against the reference recharge period. However, predictive bias occurs by running these models over a time span of several years. Using CC data with more extreme weather conditions increases the resulting bias. The potential for model predictive error increases with the difference between the climatic forcing function used in the CC predictions and the climatic forcing function used in calibration period. The difference between the reference recharge and simulated recharge from physical

[1] C.Moeck (1), P.Brunner (1) and D. Hunkeler (1)
(1) Centre für Hydrogeology and Geothermics (CHYN), University of Neuchâtel, Switzerland

based but homogenous model as well as semi-mechanistic model are smallest whereas the differences increase with the simple models. The differences are due to structural model deficits such as the limitation of reproducing preferential flow. Due to these structural model deficits also a seasonal trend in recharge difference between the reference and simplified models can be observed, whereby summer recharge is underestimated and winter overestimated.
Thus results of CC impact studies using different approach to estimate recharge, in particular simple model structures need to be interpreted with caution if extremer weather conditions in future are likely and seasonal distribution of recharge rates are in particular interest. Comparison of both uncertainties, CC and model simplification, indicate, that the highest uncertainty is related to CC, but model simplification can also introduce a significant predictive error.

3.2 Introduction

Evaluating the effect of CC on water resources is essential for their successful management under future climate conditions. Observed changes and simulations provide evidence that water resources are vulnerable and potentially affected by CC (IPCC, 2008). Therefore, many climate impact studies have been carried out to provide insight into the relationship between CC and water resources (Holman, 2006; Holman et al., 2012; Scibek and Allen, 2006a; Scibek and Allen, 2006b; Scibek et al., 2007; Sonnenborg et al., 2012; Stoll et al., 2011; Taylor et al., 2009; Taylor et al., 2013; van Roosmalen et al., 2009; van Roosmalen et al., 2011; Woldeamlak et al., 2007). An excellent review can be found in Green et al. (2011).
A major requirement in CC impact studies is a profound knowledge about groundwater recharge. It is one of the main drivers of the hydrological system (Bakker et al., 2013) and the quantification is needed for any robust model prediction. Different approaches and models exist to embed recharge simulation into CC impact studies. Serrat-Capdevilla et al. (2007) used a three-dimensional “MODFLOW” model to estimate the CC impact on groundwater in Arizona. To simulate recharge, an empirical relationship between recharge and precipitation was applied. In Loaiciga et al. (2000) recharge was calculated by utilizing a water balance of the streamflow. This calculated value was used in a two-dimensional model (“GWSIM") to evaluate the effect of CC for a karst aquifer. Yusoff et al. (2002) followed a quite similar approach, but recharge input for the “MODFLOW” model was generated by a more conventional soil water balance method. Effects of CC were simulated, also with a soil-water balance model, for a study site in Uganda (Mileham et al., 2008, Mileham et al., 2009). In the studies of Allen et al. (2004), Scibek and Allen (2006a), Scibek et al. (2007) the effect of CC on the unconfined alluvial aquifer, which is influenced by river stages, was simulated in the framework of a combined modeling approach. Recharge values are based on the “HELP” model (Schroeder et al., 1994) while groundwater flow was simulated with a three-dimensional “MODFLOW” groundwater model (Harbaugh, 2005). For a CC impact study in Denmark, Van Roosmalen et al. (2007, 2009) developed a coupled model based on “MIKE SHE”

that simulates surface water and groundwater flows simultaneously. Although, this model already integrates different components of the water balance, still a relatively simple water balance method is used to simulate water flow within the unsaturated zone. In the work of Stoll et al. (2011) the integrated "MIKE SHE" model was used for a peri-alpine catchment in Switzerland. Goderniaux et al. (2009) simulate recharge from the surface to the subsurface domain between each node at each time step. This integrated, fully coupled approach was carried out with the HydroGeoSphere code for a catchment in Belgium. Sulis et al. (2012) study the effect of differences in the downscaling approach for a study area in Canada with the model "CATCHY", which is a coupled, physically based, spatially distributed model for surface to subsurface simulations. In contrast to former mentioned catchment simulation, long-term average groundwater recharge on the global scale was estimated for the past (Döll and Fiedler 2008) and future period under climate change (Döll 2009) with the lumped model WaterGAP Global Hydrology Model (Döll et al., 2003). The model was tuned against observed average long-term river discharge to obtain unknown model parameters.

All these mentioned mathematical models are used to quantify the relationship between CC and recharge rates. These models can be simple water balance calculations, lumped modeling approaches or physically based models relying on the Richards equation. Jones et al. (2006) claim that complex, physically based and simplified models should play a different role in impact studies. Simplified models can be used to rapidly estimate the impact of possible changes in the water balance caused by CC. On the other hand, physically based models represent flow processes and land-use in a physical interconnected model domain in which all equations are simultaneously solved. Due to this coupled flow and land-use process the effect of CC can be evaluated in more detail.

Even though hydrological processes can be reproduced with a high level of detail in complex physical based models, heterogeneity in the subsurface is often not well characterized and leads to uncertainty in the model parameter distribution and therefore to uncertain predictions. Heterogeneous versus homogenous model parameter discretization represent often-missing knowledge in parameters distribution. In addition, reproducing processes in full physical detail leads to long run times and carries the risk of numerical instability. In contrast, simplified models are very attractive due to the short run times and numerical stability. Fitting of historical observations can be realized by using just a few model parameters. Compared to physically based models, the calibration of simplified models is easier due to the reduced number of calibration parameters and because the model parameters often show linear relationships to model outputs. However, the simplified model structures are limited in reproducing the complexity of hydrological processes. This simplification can also be a major source of uncertainty.

Some studies (Cooley and Christensen, 2006; Doherty and Christensen, 2011) show how model simplification can introduce predictive bias. Model parameters from simpler models must take a compensatory role during the calibration process to achieve satisfactory results but may introduce bias for predictions (Doherty and

Christensen, 2011). Structural noise, the imperfect nature of models or model parameters to reproduce reality, is often the dominant contributor to model-to-measurement misfit and can increase the uncertainty in predictions (Doherty and Welter, 2010). This model structural error, that is often the main source of predictive uncertainty and bias is typically ignored (Refsgaard et al., 2012; Rojas et al., 2009). For instance, Cuthbert and Tindimugaya (2010) show that different groundwater recharge models give similar long-term historic recharge rates but still respond very different to intensity changes of precipitation. Similar results for reproducing historical recharge observations by calibration were achieved by using 6 different water balance models (Jiang et al., 2007). Differences in recharge appear between the models when CC is applied. Velazques et al. (2013) show that the chosen hydrological model can affect the CC response of different hydrological performance indicators, especially for low flow periods.

Although, the effects of model simplification and model structure is known (e.g. Döll et al., 2008), no consistency in model use for climate impact studies can be found in the literature. We speculate that the reason for this is cause by the absence of studies, which systematically evaluate the relative importance of both uncertainties, CC and model simplification. Droogers et al. (2008) point out that a common hypothesis is, that model errors are reflected in the reference situation as well as in the CC situation so that relative accuracy (difference between reference and scenario) is higher than absolute accuracy of the model. However, it is still unclear to which extent model complexity influences the prediction of recharge and lead to uncertainty.

Another type of uncertainty in climate impact studies is the climate signal itself. Multiple GCM and RCM combinations show a high variability in possible future climatic conditions. Prediction based on the same scenario but with different climate model chains can give large differences. For instance, Jackson et al. (2011) predict for a Chalk aquifer in the UK a change in groundwater recharge between -26 to 31% based on 13 GCMs.

In this study we systematically evaluate how models with various degrees of complexity influence the prediction of recharge. This approach follows the recommendation of Holman et al. (2012). They proposed a proper consideration of the hydrogeological model structural error and model uncertainty in climate impact studies. Based on the different model types reported in the literature, we subdivided complexity into structural complexity (i.e. physically based vs. lumped models) and model discretization (i.e. spatial heterogeneous vs. homogenous model parameter discretization). The used different model complexity is applied to investigate how uncertainty in model predictions due to variable model complexity compares to uncertainty originating from variability among climate model chains. More specifically, the following questions are addressed in this study:

I. Will all chosen groundwater recharge models predict the same absolute and relative change in groundwater recharge under the different climate model chains?

II. Is variability among the different GCM-RCM combinations or model simplification the driving force for predictive uncertainty?

III. Can predictive uncertainty be reduced by choosing a certain model complexity or different calibration approaches?

To avoid additional uncertainty related to boundary condition issues or measurement errors, a synthetic modeling approach was chosen, which however closely follows observations taken from a lysimeter facility. The observations from the lysimeter include soil water content behaviour and recharge pattern. A 2D heterogeneous reference model was created and simulated recharge was taken as a calibration data set for four simplified models.
We first present the description of the synthetic references model, followed by a description of the simplified models, in which complexity is subdivided into structural complexity and model discretization. Next, we introduce the used past and future climate data applied as inputs for the models. The CC data, defined by delta change factors for three time periods of the A1B emission scenario are explained. The A1B emission scenario describes a storyline with a balance across technological emphasis between fossilintensive and no fossil energy sources. This scenario was chosen because it lies between the extremes and represents a not too pessimistic but also a not too optimistic assumption of the future world.
Then different indicators were used to evaluate the effect of model simplification and the effect of different model calibration approaches on predictions under CC. These model-scenario-equations are used to express model inaccuracies in CC impact assessment studies. A comparison is carried out for the model calibration of the simpler models against the references recharge to validate the goodness of reproducing the references recharge for the calibration and validation period. Subsequently, the best-estimated model parameters are used to systematically evaluate the model performance under past and future conditions. Then, drivers for model bias are identified based on the model-scenario equations, which may lower the model performance. Finally the effect of different calibration approaches for the model performance are evaluated, following by the summary and conclusion.

3.3 Methods

In this section a description of the 2D heterogeneous references model is given. After this the description of the four simpler models, which were calibrated against monthly groundwater recharge outputs of the complex 2D heterogeneous reference model is descripted. A schematic summary of all used simplified model structures is shown in the supporting information (Figure A3.3; supporting information). Then the used climate data and climate change scenario are explained. Finally, the different indicators (Model scenario equations) are described, which were used to evaluate the effect of model simplification and the effect of different model calibration approaches on predictions under CC.

3.3.1 Reference Model

The reference model was constructed using the fully coupled physically based model HydroGeoSphere (HGS) (Therrien et al. 2010). This integrated model simulates fully coupled 3D variably saturated groundwater flow in porous or fractured aquifers and 2D overland flow as well as solute transport in (sub)surface domains. A control volume finite element approach is used to solve Richards' equation describing 3D variably-saturated subsurface flow. The Mualem – van Genuchten model for unsaturated soil hydraulic properties (van Genuchten, 1980) is used.

$$(1-\theta_r)[1+|\alpha\psi|^{\beta}]^{-\upsilon} \qquad \text{for } \psi < 0 \tag{1}$$

$$S_w = 1 \qquad \text{for } \psi \geq 0 \tag{2}$$

$$kr = Se^{(lp)}\left[1-(1-Se^{\frac{1}{\upsilon}})^{\upsilon}\right]^2 \qquad \text{where}\left(\upsilon = 1-\frac{1}{\beta}\right) \tag{3}$$

where S_w is the water saturation [-], α is the inverse of the air-entry pressure head [m^{-1}], β is the pre-size distribution index, θ_r is the residual water saturation, ψ being the pressure head [m^{-1}], S_e is an effective saturation, given by $S_e = (S_w - S_{wr})/(1 - S_{wr})$, l_p is the pore-connectivity parameter and S_{wr} is the the residual water saturation. Precipitation is partitioned into evapotranspiration, runoff and infiltration. Based on the work of Kristensen and Jensen (1975) actual transpiration and evaporation are a function of potential evapotranspiration, soil moisture, evaporation depth, root depth, and 'Leaf Area Index' (LAI). Precipitation that exceeds evaporation and interception storage is infiltrated. A more detailed description of the model and all its components can be found in Therrien et al. (2010).

Based on this model, a vertical 2D synthetic heterogeneous reference model was created with 150 cm depth, 100 cm in the x-direction and 5 cm discretization (Figure 3.1). The model structure is highly influenced by observations from the Zürich Reckenholz lysimeter facility (Prashun et al., 2009). The lysimeter setup is transferred to our synthetic references model. Soil samples from different depths are used to create the needed variogram for the stochastic field generator to emulate the hydraulic conductivity field. Soil moisture observations are used to compare moisture dynamic from the lysimeter with the synthetic references model to be certain that a realistic soil column is represented. A specified flux boundary is used on the top of the column of the references model and a constant head boundary at the bottom. A fixed head boundary is used to allow upward fluxes from the water table during dry periods (Carrera-Hernandez et al., 2011). No flow boundary conditions are applied to the remaining borders of the soil column. Hydraulic conductivity was distributed within the model domain with the program Fieldgen (Doherty, 2010), a two –

dimensional stochastic field generator. Field generation is undertaken using the Gaussian sequential simulation principal. Using the generated hydraulic conductivity van Genuchten parameters like α, β and S_{wr} were calculated for every element based on relationships from Carsel and Parrish (1988). Reported variances around the used relationships for each van Genuchten parameter are added. That was done to include a more natural soil description with variance in all soil parameters (Figure A3.1; supporting information).

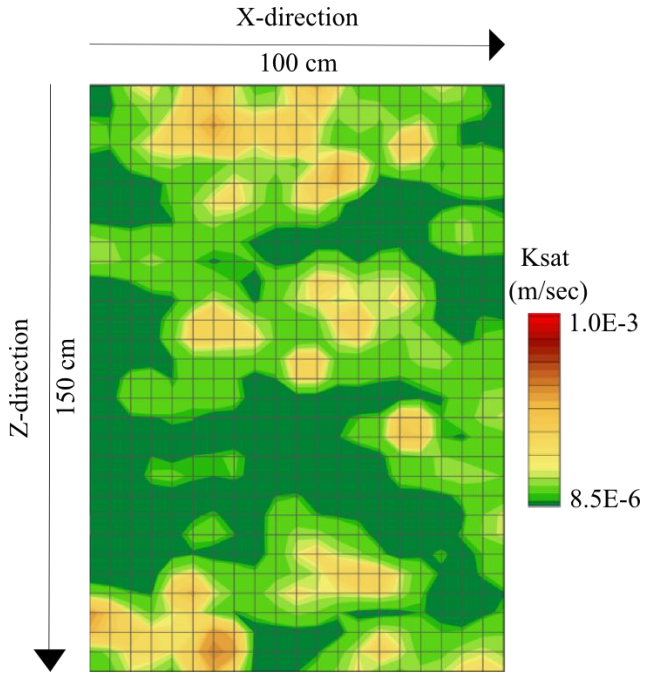

Figure 3. 5: Soil structure for the heterogeneous synthetic 2D reference model with saturated hydraulic conductivity distribution from $8.5*10^{-6}$ to $1.0*10^{-3}$ [m d^{-1}]

In addition, porosity is distributed and adapted from standard normal Gaussian distribution for the whole soil column and ranged from 0.33 to 0.38, similar to archived values from the soil samples of the lysimeter. Model parameters, such as root zone and LAI are added to the model to simulate the presence of a constant vegetation cover. Altogether 3014 parameters describe the 2D heterogeneous model domain. In order to represent spatial heterogeneity in a more robust way, 130 stochastic realizations of the soil parameters are carried out.
However, we found only small differences in recharge amount and pattern between different stochastic realizations of the soil column (Figure A3.2; supporting information). Also the calibration of the simpler models against the 130 stochastic realizations of the references model shows only small differences. Due to these small differences and long running times for each CC scenario for each realization we just used one single references model out of these 130 stochastic realizations for the further analysis to reduce the computation time.

3.3.2 Homogenous 1D model

The first simpler model (1d1l) is also a HGS model but with a homogenous model parameter discretization. The model is simplified to 1D with 1 layer of a homogenous soil while maintaining the same underlying physical processes described for the reference model.

3.3.3 Lumped parameter bucket model

The second model is the lumped parameter "bucket" model named Lumpren (Doherty, 2003).
The model provides a basic representation of major aspects of the unsaturated zone including rainfall, evapotranspiration, runoff, matrix and macropore recharge. Matrix and macropore recharge are activated after specified delay times. Lumprem calculates the actual evapotranspiration taking into account soil moisture storage and plant parameters according to:

$$E = fE_p \frac{1-e^{-\gamma \upsilon'}}{1-2e^{-\gamma}+e^{-\gamma \upsilon'}} \quad (4)$$

where E [m d^{-1}] is the water loss through evapotranspiration, E_p the potential evapotranspiration [m d^{-1}], f is a crop factor, υ' is the volume of water in the soil column and γ is a parameter determining the shape of the evaporation rate vs. stored water relationship. Water is lost from the container (Figure A3.3; supporting information) as a continuous unsaturated vertical flow. The recharge rate depends on the moisture volume in the container. This moisture volume controls the hydraulic conductivity. Decreasing moisture volume leads to decreasing hydraulic conductivity and increasing saturation leads to an increase in hydraulic conductivity. The rate of water loss is defined as:

$$R = K_s[\upsilon']^l \left[1 - (1 - [\upsilon']^{\frac{1}{m}})^m\right]^2 \quad (5)$$

where R is the rate of drainage, l is tortuosity, K_s is the saturated hydraulic conductivity and m determines the shape of relationship between the drainage rate vs. stored water.

3.3.4 Finch soil water balanced model

This soil water balance model includes, in contrast to many other soil water balance models, interception and root water uptake (Finch, 1998). It was shown that the maximum available water and the root depth have a major impact on estimates of direct groundwater recharge (Finch, 1998). Even though this model represents a more complex soil water balance model the relationships between model parameters as well as simulated recharge is predominantly linear. Direct recharge is calculated using a daily water balance equation:

$$P_i = E_{ai} + I_i + R_i + B_i + \Delta S_i \quad (6)$$

where P_i is precipitation [mm], E_{ai} is evaporation [mm], I_i is canopy interception loss [mm], R_i is runoff [mm], B_i is flow bypassing the soil water store [mm] and ΔS_i is change in soil water [mm]. No upward movement of water from groundwater to the soil layer can occur.
In this study the root zone for the Finch model is divided into four layers (Figure A3.3; supporting information). That follows the proposed pragmatic solution of Finch (1998), where a reasonable representation of physical conditions is still achieved whilst unnecessary complexity is avoided. Plant roots take up water at the given rate as long as there is no water stress.

$$A_j = \theta_{fcj} - \theta_{wpj} \quad (7)$$

$$E_{aj} = E_p S_j C_j \quad (8)$$

$$S_j = \frac{(\theta_j - \theta_{wpj}) Z_j}{A_j} \text{ where } \theta_{wpj} < \theta_j < \theta_{fcj} \quad (9)$$

$$S_j = 0 \text{ where } \theta_j \leq \theta_{wpj} \quad (10)$$

$$S_j = 1 \text{ where } \theta_{jg} \geq \theta_{fcj} \quad (11)$$

where A_j is the fractional maximum available soil water content [-], $E_{a,j}$ the actual root water uptake [mm], E_p the potential total root water uptake [mm], Z_j the layer thickness [mm], C_j the fractional proportion of roots [-], θ the current fractional soil water content [-], θ_{fc} fractional soil water content at field capacity [-] and $\theta_{wp,j}$ is the fractional soil water content at wilting point [-]. For a more comprehensive description of model details see for instance Finch (1998).

3.3.5 SWB soil water balanced model

The fourth simple model (SWB), also a soil water balance model, depends in contrast to the Finch model only on one soil storage parameter. Recharge can only occur if the threshold of this soil storage is reached and the excess water is transferred to daily recharge. Changes in storage depend on subtraction of potential evapotranspiration from precipitation as well as storage changes from the previous day. A soil function, which depends on the chosen soil storage parameter (Richter and Lillich, 1975) reduces the potential to a real water loss [mm].

3.4 Model Calibration

The simulated recharge from the reference model was used for the calibration. Calibration was carried out using the automatic parameter estimation software PEST (Doherty, 2010) for soil and vegetation parameters for each recharge model (Table A3.1; supporting information). Monthly recharge sums from the reference model were used to minimize the objective function, which calculates the differences between reference and simulated recharge for each recharge model. It is assumed that monthly recharge values could be deduced frequently from streamflow measurements and are a proper alternative for normally unknown recharge rates or dynamics. Three different calibration periods, containing an average year (2010), a wet/dry year (2002/2003) and a monthly time series (2004-2009), are used to evaluate if simpler models show less predictive model bias for actual and future periods if extreme condition and longer time series of observation are included in the calibration.

3.5 Climate data and Climate Change Scenarios

The used past and future climate data as well as the methodology to create daily climate data for future periods as inputs for all models are presented below. To simulate future weather conditions a total of 10 model chains for the A1B emission scenario, which is moderate in terms of CO_2 emission increase, are used.
Model chains consist of combinations of GCMs and RCMs (Table A3.2; supporting information). The regional scenarios are derived directly from the output of individual GCM-RCM model chains by means of the statistically downscaling technique to the MeteoSwiss monitoring network with an inverse distance weighting interpolation (Bosshard et al., 2011). These model chains provide a daily time series of delta change factors for precipitation and temperature relative to the reference period 1980-2009 for three time periods: 2035 (2021-2050), 2060 (2045-2074) and 2085 (2070-2099). The delta change method shifts an observed time series by a CC induced value (Hay et al. 2000). Future weather periods are therefore a function of the past climate conditions, with added (temperature) or multiplied (precipitation) delta change values. Daily time series of actual precipitation were used over a period from 01.01.1982 to 31.12.2011. The time series were measured at the MeteoSwiss weather station Zurich-Reckenholz, Switzerland directly located at the lysimeter facility. This weather station was chosen because our references soil model parameters are based on the observation taken from the lysimeter facility. Potential evapotranspiration was calculated using the Penman Montheith equation after Allen et al. (1994).
A general increase in temperature for all time periods compared to the reference period can be observed in figure 3.2 (temperature column). Values larger than zero are constantly added to the past temperature. The strongest increase occurs in summer with a maximum in August whereas the smallest between February and March. The delta change values for precipitation shows both, increasing and

decreasing trends. Temporal distributions for precipitation show an increase between autumn to winter and a decrease in summer until the beginning of autumn (Figure 3.2, precipitation column). However, temperature and precipitation distributions depend strongly on the chosen model chain. A total of 31 time series were created comprising 10 model chains for 3 CC periods and 1 time series for the actual weather condition. However, it should be noted that this data set is not taking future changes in inter-annual variability into account.

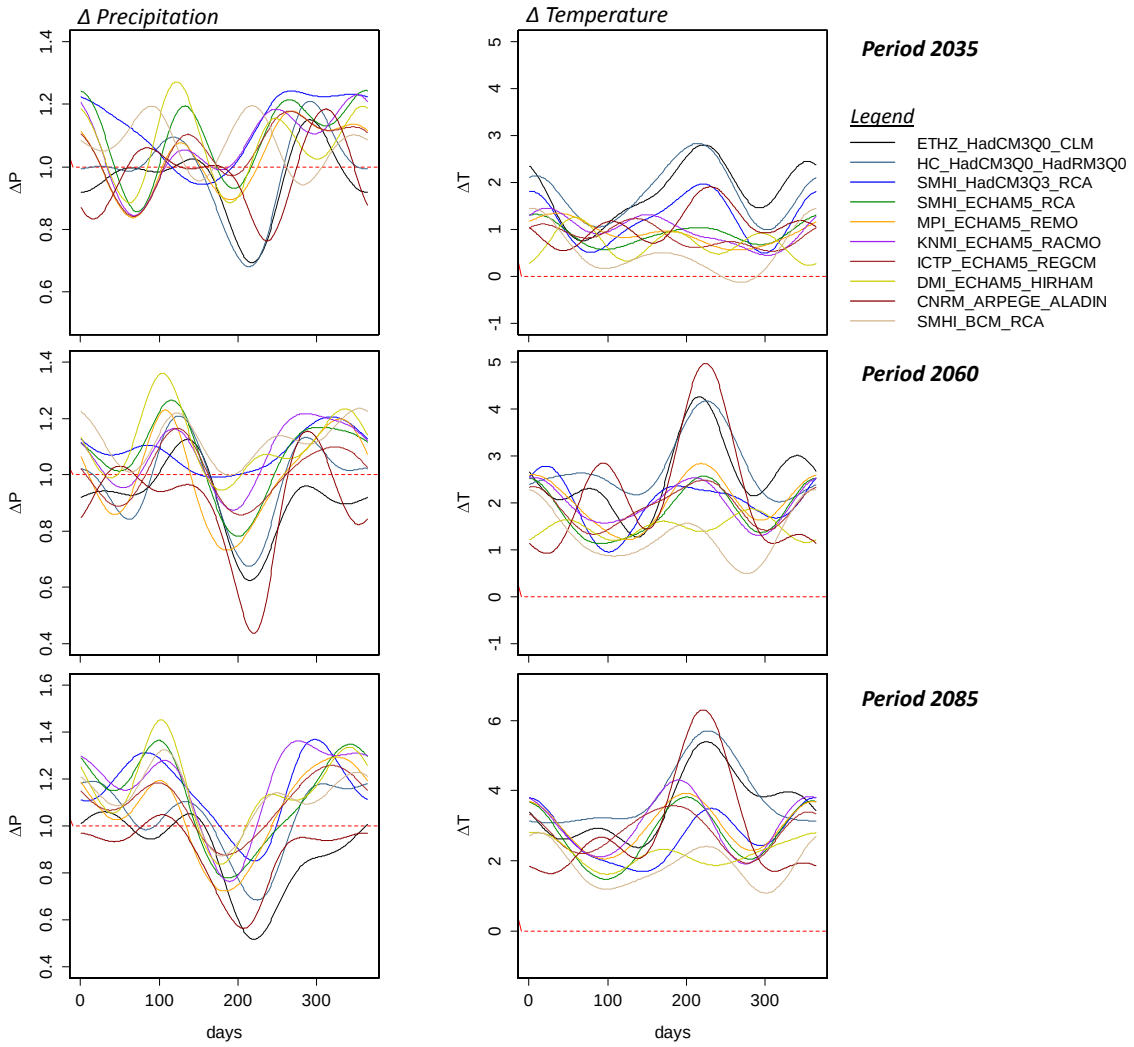

Figure 3. 6: Daily climatic change factors (delta - Change approach) for each climate model chain for the scenario A1B. Left column show changes in daily precipitation and right column in daily mean temperature for Meteoswiss weather station in Zurich-Reckenholz.

3.6 Model Scenario Equations

Different indicators were used to evaluate the effect of model simplification and the effect of different model calibration approaches on predictions under CC. Model-Scenario-Equations are used to express model inaccuracy in CC impact assessment studies. Three different model scenario equations are chosen because interpretation of the results can be challenging due to the fact that model scenario equations can emphasize with different sensitivity on observed and simulated values. It is therefore, recommended to apply different Model scenario equations to limit any weakness of the metric (Bennet et al., 2013).
Here, we introduce the applied model scenario equations. We calculated a modified Model-Scenario Ratio (MSR) (Droogers et al., 2008), which indicates to what extent the impact of a scenario contributes to the final findings compared to model simplification.

$$SI_{Ref;t} = (\text{Ref-ModelChain}_t - \text{Ref-Current}_t)/\ \text{Ref-Current}_t \quad (13)$$

$$SI_{Simple,t} = (\text{Simple-ModelChain}_t - \text{Simple-Current}_t)/\ \text{Simple-Current}_t \quad (14)$$

$$MSR_t = 1 - abs(\ SI_{Ref,t} - SI_{Simple,t}) \quad (15)$$

where SI_{Ref} is the scenario index for the reference model, SI_{Simple} the calculated scenario index for the simplified models, Ref-ModelChain the future annual recharge rate for the chosen climate model chain for the 2D reference model, Ref-Current the annual current recharge rate for the 2D reference model, t the yearly time steps. To calculate the SI_{Simple} the output of the simple model instead of the reference model is used. The model scenario index (MSR) has a range from 1 to -∞ where 1 indicates that the model simplification does not play a role and results are just a function of the scenario only. Values smaller than 0 indicate that model inaccuracy is the dominant factor for changes in recharge rates rather than the climate scenario.
Another chosen approach to evaluate the effect of model simplification for groundwater recharge predictions under CC is the well-known Nash Sutcliffe model efficiency (NSE) coefficient (Nash and Sutcliffe, 1970).

$$NSE = 1 - \frac{\sum_{t=1}^{T}(\text{Reference}_o^t - \text{Simplified}_o^t)^2}{\sum_{t=1}^{T}(\text{Reference}_o^t - \overline{\text{Refernence}_0})^2} \quad (16)$$

where Reference_o^t [mm y^{-1}] is the annual reference recharge at time step t [y], Simplified_o^t [mm y^{-1}] is the recharge from one of the simplified models at time step t [y] and $\overline{\text{Refernence}_0}$ is the mean calculated reference recharge. Like the MSR, the NSE provides also values between 1 to -∞, where 1 indicates a perfect match and no effect on prediction caused by model simplifications.

The percent of bias was calculated after Gupta et al. (1999) but in a modified version for this CC and simplification impact study.

$$\text{PBIAS (\%)} = \frac{\sum_{t=1}^{T}(\text{Reference}_o^t - \text{Simplified}_o^t) \times 100}{\sum_{t=1}^{T}(\text{Reference}_o^t)} \quad (17)$$

PBIAS provide a measure of over- or underestimation for each scenario. An optimal value would be 0% while a positive value indicates an underestimation and a negative value an overestimation of yearly recharge.

3.7 Results and Discussion

In the following section, results of the model calibration of the simpler models against the reference recharge are given (3.6.1). The best-estimated model parameters are used to systematically evaluate the model performance under past and future conditions (3.6.2). Then, drivers for model bias are identified (3.6.3) which may lower the model performance. Subsequently, a comparison between three calibration periods are carried out, in order to evaluate if simpler models show a better model performance if more "extreme" conditions or longer time series of observation are included (3.6.4).

3.7.1 Calibration and Validation

For the calibration period 2010 the simpler recharge models reproduce the reference recharge surprisingly well, even though the model complexity is different. The annual recharge agrees well between reference and simplified models (Figure 3.3).

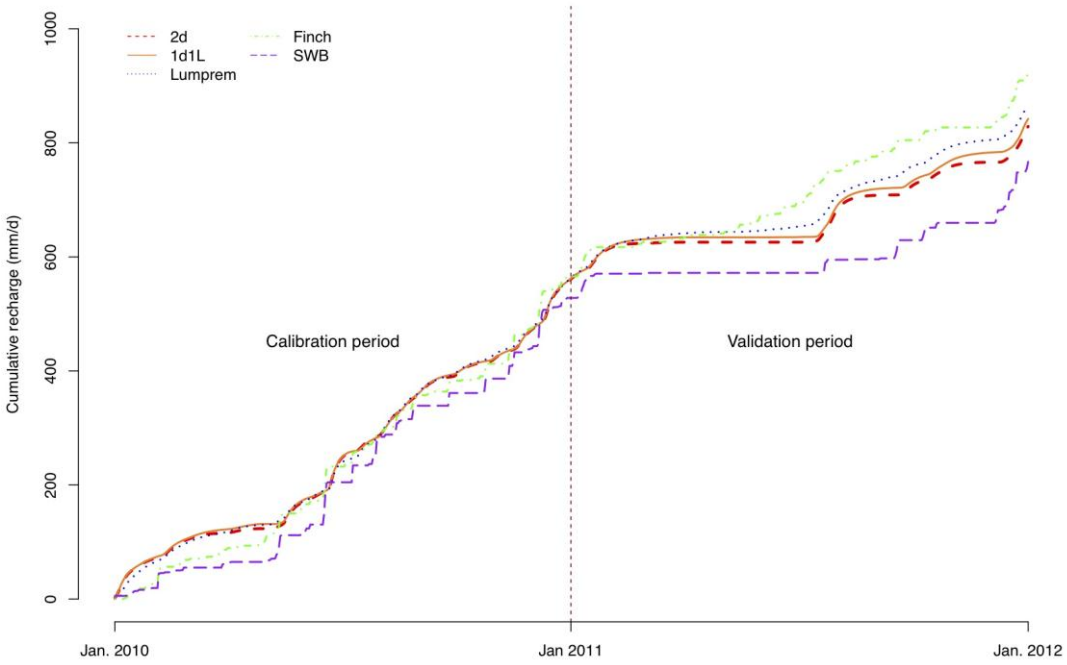

Figure 3. 7: 2D simulated cumulative reference recharge (red dashed line) and fitted recharge for 1d1l (orange line), Lumprem (blue line), Finch model (green line) and SWB (purple line). The 2D references recharge from year 2010 was used for the calibration of the simplified models. The recharge values from year 2011 were used for the validation (without data calibration).

However, differences in the annual pattern can be observed. Sharp rises of recharge after strong precipitation events appear for the SWB and Finch model while the recharge pattern is more smoothed for the other models. This effect is related to the model structure of the soil water balance model. Once the storage capacity is filled up, excess water contributes directly to recharge without a typical infiltration front for the SWB and Finch models. Therefore, the model results cannot be compared to the more complex models for small time steps like daily calculations. Only weekly or monthly values gave a good fit throughout the calibration. In this study monthly values were chosen for the calibration for all simplified models. Even though the input time step for the calibration is large, the advantage is that monthly recharge values could be deduced frequently from streamflow measurements and are a proper alternative for normally unknown recharge rates or dynamics. A comparison of stream flow measurements and seepage rates from lysimeters in another study show quite similar monthly dynamics and discharge values (Seneviratne et al., 2012) and

validate our approach. Furthermore, for CC impact studies, which typically cover a long time period, it is commonly sufficient if a model can correctly reproduce monthly values even though daily processes are not correctly simulated.
For the validation period 2011, which corresponds to a more extreme year with a long dry spell, an increase in recharge amount for all simpler models can be observed, especially for the SWB and Finch model. The Finch model overestimated recharge during the dry period because small precipitation events led directly to recharge.
However, all recharge models with the calibrated model parameter sets perform well for the past climate conditions. Simulating a 30 years period to estimate past recharge rates based on the best-estimated parameter sets shows variability among the different models. The simulation creates a model bias due to structural model differences (Figure 3.4). The SWB model underestimates (-10 %), whereas the Finch model overestimates (+7.5 %) the total recharge rate. Also, the physically based 1D and Lumprem model over- and underestimate the true value from the references model but by less than 2%. These percentages correspond to an error between 5 and 17 mm per year over a 30 years period. Generally speaking, model bias is small for a performance over 30 years.

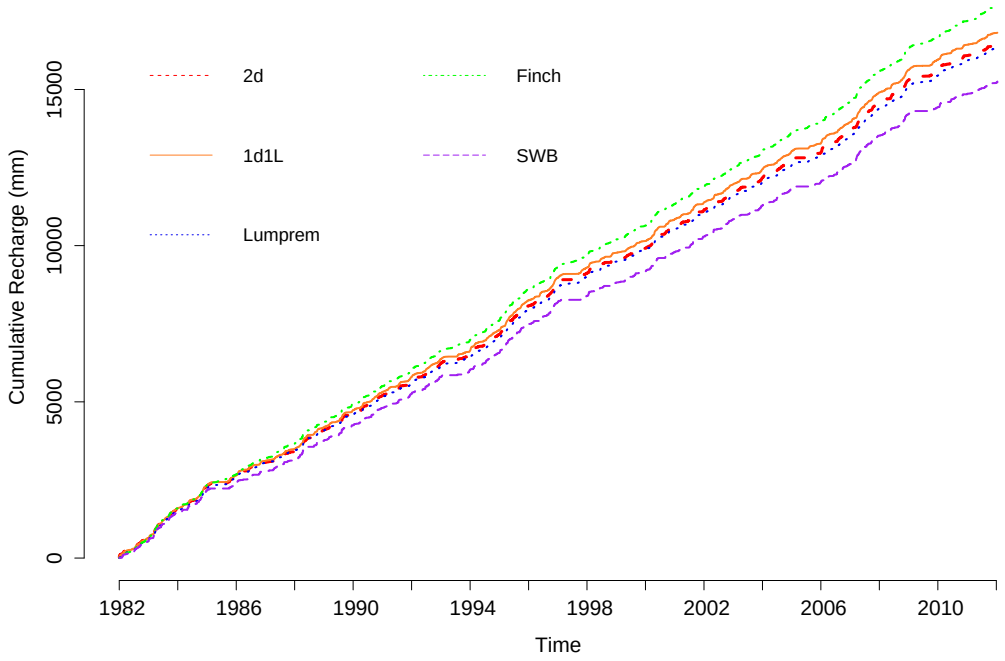

Figure 3. 8: 2D simulated cumulative reference recharge (red dashed line) and fitted recharge for 1d1l (orange line), Lumprem (blue line), Finch model (green line) and SWB (purple line). The 2D references recharge from year 2010 was used for the calibration of the simplified models. The recharge values from year 2011 were used for the validation (without data calibration).

3.7.2 Model performance for future conditions

Simulating with all models the time series generated from our baseline with additional delta change values shows a spreading in the results (Figure 3.5). For 2035, the mean groundwater recharge increases by 4.2% (+22.8 mm) for the 2D reference model considering all 10 climate model chains relative to the reference period 1982-2011.

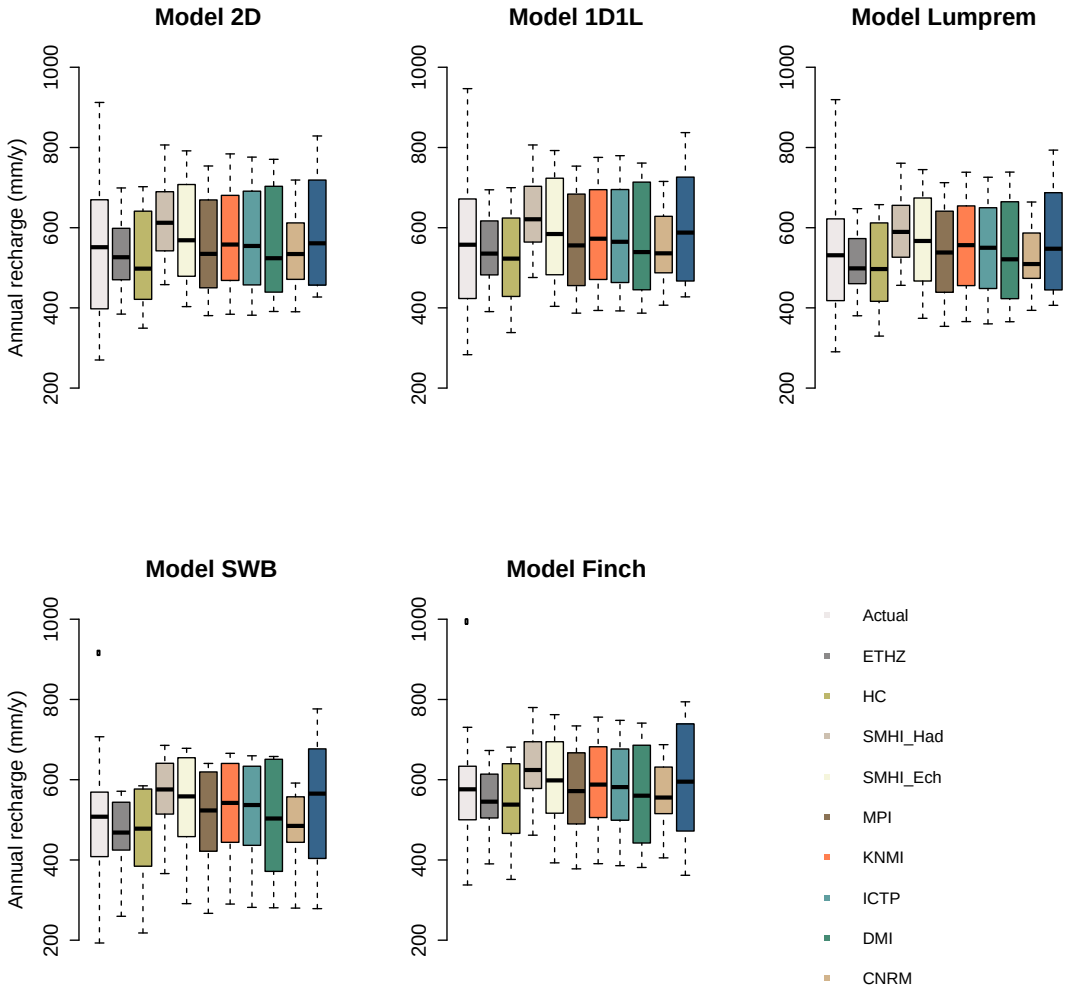

Figure 3. 5: Boxplot of 30 year past recharge and for 10 climate model chains for the period 2035 based on delta change factors. Filled boxes show the upper and lower quartile with mean value as black line within the boxes. The whisker, the vertically lines elongating the box indicate values outside the upper and lower quartile.

However, due to the variability among the different climate model chains a range of mean groundwater recharge between -4.3% (-23.3 mm) to +14.4% (+78.1 mm) is simulated. Similar ranges can be observed for all other groundwater recharge models as well (Table 3.1). However, it is interesting to note that increasing simplification of the models tends to clearly underestimate mean and minimum change in recharge compared to the reference 2D model (Table 3.1). Predicted groundwater recharge

changes depend strongly on the degree of model simplification. Evapotranspiration processes are operating differently in all models. For instance, the SWB model is highly influenced by increasing evapotranspiration (ET) due to the simple relationship between potential and actual water lost. It depends only on a uniform homogenous soil storage compartment where no additional limitations for the evaporation or transpiration depth exist. In contrast, due to the heterogeneous model structure of the 2D model, infiltration is not uniform and water can infiltrate into deeper parts of soil faster, where the effect of ET is less present. Ponded water at the surface is not available for the 2D model and reduces the actual ET whereas the model structure of the SWB model does not considered these processes. Additional limitations of ET fluxes are given by vegetation and root depth for the 2D model, where water under the root zone is not affected by ET processes.

Table 3. 1: Percentage changes for the scenario period 2035 (2021-2050) in groundwater recharge rates due to variability among the different climate model chains and through different groundwater recharge models

% Change in groundwater recharge rates				
Model	Median	Mean	Min	Max
2D	4.2	4.2	-4.3	14.4
1d1l	3.1	3.4	-5.6	14.0
Lumprem	1.1	1.6	-6.3	11.6
Finch	-1.7	-0.9	-7.7	8.0
SWB	0.9	1.4	-9.6	13.5

Even though differences in the range (min, max and mean) in simulated groundwater recharge for the period 2035 exist between the different recharge models, the trend for each climate model chain indicates similarities (Figure 3.5). For climate model chains with the largest change, all simplified models show similar groundwater recharge rates. In figure 3.6, for instance, all models indicate a decrease of recharge for the climate model chain 1.

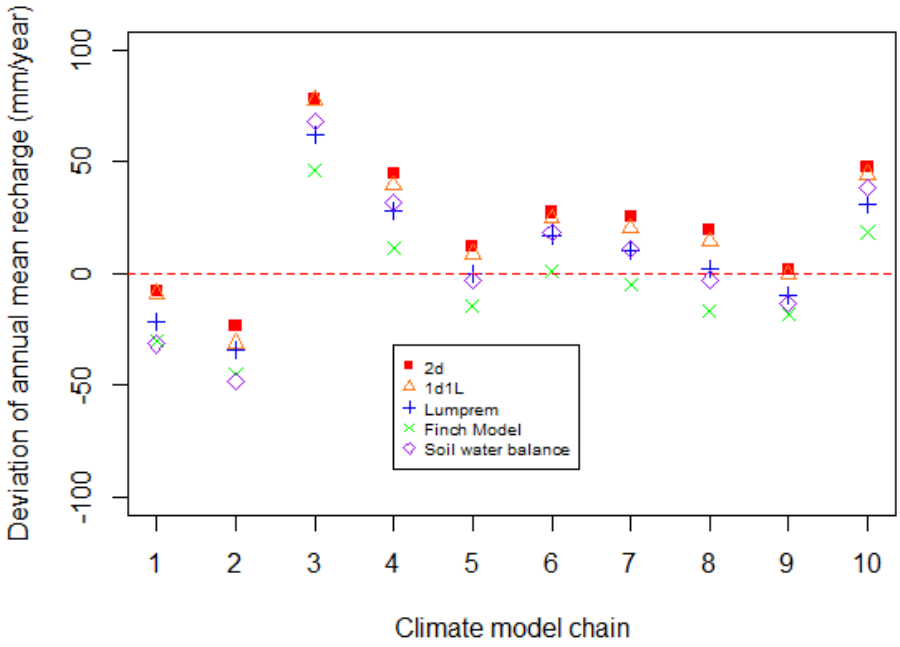

Figure 3. 6: Deviations between mean annual recharge from the baseline (past mean recharge) and for the period 2035 for 10 model chains.

A consistent order between all simplified models for each climate model chain can be observed. The smallest differences and therefore best model performance can be observed for model 1d1l which shows recharge values close to our reference 2D model. This model has exactly the same trend as the reference model in recharge changes under CC. The Finch and SWB model perform different, in particularly the Finch model. Based on the Finch model, more climate model chains would predict a decrease in recharge, whereas the reference model indicates an increase. Similar results can be found by using the lower and upper quartile as an indicator of recharge trends (Figure A3.6; supporting information).

3.8.3 Drivers for model bias

Calculations of MSR for each year are carried out to identify the drivers for model bias. It can be shown that for most years the MSR values are larger than 0.9 for each recharge model, meaning that model simplification does not play a role and changes in recharge for future climate conditions are only a function of the scenario (Figure 3.7). However, for each model some outliers appear. These outliers correspond to weather conditions with distinct different precipitation amounts and distribution, as well as temperature values, such as observed e.g. for the hot dry year 2003 (Seneviratne et al., 2012). The corresponding values for the outliers ranged between 0.85 (1d1l), 0.65 (Lumprem), 0.4 (Finch) to 0 (SWB). This order shows the sensitivity of the models to extreme years. Simple models such as SWB and Finch give similar results like the physical models for years with normal temperature and precipitation distribution. However, for extremes such as observed in the year 2003 and 2011 (validation period in the calibration) they simulated different recharge rates.

Results already drift apart for some model types, for the chosen delta change approach. This model sensitivity to extreme years can become increasingly important due to a higher probability, frequency and duration of extremes periods in future periods (Schär et al., 2005).

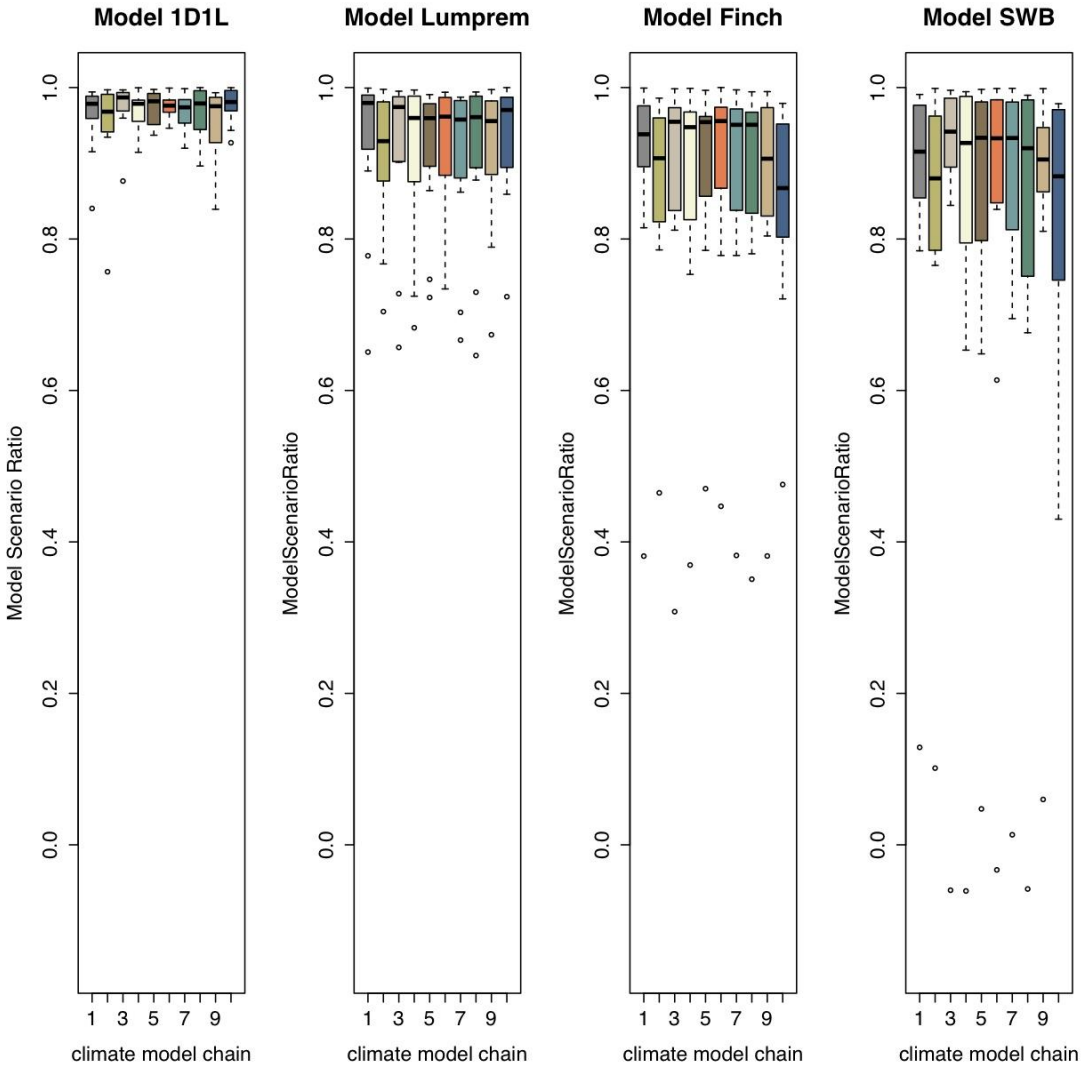

Figure 3.7: Model scenario ratio (Equation 13-15) for simplified groundwater recharge models for each climate model chain.

Calculating the NSE and PBIAS for each climate model chain, a model performance order among the different simplified models can be observed, similar to the order of model sensitivity to extreme years (Table 3.2). The NSE shows for the scenarios values between 0.89 to 0.99 for the 1d1l and 0.89 to 0.97 for the Lumprem model. For the former overestimation of the reference recharge rates based on PBIAS lies only between 2.3 to 0.89 whereas the latter underestimate this values by 1.03 to 4.17. Values for the Finch and SWB model show a NSE for the former between 0.49 and 0.93 and for the latter between 0.35 and 0.87. Values of PBIAS indicate a range of -7.52 to 7.88 and 7.21 to 12.35.

Table 3.2: Variation of NSE-Coefficient and PBIAS to different groundwater recharge models and climate model chains.

		Period 2035			
		1d1l	Lumprem	Finch	SWB
Scenario	Equation				
Past	NSE	0.99	0.97	0.87	0.87
ETH		0.93	0.9	0.6	0.23
HC		0.92	0.88	0.61	0.35
SMHI_Had		0.97	0.9	0.84	0.56
SMHI_EC		0.98	0.93	0.93	0.7
MPI		0.98	0.95	0.92	0.67
KNMI		0.98	0.96	0.93	0.75
ICTP		0.99	0.94	0.93	0.71
DMR		0.98	0.93	0.92	0.62
CNMR		0.89	0.86	0.49	0.35
SMHI_B		0.99	0.95	0.92	0.72
Past	PBIAS (%)	-2.3	1.03	-7.52	7.21
ETH		-2.12	3.62	6.71	11.75
HC		-0.89	3.1	6.64	12.35
SMHI_Had		-2.03	3.42	-1.53	7.9
SMHI_EC		-1.24	3.87	-1.26	8.9
MPI		-1.62	3.22	-2.5	9.79
KNMI		-1.73	2.75	-2.58	8.37
ICTP		-1.33	3.65	-1.83	9.35
DMR		-1.27	4.17	-0.8	10.97
CNMR		-1.87	3.18	7.88	9.99
SMHI_B		-1.59	3.77	-1.98	8.15

Smallest values for NSE and highest values of PBIAS can be found for climate model chains with the strongest increase in temperature and decrease in precipitation (Table 3.2 for the ETHZ_HadCM3Q0_CLM climate model chain). Using future time periods (Period 2060 and 2085) where the increase in temperature and change in precipitation distribution are stronger than in period 2035 the observed effect for some models increases (Figure 3.8). Over the complete time series (periods 2035-2085) for the climate model chain ETHZ_HadCM3Q0_CLM, the 1d1l model shows only a small change in model performance. NSE values are still close to 1 whereas for all other recharge models a decrease through the different climate model periods is observed. However, the decline in NSE follows again the degree of simplification where the SWB model shows the largest decrease up to a value of -2.5. Similar observations can be made using the PBIAS. The 1d1l and Lumprem model drift only

slightly, whereas Finch, followed by SWB, shows a drastic change. The decrease of efficiency results from sensitivity of models to stronger changing climate conditions.

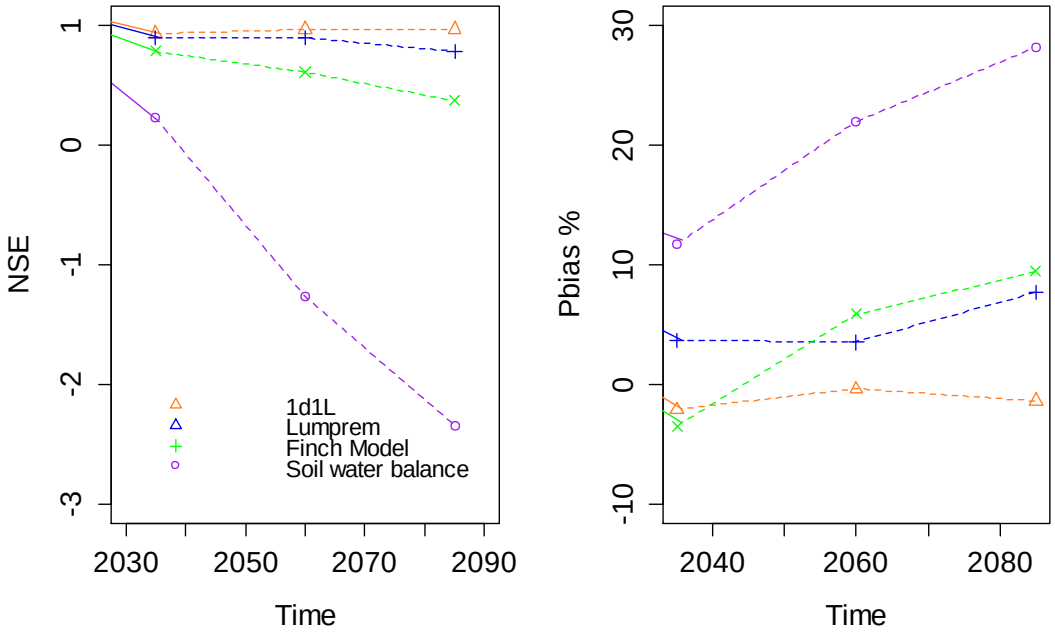

Figure 3. 8: Variations of NSE-Coefficient and PBIAS for different groundwater recharge models. ETHZ_HadCM3Q0_CLM climate model chain is used for the periods 2035, 2060 and 2085.

Monthly residuals between reference 2D model and simplified models indicate that a underestimation of reference recharge occur in the summer and spring whereas an small overestimation can be observed during winter and autumn (Figure 3.9). This seasonal trend in over- and underestimation is stable over each time period for each simplified model. An underestimation of the reference recharge during the summer indicate that the effect of rapid infiltration (preferential recharge) due to commonly strong summer precipitation events of the reference model cannot be simulated by the simplified models. In contrast, the overestimation during the winter shows that the simplified models simulate more recharge than the reference model. This indicate that the model parameters from the simplified models try to compensate the misfit during the summer in the calibration process. Thus this compensation leads to model parameter sets which maintain to higher recharge in the winter period. Still satisfactory results can be archived for annual recharge but the error between reference and simplified recharge on seasonal distribution are larger.

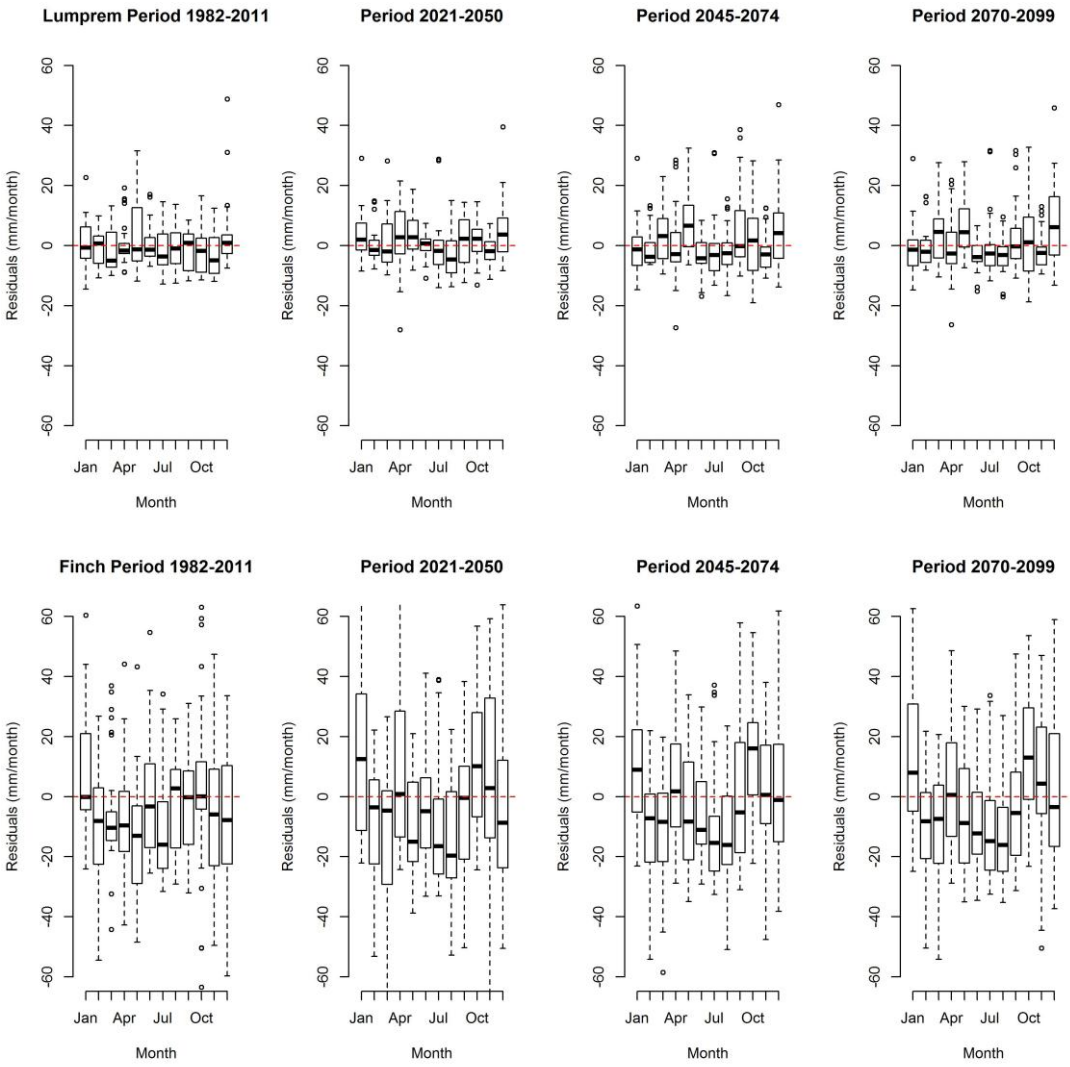

Figure 3. 9: Residuals between simulated monthly Recharge from the reference 2D model and the Lumprem (upper panel) as well as the Finch Model (lower panel) for the four simulated time slices.

3.8.4 Calibration of extreme years

To evaluate if simpler models show less predictive model bias if more extreme conditions are included in the calibration, three calibration periods, year 2010 (normal year), years 2002/2003 (wet/dry year) and time series (year 2004-2009) are chosen.

In figure 3.9, a comparison between the archived MSR under the calibration periods are shown. Under the calibration period 2002/2003 an improvement of the Finch model, especially for the outliers can be observed. This is especially caused by a better fit of the extreme years, such as 2003. The model parameter set estimated under the calibration period 2002/2003 still does not fit perfectly the reference recharge but simulate at least similar patterns for the extreme years (figure A3.7, supporting information). Consequently predictive bias for actual recharge as well as

under future time periods is smaller. Only small changes for the 1d1l and Lumprem model can be observed whereas the SWB model with the inflexible model structure shows no change. Similar improvements can be found when the calibration period 2004-2009 is used. A longer time series in the calibration period increase the model performance for all models, only the SWB model shows no improvement. The difference between the calibration period 2002/2003 and 2004-2009 is marginal, but a bit better under period 2004-2009. To note is however, that the calibration process with the time series 2004-2009 was almost three times longer than under the calibration period 2002/2003.

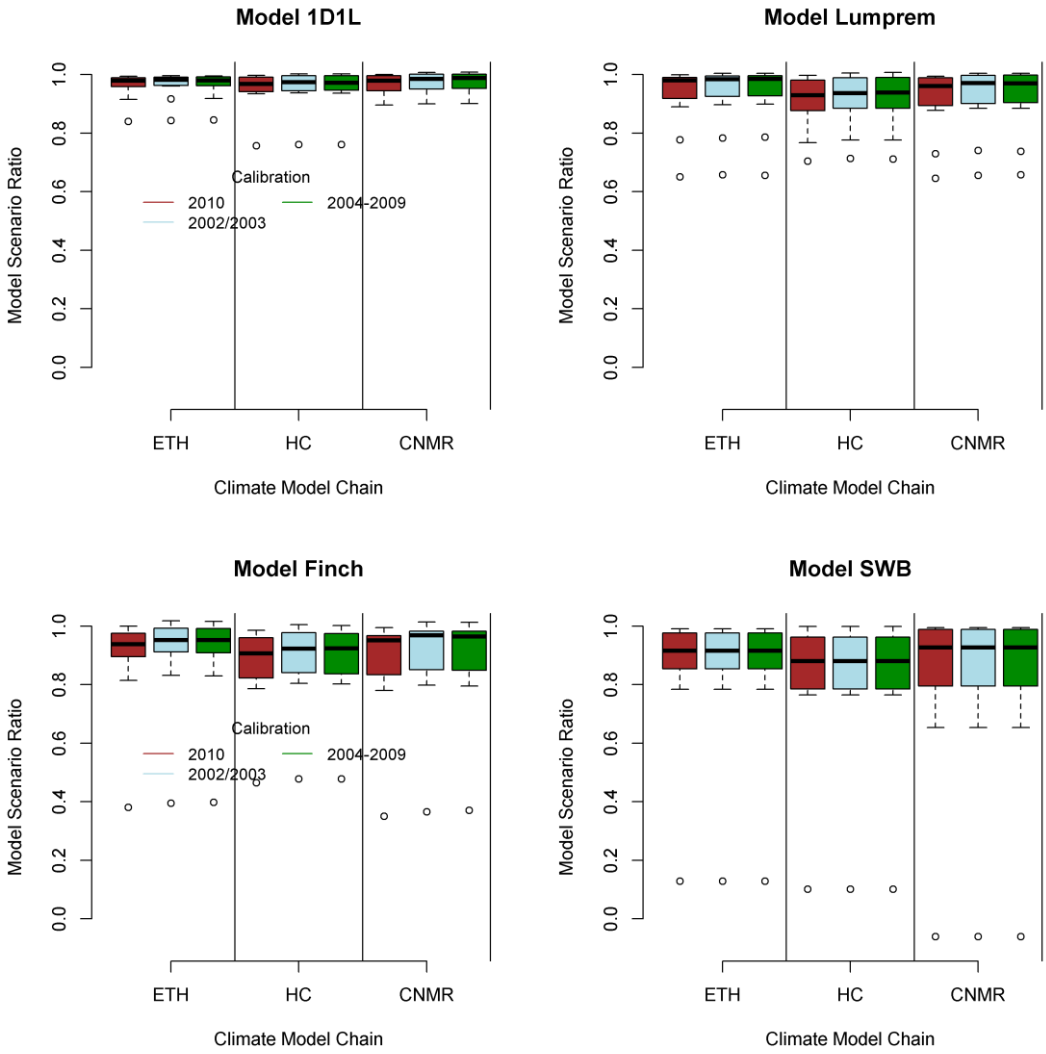

Figure 3. 10: Comparison between the archived MSR for each simplified model under the calibration period 2010 (brown color), 2002/2003 (light-blue color) and 2004-2009(green color) are shown for three model chains.

Calculation of the MSR (mean), NSE and PBIAS values under the calibration period 2002/2003 and 2010 indicate an improvement for the Finch model by using the year 2002/2003 in the calibration (Table 3.3). For instance, for the CNMR the NSE increases from 0.49 to 0.71 and PBIAS change from an overestimation of 7.88% to an underestimation of -3.83%. A strong improvement cannot be observed for 1d1l

model. Only under the climate model chain CNMR a change in PBIAS can be observed. This may be explained by the delta change values for this climate model chain. This model chain shows the longest and strongest decrease for precipitation from summer until autumn. Using the delta change values from this model chain on the past climatic conditions intensified existing extreme periods such as the drought summer period 2003. However, the recharge behavior can still be represented by model parameter sets obtained under the calibration period 2002/2003, whereas the calibration under period 2010 failed to a certain amount in reproducing realistic recharge rates. However, for the climate model chains ETH and HC no improvement due to different calibration periods is simulated. Results of NSE and PBIAS for the Lumprem model do not give a clear trend in model improvement. NSE and PBIAS indicate an improvement for the ETH climate model chain, whereas for the actual climate condition a small decrease is observed. In addition, a decrease in NSE but an increase in PBIAS for the Lumprem model performance under the climate model chain CNMR can be observed. That is probably due the different sensitivity of the model scenario equations on simulated and observed recharge behavior. For instance, the NSE is very sensitive to high recharge rates, whereas the applied equation performs better during smaller recharge rates. Similar results are found in a comparison of different efficiency criteria for hydrological model assessment study for peak and flow conditions (Krause et al., 2005). That indicates clearly that decisions should not be based only on one model performance criteria; rather a comparison of different impact calculations should be involved. Results are not improved for the SWB model due the simple and not flexible model structure of only 1 soil parameter.

Table 3. 3: Variation of NSE-Coefficient and PBIAS to different groundwater recharge models and climate model chains for calibration period 2010, 2002/2003 and 2004-2009.

Scenario		Period 2035					
		1d1l calibrationperiod			Lumprem calibrationperiod		
		2010	2002 /03	2004-2009	2010	2002 /03	2004-2009
ETH	MSR (mean)	0.96	0.97	0.97	0.93	0.94	0.94
HC		0.95	0.97	0.98	0.91	0.93	0.95
CNMR		0.95	0.96	0.96	0.92	0.93	0.93
Past	NSE	0.99	0.99	0.99	0.97	0.96	0.97
ETH		0.93	0.9	0.92	0.9	0.91	0.93
HC		0.92	0.91	0.92	0.88	0.86	0.88
CNMR		0.89	0.84	0.86	0.86	0.75	0.91
Past	PBIAS	-2.3	-2.26	-2.28	1.03	-2.84	-1.05
ETH		-2.12	-2.31	-2.26	3.62	0.08	0.05
HC		-0.89	-0.89	-0.85	3.1	-0.47	-0.35
CNMR		-1.87	0.01	-0.05	3.18	1.41	1.39
		Finch calibrationperiod			SWB calibrationperiod		
		2010	2002 /03	2004-2009	2010	2002 /03	2004-2009
ETH	MSR (mean)	0.89	0.91	0.92	0.85	0.85	0.85
HC		0.87	0.89	0.92	0.82	0.82	0.82
CNMR		0.87	0.89	0.91	0.84	0.84	0.84
Past	NSE	0.87	0.91	0.92	0.87	0.87	0.87
ETH		0.6	0.79	0.82	0.23	0.23	0.23
HC		0.61	0.78	0.79	0.35	0.35	0.35
CNMR		0.49	0.71	0.84	0.35	0.35	0.35
Past	PBIAS	-7.52	4.22	3.59	7.21	7.21	7.21
ETH		6.71	-3.5	-3.6	11.75	11.75	11.75
HC		6.64	-3.74	-3.64	12.35	12.35	12.35
CNMR		7.88	-3.83	-3.56	9.99	9.99	9.99

3.9 Summary and Conclusions

In this numerical experiment a heterogeneous 2D reference model was used to simulate past and future groundwater recharge rates based on future climatic forcing functions. Simpler models were calibrated against reference outputs and predictions of both, reference and simpler models were compared to evaluate the effect of model simplification for CC impact studies.

The most important conclusions are listed below:

All groundwater recharge models performance well for years with normal temperature ranges and precipitation amounts. However, considering small time steps the correct recharge pattern over the complete year cannot be simulated for the soil water balance models. This highlights the structural difference between the physical reference model and the soil water balance models. Only weekly or monthly input data of precipitation were useful to obtain a good model fit.

Simulations of 30 years for the past recharge and under future climate conditions using the calibrated model parameter sets for each model create a model bias, which is smaller compared to the uncertainty originated from variability among the 10 different climate model chains.

Increasing simplification of the models tend to clearly underestimate mean and minimum change in recharge compared to the reference 2D model. Predicted groundwater recharge changes depend strongly on the degree of model simplification.

Even though differences in the range (min, max and mean) in simulated groundwater recharge exist between the different recharge models, the trend for each climate model chain is similar. For climate model chains with the largest change, increase or decrease is similar for all simplified models in groundwater recharge rates. Also a persistent order between all simplified models for each climate model chain can be observed.

Analysis based on MSR, NSE-Coefficient and PBIAS show similar trends. MSR values are generally not smaller than 0.8, which shows that model simplification is not the controlling factor for recharge differences under future climatic forcing functions. Recharge changes for future periods are mainly a function of the scenario only. However, weather condition with hot dry years and distinct different precipitation amounts lead to model bias and outliers in the model scenario indexes are observed. Simple models such as SWB and Finch give reliable results for years with “normal” temperature and precipitation distribution but for extremes such as observed in the year 2003 and 2011 with additionally delta change values they failed to reproduce the reference recharge rates. This is important due to the fact that these extremes are probably more frequent in future.

Analyzing monthly residuals between reference 2D model and simplified models indicate that a underestimation of reference recharge occur in the summer and spring months whereas an small overestimation can be observed during the winter period.

The missing capability of the simplified models to simulate in a sufficient way rapid infiltration (preferential recharge) of the reference model leads to an underestimation during the summer. Due to this structural deficit of the simplified model some model parameters have a compensatory role during the calibration process to achieve satisfactory results but leads to an small overestimation during the winter period.
The aforementioned effects of extreme years on recharge and seasonal misfits can be reduced by including extreme years or a longer times series in the calibration process. The model bias can be reduced, especially for soil water balance models whereas the 1d and Lumprem model does not show a strong improvement.
The 1D physically based model reproduce best the reference recharge, followed by semi-mechanistic Lumprem model, with only small differences between reference and simulated recharge from the simpler models. However, this conclusion is based on the assumption that the physical reference model reflect the best approximation of real recharge processes for past and future conditions. Under this assumption the soil water balance models perform different compared to physical based and lumped model. This is quite important because many large scale impact studies use different kinds of soil water balance model approaches to simulate future recharge rates under CC. Thus CC impact results from these studies need to be interpreted with caution.
In addition, it should be mentioned that our 3 applied model scenario equations are slightly divergent in the results. That is due to the fact that criteria can emphasize on different types of simulated-observed behaviour with different sensitivity. Therefore, we recommend that conclusions should not be based only on one single equation to evaluate uncertainty originated from model simplification and from variability among different climate model chains. Instead comparison of different impact calculations should be involved. Limitations in this study are the assumption of a constant vegetation cover and soil structure. Increasing temperature in the future will certainly change growing periods of plants. Also, it is very likely that soils can dry out over some future periods and macropores are created due to the soil water deficit. These effects could additionally influence predictions of recharge.

3.10 Reference:

Allen, D. M., D. C. Mackie (2004). "Groundwater and climate change: a sensitivity analysis for the Grand Forks aquifer, southern British Columbia, Canada." Hydrogeology Journal 12(3): 270-290.

Bakker, M., Bartholomeus, R. P., Ferré, T. P. A., Leterme, B., Mallants, D., Jacques, D., and Nimmo, J. R. (2013). Groundwater recharge: processes and quantification. Hydrol. Earth Syst. Sci, 17, 2653-2655.

Bennett, N. D., Croke, B. F., Guariso, G., Guillaume, J. H., Hamilton, S. H., Jakeman, A. J., ... & Andreassian, V. (2013). Characterising performance of environmental models. Environmental Modelling & Software, 40, 1-20.

Bosshard, T., Kotlarski, S., Ewen, T., Schaer, C., (2011). Spectral representation of the annual cycle in the climate change signal. Hydrol. Earth Syst. Sci., 15(9): 2777-2788.

Carrera-Hernandez, J.J., Mendoza, C.A., Devito, K.J., Petrone, R.M., Smerdon, B.D., (2011). Effects of aspen harvesting on groundwater recharge and water table dynamics in a subhumid climate. Water Resour. Res., 47.

Carsel, R.F., Parrish, R.S., (1988). Developing Joint Probability-Distributions of Soil-Water Reteion Characteristics. Water Resour. Res., 24(5): 755-769.

Cooley, R.L., Christensen, S., (2006). Bias and uncertainty in regression-calibrated models of groundwater flow in heterogeneous media. Advances in Water Resources, 29(5): 639-656.

Cuthbert, M.O., Tindimugaya, C., (2010). The importance of preferential flow in controlling groundwater recharge in tropical Africa and implications for modelling the impact of climate change on groundwater resources. Journal of Water and Climate Change, 1(4): 234-245.

Döll, P., & Fiedler, K. (2007). Global-scale modeling of groundwater recharge. Hydrology & Earth System Sciences Discussions, 4(6).

Döll, P., Berkhoff, K., Bormann, H., Fohrer, N., Gerten, D., Hagemann, S., & Krol, M. (2008). Advances and visions in large-scale hydrological modelling: findings from the 11th Workshop on Large-Scale Hydrological Modelling. Advances in Geosciences, 18, 51-61.

Döll, P. (2009). Vulnerability to the impact of climate change on renewable groundwater resources: a global-scale assessment. Environmental Research Letters, 4(3), 035006.

Doherty, J., Christensen, S., (2011). Use of paired simple and complex models to reduce predictive bias and quantify uncertainty. Water Resour. Res., 47.

Doherty, J., Welter, D., 2010. A short exploration of structural noise. Water Resour. Res., 46(5): W05525.

Doherty, J. 2010. PEST- Model-Independent Parameter Estimation.Watermark Numerical Computing.peshomepage.org.

Doherty, J.E., Fienen, M.N., and Hunt, R.J.: Approaches to highly parameterized inversion: Pilot-point theory, guidelines, and research directions: U.S. Geological Survey Scientific Investigations Report 2010–5168, 36 p., 2010

Droogers, P., Van Loon, A., Immerzeel, W.W., (2008). Quantifying the impact of model inaccuracy in climate change impact assessment studies using an agro-hydrological model. Hydrol. Earth Syst. Sci., 12(2): 669-678.

Finch, (1998). Estimating direct groundwater recharge using a simple water balance model – sensitivity to land surface parameters.

Green, T.R. et al., 2011. Beneath the surface of global change: Impacts of climate change on groundwater. Journal of Hydrology, 405(3-4): 532-560.

Gupta, H. V., S. Sorooshian, and P. O. Yapo. (1999). Status of automatic calibration for hydrologic models: Comparison with multilevel expert calibration. J. Hydrol. Eng. 4(2): 135-143.

Holman, I.P., (2006). Climate change impacts on groundwater recharge-uncertainty, shortcomings, and the way forward? Hydrogeology Journal, 14(5): 637-647.

Holman, I.P., Allen, D.M., Cuthbert, M.O., Goderniaux, P., (2012). Towards best practice for assessing the impacts of climate change on groundwater. Hydrogeology Journal, 20(1): 1-4.

Intergovernmental Panel on Climate Change (IPCC) (2008), Climate change and water, edited by B.C. Bates et al., Tech. paper of the IPCC, pp. 210, IPCC Secretariat, Geneva.

Jackson, C.R., Meister, R., Prudhomme, C., (2011). Modelling the effects of climate change and its uncertainty on UK Chalk groundwater resources from an ensemble of global climate model projections. Journal of Hydrology, 399(1-2): 12-28.

Jiang, T., Chen, Y. D., Xu, C. Y., Chen, X., Chen, X., & Singh, V. P. (2007). Comparison of hydrological impacts of climate change simulated by six hydrological models in the Dongjiang Basin, South China. Journal of Hydrology, 336(3–4): 316-333.

Jones, R.N., Chiew, F.H.S., Boughton, W.C., Zhang, L., (2006). Estimating the sensitivity of mean annual runoff to climate change using selected hydrological models. Advances in Water Resources, 29(10): 1419-1429.

Krause, P., Boyle, D. P., and Bäse, F. (2005): Comparison of different efficiency criteria for hydrological model assessment, Adv. Geosci., 5, 89-97, doi:10.5194/adgeo-5-89-2005.

Kristensen, K.J. and S.E. Jensen. (1975). A model for estimating actual evapotranspiration from potential evapotranspiration. Nordic Hydrol., 6:170-88.

Nash, J. E. and J. V. Sutcliffe (1970), River flow forecasting through conceptual models part I -A discussion of principles, Journal of Hydrology, 10 (3), 282-290

Prasuhn V., Spiess E. und Seyfarth M. (2009): Die neue Lysimeteranlage Zürich-Reckenholz. In: Perspektiven in Forschung und Anwendung. Bericht über die

13. GumpensteinerLysimetertagung, Irdning, 21.-22.4.09. LFZ Raumberg-Gumpenstein, Irdning, 11-16

Refsgaard, J. C., Christensen, S., Sonnenborg, T. O., Seifert, D., Højberg, A. L., & Troldborg, L (2012). Review of strategies for handling geological uncertainty in groundwater flow and transport modeling. Advances in Water Resources, 36(0): 36-50.

Richter, W. &Lillich, W. (1975): Abriß der Hydrogeologie.- Schweizerbarth Verlag, Stuttgart.

Rojas, R., Feyen, L., Dassargues, A., (2009). Sensitivity analysis of prior model probabilities and the value of prior knowledge in the assessment of conceptual model uncertainty in groundwater modelling. Hydrol. Process., 23(8): 1131-1146.

Schär, C. and G. Jendritzky (2004). "Climate change: Hot news from summer 2003." Nature 432(7017): 559-560.

Scibek, J., Allen, D.M., (2006a). Comparing modelled responses of two high-permeability, unconfined aquifers to predicted climate change. Global and Planetary Change, 50(1-2): 50-62.

Scibek, J., Allen, D.M., (2006b). Modeled impacts of predicted climate change on recharge and groundwater levels. Water Resour. Res., 42(11).

Scibek, J., Allen, D.M., Cannon, A.J., Whitfield, P.H., (2007). Groundwater-surface water interaction under scenarios of climate change using a high-resolution transient groundwater model. Journal of Hydrology, 333(2-4): 165-181.

Seneviratne, S. I., Lehner, I., Gurtz, J., Teuling, A. J., Lang, H., Moser, U., .and Zappa, M. (2012). Swiss prealpine Rietholzbach research catchment and lysimeter: 32 year time series and 2003 drought event. Water Resour. Res., 48.

Sonnenborg, T.O., Hinsby, K., van Roosmalen, L., Stisen, S., (2012). Assessment of climate change impacts on the quantity and quality of a coastal catchment using a coupled groundwater-surface water model. Climatic Change, 113(3-4): 1025-1048.

Stoll, S., Franssen, H.J.H., Butts, M., Kinzelbach, W., (2011). Analysis of the impact of climate change on groundwater related hydrological fluxes: a multi-model approach including different downscaling methods. Hydrol. Earth Syst. Sci., 15(1): 21-38.

Sulis M., C. Paniconi, M. Marrocu, D. Huard, D. Chaumont (2012). Hydrologic response to multimodel climate output using a physically based model of groundwater/surface water interactions, Water Resour. Res., 48, W12510, doi:10.1029/2012WR012304.

Taylor, R.G., Koussis, A.D., Tindimugaya, C., (2009). Groundwater and climate in Africa—a review. Hydrological Sciences Journal, 54(4): 655-664.

Taylor, R. G., Scanlon, B., Döll, P., Rodell, M., Van Beek, R., Wada, Y., ... & Treidel, H. (2013). Ground water and climate change. Nature Clim. Change, 3(4): 322-329.

Therrien, R. McLaren, R.G., Sudicky, E.A. (2007): HydroGeoSphre-a three dimensional numerical model describing fully integrated subsurface and surface flow and solute transport, Groundwater Simulations Group, University of Waterloo.

van Roosmalen, L., Sonnenborg, T.O., Jensen, K.H., (2009). Impact of climate and land use change on the hydrology of a large-scale agricultural catchment. Water Resour. Res., 45.

van Roosmalen, L., Sonnenborg, T.O., Jensen, K.H., Christensen, J.H., (2011). Comparison of Hydrological Simulations of Climate Change Using Perturbation of Observations and Distribution-Based Scaling. Vadose Zone Journal, 10(1): 136-150.

Velázquez, J. A., Schmid, J., Ricard, S., Muerth, M. J., Gauvin St-Denis, B., Minville, M., Chaumont, D., Caya, D., Ludwig, R., and Turcotte, R. (2013): An ensemble approach to assess hydrological models' contribution to uncertainties in the analysis of climate change impact on water resources, Hydrol. Earth Syst. Sci., 17, 565-578, doi:10.5194/hess-17-565-2013.

Woldeamlak, S.T., Batelaan, O., De Smedt, F., (2007). Effects of climate change on the groundwater system in the Grote-Nete catchment, Belgium. Hydrogeology Journal, 15(5): 891-901.

Yusoff, I., Hiscock, K.M., Conway, D., (2002). Simulation of the impacts of climate change on groundwater resources in eastern England. Geological Society, London Special Publications 193 (1), 325–344.

3.9 Supporting information

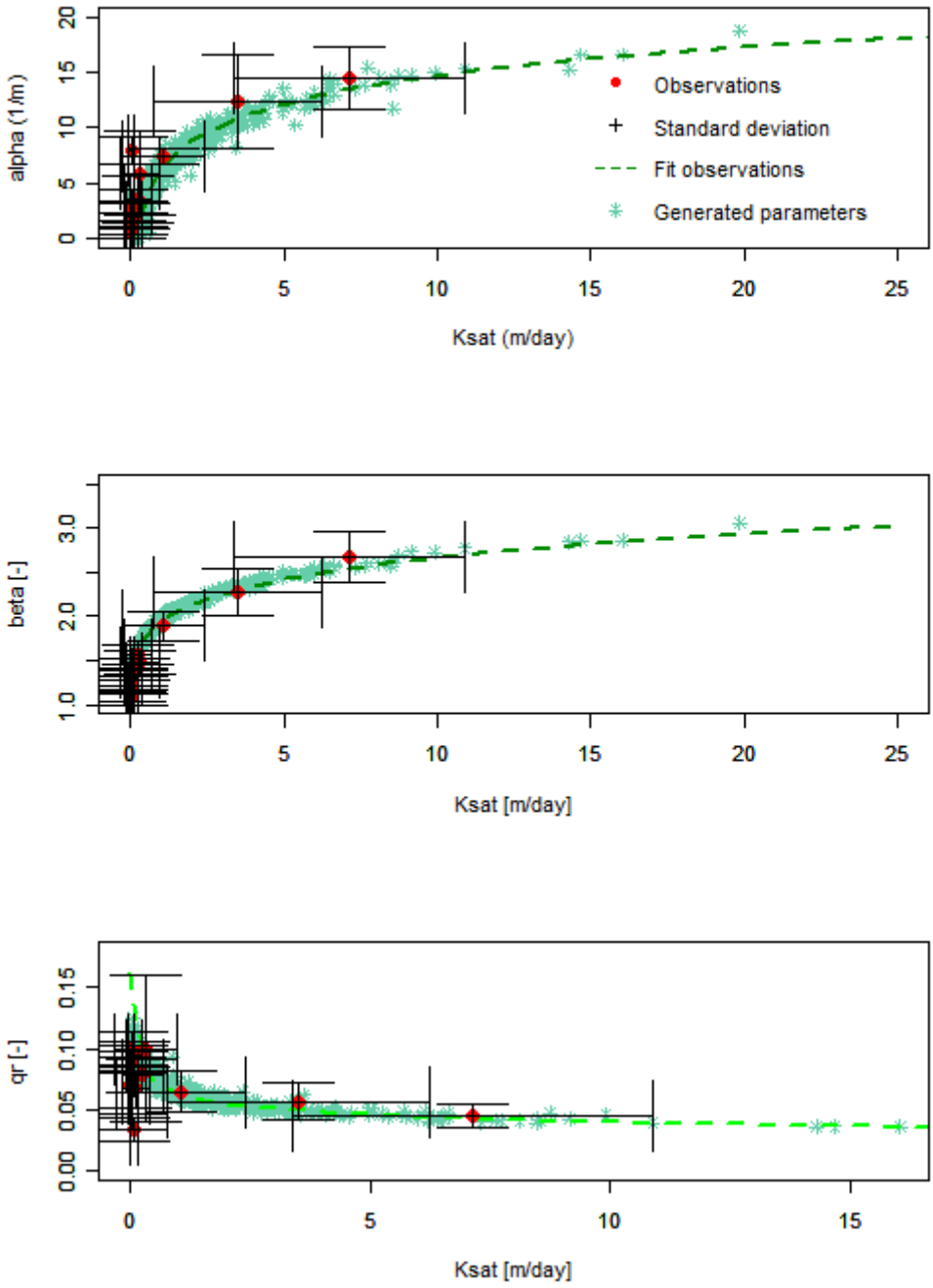

Figure A3. 5: Relationship of the van Genuchten parameters alpha, beta and residual water content (qr) with saturated hydraulic conductivity (K_{sat}).

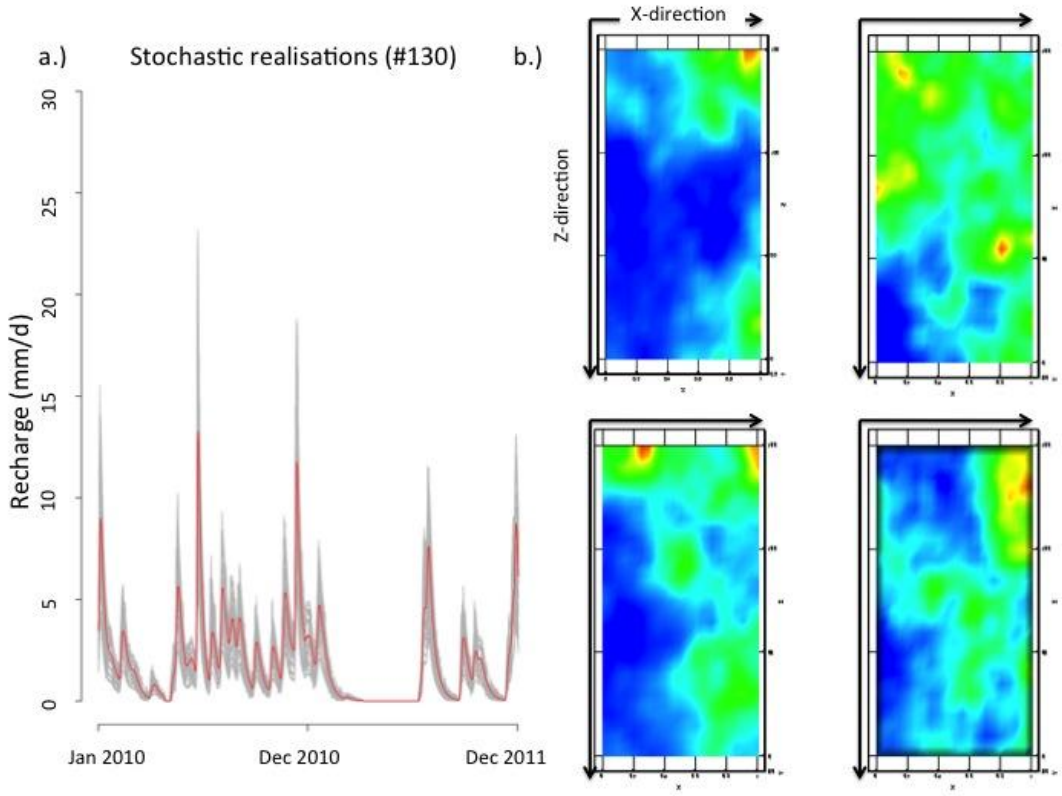

Figure A3. 6: a.) Daily recharge pattern (mm/day) for year 2010 and 2011 for 130 stochastic hydraulic parameter fields used in the references 2D field. The red line shows the mean recharge from all 130 simulations whereas the gray lines display the variations b.) Four hydraulic conductivity fields from the 130 stochastic realizations.

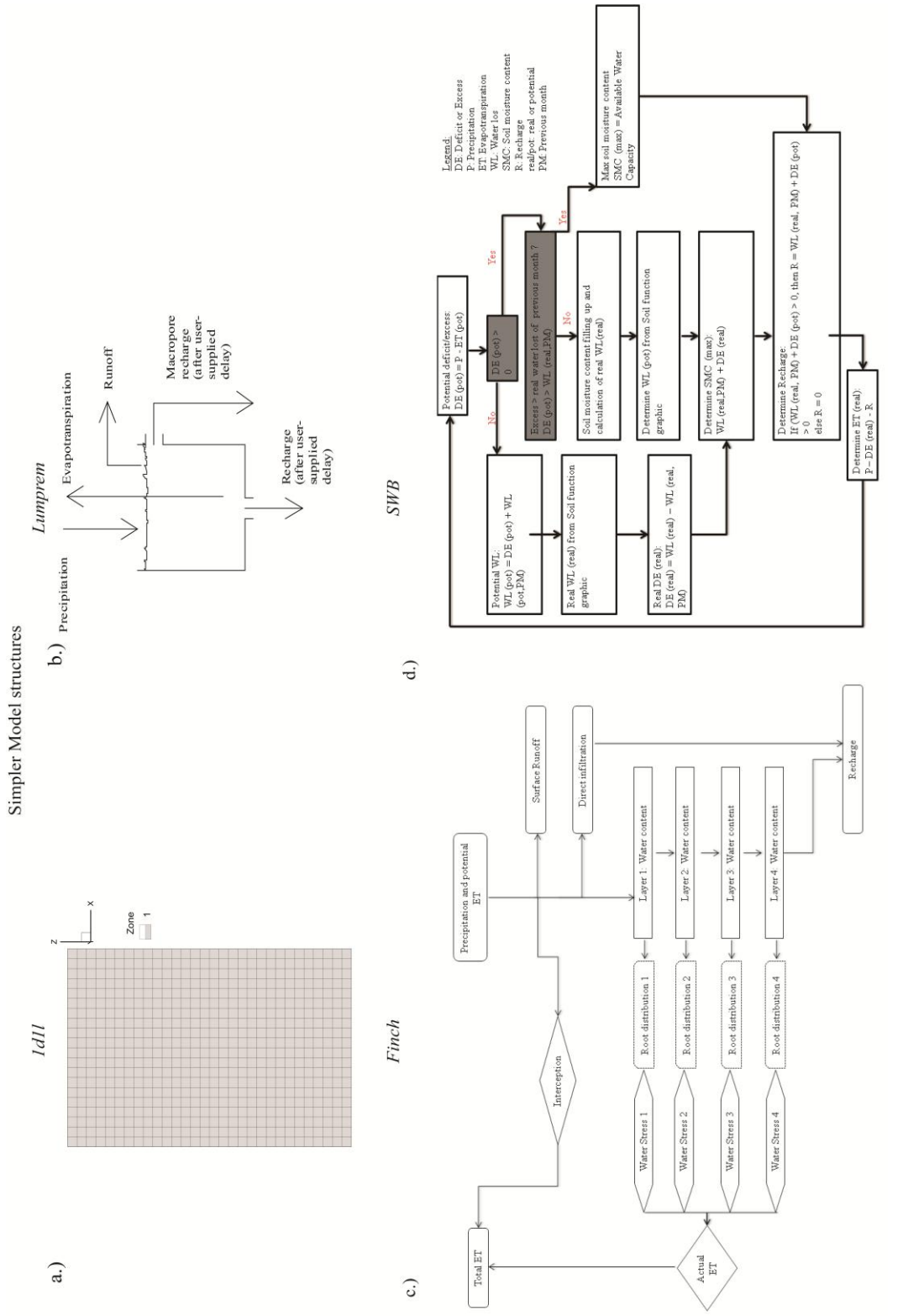

Figure A3. 7: Structure of simplified models for a.) 1D homogeneous soil structure with 1layer (1d1l), b.) Semi-mechanistic model (Lumprem), c.) Soil water balance model with 4 layers and root distribution (Finch) and d.) Simple 1 soil column model without runoff, interception or direct recharge (SWB).

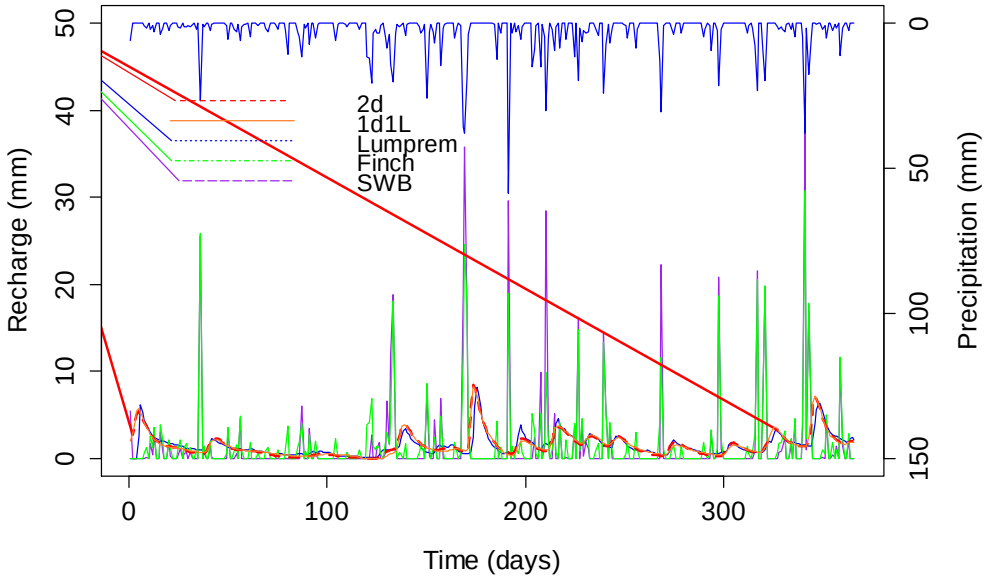

Figure A3. 8: Daily recharge pattern for all applied recharge models for the year 2010.

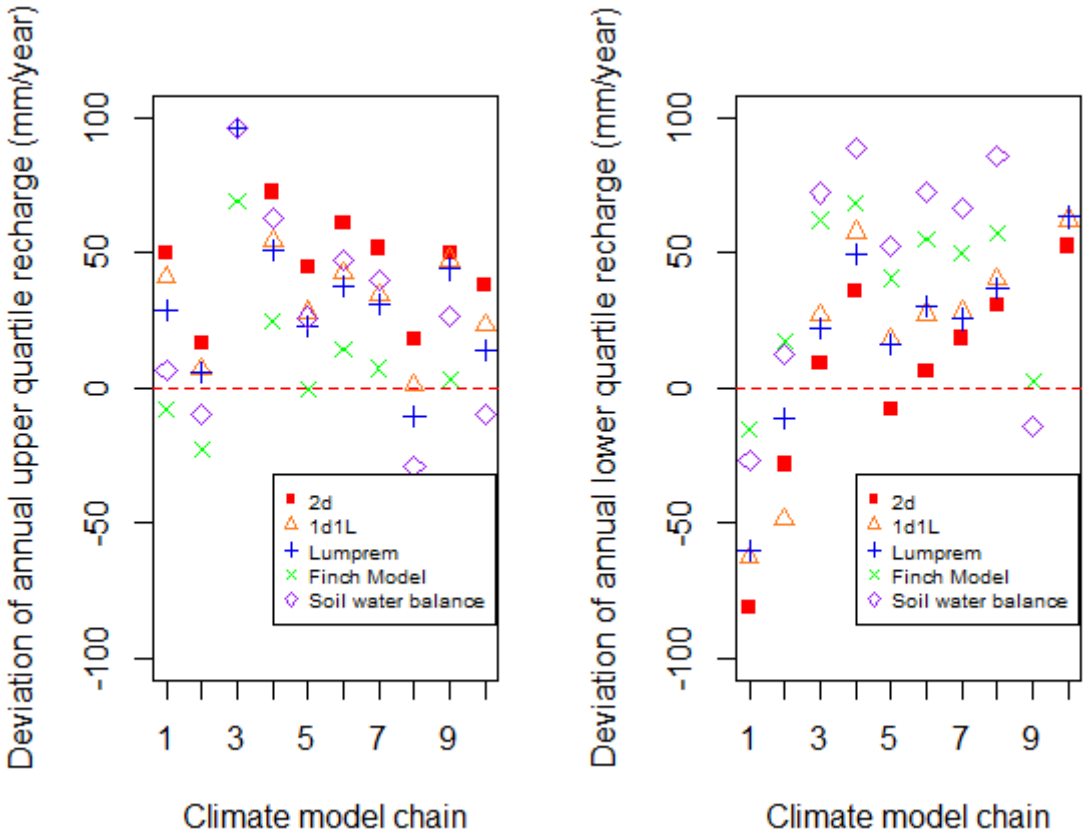

Figure A3. 5: Deviations between upper (left panel) and lower (right panel) annual recharge from the baseline (past mean recharge 30 years) and for the period 2035 for 10 model chains.

Table A3. 1: Calibrated model parameter for each recharge model with initial and lower as well as upper bound values for each calibrated model parameter.

Model	Parameter	Initial value	lower bound	upper bound
1d1l	Ksat	1	0.01	20
	Porosity	0.4	0.3	0.6
	vanGenuchten alpha	5	2	16
	vanGenuchten beta	1.8	1.01	2.6
	Qr	0.04	0.01	0.069
	Wilting point	0.01	0.01	0.09
	Field capacity	0.204	0.091	0.29
	Oxic limit	0.495	0.3	0.65
	Anoxic limit	1	0.66	1
	Root depth	1	0.01	1.5
	Evaporation depth	1	0.01	1.5
	LAI	1	0.01	5
Finch	Field capacity	0.26	0.25	0.32
	Wilting point	0.1	0.01	0.24
	Water saturation	0.34	0.05	0.4
	Bypass flow	15	0.00001	20
	Bypass portian	0.02	0.00001	0.5
	Steam portion	0.017	0.00001	0.06
	Steam strorage	0.016	0.005	0.05
	Canopy	1.1	0.5	1.5
	Canopy Fraction	0.5	0.2	1
	Canopy capacity	1.1	0.5	1.5
	Root portion	2	1	5
	Root depth	2	0.00001	3
Lumprem	Crop factor1	0.25	0.01	5
	Crop factor2	0.25	0.01	5
	Gamma1	2	0.01	10
	Gamma2	2	0.01	10
	Ksat	0.01	0.01	1
	vanGenuchten m	0.2	0.01	2
	Matrix flow	0.2	0.01	1
	Macropore delay	2	0.01	10
	Matrix delay	0.4	0.01	10
SWB	Soil storage	75	50	250

Table A3. 2: Climate change scenarios with associated GCMs and RCMs.

Institution	GCM		RCM	UsedAcronym
SMHI	BCM		RCA	SMHI_B
ETHZ	HadCM3	standardsensitvity (HadCM3Q0)	CCLM	ETH
HC		standardsensitvity (HadCM3Q0)	HadRM3Q0	HC
SMHI		lowsensitivity (HadCM3Q3)	RCA	SMHI_Had
MPI	ECHAM5		REMO	MPI
DMI			HIRHAM	DMI
KNMI			RACMO	KNMI
SMHI			RCA	SMHI_ECH
ICTP			REGCM3	ICTP
CNRM	ARPEGE		ALADIN	CNRM

Chapter 4

4. Evaluating the effect of climate change on groundwater recharge under different crops[ii]

4.1 Abstract

Numerous studies have already been conducted to investigate the effect of climate change (CC) on recharge rates. The conclusions drawn based on obtained results from most studies are limited in their explanatory power. Most studies have difficulties to reproduce the detailed effects of different crops on recharge rates due to the simulated large scale of the catchment and associated simplification in the model. In addition, studies often deal with sparse soil observations and data describing crops and growths, such as temporal leaf area indexes. Consequently, prediction for different soil types and vegetation are highly uncertain.

This paper attempts to systematically explore the combined effect of CC and changes in land use on groundwater recharge. We address these questions by combining numerical modeling techniques with a significant amount of high quality lysimeter data. These data comprised information on the effect of land use, crops and soils on recharge rates. Results based on 1D numerical model simulations indicate that for most crops a decreasing trend in recharge occurs (between -5 to -60%) during their specific vegetation period. However, for catch crops such as Phacelia and Temporary grassland an increasing trend can be observed. Using these crops in a crop sequence buffer the decreasing trend in future recharge rates, but the amplitude depends strongly on the growing season where catch crops are used. Therefore, using actual crop sequences from the lysimeter facility representative for most agriculture areas in Switzerland indicates only a decrease in recharge of 7 to 11%.

Crop parameters such as leaf area index (LAI) and root depth (RD) a controlling strongly the recharge rates but they will probably change in future due to increasing water stress. Therefore, an analysis of the sensitivity of LAI and RD on future recharge rates was carried out. It was found that simulated recharge is inversely related to LAI and RD, where recharge is more sensitive to a decrease in LAI than to RD. Therefore, final recharge estimates under original literature LAI and RD values probably represent an upper boundary on recharge rate changes for the future. In addition, all simulations indicate a high predictive uncertainty in recharge due to

[ii] Christian Moeck (1), Volker Prasuhn (2), Philip Brunner (1), Daniel Hunkeler (1)

[1]Centre d'Hydrogéologie et de Géothermie (CHYN), University of Neuchâtel, Neuchâtel, Switzerland

[2]Agroscope Reckenholz-Tänikon ART, Zurich, Switzerland

variability originated among general circulation model (GCM) and regional climate model (RCM) combinations and stochastic realisations of the future climatic conditions. We can conclude that crops can have an effects on recharge rates similar as changes due to CC.

4.2 Introduction

The spatial and temporal distribution of groundwater recharge is controlled by soil type, vegetation and meteorological conditions. Predicted changes in meteorological conditions due to CC will alter future groundwater recharge rates and thus influence the water balance (Goderniaux et al., 2009, Scibek, 2006, 2007, Scibek and Allen, 2006, Serrat-Capdevila et al., 2007, Stoll et al., 2011, Woldeamlak et al., 2007). However, it is unlikely to assume that societal, political and economic conditions will remain unchanged into future, and that CC alone is the driving force for changes in recharge rates (Holman et al., 2012). In this context of CC and the other mentioned multiple forces, changes in land use can occur, which directly also impact the water balance (Eitzinger et al., 2003, Holman, 2006, Holman et al., 2012, Scanlon et al., 2005, Scanlon et al., 2007).

Numerous studies have already been conducted to investigate the effect of CC on recharge rates. For instance, a significant decrease in groundwater levels and in surface water flow rates by the end of the century has been predicted by Godernniaux et al. (2009) using numerical simulations for a catchment in Belgium. These simulations contained four land use types to cover the model domain. The land use was not varied for the simulated time period. Stoll et al. (2011), used a hydrological model with two fixed defined land use types where land use model parameters were specified according to literature values. They found a small increase in recharge for a pre-alpine region in northern Switzerland. In the study of van Roosmalen (2009), land use was taken into account by using six different land use types based on literature values. Increasing recharge in Denmark was predicted due to the increase in winter precipitation.

The conclusions drawn based on obtained results from most studies are limited in their explanatory power when different crop types controls recharge rates and pattern. It is of course challenging in large scale studies to represent small scale processes such as the detail description of crop parameters and growth. Therefore, model simplification has to be included. In addition, often these catchment CC impact studies deal with sparse soil observations and data describing crops. Consequently, prediction for different soil types and vegetation are highly uncertain (Eckhardt et al., 2003).

To prevent neglecting local effects and still have reasonable computation times, high quality lysimeter data could be used. Lysimeters are frequently used in several inverse modeling studies solving the Richards equation (Mertens et al., 2009, Mertens et al., 2006, Stumpp and Hendry, 2012, Stumpp and Maloszewski, 2010, Stumpp et al., 2012, Stumpp et al., 2009, Vrugt et al., 2003, Vrugt et al., 2001a, Vrugt et al., 2001b, Wohling and Vrugt, 2011). Fully aware that only local processes

are described and upscaling to the catchment is still challenging (Vereecken et al., 2010, Zhao et al., 2013), some studies indicate that lysimeter measurements are representative for larger regions (Seneviratne et al., 2012).
Only a limited number of studies in both catchment and local scale focuses on the combined effect of future climatic conditions and land use for groundwater recharge rates. The vegetation parameters are typically held constant and land use changes are seldom taken into account. This indicates that a systematic analysis of CC under different crops is still missing, although knowledge of the extent of recharge changes induced by CC under different crops might crucial for a sustainable water management.
This paper attempts to explore the combined effect of CC and changes in land use on groundwater recharge. More specifically, this study aims at addressing the following research questions:

- What is the combined influence of different soil types, different crops and CC for future groundwater recharge rates?
- Will and how CC affect the recharge rates and temporal patterns?
- Which land use strategy is most efficient to buffer changes in recharge rates originated from the CC signal?
- How large is the corresponding uncertainty originating from the variability among the different climate model chains for groundwater recharge rates compared to changes in interannual variability expressed in a stochastic modelling framework?

We address these questions by numerical modeling techniques based on a significant amount of high quality lysimeter data. These data comprised information on the effect of land use, crops and soils on recharge rates. Precise observations of seepage water, soil moisture and actual evapotranspiration (ET_a) were used in the calibration process. The use of all observations in a simulated coupled flow process enables us to validate the correctness of all components of the water balance.
In this framework five 1D homogenous numerical soil models were created to simulate past and future recharge for five crop sequences. In this crop sequences the three dominant soil types of Switzerland are represented. Changes in future recharge rates are simulated for each crop type in the crop sequences for the three soils considered. All simulations of future recharge rates were carried out by combining the use of delta change values from different GCM-RCM combinations with a stochastic weather generator. This stochastic approach enables to simulate climatic variability more realistically compared to the simple delta change downscaling approach (Goderniaux et al., 2011). In addition, uncertainty linked to the chosen climate model chains and natural variability in the climatic forcing functions can be determined. The possible range of variation for projected recharge has been evaluated using seven different GCM-RCM combinations and 10 stochastic realisations to represent natural variability of the climatic conditions.

Results of relative changes in daily recharge rates for the lysimeter with the associated crops and soils until 2085 are simulated. This time period was chosen based on the temporal data availability of GCM-RCMs. A temporal analysis of recharge was carried out to identify the effect of different growing seasons and crop parameters under future weather conditions. In addition to changes in recharge rates induced only by CC, a sensitivity analyses for the crop model parameters root depth (RD) and leaf area index (LAI) was carried out. This sensitivity analysis is based on the fact that water stress will likely become more frequent and can affect the crop parameters. As transpiration can decrease significantly under dry conditions (Eitzinger et al., 2003), the crucial effect of changing crop parameters was evaluated.

4.3 Reckenholz Lysimeter

The lysimeter facility in Zurich-Reckenholz, northern Switzerland (444m a.s.l), contains 72 cultivated lysimeters where 12 are weighable. The lysimeters have a surface of $1m^2$ and depth of 1.5m. The steel cylinders are filled with undisturbed material from three dominant soil types for Switzerland (Prasuhn et al., 2009). The soils were removed intact as monoliths using a special milling technology. The Grafenried soil, a cambisol from the Bernese region comprises 18% clay, 27% silt and 55% sand. The Pseudo-gleyed cambisol directly taken from Zurich-Reckenholz comprises 25% clay, 55% silt and 20% sand whereas the luvisol from Schafisheim, Aargau Region has 25% clay, 24% silt and 51% sand. The average bulk density is 1.6, 1.4 and $1.5g/cm^3$, respectively for the entire soil columns. The lysimeter facility surface and basement as well as the present soils are shown in figure 4.1.

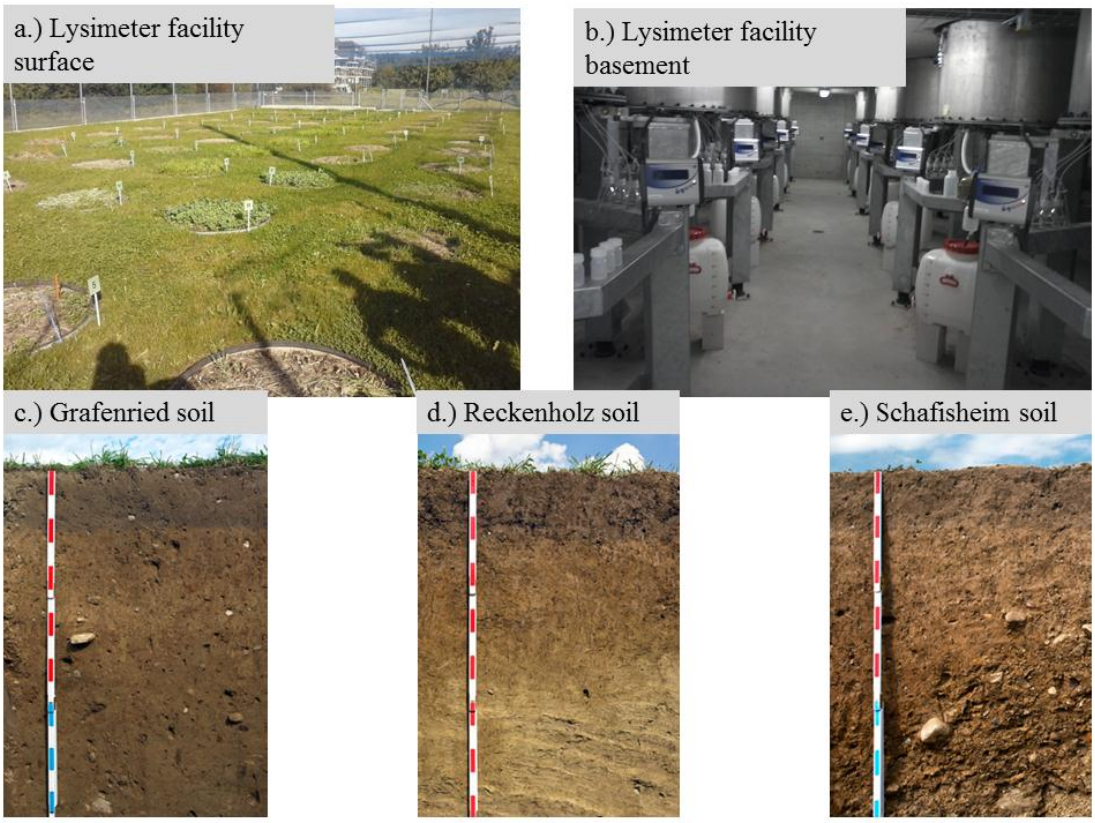

Figure 4. 3: Lysimeter facility surface (a.) and basement (b.) as well as the three present soil types (c-e).

The lysimeters are cultivated by different crop sequences representative for most agriculture areas in Switzerland. Each crop sequence is planted in triplicates and are conducted in parallel on the three different soils in order to determine the influence of the soil. In this study, five lysimeters which cover the available three soil types and represent the most occurring crop sequences in Switzerland were chosen. The covered time periods between 01.04.2009 and 12.07.2012 (based on the data availability) as well as the crop sequences investigated in this study are listed in table 4.1.

Table 4. 1: Crop sequences for the five different lysimeters represent three different soil types. The sowing and harvesting time is given for each crop.

Lysimeter	Soil type	Crop	Sowing date	Harvest date
3	Cambisol	Winter barley	01.10.2009	09.07.2010
		Phacelia	02.09.2010	21.03.2011
		Sugar beets	22.03.2011	04.10.2011
		Feed wheat	25.10.2011	12.07.2012
9	Cambisol	Winter wheat	01.11.2009	19.07.2010
		Colza	03.09.2010	27.06.2011
		Temporary grassland	17.08.2011	23.04.2012
10	Cambisol	Spelt	01.11.2009	19.07.2010
		Temporary grassland	03.09.2010	14.03.2011
		Field peas	15.03.2011	05.07.2011
		Colza	30.08.2011	04.07.2012
5	Pseudo-gleyed cambisol	Maize	22.05.2009	22.10.2009
		Winter wheat	31.10.2009	19.07.2010
		Phacelia	02.09.2010	14.03.2011
		Field peas	15.03.2011	05.07.2011
		Colza	31.08.2011	04.07.2012
6	Luvisol	Maize	22.05.2009	22.10.2009
		Winter wheat	31.10.2009	19.07.2010
		Phacelia	02.09.2010	14.03.2011
		Field peas	15.03.2011	05.07.2011
		Colza	31.08.2011	04.07.2012

The amount of seepage water at the bottom of the soil columns is measured in 100 ml steps with a tipping bucket. The drainage occurs only by gravitation. A filter layer (gravel and sand) installed between 1.35 and 1.5m depth is used to avoid irregularities of water fluxes and pressure at the interrupted lysimeter bottom. Twelve of the 72 lysimeters have highly precise scales with a resolution of 10 g. Due to weighing of these soil columns, quantitative measurements of actual evapotranspiration (ET_a) can be calculated with:

$$ET_a = P - Q \pm \Delta S \quad (1)$$

where P is precipitation [mm], Q is the amount of seepage water [mm] (representing recharge in this study), and ΔS is the change in stored water volume [mm] calculated from the change in lysimeter mass.

The precise estimation of ET_a depends on the surface and depth of the lysimeter (Young et al., 1996, Rana and Katerji, 2000). Only a sufficent surface and depth helps to minimize boundary effects which limits the realiability of ET estimations. The lysimeter surface and depth from this facility allowed making accurate measurements of ET_a comparable to ET_a estimated fluxes by flux stations or satellite imagery. The lysimeter also contains various measuring probes (soil-temperature sensors, tensiometers for measuring the surface tension of water, FDR sensors for measuring soil water content, suction cups for water removal) at four different soil depths (0.1, 0.3, 0.6 and 0.9m) with two repetitions where data acquisition takes place every five minutes. Precipitation was recorded at the official MeteoSwiss meteorological station located close to the lysimeters (at 10m distance). The amount of seepage water for the total time period corresponds to 32-36 % of the total precipitation amount. Comparing grass reference ET_0 (calculated with the Penman-Monteith equation) with measured ET_a, we can observe that ET_a is 10 to 35 % higher, depending on the crops.

A lysimeter data set, comprising amount and pattern of seepage and precipitation, mean calculated soil water content (SMC) and calculated ET_a based on weight changes in the lysimeter column is shown as an example (Figure 4.2). It can be observed that smaller precipitation events lead not always to seepage if the water content is lower than ≈0.3 Vol%. In addition, a long dry period with high ET_a in 2011 can be observed where only seepage occur during the autumn and winter period.

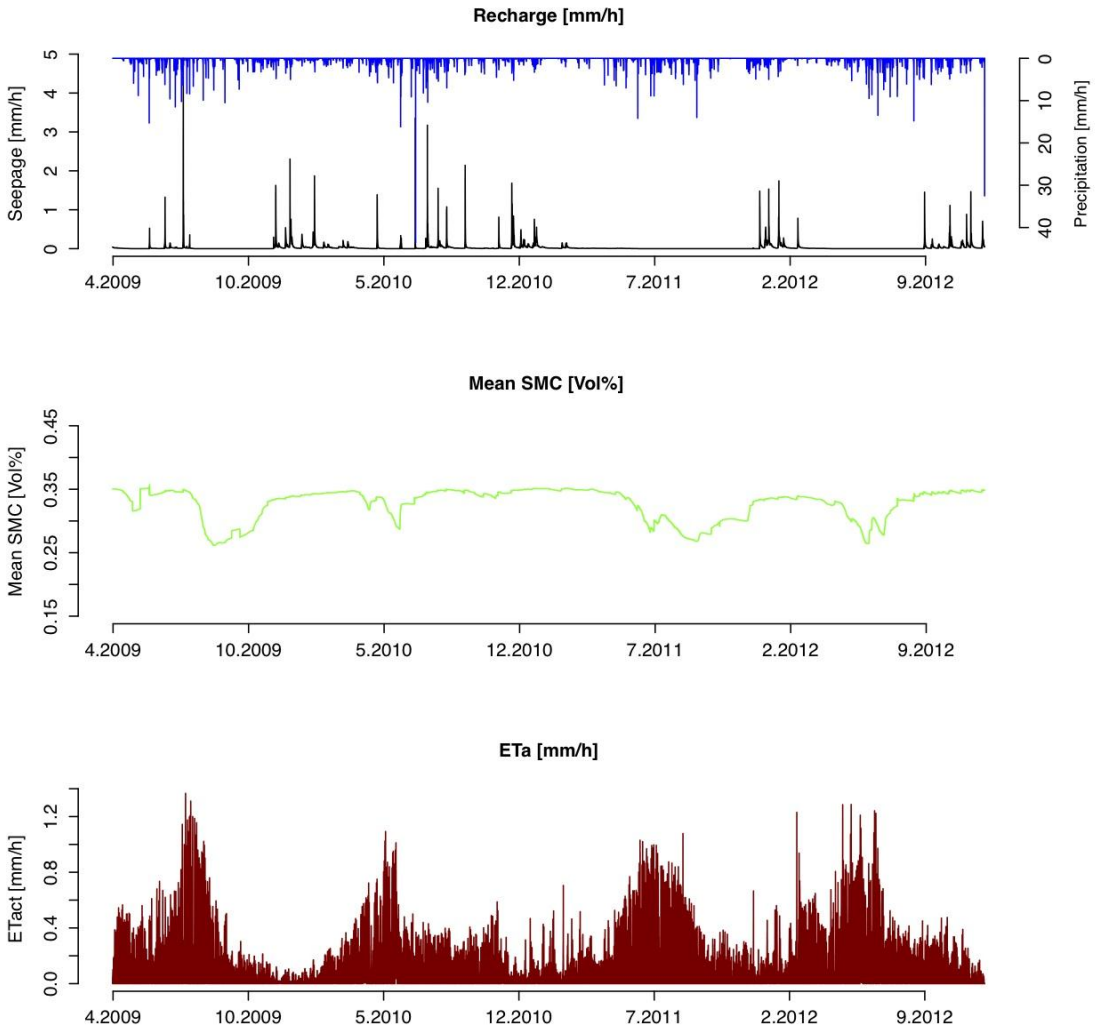

Figure 4.2: Lysimeter data with recharge (mm/h), precipitation (mm/h), mean soil moisture content (SMC in Vol%) and calculated ET_a (mm/h) for lysimeter 3 with the soil type Cambisol.

4.4 Historical Effects of Crops

In order to highlight the effect of land use on recharge in terms of different crop types and sequences an example from the measured historical data is given. Water content in four different depths from three different lysimeter is displayed (Figure 4.3) as well as daily seepage pattern and cumulative rates for the entire time series and smaller time slot (Figure 4.4). The lysimeters contains the same soil type but are operated with different crop types. The variations in among the lysimeters are generally small (Figure 4.3). However, in spring/summer 2011 considerable differences in water content occur due to different crop types and the associated different water demand. The effect for seepage rates is, however, small due to the already mentioned long dry period in 2011. Unfortunately during this period the most

significant difference in water content occur but the explanation power for recharge is limited.

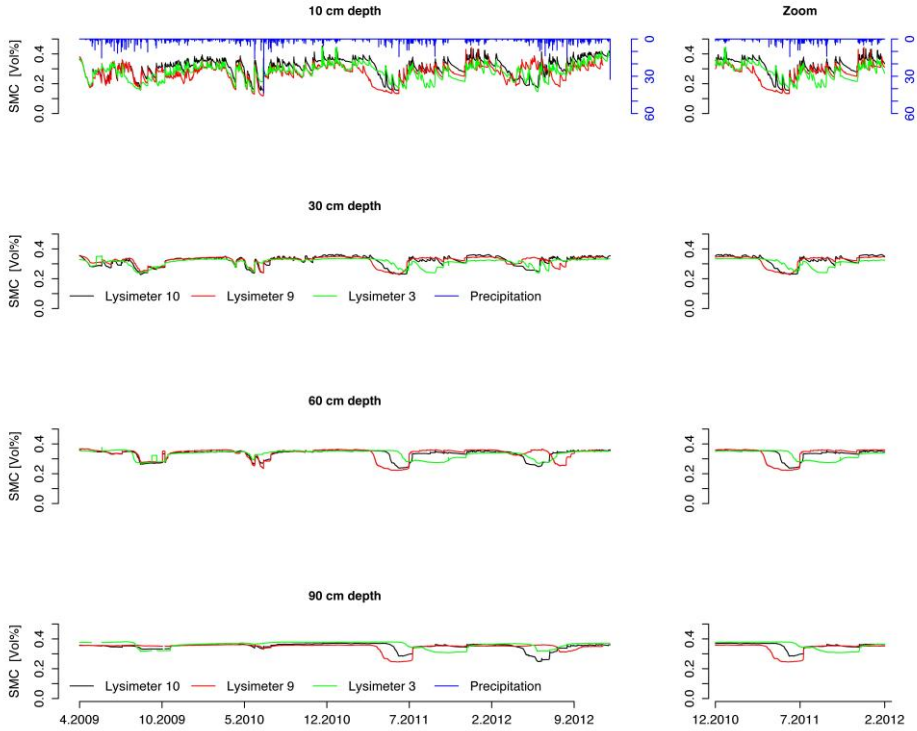

Figure 4.3: Soil moisture content (SMC) for lysimeter 3 in 4 different depths for the entire time series (left panel) and a chosen time slot where differences in SMC occur (right panel).

Considering just the time slot from 2011 (spring/summer) shows that plants with larger root depth and LAI lead to reduced water content and partly seepage. For instance, colza (Figure 4.3 and 4.4, red colour) with deep roots and large LAI induce reduced water content up to a depth of 90 cm. In contrast, using peas (Figure 4.3 and 4.4, green colour) instead of colza leads to delayed decrease in water content and a dumped reduction. For instance, in 90 cm depth only a minor reduction in water content can be observed.

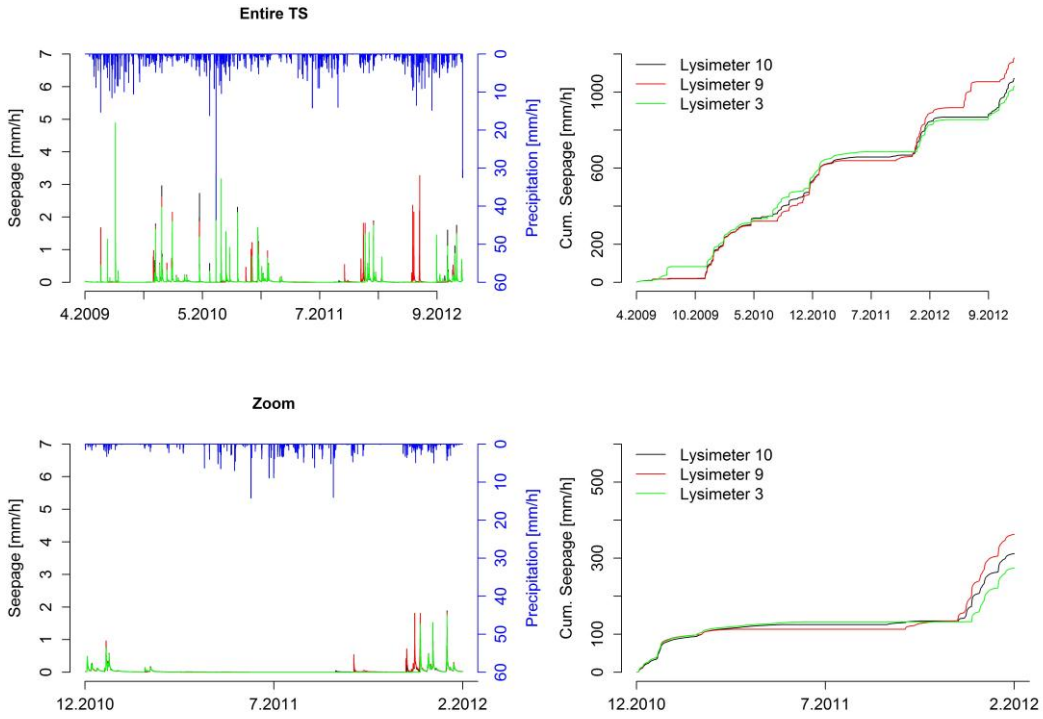

Figure 4.4: Hourly (left panel) and cumulative seepage (right panel) for lysimeter 3 for the entire time series (top row) and a chosen time slot (bottom row).

4.5 Climate input data

In this section, the used past and future climatic data for the 1D models are described. The applied methodology, which combines delta change values from seven different GCM-RCM combinations with a stochastic weather generator, is presented. To estimate the uncertainty linked to differences in GCMs and RCMs, a multi-model ensemble approach is used, whereas the uncertainty linked to the inter-annual variability of the climate is evaluated by using different stochastic realizations of the possible climatic conditions. The combined method was applied to generate daily transient climatic input data to identify temporal change in recharge rates for each crop under the specific vegetation period.

4.5.1 Past climatic data

Measured data from the MeteoSwiss weather station Zurich-Reckenholz, Switzerland were used to calculate grass references potential evapotranspiration using the Penman Montheith equation (Allen et al., 2005). This grass reference evapotranspiration was adjusted by crop coefficients (Allen et al., 2005) for the each respective crop.

$$ET_c = ET_0 * K_c \quad (2)$$

where Et_c is the crop evapotranspiration [mm/day], ET_0 is the reference crop evapotranspiration [mm/day] and K_c is the dimensionless crop factor for the specific crop type.

4.5.2 Future climatic data

A total of seven model chains for the A1B emission scenario are used for the simulation under future climate conditions (Supporting information, table A4.2). These model chains consist of a GCM driving a RCM. Regional scenarios are derived directly from the output of individual GCM-RCM model chains by means of the statically downscaling technique to the MeteoSwiss monitoring network with an inverse distance weighting interpolation (Bosshard et al., 2011) and are provided by the Center for Climate Systems Modeling (C2SM; http://www.c2sm.ethz.ch/). The applied model chains provide a daily time series of delta change factors for precipitation and temperature for three periods (2035, 2060 and 2085) relative to the reference period 1980-2009 (Figure 4.5).

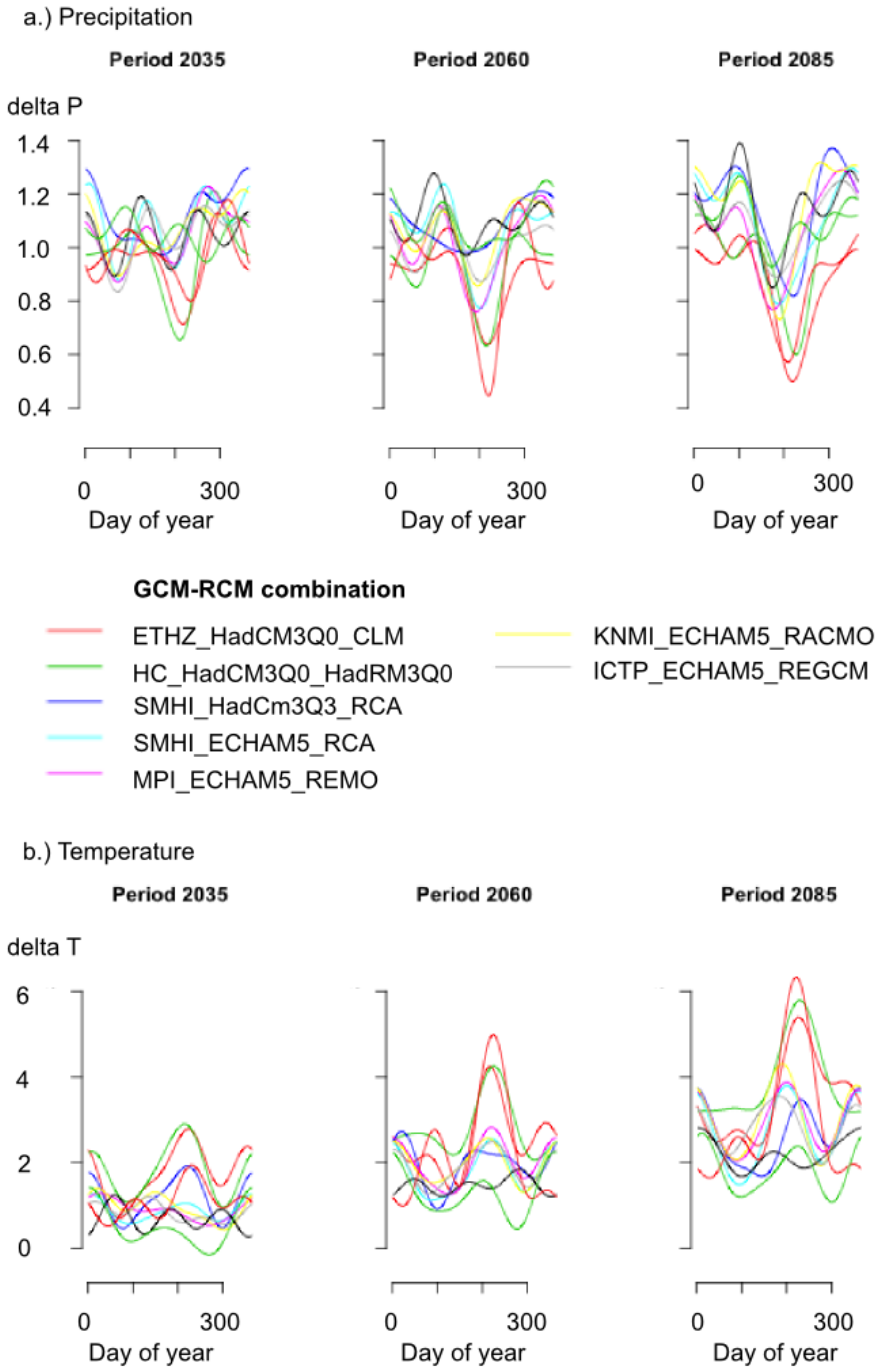

Figure 4. 5: Daily climatic change factors (Delta-Change Approach) for each climate model chain for the scenario A1B. a.) Daily precipitation and b.) Daily mean temperature from Meteoswiss weather station in Zurich-Reckenholz.

Subsequently, a technique, which combines the delta change factor and stochastic weather generator approach, is used to generate transient CC scenarios. Linear interpolation was carried out between the three periods with delta change values in order to obtain a continuous time series for each day and each year between 2011 and 2085. This continuous time series of delta change values are then used in a stochastic

weather generator (LARS-WG, Racsko et al. 1991, Semenov and Barrow 1997, Semenov et al. 1998) to create 10 different realisations of future precipitation and temperature values for each of the seven model chains. The 10 different realisations are required to represent possible future weather patterns. This stochastic approach enables to simulate climatic variability more realistically compared to the simple delta change downscaling approach (Goderniaux et al., 2011). Using that methodology, we are able to analyze the timing of an expected change in recharge rates, whereas the delta change method predicts increase or decrease of recharge only for the three stationary time periods. The conceptual approach is shown as an example in figure 4.6 for the climate model chain "ETHZ_HadCM3Q0". The linear interpolation between the years 2011, 2035, 2060 and 2085 for temperature and precipitation for each year from 2011 to 2085 and each day during the year is demonstrated.

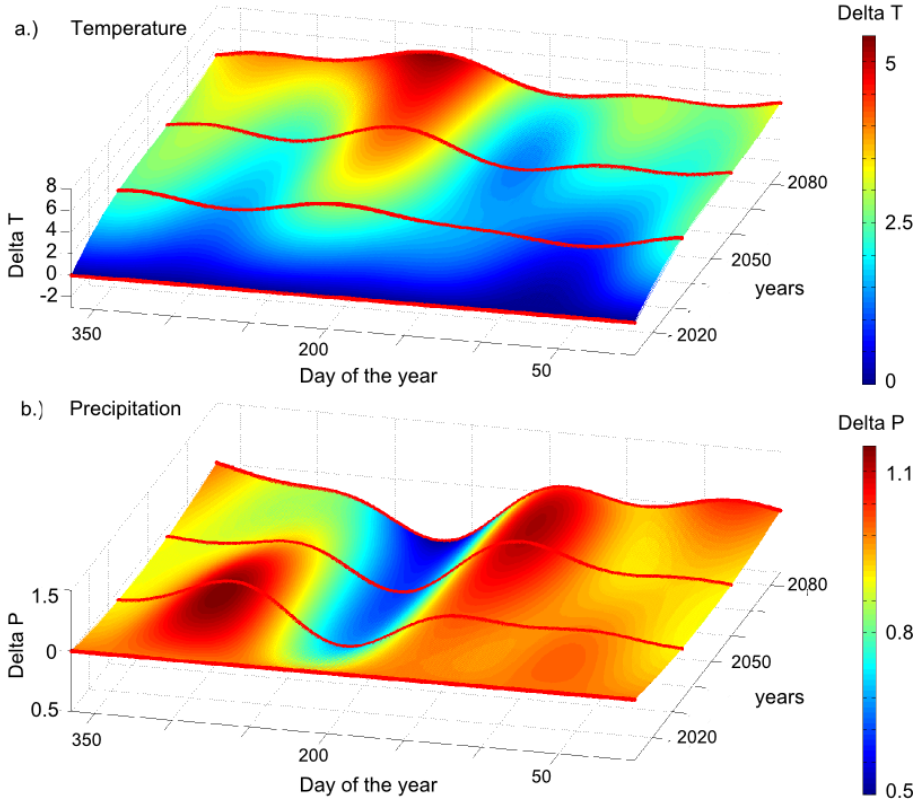

Figure 4. 6: Linear delta change factor interpolation between the year 2011 and the three-time period 2035, 2060 and 2085 (red lines) for a.) Temperature and b.) Precipitation for each year from 2011 to 2085 and each day is shown. Red and blue colors indicate an increase and decrease trend, respectively.

Only 10 different realisations for each climate model chain and each year were carried out in order to reduce the simulation time. More realisations of the weather pattern would certainly cover the CC effect in a still more realistic way. However, already 5320 simulations for each crop type and scenario were carried out and reached therefore a certain limit of computation time (76 years (year 2011-2085)

multiplied by 7 GCM-RCMs and 10 stochastic realisations of temperature and precipitation give 5320 simulations. This value must be further multiplied with 16 different crops for 4 lysimeters used in the ongoing study and 2 different crops with each 4 scenarios in the sensitivity analysis). In total 127680 simulations were carried out.

4.6 Model and modeling strategy

In this section, the mathematical modeling framework is presented. Subsequently, the conceptual numerical model structure is introduced. Then the calibration strategy and chosen model validation criteria are presented. In the last part, the scenario simulation approach will be explained.

4.6.1 Mathematical model framework

In this study the numerical finite element model HydroGeoSphere (HGS) was used (Therrien et al., 2007). In HGS, a control volume finite element approach is used to simultaneously solve Richards' equation describing 3D variably-saturated subsurface flow.

$$-\nabla(q) + \Sigma\Gamma_{ex} \pm Q = \frac{\partial}{\partial t}(\theta_s S_W) \tag{3}$$

where S_w is the water saturation [-], Γ_{ex} is the volumetric fluid exchange rate [$L^3 L^{-3} T^{-1}$] between the subsurface domain and all other domains used in the model, Q is the fluid exchange rate from boundary conditions [$L^3 L^{-3} T^{-1}$] and θ_s is the saturated water content [-]. The fluid flux q [$L T^{-1}$] is subsequently given as

$$q = K k_r \nabla(\psi + z) \tag{4}$$

where ψ is the pressure head [L^1], k_r the relative permeability [-] of the medium, K the saturated hydraulic conductivity [$L T^{-1}$] and z the elevation head [L].
The unsaturated hydraulic conductivity is defined using the Mualem – van Genuchten model (vanGenuchten, 1980) for unsaturated soil hydraulic properties.

$$k_r = Se^{(l)}\left[1 - (1 - Se^{\frac{1}{\upsilon}})^{\upsilon}\right]^2 \text{ where } \left(\upsilon = 1 - \frac{1}{\beta}\right) \tag{5}$$

where α is the inverse of the air-entry pressure head [L^{-1}], β is the pre-size distribution index, θ_r is the residual water content [-], Se is an effective saturation, given by $S_e = (\theta_s - \theta_r)/(1 - \theta_r)$ and l is the pore-connectivity parameter. Precipitation is partitioned automatically in the model into evapotranspiration, runoff and infiltration (Goderniaux et al., 2009b). According to the work of Kristensen and Jensen (1975), actual transpiration (T_p) and evaporation (E_s) is a function of potential evapotranspiration (E_{pot}) [$L T^{-1}$], soil moisture [-], evaporation depth [L], root

distribution function over a given depth (*RDF*) [L], and Leaf Area Index (*LAI*). T_p is given as

$$T_p = f_1(LAI) f_2(\theta) RDF (E_{pot} - E_{can}) \quad (6)$$

where E_{can} is the tree canopy evaporation [L T^{-1}]. The linear relationship between T_p and *LAI* give the vegetation function (f_1)

$$f_1(LAI) = max\{0, min(C_2 + C_1 LAI)\} \quad (7)$$

where *C1* and *C2* are fitting parameters [-].

The *RDF* is given by

$$RDF = \frac{\int_{z'_1}^{z'_2} r_f(z')dz'}{\int_0^{Lr} r_f(z')dz'} \quad (8)$$

where L_r is the effective root length [L] and *z* the depth beneath the soil surface [L]. The root extraction function is given by $r_f(z')$ [L^3 T^{-1}]. The moisture content function (f_2) relates T_p to the moisture state and has the form as:

$$f_2(\theta) = \begin{cases} 0 & 0 \le \theta \le \theta_{wp} \\ f_3 & \theta_{wp} \le \theta \le \theta_{fc} \\ 1 & \theta_{fc} \le \theta \le \theta_{ox} \\ f_4 & \theta_{ox} \le \theta \le \theta_{an} \\ 0 & \theta_{an} \le \theta \end{cases} \quad (9)$$

where $f_3 = 1 - \left(\frac{\theta_{fc} - \theta}{\theta_{fc} - \theta_{wp}}\right)^{C3}$ (10)

$$f_4 = 1 - \left(\frac{\theta_{fc} - \theta}{\theta_{an} - \theta_o}\right)^{C3} \quad (11)$$

C3 is a fitting parameter [-], θ_{fc} is the moisture content at field capacity, θ_{wc} is the moisture content at the wilting point, θ_o is the moisture content at the oxic limit and θ_{an} is the moisture content at the anoxic limit. Below the wilting-point moisture content, transpiration is zero; transpiration then increases with moisture content to a maximum at the field-capacity moisture content. This maximum is maintained up to the oxic moisture content beyond which the transpiration decreases to zero at the anoxic moisture content. When the available moisture content exceeds the anoxic moisture content, the roots become inactive due to a lack of aeration.

In HGS, evaporation from the surface and sub-surface soil layers is a function of nodal water content and an evaporation distribution function (*EDF*) over a prescribed

extinction depth. The model assumes that evaporation occurs together with transpiration, this resulting from energy that penetrates the vegetation cover. It is expressed as:

$$E_s = \alpha^*\left(E_p - E_{can} - T_p\right)EDF \tag{12}$$

The wetness factor α^* is given by:

$$\alpha^* = \begin{Bmatrix} \frac{\theta-\theta_{e2}}{\theta_{e1}-\theta_{e2}} & for\ \theta_{e2} \leq \theta \leq \theta_{e1} \\ 1 & for\ \theta > \theta_{e1} \\ 0 & for\ \theta < \theta_{e2} \end{Bmatrix} \tag{13}$$

where θ_{e1} is the moisture content at the end of the energy limiting stage (above which full evaporation can occur) and θ_{e2} is the limiting moisture content below which evaporation is zero.

An *EDF* is an evaporation density function defined by the user. It is assumed that the amount of available energy for evaporation decreases with increasing depth. Here, we have chosen a linear function to describe the rate of decrease between the soil surface and the extinction depth L_E (L).

The rate of transpiration for a given node i (T_{pi}) can be estimated by substituting θ in equation (11) with the nodal water content θ_i. The total transpiration rate is then calculated using:

$$T_p = \sum_{i=1}^{n_r} T_{pi} \tag{14}$$

where n_R is the number of nodes that lie within the depth interval $0 \leq z \leq L_r$. The rate of evaporation for node i can then be estimated by substituting the nodal water content i and nodal evaporation distribution function EDF_i into equations (6)–(11).

4.6.2 Numerical model and calibration

The 1-D models were created with 135cm depth and 5cm vertical discretization. Specific flux boundary was used on the top of the column (potential ET and precipitation), while a seepage boundary at the bottom was applied. Several studies shows that the water dynamics could be reasonably described using the assumption of homogenous soil conditions even for strongly differing textures (Schelle et al., 2012). However, based on soil samples and moisture measurements throughout the depths of the Reckenholz lysimeter, only small differences in texture were observed, a homogenous model structure was chosen. Runoff was completely neglected due to the lysimeter steel cylinder edge (higher than the surfaces), which prevented runoff during precipitation events.

The calibration of the 1D model was carried out using PEST (Doherty, 2010). The time between cropping and harvesting for each crop type was subdivided into two

parts. The first half was used for the calibration and the second for the validation. Daily values of cumulative seepage water amount (referred also as groundwater recharge), water content averaged over the depths 30-90cm, and ET_a were used as observed data for the calibration. Mertens et al. (2006) demonstrate that using average moisture content in the calibration enables to identify reliable retention and hydraulic conductivity curves, although local fluctuations in different depths are neglected. In addition, Brunner et al. (2012) show for a 1D modeling study that the use of ET_a data in the calibration can help increasing the model parameter identification capacity and reduce predictive uncertainties, but the efficient of the calibration with ET_a depends on the depth to the water table. Due to the shallow boundary in 1.35m for the lysimeters used in this study, it is expected that the information content of ET_a is considerable for the model calibration. Furthermore, the simulated coupled flow process enable to validate all components of the water balance against the observations. The bias induced by the calibration is easier to detect than using only soil moisture content observations to calibrate the model.

The used weight for each observation group reflects $1/\sigma$, where σ is the measurement error. A measurement error of 0.1kg precision for the collection of drainage water (0.1mm of water column on the lysimeter) and 0.05 Vol% of the water content was used due to the reported accuracy of the used sensors. For ET_a 0.01mm was used based on the 0.01kg weighting precision for the lysimeter mass. The weighting of the mass are used in equation 1 as a storage change (ΔS). It should be mentioned that the measurement uncertainty of ET_a can be higher due the interplay of precipitation and seepage water amount measurement errors.

Initial values for the calibration of the soil model parameters such as K, α, β and θ_r were estimated using the program Rosetta (Schaap et al., 2001), a pedo-transfer model which predicts soil hydraulic parameters from soil textures. These parameters were calibrated subsequently for each soil type. The estimated soil model parameters for the first crop type were fixed as a "basic" value. Re-calibration of theses parameters in a range of -10 to 10% for each new appearing crop was carried out to account for possible changes in soil structure due to different crops and root growth. Although a maximum change of -10 to 10% was permitted, the archived retention curves based on the van Genuchten parameters differ only slightly (not shown). Vegetation model parameters such as LAI and RD were taken from the literature (Table 4.1; supporting information) (Breuer et al., 2003, Yunusa et al., 1993, Garcia et al., 1988, ORNL 2001, Jamieson et al., 1995, Jipp et al., 1998) and only parameters *C1* to *C3* were calibrated in a range of 0 to 1 for each crop type.

4.6.3 Model validation

Four model performance criteria were used to characterize the model results from the five different lysimeters under different crop sequences (section 5.1). These model scenario equations were chosen because the results interpretation can be challenging due to the fact that model scenario equations can emphasize on different types of simulated-observed behaviors with different sensitivity. For instance, R^2 is

oversensitive to high extreme values and unaffected by proportional differences between predictions and observations.
Nevertheless, the coefficient of determination R^2 was first used to verify whether a linear relationship (R^2=1) existed between the simulated and measured values.
Secondly, the Nash Sutcliffe model efficiency (NSE), which is a normalized value that determines the relative magnitude of the residual variance compared to the measured data variance (Nash and Sutcliffe, 1970), was applied.

$$NSE = 1 - \frac{\sum_{i=1}^{n}(Y_i^{obs} - Y_i^{sim})^2}{\sum_{i=1}^{n}(Y_i^{obs} - Y_i^{mean})^2} \quad (15)$$

where Y_i^{obs} is the observed value , $Y_i^{sim}$is the simulated value, Y_i^{mean} is the mean calculated value from all observation and n is the number of observations. NSE provides values between 1 to -∞, where 1 indicates a perfect match.
The percent of bias (PBIAS) was calculated according to the method given by Gupta et al. (1999).

$$\text{PBIAS} = \left[\frac{\sum_{i=1}^{n}(Y_i^{obs} - Y_i^{sim}) * 100}{\sum_{i=1}^{n}(Y_i^{obs})}\right] \quad (16)$$

PIBAS provides a measure of over- or underestimation for each observation group.
An optimal value is 0% while a positive value indicates an underestimation and a negative value an overestimation.
The last method used to validate the calibration is the Kling-Gupta efficiency (KGE′). Developed by Gupta et al. (2009) and revised subsequently by Kling et al. (2012), this method ensures that bias and variability ratios are not-cross-correlated and provide a diagnostically decomposition of the Nash-Sutcliffe efficiency into correlation, bias term and variability term.

$$\text{KGE}' = \sqrt{(r-1)^2 + (\beta'-1)^2 + (\gamma'-1)^2} \quad (17)$$

$$\beta' = \frac{\mu_s}{\mu_o} \quad (18)$$

$$\gamma' = \frac{CV_s}{CV_o} = \frac{\delta_s/\mu_s}{\delta_0/\mu_o} \quad (19)$$

where KGE′ is the modified KGE-statistic (dimensionless), r is the correlation coefficient between simulated and observed values (dimensionless), β' is the bias ratio (dimensionless), γ' is the variability ratio (dimensionless), μ is the mean value used in the analysis, *CV* is the coefficient of variation (dimensionless), δ is the standard deviation of used values in the analysis, and the indices *s* and *o* represent simulated and observed values.

4.6.4 Simulations

Simulations were carried out for four lysimeters involving the soil type cambisol (Lysimeter 3, 9 and 10) and pseudo-gleyed cambisol (Lysimeter 5) with the associated crops. Since lysimeters 5 and 6 have similar soil textures and crop sequence, gave comparable field data and similar results in the calibration, lysimeter 6 was omitted to reduce computational time. The simulated crop sequence is same to the crop sequence in the lysimeter experiment (Table 4.1).

Each crop type was simulated between the sowing and harvesting times. For crop sequence where after the harvesting a time lag occur until the next crop was planted a fallow land use was implemented. Throughout all simulations, a warm-up phase for the first crop type in each crop sequence of six months was chosen to minimize effects related to the initial conditions. Except for the first crop type in each sequence, the last moisture content distribution of the previous simulation was taken as initial condition for the following appearing crop. Daily values of potential ET and precipitation were used as input for the model. Simulations of groundwater recharge for 76 years (time series without the delta change factors, past recharge/seepage) were carried out in order to provide a baseline, which can be compared to future groundwater recharge rates. All subsequently simulated future recharge rates are based on predicted CC established by delta change values for each year and day for the A1B scenario until 2085 and 10 stochastic realisation.

In addition to these simulations a scenario modeling approach was carried out to evaluate the sensitivity of recharge rates on LAI and RD values. A change in LAI and RD values is assumed, as water stress (considerable reduced water content in the lysimeter) will likely become more frequent. Water stress frequently leads to a reduction in yield and LAI as observed in field studies (Claasen and Shaw 1970). Water stress during vegetative growth reduced LAI values due to a reduced size of the leaves. Water stress causes early loss of lower leaves and decreases dry matter weight and grain yield as a result of reduced intercepted radiation (Cakir 2004). Therefore, under drought conditions, transpiration decreases significantly (Eitzinger et al., 2003) and it is thus crucial to evaluate the effect of changing crop parameters such as LAI and RD. The chosen scenario modeling approach of this sensitivity analysis is subdivided in two different parts. In scenario 1, changes in recharge compared to the baseline are a function of the climatic conditions and adjusted LAI values. The LAI values were reduced by 5, 10 and 20% followed by an increase of 20%. In scenario 2, the RD is systematically changed by -10, - 25 and -50% followed by an increase of 50%. The sensitivity analyses were conducted for lysimeter 3 because it represents a range of different crops typically used in agriculture for Switzerland.

4.7 Results and Discussion

In this section, the calibration results are given to evaluate the goodness of the fit based on the model performance criteria. The simulated relative change for each crop type until 2085 based on the best-estimated model parameters obtained by the calibration is presented. Based on the obtained results, some specific crops were taken to study the temporal differences in recharge rates during the applied transient CC simulation in more detail. The effect of sowing and harvesting time and plants parameter is analysed as well. The results of a sensitivity analysis are then discussed to demonstrate the importance of changes in model crop parameters.

4.7.1 Calibration

A comparison between simulated and observed moisture content, cumulative seepage and cumulative ET_a is given based on graphical interpretation and model performance criteria to validate the goodness of the calibration. A good fit of average soil moisture content, cumulative seepage water amount (recharge) and cumulative ET_a (Figure 4.7) for lysimeter 3 under all four crops was observed. Small discrepancies occur between simulated and observed ET_a for all crops, whereas the moisture content and the amount of seepage water are well reproduced.

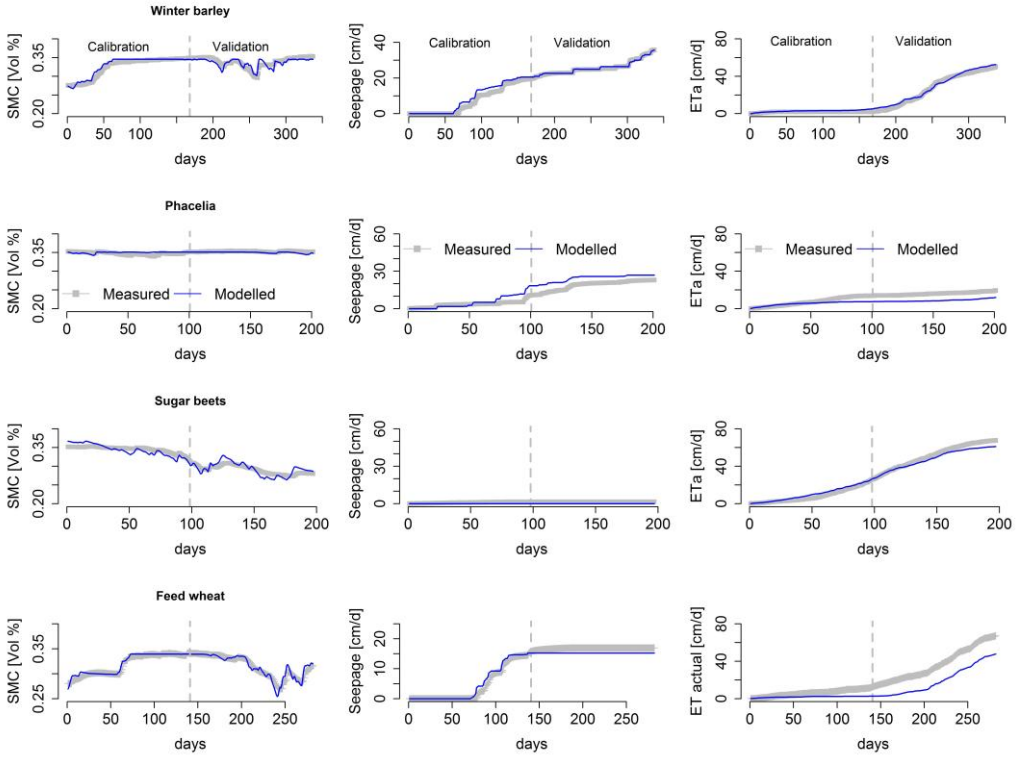

Figure 4. 7 :Fit between measured (grey) and simulated (blue) soil moisture content (SMC) (top row), cumulative seepage (middle row) and cumulative ET_a (bottom row) for Winter barley, Phacelia, Sugar beets and Feed wheat for lysimeter 3. The vertical gray line distinguish between calibration and validation period.

The performance criteria listed in table 4.2 summarises the calibration results for each crop and soil type. They are in good agreement with the graphical interpretation. Low performance criteria values are obtained for the crop Phacelia, Temporary grassland and Field peas. This is due to small variations in moisture content, seepage water amount and ET_a rates. These observations are stable in time (only minor variations), which lower the information content to identify "reliable" model parameters during the calibration process. The relatively short calibration time for Field peas also lowered the calibration results. The largest differences between simulated and observed values appear for ET_a which shows the highest measurement uncertainty and inaccuracy in K_c taken from FAO literature guidelines (Allen et al., 2005). However, the performance criteria for most crops indicate an accurate fit between all simulated and observed components of the water balance.

It should still be mentioned that the applied model scenario criteria show diverging results due to different sensitivity on the simulated and observed values. The lysimeter 10, which contains Field peas, for instance, shows a perfect fit between the observed and the simulated ET_a for the criteria R^2, and only a small underestimation in PBIAS whereas the NSE and KGE indicate a less good fit. To validate the calibration, we gave finally more weight on NSE and KGE. For instance, KGE was assumed to be the better criteria than R^2 because it ensures that bias and variability ratios are not-cross-correlated and provide a diagnostically decomposition of the Nash-Sutcliffe efficiency into correlation, bias term and variability term. We assumed that the decomposition helps to provide a more robust validation of the calibration. However, a detail discussion of strengths and weaknesses of model performance criteria is not the aim of this work but we indicate that the evaluation of the model performance should not be based only on one model performance criterion, but rather a comparison of different criteria should be involved. A good review about the pros and cons of different model performance criteria can be found in Bennet et al. (2013).

Table 4. 1: Table of the used performance criteria to evaluate the fit between simulated and observed moisture content (MC), seepage water amount and ET_a for each crop and lysimeter.

Chapter 4

	Lysimeter 3					*Lysimeter 10*		
observation typ	Criteria	Winter barley	Phacelia	Sugar beets	Feed wheat	Spelt	mporary grassla	Field peas	Colza
Moisture content	growing days	336	201	197	282	306	193	113	365
	PBIAS %	-0.3	0	0.1	-0.3	0.8	0	0	0
	NSE	0.86	-4.53	0.89	0.92	-0.13	-4.05	0.99	0.84
	R2	0.89	0.01	0.89	0.92	0.09	0.24	0.99	0.86
	KGE	0.89	-0.51	0.93	0.96	0.26	-0.64	0.99	0.77
	Range	0.08	0.02		0.07	0.06	0.02	0.1	0.1
Seepage water	PBIAS %	-0.4	63.3	-	4.9	2.2	46.8	1053.4	-14.6
	NSE	0.99	-4.69	-	0.96	0.97	-2.53	-464.2	0.95
	R2	0.99	0.92	-	0.98	0.99	0.93	0.92	0.99
	KGE	0.96	-0.48	-	0.88	0.88	-0.24	-12.4	0.82
	Sum (cm)	42.77	22.97	1.51	16.97	37.95	24.56	1.35	20.97
ET_a	PBIAS %	6.5	-23.8	1.9	100.7	61.7	7.2	53.6	28.5
	NSE	0.94	0.8	0.98	0.1	0.19	0.96	0.25	0.31
	R2	0.99	0.95	1	0.94	0.57	0.98	1	0.98
	KGE	0.93	0.68	0.86	-0.1	0.15	0.86	0.27	0.37
	Sum (cm)	102.3	19.48	67.55	67.15	45.37	17.6	39.65	88.31

	Lysimeter 5					*Lysimeter 9*		
observation typ	Criteria	Maize	Winter wheat	Phacelia	Field peas	Colza	Winter wheat	Colza	Temporary grassland
Moisture content	growing days	161	306	194	112	365	307	348	251
	PBIAS %	1.2	0.3	0	-0.9	0	0.7	-0.1	-0.1
	NSE	0.95	0.83	-151.87	0.95	0.83	0.65	0.89	0.43
	R2	0.99	0.85	0.01	0.96	0.83	0.76	0.92	0.53
	KGE	0.8	0.79	-10.44	0.96	0.9	0.8	0.85	0.73
	Range	0.09	0.09	0.02	0.1	0.11	0.08	0.13	0.03
Seepage water	PBIAS %	-	-0.1	-17	-8.3	-15.7	-4.3	-6	-13.5
	NSE	-	0.98	0.88	-2.3	0.93	0.96	0.97	0.71
	R2	-	0.98	0.95	0.19	0.97	0.98	0.99	0.95
	KGE	-	0.95	0.78	-0.11	0.81	0.92	0.93	0.78
	Sum (cm)	3.57	35.74	25.12	1.23	15.74	35.13	27.03	27.84
ET_a	PBIAS %	-6.6	-0.3	74.6	11.3	7.9	4.1	83.3	-8.2
	NSE	-0.65	0.99	-7.19	0.93	0.89	0.98	0.08	0.95
	R2	0.88	1	0.93	0.99	0.98	0.99	0.95	0.98
	KGE	0.46	0.9	-0.82	0.76	0.72	0.87	0.09	0.85
	Sum (cm)	61.06	49.2	20.87	42.9	77.96	58.74	71.07	16.84

4.7.2 Changes in recharge rates

In this section, the relative (%) and absolute cumulative (mm) change in recharge rate until 2085 compared to the baseline (past recharge) of each crop used in this study is shown. The maximal simulated change under different GCM-RCM combinations in a stochastic framework is analysed and uncertainties in the predictions are given (Figure 4.8).

Most crops show a percental decrease in recharge rates until 2085, but in a wide range of different amplitudes depending on the GCM-RCM combinations and stochastic realisations. The strongest decrease is simulated for Grain maize, which grows from May until October when the strongest increase in temperature and decrease in precipitation is predicted, followed by Field peas, which grows also during summer. Only Phacelia and the two Temporary grasslands indicate for some model chains an increase in recharge. For the crop Phacelia, a mean increase of 6.9%, is simulated, but in a range of –1.4 to 15.1% depending on the chosen climate model chains. The two Temporary grasslands under different soil types indicate a mean increase of 8.5% (Lysimeter 10) and a mean decrease of -0.6% (Lysimeter 9) under all climate model chains. The differences in recharge between lysimeter 9 and 10 with temporary grassland can be linked to different soil types, where already in the historical recharge data a difference between the soil types from these lysimeter of 5 to 10% can be observed.

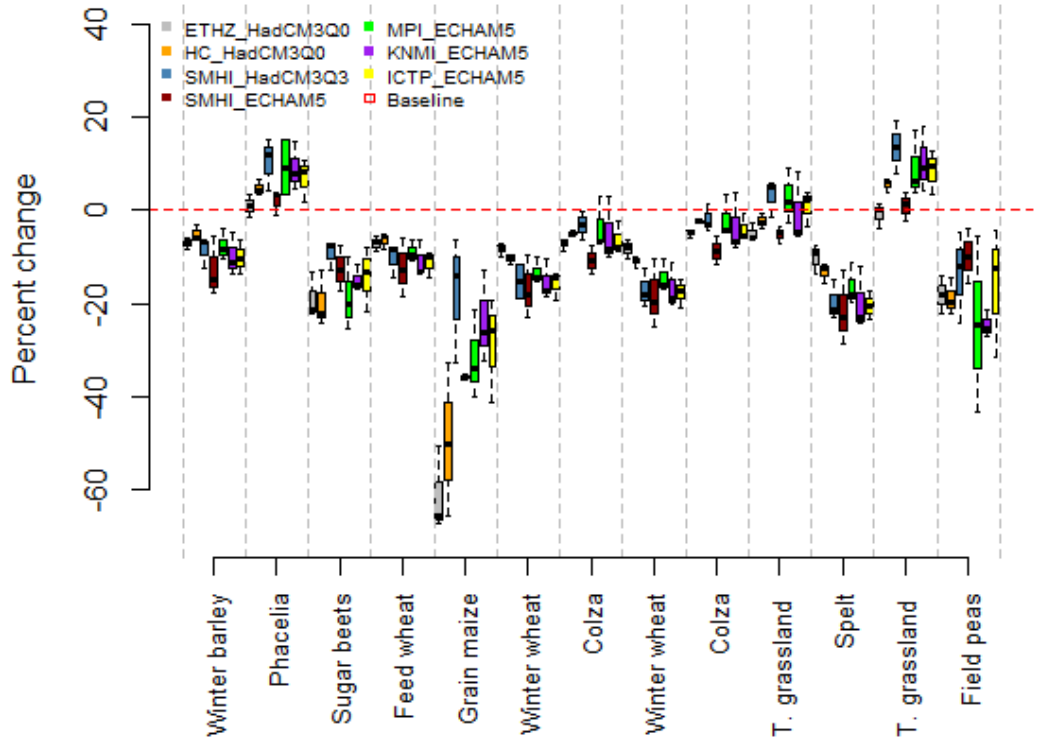

Figure 4. 8: Boxplot summary of all simulations for each crop type and lysimeter as well as climate model chain and 10 stochastic realisations for 2085 is shown (Period from 2011 to 2085). The percentile change compared to the baseline (past recharge) is displayed. A positive value indicates a recharge increase and a negative a decrease compared to the baseline. The different colours of each boxplot represent the seven different GCM-RCM combinations.

In order to understand underlying processes of recharge changes associated with growing period and crop parameters such as LAI and RD the absolute change for chosen soils and associated crop types are shown in figure 4.9 (LAI) and 4.10 (RD). The vertical arrows show the combined uncertainty originated from GCM-RCM combinations and stochastic realisation of the interannual variability in precipitation and temperature. The size of the rectangle shows the model parameter value for the related crop, whereas the position indicate the mean simulated change out of the different from GCM-RCM combinations and stochastic realisation. The horizontal arrows show the growing period. For instance for Lysimeter 9 (figure 4.9; bottomleft panel), we can observed that with increasing LAI value the absolute change from the reference period in recharge increase. Winter wheat with a large LAI shows the highest difference between past and future recharge rates, whereas for temporary grassland changes are negligible.

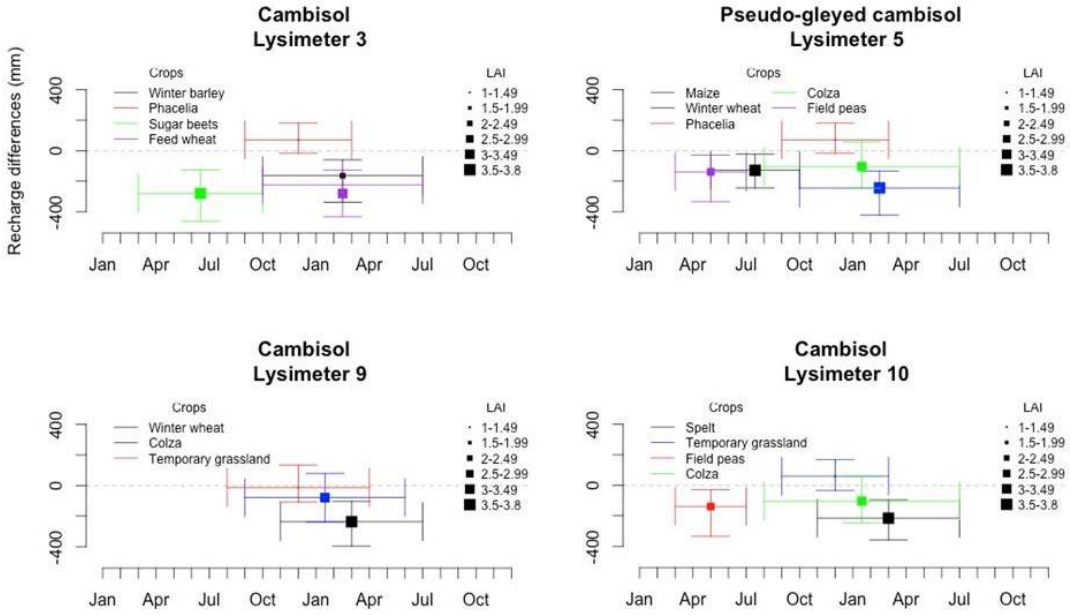

Figure 4. 9: Absolute change in recharge rate from the reference period for each chosen lysimeter and associated crop types. The vertical arrows show the combined uncertainty originated from GCM-RCM combinations and stochastic realisation of the interannual variability in precipitation and temperature. The size of the rectangle shows the model parameter value Leaf area index (LAI) for the related crop, whereas the position indicate the mean simulated change out of the different from GCM-RCM combinations and stochastic realisation. The horizontal arrows show the growing period.

Recharge changes depends strongly on the value for LAI, rather than on RD (Figure 4.9 and 4.10) Using again the aforementioned example from lysimeter 9 for the model parameter RD (figure 4.10; bottomleft panel), we can observed that simulation with a small RD for Winter wheat still gives large differences between future and past recharge. That indicate already that recharge is more sensitive to LAI rather than to RD.

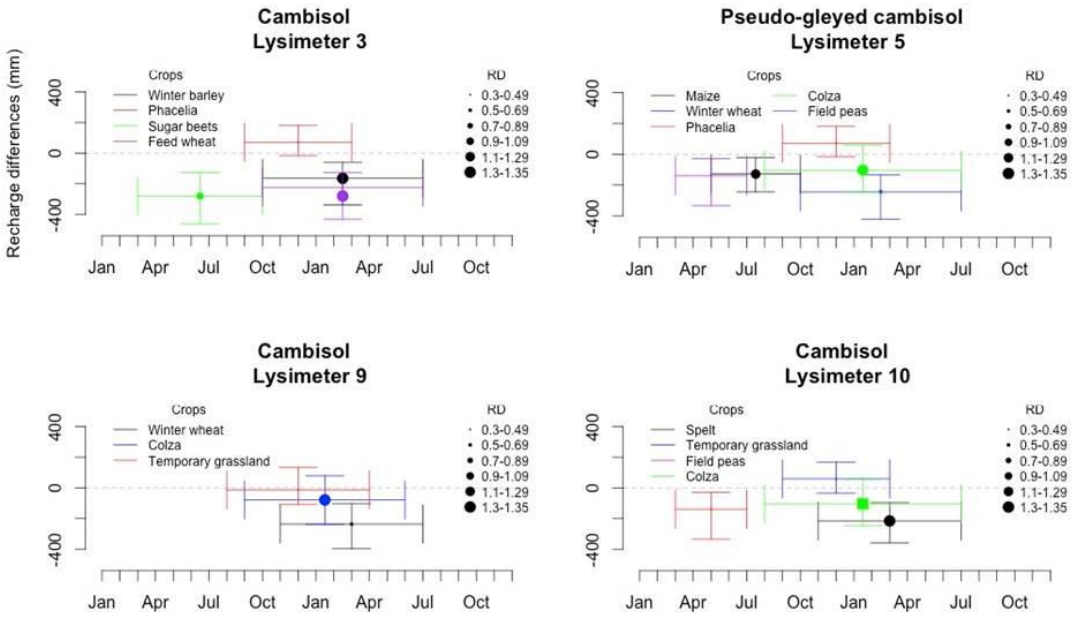

Figure 4. 10: Absolute change in recharge rate from the reference period for each chosen lysimeter and associated crop types. The vertical arrows show the combined uncertainty originated from GCM-RCM combinations and stochastic realisation of the interannual variability in precipitation and temperature. The size of the rectangle shows the model parameter value root depth (RD) for the related crop, whereas the position indicate the mean simulated change out of the different from GCM-RCM combinations and stochastic realisation. The horizontal arrows show the growing period.

For the different crop sequences (see table 4.1 for the crop sequence for each lysimeter), a decrease in recharge of 7 to 11% is simulated. Single crops indicate recharge decrease, but in the crop sequences, the catch (intermediate) crops (fast-growing crop that is grown between successive plantings of a main crop) such as Temporary grassland and Phacelia, where increasing recharge is predicted buffer to a certain amount the decreasing recharge rates.
Assuming a change in agriculture practice from the historical used crops to Temporary grassland would mostly create an increase in recharge. However, the timing in the seasonality when the changes to Temporary grassland occur influences the amplitude of changes in recharge rates. In table 4.3, the differences for lysimeter 3 from the historical used crops to Temporary grassland are presented. This lysimeter was chosen as an example because it covered common used crops in Switzerland and has different growing periods with the longest time series of historical data. This change from crops used agriculture to Temporay grassland is in particular interesting due to the topic of intensivation of agriculture and vice versa. Especially by high Nitrate concentration in aquifers used for drinking water supply a change in agriculture practice is common, often related to a change to grassland (e.g. Fischer et al., 2010).

Only small differences in future recharge rates can be observed when Winter barley is replaced by Temporary grassland, whereas the alteration is higher when Sugar beets are replaced. This indicates again the seasonal effect of crops growing period for recharge rates. Sugar beets grow from spring to autumn, while the strongest increase in temperature and decrease in precipitation is predicted in summer and autumn. A crop change to Temporary grassland, with smaller RD and LAI values than Sugar beets reduce ET_a and more recharge can occur. Winter barley, in contrast, grows during winter and spring where water deficits are uncommon and recharge rates are less affected by different crops. Therefore, a change to catch crops would be most efficient during late spring until autumn. However, considering also yield and cost for agriculture will restrict or complicated certainly a land use strategy as mentioned.

Table 4. 3: Percentage differences in future recharge rates for original crops and with an assumed change from agriculture crop sequence to Temporary grassland for the period 2011-2085. The absolute values indicate the change compared to the baseline (past recharge).

	Change in recharge from baseline				
Previous crop	Mean change (%)	absolute value (mm/a)	Switch to	Mean change (%)	absolute value (mm/a)
Feed wheat	-10	-39	Temporary grassland	6	23
Winter barley	-8	-25	Temporary grassland	-2	-6
Sugar beets	-15	-38	Temporary grassland	5	13

4.7.3 Transient climate change simulation

In this section, a temporal analysis for the entire time series of future and baseline (past) recharge rates is given. Using this approach, we are able to analyze the timing of an expected change in recharge rates. The temporal trend of recharge rates for Temporary grassland, Colza and Feed wheat is provided in figure 4.8 for their specific vegetation period. These crops were chosen as an example because they have distinctly different temporal trends of changes between baseline and future groundwater recharge rates. Furthermore, they have nearly the same sowing and harvesting time and can be therefore used to identify the effect of different crops for future recharge trends. For the remaining crops the temporal recharge trends can be found in the supporting information (figure A4.1 and A4.2).

For Temporary grassland, future recharge rates show both an increase and a decrease compared to the baseline, depending on the chosen model chain and stochastic realisation (Figure 4.11a). In contrast, Colza shows a recharge trend comparable with Temporary grassland until the year 2035, followed by a decreasing trend compared to

the baseline (Figure 4.11b) until 2085. However, still three out of 70 (4%) realizations show a small increase until the end of the century. For Feed wheat, a similar trend as reported for the other two crops until the year 2035 can be observed, whereas the decrease in recharge rates for all climate model chains is strongest (Figure 4.11c). While Temporary grassland and Colza still show an increase in recharge for some equiprobable stochastic realisations until 2057 (Temporary grassland 9 % and Colza 4 %), the predictions for Feed wheat do not indicate that. This observed temporal trend in recharge rates for Feed wheat is transferable to most crops (Figure A4.1 and A4.2, supporting information). The temporal differences between recharge rates from the used crops in this example depend on the crop parameters. A maximum LAI value of 1 and RD of 35cm for Phacelia has a less negative effect on recharge than Colza (LAI 3.1, RD 135cm) or Feed wheat (LAI 3.3, RD 135cm). Effects of the different soil types can be excluded because it gives only minor (less than 10 %) differences in recharge rates and patterns.

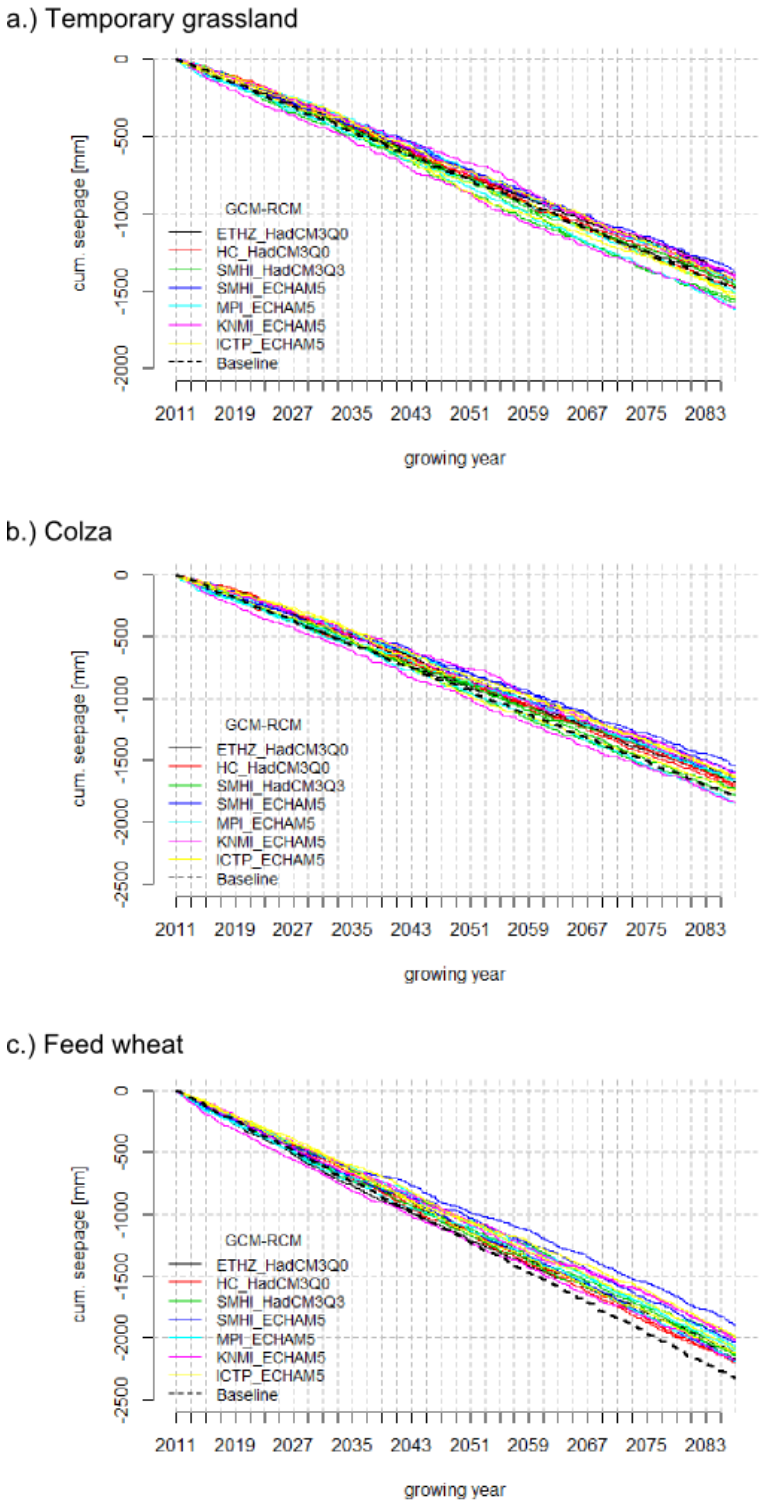

Figure 4. 11: Cumulative seepage water amount between 2011 and 2085 of the transient CC simulation for a.) Temporary grassland, b.) Colza and c.) Feed wheat during their specific vegetation period is shown. The dashed black line represents the baseline (past recharge) whereas the coloured solid lines displayed the seven different GCM-RCM combinations with the associated equiprobable stochastic realisations.

4.7.4 Sensitivity analysis

In order to evaluate the possible effects on recharge rates due to changes in LAI and RD a sensitivity analysis was carried out. A change in LAI values and RD is assumed to be required as water stress become more frequent. Water stress can causes changes in RD and LAI. The crops, Sugar beets and Feed wheat from lysimeter three were chosen as an example because they covered different growing periods. Sugar beets are sawed in spring and harvested in autumn, where the temperature increase and precipitation decrease are highest (Figure 4.2 and 4.3). In contrast, the Feed wheat is sawed in autumn and harvested in the following summer. An increase in precipitation is predicted especially over late winter and early spring.

Simulations with changing LAI and RD values for Feed wheat indicate a variability of recharge rates (Figure 4.10). Simulated recharge is inversely related to LAI and RD (Figure 4.10 and table 4.4). Decreasing of LAI and RD leads to an increase in recharge where simulated recharge is more sensitive to a decrease in LAI than to RD, which is consistent with the findings of Kesse et al., (2005). A reduced LAI value of 20% for Feed wheat leads to a simulated increase of recharge of 7.9% while an increase of 20% leads to a decrease of 9.2%. The result under a 20% decrease in LAI is interesting because simulated recharge is subsequently close to the baseline recharge (past recharge, red dashed line).

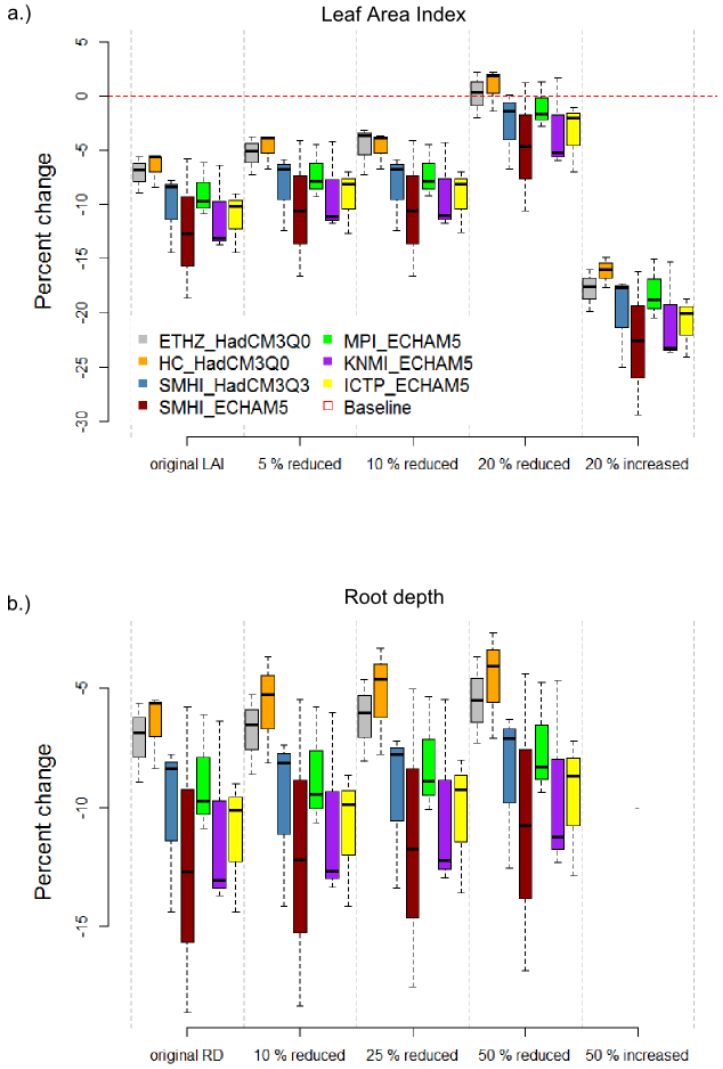

Figure 4. 14: Sensitivity of recharge rates on the Feed wheat a.) LAI and b.) RD. In the references scenario ("original" LAI or RD) LAI and RD corresponds to the original literature values. The red dashed line corresponds to the past recharge rates (baseline). A RD increase for Feed wheat could not be simulated because the actual RD already reaches the bottom depth of the lysimeter.

A RD decrease of 50 % leads to a recharge increase of 2% for Feed wheat (Table 4.4). A RD increase for Feed wheat could not be simulated because the actual RD already reaches the bottom depth of the lysimeter. It is very likely that the LAI and RD values will change in for future time periods and used actual literature values lead to an over-estimation of the impact of CC. Therefore, recharge estimates under original LAI and RD values may represent an upper boundary of recharge rate changes for the future.

Table 4. 4: Sensitivity of recharge rates to variations in Leaf area index (LAI) and root depth (RD) for lysimeter 3 and two crops.

Parameter	LAI				RD			
	Reduced			Increased	Reduced			Increased
	5%	10%	20%	20%	10%	25%	50%	50%
Sugar beets	1.52	3.13	9.59	-5.98	0.18	0.42	0.83	-0.65
Feed wheat	2.04	2.45	7.90	-9.20	0.82	1.26	1.89	-

4.8 Conclusions and Recommendation

In this study 1D unsaturated zone models were used to simulate future recharge rates for different crops and three considered soils. The numerical modeling technique was combined with a significant amount of high quality lysimeter data to ensure a reliable representing of historical and future recharge rate under different crop types. The lysimeter data comprised information on the effect of land use, crops and soils on recharge rates.

Several conclusions can be drawn from the investigation of the combined effect of CC and crops on groundwater recharge. Climate, vegetation and soils have control on the recharge rates. Using the available three soil types, differences in recharge rates of around 10% could be identified. These differences between the soils are observed in the field data for the time periods where the crops are identically and in the simulated future recharge values. But this is the least significant factor compared to climate and vegetation in this study.

Simulations indicate that for most crops a decreasing trend occurs compared to past recharge during their specific vegetation period. The differences here are functions of crop parameters, vegetation period with the associated change in precipitation and ET due to CC and uncertainty linked to variability between GCM-RCM combinations as well as the interannual variability of the climate. In contrast to most other crops, for catch crops such as Phacelia and Temporary grassland an increasing trend can be observed. Small RD and LAI values lead to less ET_a and consequently to increasing recharge. Simulations with used crop sequences from the lysimeter facility indicates only a decrease in recharge of 7 to 11% (mean annual recharge is around 330 mm). Using the catch crops in a crop sequence a buffering of the decreasing trend in future recharge rates can be realised, but the buffer capacity depends strongly on the growing season where catch crops are used.

Simulated recharge is inversely related to LAI and RD, where simulated recharge is more sensitive to a decrease in LAI than to RD. It is very likely that LAI and RD will change in the future due to water stress induced by CC. Therefore, final recharge estimates under original LAI and RD values probably represent an upper boundary on recharge rate changes for the future.

Considering the uncertainty of simulated future recharge, we can conclude that the highest uncertainty is linked first due to the GCM-RCM combinations and then to the

interannual variability expressed by the stochastic weather realisations. Uncertainty due to the model calibration seems to be smaller than the former uncertainties, expected crops where only low information content of the observations are available.
It should be note the used methodology which create transient CC climatic input data and give the possibility to detailed analysis when an expected change in recharge rates occur. This is in contrast to the delta change method where an increase or a decrease of recharge can be predicted only for the three stationary time periods. Therefore, if the temporal change in recharge is in particular interested the transient CC scenario is the proposed method to use.
Although a physical based model with an uncommon calibration dataset, including precise ET_a ,seepage and water content values covering all component of the water balance was used in this study, some open issues to evaluate the effect of CC on recharge are out of scope of this study. That is why recommendations are drawn for future studies. Already the simple sensitivity analysis indicates the strong dependency of recharge rates on changes in crop parameters such as LAI and RD. From this analysis, we can conclude that one of the most fundamental conceptual aspects is the vegetation dynamics. Growing periods will probably adapt to changing weather distribution, which is not taken into account here. The already coupling between vegetation and soil moisture content for the different scenarios should be extended to include changes in growing periods of the plants and provide consequently an increasing physical description of the system. In addition, this study represents a simplified approach to estimate recharge using a homogenous 1D model. More complex representations of the soil structure (if needed) will probably change the results. For instance macropores, which can occur more frequently in the future due to more drought periods and drying-out cracks, can have a strong influence on recharge rates.

Acknowledgements

The authors gratefully acknowledge the financial assistance provided by the Swiss National Science Foundation, Project NFP 61, Sustainable Water Management. The CH2011 data were obtained from the Center for Climate Systems Modeling (C2SM).

4.8 Reference:

Beniston, M. (2006). August 2005 intense rainfall event in Switzerland: Not necessarily an analog for strong convective events in a greenhouse climate. Geophysical Research Letters 33(5): L05701.

Bennett, N. D., Croke, B. F., Guariso, G., Guillaume, J. H., Hamilton, S. H., Jakeman, A. J., ... & Andreassian, V. (2013). Characterising performance of environmental models. Environmental Modelling & Software, 40, 1-20.

Bosshard, T., Kotlarski, S., Ewen, T., and Schaer, C.: Spectral representation of the annual cycle in the climate change signal, Hydrol. Earth Syst. Sci., 15, 2777-2788, 10.5194/hess-15-2777-2011, 2011.

Breuer, L., Eckhardt, K., and Frede, H.-G.: Plant parameter values for models in temperate climates, Ecological Modeling, 169, 237-293, http://dx.doi.org/10.1016/S0304-3800(03)00274-6, 2003.

Brunner, P., Doherty, J., and Simmons, C. T.: Uncertainty assessment and implications for data acquisition in support of integrated hydrologic models, Water Resour. Res., 48, n/a-n/a, 10.1029/2011wr011342, 2012.

BUWAL, BWG, MeteoSchweiz, 2004: Auswirkungen des Hitzesommers 2003 auf die Gewässer. Bundesamt für Umwelt, Wald und Landschaft, Berne, 174 pp.

Çakir, Recep. Effect of water stress at different development stages on vegetative and reproductive growth of corn. Field Crops Research, 2004, vol. 89, no 1, p. 1-16.

Claasen, M. M. and R. H. Shaw. 1970. "Water Deficit Effects on Corn:II Grain Components." Agron. J. 62:652-655.

Doherty, J. (2010), PEST: Model independent parameter estimation, User Manual, Watermark Numer. Comput., Brisbane, Australia.

Eckhardt, K., Breuer, L., and Frede, H.-G.: Parameter uncertainty and the significance of simulated land use change effects, Journal of Hydrology, 273, 164-176, http://dx.doi.org/10.1016/S0022-1694(02)00395-5, 2003.

Eitzinger, J., Stastna, M., Zalud, Z., and Dubrovsky, M.: A simulation study of the effect of soil water balance and water stress on winter wheat production under different climate change scenarios, Agricultural Water Management, 61, 195-217, 10.1016/s0378-3774(03)00024-6, 2003.

Fischer, G., Prieler, S., van Velthuizen, H., Berndes, G., Faaij, A., Londo, M., and de Wit, M. (2010). Biofuel production potentials in Europe: Sustainable use of cultivated land and pastures, Part II: Land use scenarios. Biomass and bioenergy, 34(2), 173-187.

Garcia, R., E.T. Kanemasu, B.L. Blad, A. Bauer, J.L. Hatfield, D.J. Major, R.J. Reginato and K.G. Hubbard (1988) Interception and use efficiency of light in Winter wheat under different nitrogen regimes. Agricultural and Forest Meteorology 44, 175-186.

Goderniaux, P., Brouyere, S., Fowler, H. J., Blenkinsop, S., Therrien, R., Orban, P., and Dassargues, A.: How can large scale integrated surface - subsurface

hydrological model be used to evaluate long term climate change impact on groundwater reserves, Calibration and Reliability in Groundwater Modeling: Managing Groundwater and the Environment, edited by: Wang, Y. X., 137-140 pp., 2009a.

Goderniaux, P., Brouyere, S., Fowler, H. J., Blenkinsop, S., Therrien, R., Orban, P., and Dassargues, A.: Large scale surface-subsurface hydrological model to assess climate change impacts on groundwater reserves, Journal of Hydrology, 373, 122-138, 10.1016/j.jhydrol.2009.04.017, 2009b.

Goderniaux, P., Brouyere, S., Blenkinsop, S., Burton, A., Fowler, H. J., Orban, P., and Dassargues, A.: Modeling climate change impacts on groundwater resources using transient stochastic climatic scenarios, Water Resour. Res., 47, W1251610.1029/2010wr010082, 2011.

Gupta, Hoshin V., Harald Kling, Koray K. Yilmaz, Guillermo F. Martinez. Decomposition of the mean squared error and NSE performance criteria: Implications for improving hydrological modeling. Journal of Hydrology, Volume 377, Issues 1-2, 20 October 2009, Pages 80-91. DOI: 10.1016/j.jhydrol.2009.08.003. ISSN 0022-1694

Hohenegger, C., A. Walser, et al. (2008). Cloud-resolving ensemble simulations of the August 2005 Alpine flood. Quarterly Journal of the Royal Meteorological Society 134(633): 889-904.

Holman, I. P.: Climate change impacts on groundwater recharge-uncertainty, shortcomings, and the way forward?, Hydrogeology Journal, 14, 637-647, 10.1007/s10040-005-0467-0, 2006.

Holman, I. P., Allen, D. M., Cuthbert, M. O., and Goderniaux, P.: Towards best practice for assessing the impacts of climate change on groundwater, Hydrogeology Journal, 20, 1-4, 10.1007/s10040-011-0805-3, 2012.

Jamieson P.D., R.J. Martin, G.S. Francis and D.R. Wilson (1995) Drought effects on biomass production and radiation-use efficiency in barley. Field Crops Research 43, 77-86.

Jaun, S., Ahrens, B., Walser, A., Ewen, T., & Schar, C. (2008). "A probabilistic view on the August 2005 floods in the upper Rhine catchment." Natural Hazards and Earth System Sciences 8(2): 281-291.

Jipp PH, Nepstad DC, Cassel DK, De Carvalho CR (1998). Deep soil moisture storage and transpiration in forests and pastures of seasonally-dry Amazonia. Climatic Change 39: 395-412.

Keese, K. E., Scanlon, B. R., and Reedy, R. C.: Assessing controls on diffuse groundwater recharge using unsaturated flow modeling, Water Resour. Res., 41, W0601010.1029/2004wr003841, 2005.

Kling, H., Fuchs, M., and Paulin, M.: Runoff conditions in the upper Danube basin under an ensemble of climate change scenarios, Journal of Hydrology, 424–425, 264-277, http://dx.doi.org/10.1016/j.jhydrol.2012.01.011, 2012.

Kristensen KJ, and Jensen SE. "A model for estimating actual evapotranspiration from potential evapotranspiration." Nordic Hydrology 6.3 (1975): 170-188.

Mertens, J., Stenger, R., and Barkle, G. F.: Multiobjective inverse modeling for soil parameter estimation and model verification, Vadose Zone Journal, 5, 917-933, 10.2136/vzj2005.0117, 2006.

Mertens, J., Kahl, G., Gottesbueren, B., and Vanderborght, J.: Inverse Modeling of Pesticide Leaching in Lysimeters: Local versus Global and Sequential Single-Objective versus Multiobjective Approaches, Vadose Zone Journal, 8, 793-804, 10.2136/vzj2008.0029, 2009.

Nash, J. E., and Sutcliffe, J. V.: River flow forecasting through conceptual models part I — A discussion of principles, Journal of Hydrology, 10, 282-290, http://dx.doi.org/10.1016/0022-1694(70)90255-6, 1970.

Overman, A.R., Scholtz, R.V., 2002. Mathematical Models of Crop Growth and Yield. Marcel Dekker, Inc., New York.

Patane, C. Leaf area index, leaf transpiration and stomatal conductance as affected by soil water deficit and VPD in processing tomato in semi arid Mediterranean climate. Journal of Agronomy and Crop Science, 2011, vol. 197, no 3, p. 165-176.

Prasuhn V., Spiess E. und Seyfarth M. (2009): Die neue Lysimeteranlage Zürich-Reckenholz. In: Perspektiven in Forschung und Anwendung. Bericht über die 13. Gumpensteiner Lysimetertagung, Irdning, 21.-22.4.09. LFZ Raumberg-Gumpenstein, Irdning, 11-16.

Racsko, P., Szeidl, L., & Semenov, M. (1991). "A Serial Approach to Local Stochastic Weather Models." Ecological Modeling 57(1-2): 27-41.

Rana, G., and Katerji, N.: Measurement and estimation of actual evapotranspiration in the field under Mediterranean climate: a review, European Journal of Agronomy, 13, 125-153, 10.1016/s1161-0301(00)00070-8, 2000.

Scanlon, B. R., Reedy, R. C., Stonestrom, D. A., Prudic, D. E., and Dennehy, K. F.: Impact of land use and land cover change on groundwater recharge and quality in the southwestern US, Global Change Biology, 11, 1577-1593, 10.1111/j.1365-2486.2005.01026.x, 2005.

Scanlon, B. R., Reedy, R. C., and Tachovsky, J. A.: Semiarid unsaturated zone chloride profiles: Archives of past land use change impacts on water resources in the southern High Plains, United States, Water Resour. Res., 43, W06423, 10.1029/2006wr005769, 2007.

Schaap, M. G., Leij, F. J., and van Genuchten, M. T.: ROSETTA: a computer program for estimating soil hydraulic parameters with hierarchical pedotransfer functions, Journal of Hydrology, 251, 163-176, 10.1016/s0022-1694(01)00466-8, 2001.

Schelle, H., Iden, S. C., Fank, J., and Durner, W.: Inverse Estimation of Soil Hydraulic and Root Distribution Parameters from Lysimeter Data, Vadose Zone Journal, 11, 10.2136/vzj2011.0169, 2012.

Scibek, J., and Allen, D. M.: Modeled impacts of predicted climate change on recharge and groundwater levels, Water Resour. Res., 42, W1140510.1029/2005wr004742, 2006.

Scibek, J.: Groundwater–surface water interaction under scenarios of climate change using a high-resolution transient groundwater model, 2007.

Semenov, M. A. and E. M. Barrow (1997). "Use of a stochastic weather generator in the development of climate change scenarios." Climatic Change 35(4): 397-414.

Semenov, M. A., Brooks, R. J., Barrow, E. M., & Richardson, C. W. (1998). "Comparison of the WGEN and LARS-WG stochastic weather generators for diverse climates." Climate Research 10(2): 95-107.

Serrat-Capdevila, A., Valdes, J. B., Perez, J. G., Baird, K., Mata, L. J., and Maddock, T., III: Modeling climate change impacts and uncertainty on the hydrology of a riparian system: The San Pedro Basin (Arizona/Sonora), Journal of Hydrology, 347, 48-66, 10.1016/j.jhydrot.2007.08.028, 2007.

Stoll, S., Franssen, H. J. H., Butts, M., and Kinzelbach, W.: Analysis of the impact of climate change on groundwater related hydrological fluxes: a multi-model approach including different downscaling methods, Hydrol. Earth Syst. Sci., 15, 21-38, 10.5194/hess-15-21-2011, 2011.

Stumpp, C., Stichler, W., and Maloszewski, P.: Application of the environmental isotope delta O-18 to study water flow in unsaturated soils planted with different crops: Case study of a weighable lysimeter from the research field in Neuherberg, Germany, Journal of Hydrology, 368, 68-78, 10.1016/j.jhydrol.2009.01.027, 2009.

Stumpp, C., and Maloszewski, P.: Quantification of preferential flow and flow heterogeneities in an unsaturated soil planted with different crops using the environmental isotope delta O-18, Journal of Hydrology, 394, 407-415, 10.1016/j.jhydrol.2010.09.014, 2010.

Stumpp, C., and Hendry, M. J.: Spatial and temporal dynamics of water flow and solute transport in a heterogeneous glacial till: The application of high-resolution profiles of delta O-18 and delta H-2 in pore waters, Journal of Hydrology, 438, 203-214, 10.1016/j.jhydrol.2012.03.024, 2012.

Stumpp, C., Stichler, W., Kandolf, M., and Simunek, J.: Effects of Land Cover and Fertilization Method on Water Flow and Solute Transport in Five Lysimeters: A Long-Term Study Using Stable Water Isotopes, Vadose Zone Journal, 11, 10.2136/vzj2011.0075, 2012.

Therrien, R., McLaren, R.G., Sudicky, E.A. (2007). HydroGeoSphere—a three-dimensional numerical model describing fully integrated subsurface and surface flow and solute transport Groundwater Simulations Group, University of Waterloo

Thornley, John HM, and Ian R. Johnson. Plant and crop modeling. Oxford: Clarendon Press, 1990.

UT-BALL-ELLE, Managed by. Worldwide historical estimates of leaf area index, 1932-2000. ORNL, 2001, vol. 27, p. 4-00.

van Roosmalen, L., Sonnenborg, T. O., and Jensen, K. H.: Impact of climate and land use change on the hydrology of a large-scale agricultural catchment, Water Resour. Res., 45, W00A15, 10.1029/2007wr006760, 2009.

vanGenuchten: A Closed-form Equation for Predicting the Hydraulic Conductivity of Unsaturated Soils, 1980.

Vereecken, H., Weynants, M., Javaux, M., Pachepsky, Y., Schaap, M. G., and van Genuchten, M. T.: Using Pedotransfer Functions to Estimate the van Genuchten-Mualem Soil Hydraulic Properties: A Review, Vadose Zone Journal, 9, 795-820, 10.2136/vzj2010.0045, 2010.

Vrugt, J. A., Bouten, W., and Weerts, A. H.: Information content of data for identifying soil hydraulic parameters from outflow experiments, Soil Science Society of America Journal, 65, 19-27, 2001a.

Vrugt, J. A., van Wijk, M. T., Hopmans, J. W., and Simunek, J.: One-, two-, and three-dimensional root water uptake functions for transient modeling, Water Resour. Res., 37, 2457-2470, 10.1029/2000wr000027, 2001b.

Vrugt, J. A., Bouten, W., Gupta, H. V., and Hopmans, J. W.: Toward Improved Identifiability of Soil Hydraulic Parameters: On the Selection of a Suitable Parametric Model, Vadose Zone Journal, 2, 98-113, 2003.

Wohling, T., and Vrugt, J. A.: Multiresponse multilayer vadose zone model calibration using Markov chain Monte Carlo simulation and field water retention data, Water Resour. Res., 47, W0451010.1029/2010wr009265, 2011.

Woldeamlak, S. T., Batelaan, O., and De Smedt, F.: Effects of climate change on the groundwater system in the Grote-Nete catchment, Belgium, Hydrogeology Journal, 15, 891-901, 10.1007/s10040-006-0145-x, 2007.

Young, M. H., Wierenga, P. J., and Mancino, C. F.: Large weighing lysimeters for water use and deep percolation studies, Soil Science, 161, 491-501, 10.1097/00010694-199608000-00004, 1996.

Yunusa, I.A.M., K.H.M. Siddique, R.K. Belford and M.M. Karimi (1993) Effect of canopy structure on efficiency of radiation interception and use in spring wheat cultivars during the preanthesis period in a Mediterranean-type environment. Field Crops Research 35, 113-122.

Zhao, L., Yang, K., Qin, J., Chen, Y. Y., Tang, W. J., Montzka, C., Wu, H., Lin, C. G., Han, M. L., and Vereecken, H.: Spatiotemporal analysis of soil moisture observations within a Tibetan mesoscale area and its implication to regional soil moisture measurements, Journal of Hydrology, 482, 92-104, 10.1016/j.jhydrol.2012.12.033, 2013.

4.9 Supporting information

Table A4. 1: Vegetation model parameters such as maximum root depth (cm) and maximum leaf area index (LAI) and transpiration limiting saturation parameters. The calibrated transpiration fitting parameters C1 to C3 are shown as well.

Crops	Max Root depth	Max LAI	Transpiration limiting saturations				Transpiration fitting parameters		
			Wiliting point	Field capacity	Oxic limit	Anoxic limit			
	(cm)	(-)					C1	C2	C3
Spelt	130	3.7	0.10	0.30	0.40	0.99	1.0E-05	1.9E-01	5.4E-01
Temporay grassland	35	1	0.10	0.30	0.40	0.99	1.0E-01	1.0E-03	3.6E-01
Field peas	90	2.5	0.10	0.30	0.40	0.99	3.1E-01	2.3E-01	4.7E-01
Colza	135	3.2	0.10	0.30	0.40	0.99	1.0E-05	2.9E-01	1.0E+00
Winter wheat	135	3.8	0.10	0.30	0.40	0.99	6.3E-02	1.3E-01	1.0E+00
Grain maize	120	3.8	0.10	0.30	0.40	0.99	1.4E-01	4.6E-02	1.0E-03
Phacelia	30	1	0.10	0.30	0.40	0.99	1.0E-05	1.0E-03	3.6E-01
Field peas	90	2.5	0.10	0.30	0.40	0.99	7.9E-02	1.7E-01	3.7E-01
Raps	135	3.2	0.10	0.30	0.40	0.99	1.0E-05	1.0E-03	1.0E+00

Table A4. 2: Climate change scenarios with associated GCMs and RCMs.

Institution	GCM		RCM	UsedAcronym
ETHZ	HadCM3	standardsensitvity (HadCM3Q0)	CCLM	ETH
HC		standardsensitvity (HadCM3Q0)	HadRM3Q0	HC
SMHI		lowsensitivity (HadCM3Q3)	RCA	SMHI_Had
MPI	ECHAM5		REMO	MPI
KNMI			RACMO	KNMI
SMHI			RCA	SMHI_ECH
ICTP			REGCM3	ICTP

Figure A4. 1: Cumulative seepage water amount between 2011 and 2085 of the transient CC simulation for crops on lysimeter 3 and 5 during their specific vegetation period is shown. The dashed black line represents the baseline (past recharge) whereas the coloured solid lines displayed the seven different GCM-RCM combinations with the associated equiprobable stochastic realisations.

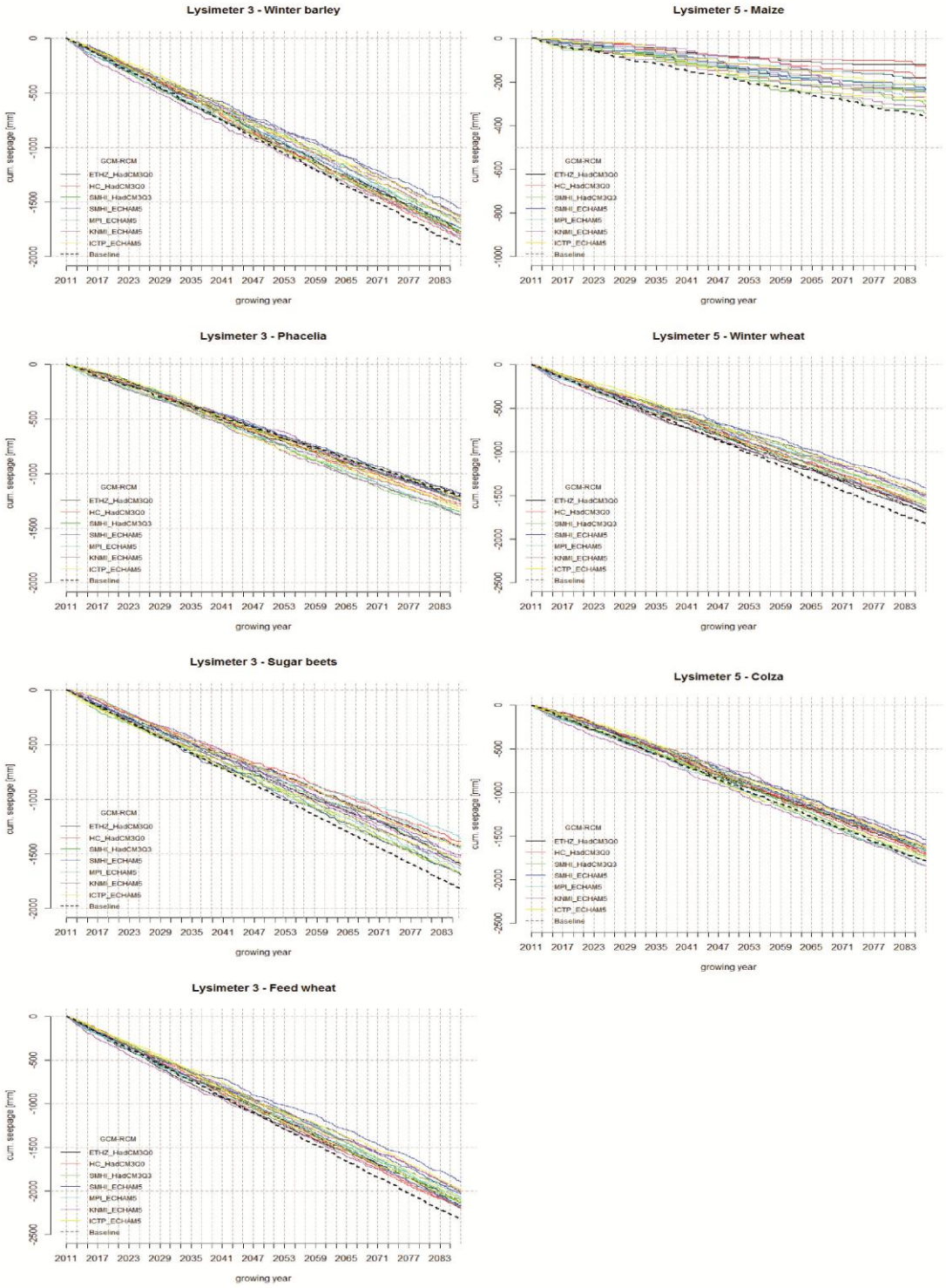

Figure A4. 2: Cumulative seepage water amount between 2011 and 2085 of the transient CC simulation for crops on lysimeter 9 and 10 during their specific vegetation period is shown. The dashed black line represents the baseline (past recharge) whereas the coloured solid lines displayed the seven different GCM-RCM combinations with the associated equiprobable stochastic realisations.

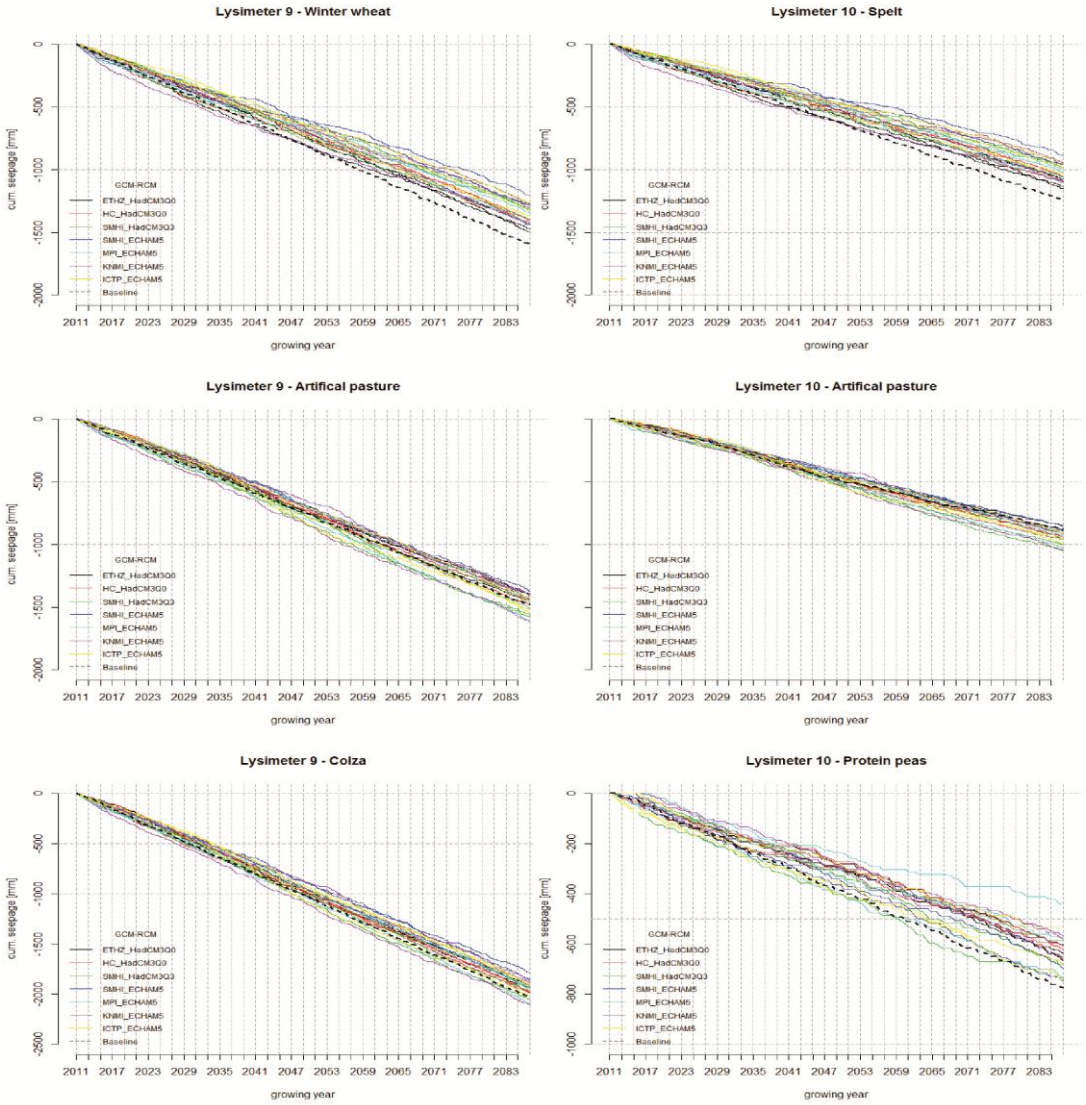

Chapter 5

5. Hydrogeological modeling of climate change impacts on a small-scale aquifer[3]

5.1 Abstract

This study explores how changes in groundwater recharge might influence groundwater levels for a small glacio-fluvial aquifer in northern Switzerland. Seasonal shifts of groundwater recharge can lead to water shortage, although annual changes in recharge or groundwater levels can be insignificant.

The physically-based model HydroGeoSphere (HGS) was used to simulate changes in recharge rates and groundwater levels based on 10 GCM (Global Circulation Model) x RCM (Regional Climate Model) combinations for the A1B emission scenario. Future recharge rates were compared to rates observed during historical drought periods and the recharge drought frequency was quantified using a threshold approach.

Temporal analysis of future recharge rates illustrates that the strongest effect of CC occurs in autumn and not in summer, when the temperature changes are the highest. For the winter season recharge rates increase for almost all climate model chains and periods.

Similar to recharge rates, the simulated groundwater levels show uncertainty for all time periods related to the climate model chain variability. The mean calculated groundwater levels, based on the 10 model chains, illustrate, however, quite a similar performance as that simulated for the past. For the seasonal variation in groundwater levels quite similar changes as observed for recharge are predicted, although the variations in groundwater levels are small. In summer and autumn temporal water stress can occur but the intensity depends on the chosen climate model chain. The uncertainty, which originated from variability among different model chains, is large, although all climate model chains shows the same trend for the changes in the seasonality of recharge and groundwater levels. Estimation of drought frequency for a "worst-case" scenario indicates an increase in frequency and intensity under predicted

---

[3] C. Moeck (1), A. Baillieux (1,3), P. Brunner (1), M.Schirmer (1,2), D. Hunkeler (1)

[1] Centre of Hydrogeology and Geothermics (CHYN), University of Neuchâtel, Switzerland

[2] Eawag, Swiss Federal Institute of Aquatic Science and Technology, Dübendorf, Switzerland

[3] INRA, Université d'Avignon, France

CC. For the water supply in Wohlenschwil water shortage will most likely more frequently occur in summer and autumn, whereas for all other seasons no water stress is predicted.

5.2. Introduction

There is strong evidence that changing climate will alter groundwater recharge rates and levels (Green et al., 2011). Seasonal shifts of groundwater recharge can lead to water shortage (Scibek and Allen 2006a). Annual changes in recharge or groundwater levels can be insignificant, but present strongly different seasonal signals when compared with past conditions. These changes in the seasonality are already mentioned in a few studies. For instance, Yusoff et al. (2002) predict for the Chalk aquifer in eastern England a decrease in recharge, especially during autumn. For this study area longer and drier summers are expected. Woldeamlak et al. (2007) simulate an increase in groundwater recharge and surface runoff for all seasons, expect for the summer for a sandy aquifer in Belgium. In contrary Brouyère et al. (2004) found that future climate changes could result in a decrease in groundwater levels, whereas the seasonal variation did not change in a relatively small watershed in Belgium. These studies show that simulations of recharge can give different responses to CC due to different study locations and groundwater systems.

While recharge and groundwater level predictions are still challenging, mathematical models can help to simulate recharge rate and groundwater level changes resulting from climate change (CC) and consequent effects on groundwater flow systems (Green et al., 2011). A common approach in CC impact studies is to use soil water balances to calculate recharge (Woldeamlak et al. 2007, Brouyère et al., 2004, Mileham et al., 2008, Mileham et al., 2009). A soil water balance is calculated with a dedicated code and the output is then sequentially used as input for a groundwater flow model. This approach is particularly appealing for large scale models as only a small number of parameters are required. Other studies have used larger scale water balances to quantify recharge e.g. by relating stream flow to groundwater recharge (Loaiciga et al., 2000, Allen et al. (2004), Scibek and Allen 2006a, Scibek et al. 2007).

Fully integrated hydrological models are increasingly used in CC impact studies (Roosmalen et al., 2007, 2009, Stoll et al., 2011) like MIKE SHE (Refsgaard and Storm 1995). Surface water and groundwater flows are simultaneously modeled with water exchanges between both domains. However, a relatively simple water balance method to compute water flows in the partially saturated zone is applied to estimate recharge. While this kind of simplification could be used in areas where the influence of the partially saturated zone is limited (for instance arid regions) and recharge occur mainly due to the interaction with rivers, it creates serious limitation in humid regions where direct recharge mainly occur.

In the past years, a range of fully coupled, physically based models such as PARFLOW (Ashby and Falgout, 1996), InHM (Vanderkwaak and Loague, 2001) and HydroGeoSphere (HGS) (Therrien et al., 2007) have been developed. These types of

models simulate simultaneously processes between the surface and subsurface for each node and time step. In contrast to the integrated models like MIKE SHE, in e.g. HGS also recharge is physically based estimated. These models are the most powerful tools for simulating hydrological processes at the moment, assuming that the necessary historical observation are available. Although the model methodology is very attractive for CC impact studies due to the fact that interconnected flow processes, such as groundwater recharge, are physical based represented, they have only been applied in a few CC impact studies so far (e.g. Sulis et al., 2012, Goderniaux et al., 2009).

The objective within the presented study is to evaluate if seasonal shifts of groundwater recharge can lead to lower groundwater levels and a potential water shortage. Such effects are mainly expected for highly transmissive systems with a low storage capacity that are expected to react rapidly to seasonal variations in recharge. Therefore, a small aquifer in Switzerland consisting of highly permeable glacio-fluvial deposits was selected. In Switzerland seasonal changes are in particular interest because according to climate models, temperatures are expected to increase in the coming decades in Switzerland, particularly large in summer (CH2011), which will raise the evapotranspiration rates. Trends for precipitation show instead differences between the summer and the winter. Projected summer precipitation will decrease, whereas winter precipitation will increase. Therefore, it is crucial to evaluate seasonal shifts of groundwater recharge to identify water shortage.
The physically-based model HGS was used to simulate the effect of CC on recharge rates and consequently on groundwater levels. The model integrates saturated and partially saturated zones, with a simultaneous solution of the flow equations in both domain using finite elements. The build 3D HGS model is based on a wide range of data, including extensive geophysical data, information from drill logs, pumping tests as well as tracer tests in both the saturated and unsaturated zone. Calibration was carried out using PEST applying a combination of pilot points method and mathematical regularization to obtain model parameter sets. Changes in recharge rates and groundwater levels were simulated based on 10 model chains (GCM-RCM combinations) for the A1B emission scenario. The A1B scenario belongs to a scenario family describing a future world of very rapid economic growth and is characterized by a balance across technological emphasis between fossilintensive and no fossil energy sources. For the applied scenario 10 different climate model chains were used in order to estimate the predictive uncertainty coming from different GCM-RCM combinations. Furthermore, future recharge rates were compared to rates observed during historical drought periods and the recharge drought frequency was quantified using a threshold approach. Changes in drought frequencies were considered due to the fact that not only the mean climate is expected to change, but also extremes such as dry spells. Finally, the effect on groundwater levels was explored. This study provide robust projections of seasonal changes in northern Switzerland, drought

frequency and consequence for the water supply system on site based on the most sophisticated model currently available for CC impact studies.

5.3. Conceptual Model Wohlenschwil aquifer

The Wohlenschwil aquifer is located in northern Switzerland, southwest of the city of Zurich. The aquifer has an approximate extension of 3km^2. The geology consists of quaternary deposits of the Würm glacial period (Figure 5.1 and 5.2a). Three different hydrological units were observed based on 10 drilling logs of 20m depth and an intensive geophysical survey, which produced 24 electrical resistivity profiles (Supporting information; figure A5.1). Old lake deposits made of stratified silt-clay material and moraine consisting of loam with a small sand content act an aquitard. The sand-gravel aquifer has a variable thickness between 3m near the northern border of the catchment and approximate 30m near the pumping station. Silty gravel can be found in the upper part of the aquifer (between 1 and 5m of the total thickness depending on the location in the catchment area) whereas the deeper zones are silt free. Hydraulic conductivity was estimated using pumping tests and ranged from $2*10^{-2}$ to $1*10^{-5}$ m day^{-1}. The latter value corresponded to the well 96-5 (Figure 5.1) where high loam content is present locally. A relative small channel in the eastern part of the aquifer, which has likely a high hydraulic conductivity, was found by the electrical resistivity profiles. This acts probably as a preferential flow path. The unsaturated zone in the plain can be described as sandy loam mix (variable in thickness but with a maximum of 12m), whereas the first 2m from surface comprise mainly loam.

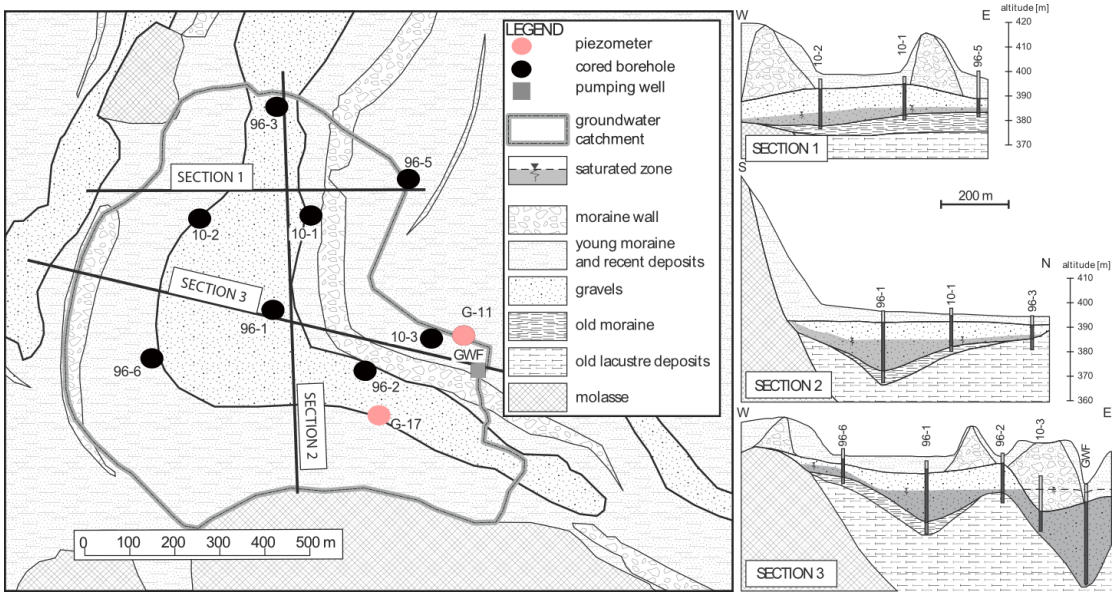

Figure 5. 11: Schematic simplified geological plane view and cross-sections of the Wohlenschwil catchment (modified from geological map).

The Wohlenschwil aquifer is used for local drinking water supply with a mean water abstraction rate of 395m^3/day. It represents a volume of around 15% of the mean annual precipitation of ≈980mm in the catchment area. The peak displacement

method was used to estimate groundwater recharge based on a tracer test. This commonly applied method (Cook et al., 1994, Scanlon et al., 2007, Healy, 2010) uses profiles of tracer concentrations and water contents obtained at different times. Vertical tracer velocity was calculated by dividing the change in penetration depth by the length of time between two sampling campaigns. Drainage rate (recharge) was calculated for the Wohlenschwil aquifer by multiplying the vertical tracer velocity (supporting information, A5.3) with measured average water content (supporting information, A. 5.5).
A groundwater budget calculation indicates additional groundwater losses through the southeastern boundary near the pumping station, where the aquifer thickness is largest. This water is most likely discharging to the river Reuss, a few kilometers downstream. The main existing vegetation cover is grassland, whereas forest only exists near the western model borders and is neglected.

5.4. Modeling

In this section the modeling approach is described. It includes model geometry and specified fluxes, followed by the calibration and scenario modeling strategy.

5.4.1 Mathematical model framework

The fully coupled hydrological model HGS (Therrien et al., 2007) was used to construct a 3D model of the Wohlenschwil study area. In HGS a control volume finite element approach is employed to simultaneously solve Richards' equation describing 3D variably-saturated subsurface flow. The fluid flux q [L T^{-1}] is given as

$$q = K k_r \nabla(\psi + z) \quad (1)$$

where ψ being the pressure head [L], k_r is the relative permeability [-] of the medium, K is the saturated hydraulic conductivity [L T^{-1}] and z is the elevation head [L].
The unsaturated hydraulic conductivity is defined by using the Mualem – van Genuchten model (vanGenuchten, 1980). Based on the work of Kristensen and Jensen (1975) actual transpiration and evaporation is simulated as a function of potential evapotranspiration, soil moisture, evaporation depth, the root distribution function over a given depth and the Leaf Area Index (Figure 5.2a). The model assumes that evaporation occurs together with transpiration. This results from the energy that penetrates the vegetation cover. For a more detailed description, the interested reader is referred to Therrien et al. (2007), Brunner et al. (2012) and Goderniaux et al. (2009)

5.4.2 Model Geometry and Specified fluxes

The model geometry was based on a wide range of data, including extensive geophysical data, piezometers installed with the direct Push technology and

information from drill logs. Pumping tests data and tracer test results in both, the saturated and unsaturated zones were further used to validate model parameterization and conceptual model structure (see supporting information).
The topography within the model domain was represented with a digital elevation model using a spatial resolution of 2m. The model domain was discretized into grid cells of approximately 30m. In the eastern part near the pumping station an outlet was simulated with a constant head boundary, perpendicular to a groundwater flow line. This boundary was assumed to be constant in time. Fully aware of possible unrealistic inflow from the constant head boundary into the model domain and consequently influence on the water balance, a modified boundary condition was used. Once the head at the boundary switched from outflow conditions to inflow, the flowrate was set to zero, which, however, occurred only twice for a short period during the scenario period 2060. Although the conceptual assumption of e.g. water loss (discharging water) is uncertain, it is the most realistic conceptual modeling approach based on the available geological information.
The model domain was divided into 21 model sub-layers vertically. A vertical variable model nodal distance is applied. The vertical discretization is variable where nodal distance (distance between the 21 model sub-layers) is less than 5cm near the surface and approximately 2m at the bottom of the model domain. The small layer thickness near the surface was chosen to avoid over- or under-estimation of infiltration and evaporation fluxes, which can occur by nodal distances larger than 5cm (van Dam and Feddes, 2000). The first geological unit can be descripted as loam and reach a maximum depth of 2m (Figure 5.2a). The second geological unit is referred as sand to a loamy sand mix. Hydraulic parameters of the unsaturated zone were estimated using the program Rosetta (Schaap et al., 2001), a pedo-transfer model, which predicts soil hydraulic parameters from soil textures. Information about the soil texture up to a depth of 20m was obtained from grain size analysis at three locations in the catchment. For the remaining geological unit parameters are distributed referred to gravel sand mix where hydraulic conductivity values and distributions were calibrated with a pilot point calibration approach. A van Genuchten parameterisation was applied and the depth of the unsaturated zone is controlled by the groundwater table itself. Three types of specified hydrological fluxes were used. These fluxes are daily precipitation and daily potential evapotranspiration as well as weekly groundwater abstraction rates at the pumping well taken as inputs to the model.

5.4.3 Calibration, Model parameters and Modeling strategy

Calibration of the distributed hydraulic conductivity of the saturated zone (bottom layer, sand-gravel geological unit) of the 3D model was carried out using PEST (Doherty, 2010) (Figure 5.2b). Daily values from March 2009 to May 2011 from groundwater levels (Figure 5.1) were used as observations for the calibration. The weight of the observation corresponded to $1/\sigma$, where σ was the measurement error of 0.02 m. Initial values for the aquifer material were based on pumping test results.

Hydraulic conductivities were calibrated subsequently with a pilot points approach (Doherty, 2003), using 14 pilot point locations. Calibration of a model using pilot points involves the following steps. Pilot points were distributed over the model flow domain, the mesh network emulating the study site. The model hydraulic conductivity parameters were associated with each pilot point. Once the pilot points were defined, PEST interpolates the values between the pilot points. The model was then run with the given parameter field, and an objective function was calculated by comparing measured and simulated observations.
In the subsequent calibration, pilot point values were varied and the corresponding objective function was calculated. PEST modifies the pilot point values to minimize the objective function. This procedure was repeated until PEST aborts the calibration process following the predefined convergence criteria. Additionally in this calibration exercise, mathematical regularisation, Tikhonov regularization and Singular value decomposition (SVD) was applied. Prior information (pumping test values for the hydraulic conductivity) was used to include expert knowledge in the calibration process. Mathematical regularisation avoids further over-fitting and numerical instability caused by the generated heterogeneity of the model hydraulic conductivity. All remaining model parameters were not calibrated and were based on literature values or field test data. Table 5.1 present the used model parameters.

Table 5. 1: Van Genuchten parameters, residual water saturation, total porosity, specific storage and saturated hydraulic conductivity. The hydraulic conductivity range for the gravel-sand aquifer is obtained by the calibration.

	Van Genuchten parameters		Residual water saturation	hydraulic conductivity
	α [1/m]	β [-]	S_{wr} [-]	K [m/sec]
Upper soil	3.6	1.6	0.078	$2.9E^{-6}$
lower soil	14.5	2.7	0.045	$8.3E^{-5}$
Gravel-sand aquifer	14.5	2.7	0.045	$7.4E^{-5}$ - $9.2E^{-3}$

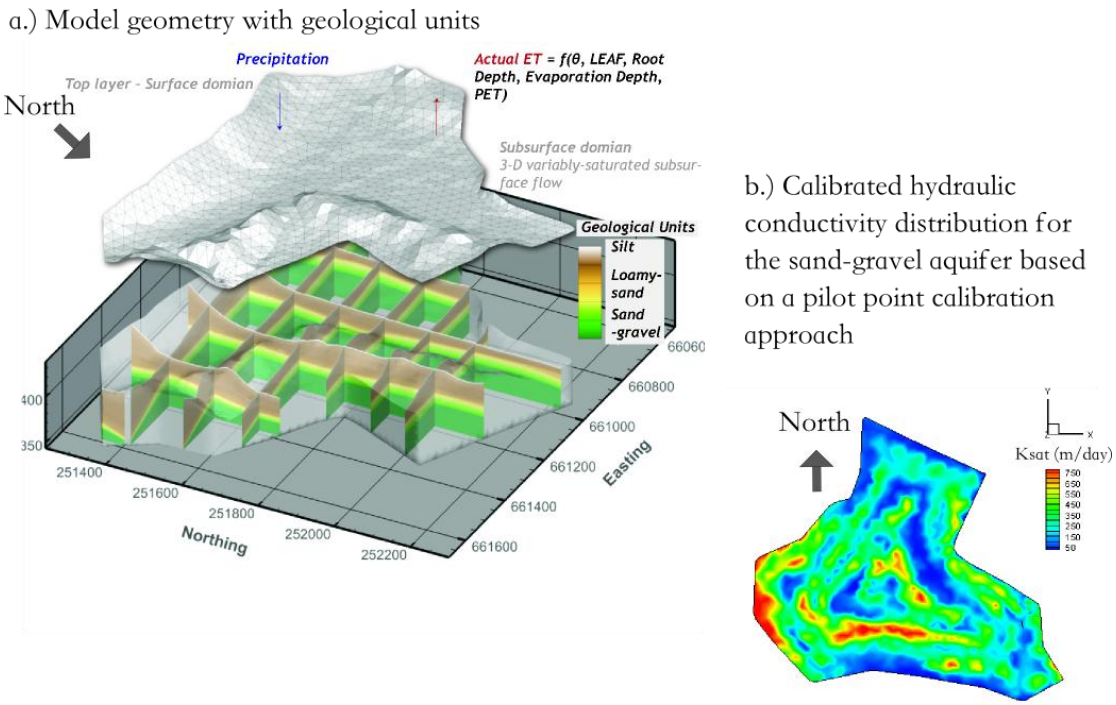

Figure 5. 12: a.) Model geometry with finite element model mesh and geological units b.) Calibrated hydraulic conductivity (K_{sat} m/day) distribution for the sand-gravel aquifer based on the pilot point calibration approach.

The modelling strategy includes simulations for the 3D model for the past time series (1983-2012) as well as for the three future time periods (2035 (2021-2050), 2060 (2045-2074) and 2085 (2070-2099)) in order to compare changes in recharge rates, groundwater levels and drought frequency under CC. Recharge rates were estimated as the vertical fluid flux reaching the water table. Initial head conditions for each time period were obtained by running a steady-state model with mean climatic input data of the chosen time scenario.

5.5. Climate change scenarios

In this section, the past and future climatic data are presented. They are used as daily inputs for the numerical model. The past weather conditions are used to simulate past conditions. Those can be compared against the simulated recharge rates and groundwater levels changes of future time periods.

5.5.1 Past climatic data

Meteorological data from 01.01.1983 to 31.12.2012 was used on a daily time step. The time series was measured at the MeteoSwiss weather station in Buchs, Switzerland 10 km away. Following the FAO guidelines (Allen et al., 2005) the potential evapotranspiration was calculated using the Penman Montheith equation.

5.5.2 Future climatic data

To simulate future weather conditions, a total of 10 model chains for the A1B emission scenario, which are moderate in terms of CO_2 emission increases, are used (Nakicenovic et al., 2000). Model chains consist of combinations between general circulation models (GCM) and regional climate models (RCM) (Table 5.2).

Table 5. 2: Climate change scenarios with associated GCMs and RCMs.

Institution	GCMs		RCMs	Used Acronym
SMHI	BCM		RCA	SMHI_B
ETHZ	HadCM3	Standard_sensitvity (HadCM3Q0)	CCLM	ETH
HC		Standard_sensitvity (HadCM3Q0)	HadRM3Q0	HC
SMHI		Low_sensitivity (HadCM3Q3)	RCA	SMHI_Had
MPI	ECHAM5		REMO	MPI
DMI			HIRHAM	DMI
KNMI			RACMO	KNMI
SMHI			RCA	SMHI_ECH
ICTP			REGCM3	ICTP
CNRM	ARPEGE		ALADIN	CNRM

For regional scenarios delta change values provide by MeteoSwiss for selected stations were used. These daily time series of delta change factors for precipitation and mean temperature relative to the reference period of 1980-2009 are provide for three scenario periods. These scenario periods are 2035 (2021-2050), 2060 (2045-2074) and 2085 (2070-2099).

An increase in temperature for all periods compared to the reference period can be observed (Figure 5.3; temperature column). The strongest increase occurs in summer with a maximum in August whereas the smallest change in temperature was predicted between February and March. Temporal distributions for precipitation show an increase between autumn and winter as well as a decrease in summer until autumn (Figure 5.3, precipitation column). The GCM-RCM combinations create an uncertainty range for precipitation and temperature, which shows that predictions depend strongly on the chosen model chain. In this climate data set, the dry or wet spell duration will not change under future time periods and indicate clearly the restriction of the delta change approach.

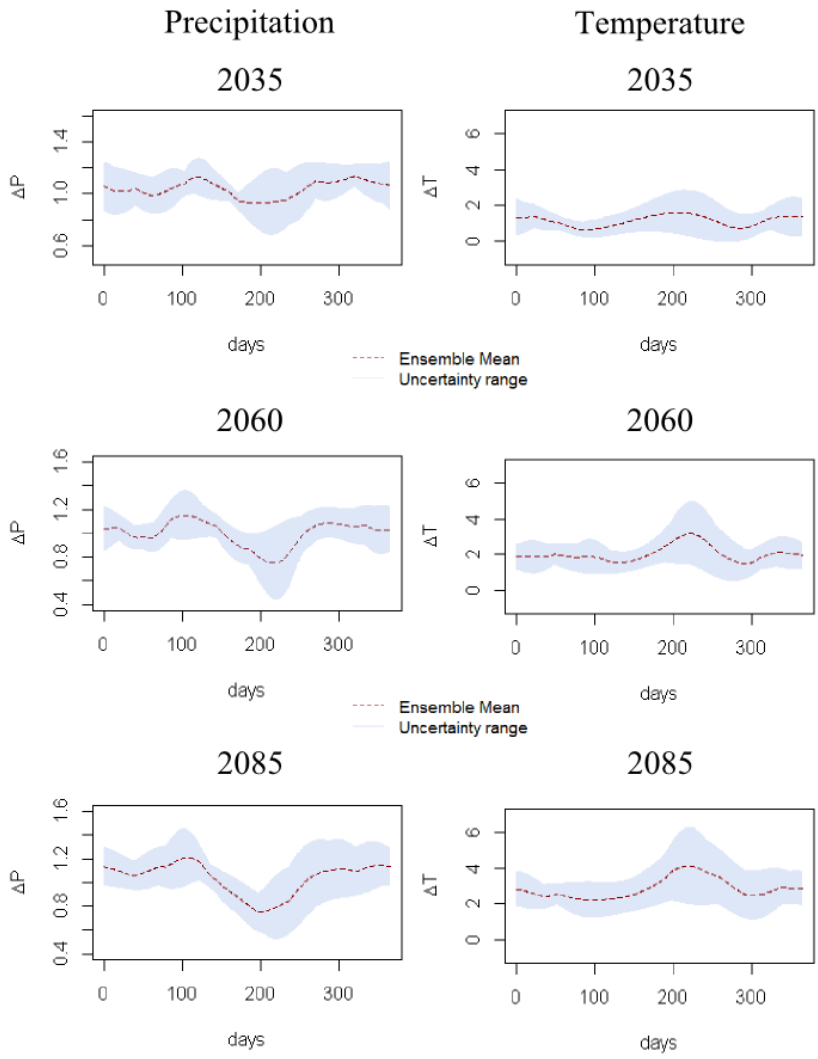

Figure 5. 13: Ensemble means (red dashed line) and uncertainty ranges (gray shaded area) of daily climatic change factors for 10 GCM-RCM combinations of the A1B scenario. Left column show changes in daily precipitation and right column in daily mean temperature for the time period 2035, 2060 and 2085 for the Meteoswiss weather station Buchs.

5.6 Results and discussion

At first, some results are presented that illustrated how well the model fit observations. Then the simulated recharge rates for past and future periods are introduced. Simulated annual past and future recharge rates are shown, followed by a discussion about the seasonal effect of CC on recharge rates, to identify possible future water stress. After a detailed analysis of simulated recharge rate, the change in groundwater levels is presented to consider both recharge and groundwater level fluctuation under CC. Finally, the change in "drought" frequency is considered based on a threshold approach.

5.6.1 Calibration

A comparison between simulated and observed transient groundwater levels is given for six selected piezometers in the study area between March 2009 and May 2011. Continuous and manual measurements were used, where half of the time series were used for the calibration and the second for the validation. The best fit is observed for well 961 where most observations are available (Figure 5.4). A different weighting strategy might increase the calibration for some wells but this is not the scope of this study. However, for the whole time series, simulated groundwater levels reproduce the observed variations in historical data quite satisfactory with a mean absolute error of 0.10m for all observations. There are two sharp increases in the simulated groundwater levels for all wells between June of 2009 and September of 2010. The assumption of horizontal uniform soil hydraulic parameter distribution presents a conceptual model simplification. This can lead to local misinterpretation of recharge fluxes and groundwater level fluctuations. However, the simulated first peak in the groundwater levels for piezometer 965 is also observed in the historical groundwater levels. Another, quite important limitation is the unknown model border where groundwater is discharging to the river Reuss. This boundary condition may not be verified locally. The groundwater loss, for instance, might be variable along this border but was simulated to have a uniform loss. Also, the low time resolution of pumping data (only weekly information was available) implies a limitation for the calibration. This fact can lead to a non-agreement of simulated and observed daily groundwater levels.

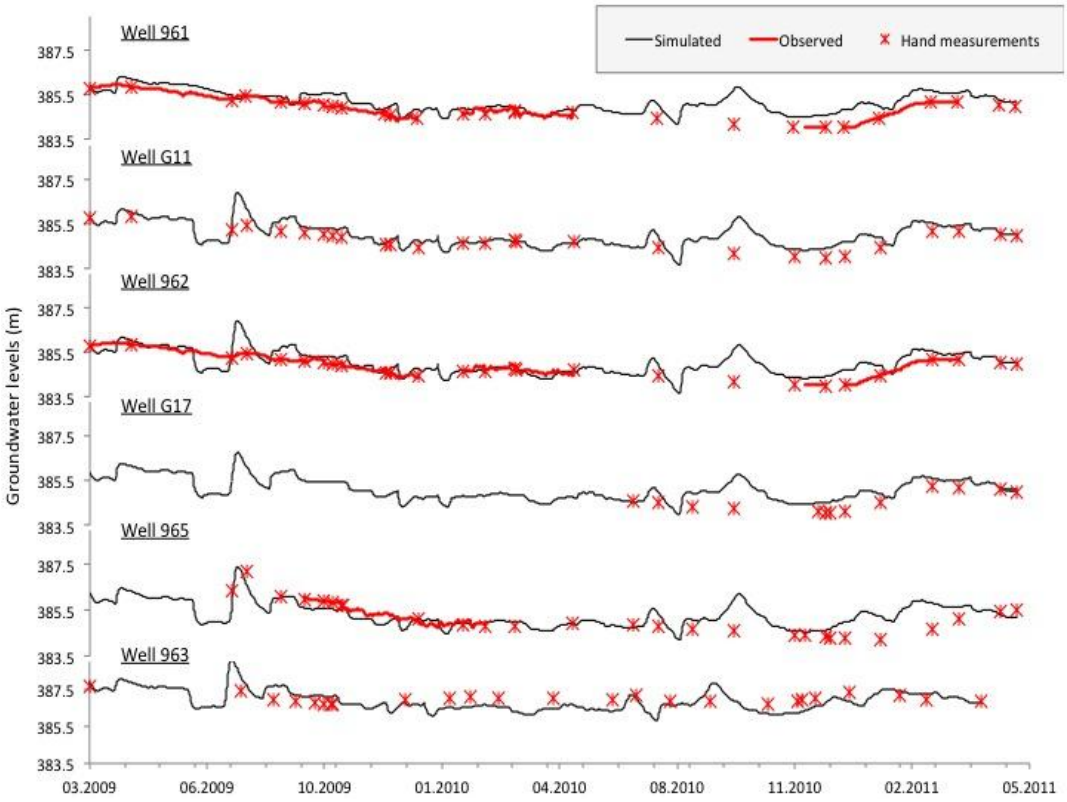

Figure 5. 14: Transient calibration of groundwater levels for six piezometers from March 2009 to May 2011.

5.6.2 Projected annual change in recharge

Using the calibrated model and 10 climate model chains for each time period, simulations were run to project the CC impact on groundwater recharge at the Wohlenschwil catchment and project the predictive uncertainty originating from climate model chain variability. In Figure 5.5, the change between the past to future annual recharge is presented for the three time periods. The mean simulated past recharge is 352mm. A similar recharge rate (370 to 390 mm) was also obtained with salt tracer tests in the catchment at two locations with the peak displacement method.

Furthermore, comparing past with future mean recharge rates indicates both, increasing and decreasing trends in recharge rates depending on the chosen climate model chain. Variations in predicted recharge rates can be observed to originate from the variability among the different GCM-RCM combinations for all periods.

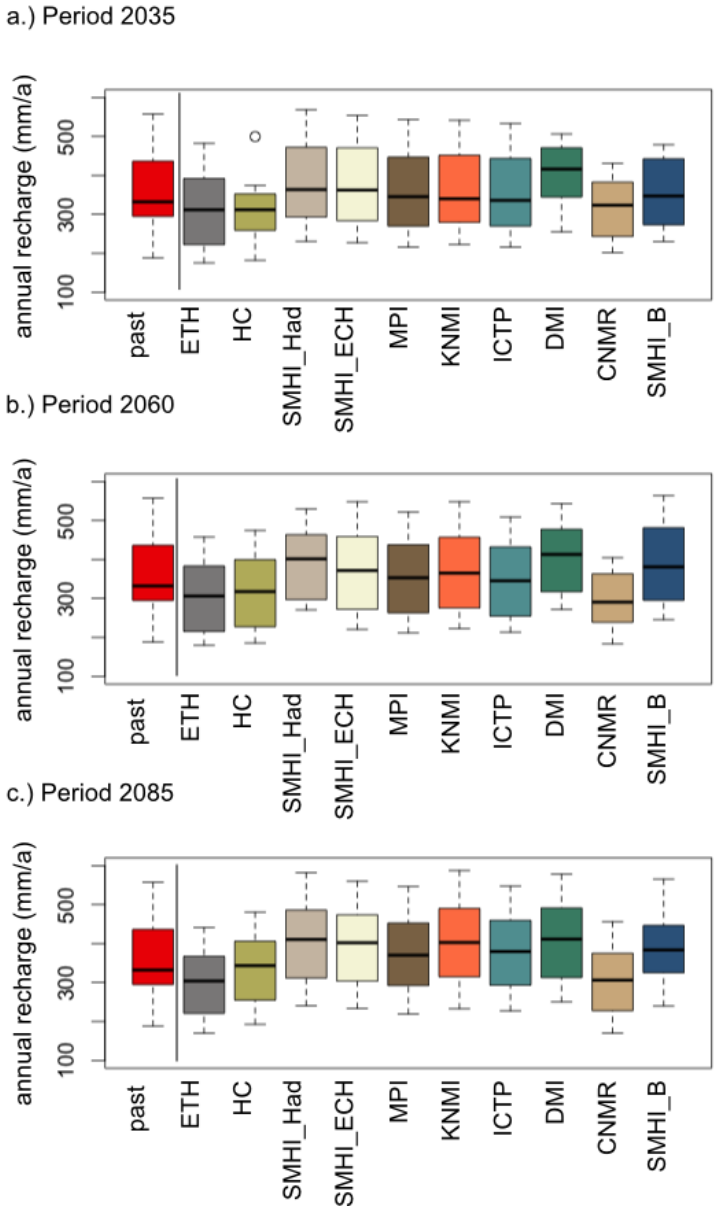

Figure 5. 15: Boxplot of annual recharge (mm/a) evaluation for 10 model chains for time periods a) 2035, b.) 2060 and c.) 2085.

Although predicted recharge rates show variability, a mean decrease of only -0.2% for the period 2035 is obtained (Table 5.3). This value, however, lies between a maximum increase of 15.6% (55mm) and decrease of 13.1% (46mm) (Table 5.3 and figure 5.5). Under the period 2065 similar results for recharge are obtained (Figure 5.5b). A mean decrease of -0.6% is simulated but again with a wide recharge rate spreading originated by variability among the different GCM-RCM combinations. For the period 2065, each model chain predicated a change in the same direction as in 2035. For the period 2085, a small increase in mean recharge of all model chains (2.6%; 9mm) can be observed compared to the past recharge but with an uncertainty range of -16.2% to 12.8%. For a few climate model chains the trend changes from a decreasing to an increasing annual recharge (Table 5.3), which is mainly due to a recharge increase during winter (see next section; projected seasonal change).

The values on the lower whisker for the past annual recharge rate correspond to more extreme years such as that observed in 2003, a well acknowledged European summer heatwave (Seneviratne et al. 2012, Schaer and Jendritzky 2004). In this year, documented water shortages occurred at the Wohlenschwil site. The pumping rates had to be reduced and the community was required to switch to an alternative source of water. Because of this water shortage in 2003 in Wohlenschwil, the most extreme climate model chains are particularly interesting. The model chains ETH, HC and CNMR project the highest temperature increase and precipitation decrease. It is interesting to note that values on the lower whisker for the past annual recharge rates are no longer "extremes" for the ETH, HC and CNMR climate model chains. Of these model chains, a large part of the 50% range (box) of the annual future recharge rates is shifted down. The predicted values are now partly congruent with the lower whisker under the past recharge conditions. The whisker is the vertically line prolonging from the box (lower and upper quartile). It shows values and variability outside the upper and lower quartile. In contrast, using the model chains DMI, SMHI_Had and KNMI as inputs for the hydrological model, the highest increase in recharge rates are simulated due to less extreme climatic conditions for the entire year.

Table 5. 3: Percentage change in mean annual recharge for each climate model chain and statistics for each time period.

Percental (%) change in mean annual recharge			
Period	*2035*	*2060*	*2085*
ETH	-13.1	-14.5	-16.2
HC	-11.6	-11.1	-7.1
SMHI_Had	6.5	11.1	12.5
SMHI_ECH	5.4	3.4	9.1
MPI	0.3	-1.7	3.7
KNMI	1.7	2.8	11.9
ICTP	-0.3	-3.1	5.4
DMI	15.6	14.5	12.8
CNMR	-7.4	-16.5	-15.1
SMHI_B	1.1	8.8	8.8
Min	-13.1	-16.5	-16.2
Max	15.6	14.5	12.8
Mean	-0.2	-0.6	2.6

5.6.3 Projected seasonal change in recharge

The predicted changes in seasonality were investigated. The mean recharge rate for each month is calculated for a 30 years period of each time period. It is shown that seasonal recharge under future climate conditions has a distinctly different temporal distribution compared to the past condition (Figure 5.6). For January and February, calculated monthly mean recharge rates increase for all climate model chains and time periods compared to past conditions. Although a temperature increase is predicted, the precipitation amount will also increase during these months, especially for the 2085 period. The strong precipitation increase during these months is therefore the controlling factor for increasing recharge. For March and April, a recharge increase can be observed for the 2085 period due to higher precipitations, whereas for the 2035 and 2060 periods a decrease is predicted (Figure 5.3) as precipitation changes little while temperatures increase. Interestingly, the strongest effect of climate change occurs in late summer and autumn for all periods (September, October and November) and not in mid-summer, when the temperature changes are the highest. One reason is that summer evapotranspiration exceeds precipitation and hence an increase in the evapotranspiration rates in this period does not have much effect on recharge. Another reason is an elongation of the "summer" period into autumn which is induced in the first place by a change in the climatic forcing functions due to CC (delta change signals). The higher temperature and less precipitation in autumn can be considered as an elongation of the summer period. Another effect is the soil moisture memory. A stronger drying out of the soil during hotter and drier summers leads to less recharge. As a result of the depleted unsaturated zone with less soil moisture (see figure A5.5; supporting information), a larger amount of precipitation is required in autumn until considerable recharge occurs compared to the past conditions.
Interestingly, some shifts in the recharge regime, such as those observed for January-February as well as September-October, are obvious under all periods and climate model chains. Although the climate model chains show a large predictive uncertainty for annual recharge rates they have similar changes in the seasonality.

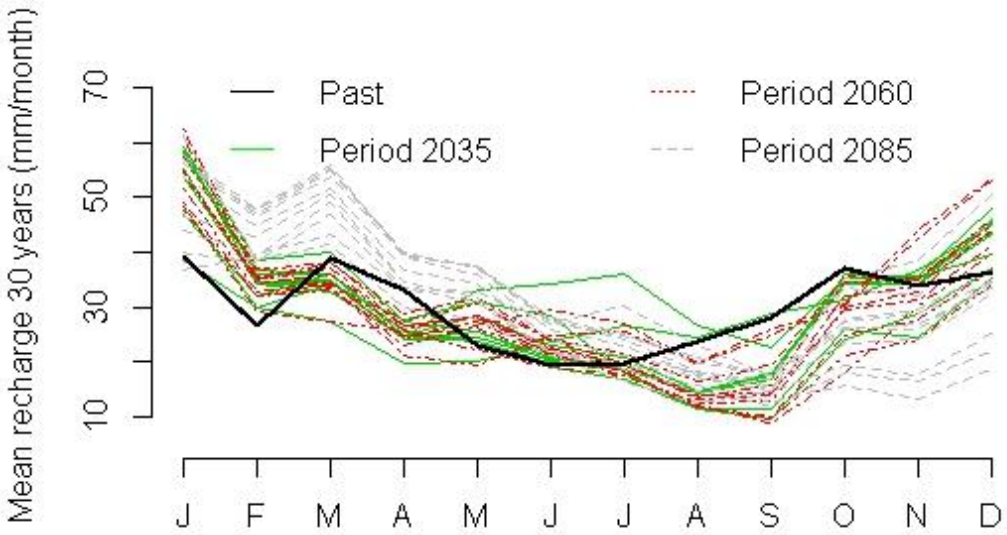

Figure 5. 16: Monthly mean recharge rates for the three time periods over 30 years simulation and past conditions (black line). Seasonal decomposition was done for all model chain.5.7.4 Projected change in groundwater level

The temporal evolution of the groundwater levels at the observation well 96-1 for 30 years for each time period (Past, 2035, 2060 and 2085) is given in figure 5.7. This observation well was chosen because well 96-1 represents the dynamics of the whole aquifer quite well. In figure 5.7, an increasing as well as decreasing trend (grey area) can be observed compared to the baseline groundwater level (black line) according to the considered model chain. The simulated groundwater levels show a large uncertainty for all time periods originated from variability among the climate model chains (grey shaded areas). Comparatively, however, the mean calculated groundwater level (green line), based on the 10 model chains, show quite a similar behavior as that simulated for the past.

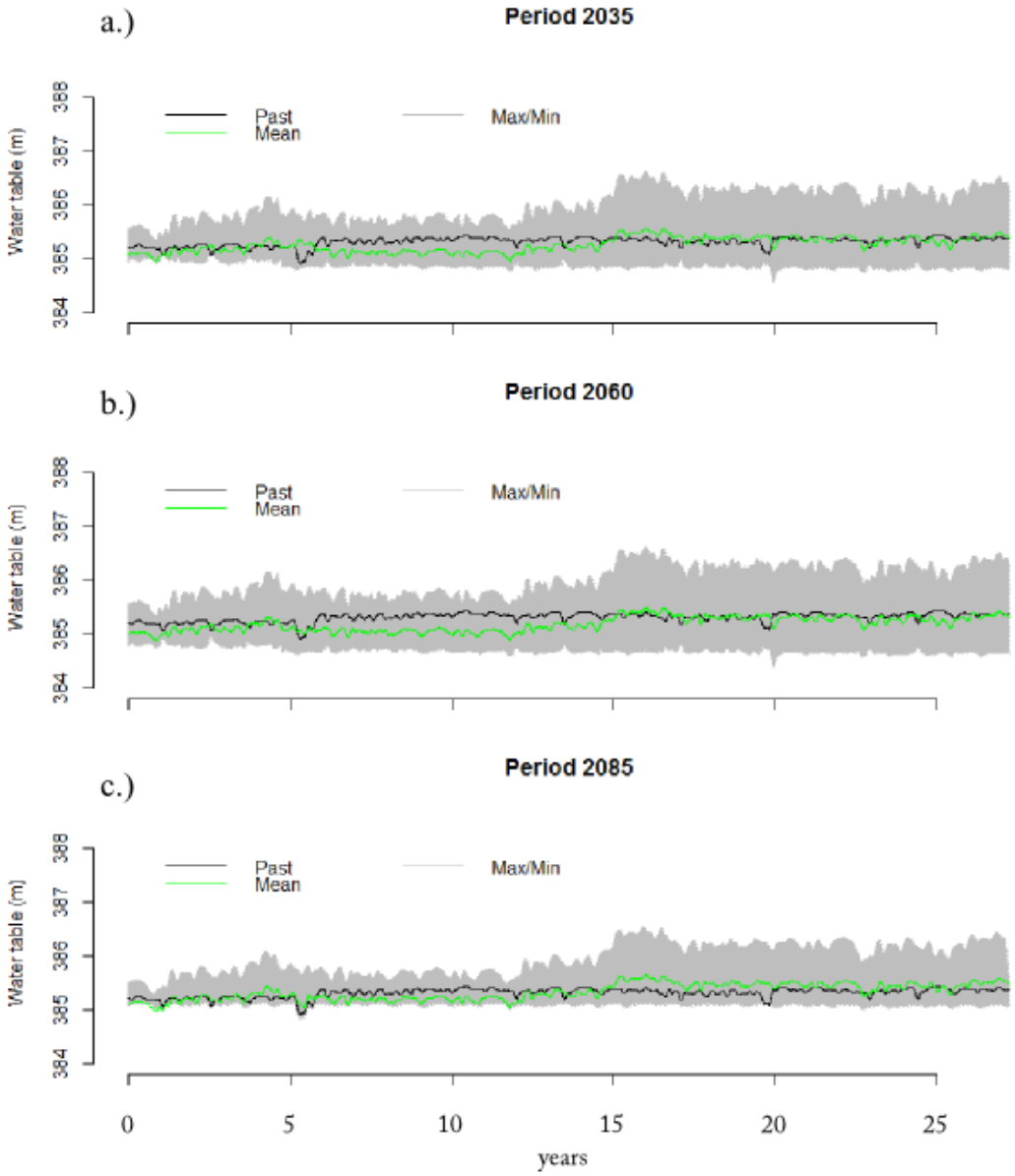

Figure 5. 17: Evolution of the groundwater levels (Water table) at well 96-1 for a.) Period 2035 (2021-2050), b.) Period 2060 (2045-2074) and c.) Period 2085 (2070-2099). The grey shaded line shows the uncertainty range originated from variability among the 10 climate model chains. The black line shows the references period, whereas the green line displays the mean calculated groundwater level based on the simulations under the 10 different climate model chains.

Only small differences exist between all the periods (Table 5.4), where a small decrease is predicted in mean groundwater levels for the period 2035 and 2060 (-0.05 and -0.03m) and an increase for period 2085 (0.02m). However, the uncertainty range (min/max) is clearly higher, but generally speaking, the changes in groundwater levels are still small.

Table 5. 4: Changes in groundwater levels (Δ h) for 2035 (2021-2050), 2060 (2045-2074) and 2085 (2070-2099) for 10 model chains compared to the reference period.

	Period 2035			Period 2060			Period 2085		
	min	max	mean	min	max	mean	min	max	mean
Δ h (m)	-0.45	0.69	-0.03	-0.61	0.45	-0.05	-0.23	0.67	0.02

5.6.5 Projected seasonal change in groundwater level

Change in seasonality for groundwater levels at well 96-1 is investigated in a similar manner like done for recharge. Only small variations in groundwater levels are observed (Figure 5.8), contrastingly to the recharge rates where a marked change in the seasonality is present (see section 5.3). The changes in the seasonality for groundwater levels are, however, consistent with the simulated changes in recharge seasonality. Only the groundwater levels are more smoothed. Lower groundwater levels are predicted for autumn (mainly September and October) compared to the past condition. The already observed shift in the lowest values from summer into autumn from recharge occurs again for groundwater levels, which is induced by the change in recharge inputs. In March and April a small increase is present such as observed also for recharge.

It can be speculated why the simulated and also observed variations in groundwater level seasonality are smaller than the simulated recharge. On one hand inflow from southern and western borders are possible, where the hydraulic conductivity is lower than in the model plain (see Figure 5.2b), where all groundwater observations are present. The lower hydraulic conductivity inhibits a rapid flow into the plain. Therefore, inflow from the border discharge into the model plain with a delay and leads to smooth groundwater levels. On the other hand, low hydraulic conductivity are also present close to the boundary, where water is most likely discharging to the river. Again a rapid outflow is inhibited and leads that water in the plain are enclose by low hydraulic conductivity. Strong fluctuations in the groundwater levels cannot occur, because water is only slow discharging. In any case, the simulated seasonal fluctuation and magnitude of groundwater levels are consistent with field observations.

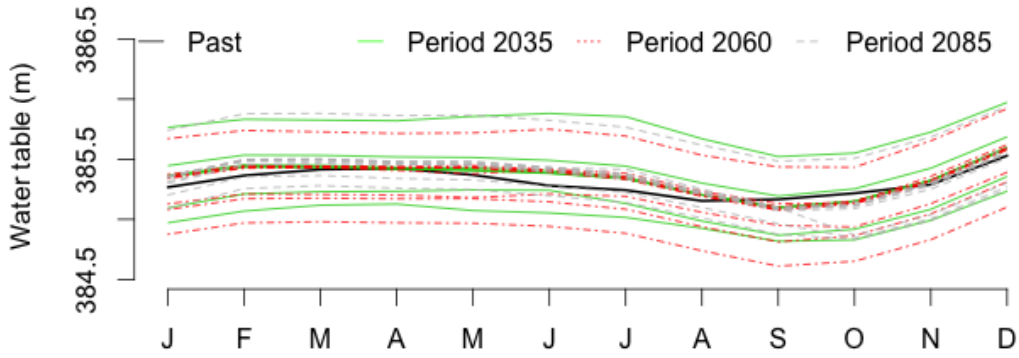

Figure 5. 18: Monthly mean groundwater levels for the three time periods for the past and future periods.

5.6.6 Drought frequency

Up to now, mean changes in annual and monthly recharge or groundwater levels are discussed, but how drought frequencies altered under CC has not been considered. The changes in drought frequency, however, are crucial for an efficient water management, and not changes in mean conditions. Schär et al. (2004) pointed out that by the end of 2100 every second summer could be as warm as the summer of 2003, a well-acknowledged European summer heatwave (e.g. Stott et al. 2004, Orsolini and Nikulin 2006). In addition, as suggested by the recharge calculations, less recharge such as the one that occurred in the years 2003 and 2011 (are referred as a recharge "drought") are expected to occur more frequently for some specific model chains (see section 5.2). The ETH model chain was chosen because this model chain shows the highest potential that recharge droughts such as that observed for 2003 are shifted from values of the lower whisker to normal conditions and acts therefore as a "worst-case" scenario.

In this study droughts are defined by a threshold level approach (Peters et al., 2005), where values smaller than the threshold are considered as droughts. The calculation is based on recharge or groundwater levels difference, where first the mean monthly values from the entire past period were calculated and used as a baseline. Then the monthly mean values for each period (Past, 2035, 2060 and 2085) were calculated and subtracted by the former calculated values from the entire past period. This calculation was carried out to remove normal seasonality effects. To obtain threshold values, which correspond to the heat wave in 2003 recharge differences between the year 2003 and the mean monthly values from the entire past period were calculated. The chosen threshold values from this calculation correspond to the months June and

September from the summer heat waves 2003, two distinct periods of exceptional heat developing (Fischer et al., 2007).

In Figure 5.9, recharge differences for each time period are shown, where higher recharge values than the mean monthly recharge from past conditions are displayed in red colors and lower values in white. The light red lines correspond to the threshold values (June (upper) and September (lower line) from the summer heat waves 2003. For all periods most values are located over the threshold lines, but with increasing time period the already dry periods with less recharge are intensified and reaching the threshold values. As expected from the climatic input data, the already wet climate conditions and seasons like spring are intensified and recharge rates increase, whereas dryer period become dryer. However, using the delta change approach, as was done in this study, only the frequency and intensity of droughts can be investigated. Changes in duration cannot be considered. This is due to the fact that the weather statistic not changed for future periods. By using the delta change approach historical measured climatic conditions were repeated with the associated shift caused by the delta values for precipitation and temperature.

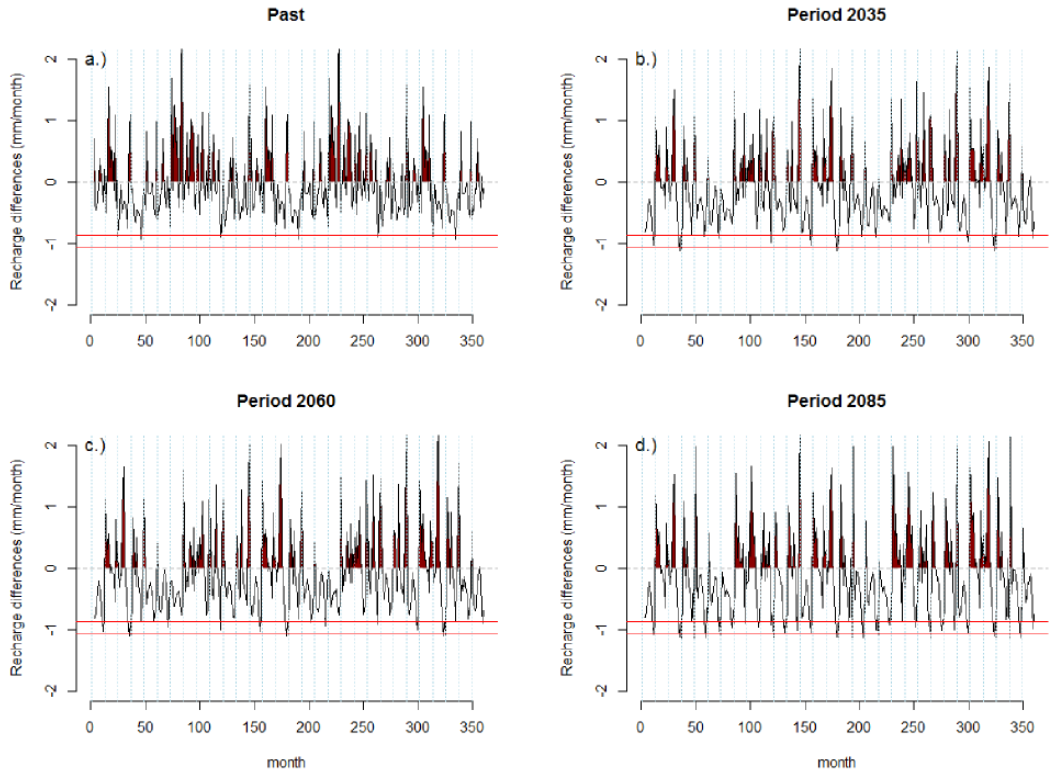

Figure 5. 19: Monthly recharge differences (mm/month) from mean monthly recharge values from the reference period (1983-2012, 360 months) for the a.) Past (1983-2012), b.) Period 2035, c.) Period 2060 and d.) Period 2085. Red lines correspond to the threshold values from the summer heatwave 2003.

The mean of the recharge differences distribution does not change under all future periods (Figure 5.10a). In contrary the skewedness of the distribution is variable under CC. A shift in the distribution of recharge rates towards a recharge deficit (values smaller than 0) can be observed. Due to this change calculated recharge

difference exceeding the threshold more frequently. The amount of months lying under the chosen threshold increase with increasing time period and a few simulated recharge differences in future can be considered as droughts such as that observed for 2003 or stronger. For the past period only eighth months are simulated under the smaller threshold value. For the 2035 period 15 events under the smaller threshold are found with additionally six events stronger than the heat wave of 2003 (larger threshold value). When comparing period 2035 and 2060, only small differences in drought frequency are observed, whereas Period 2060 has only four events more but still a similar amount of stronger drought events. For the period 2085 39 recharge differences values are found under the threshold. In addition, 17 events are stronger than the extreme heat wave of 2003. A comparison of drought frequency under past conditions and 2085 period indicate an increase in drought frequency from 2.2 (past condition) to 10.8% (2085 period).

Also the drought potential increase for groundwater levels with increasing time period. Under the 2035 and the 2060 period, an increasing potential of droughts is shown. For period 2035, 6% of the simulated months can be considered as drought but not stronger than 2003. In contrast, for period 2060 additionally 3% of all months over the simulation time can be considered as droughts stronger than 2003. For the period 2085, more than 50% of data can be determine as droughts, which seems to be very high and is probably influence directly by the estimated initial conditions from the steady state model run (see section 3.4). As mentioned already, the initial heads for each time period were obtained by running a steady-state model with mean climatic input data of the chosen time scenario. The already low simulated initial heads are close to the threshold values and simulated recharge rates for the future periods are not able to increase groundwater levels. Certainly, a “worst case scenario is investigated here and is not representative for all climate model chains. However, the threshold can be considered as a very extreme case and uncommon in past events. Due to this chosen extreme threshold, simulated increase in drought frequency in the future described probably only the upper bound of drought frequency increase. In this context unsevere droughts are not investigated. Nevertheless, this “extreme case” already shows clearly an increasing potential in frequency.

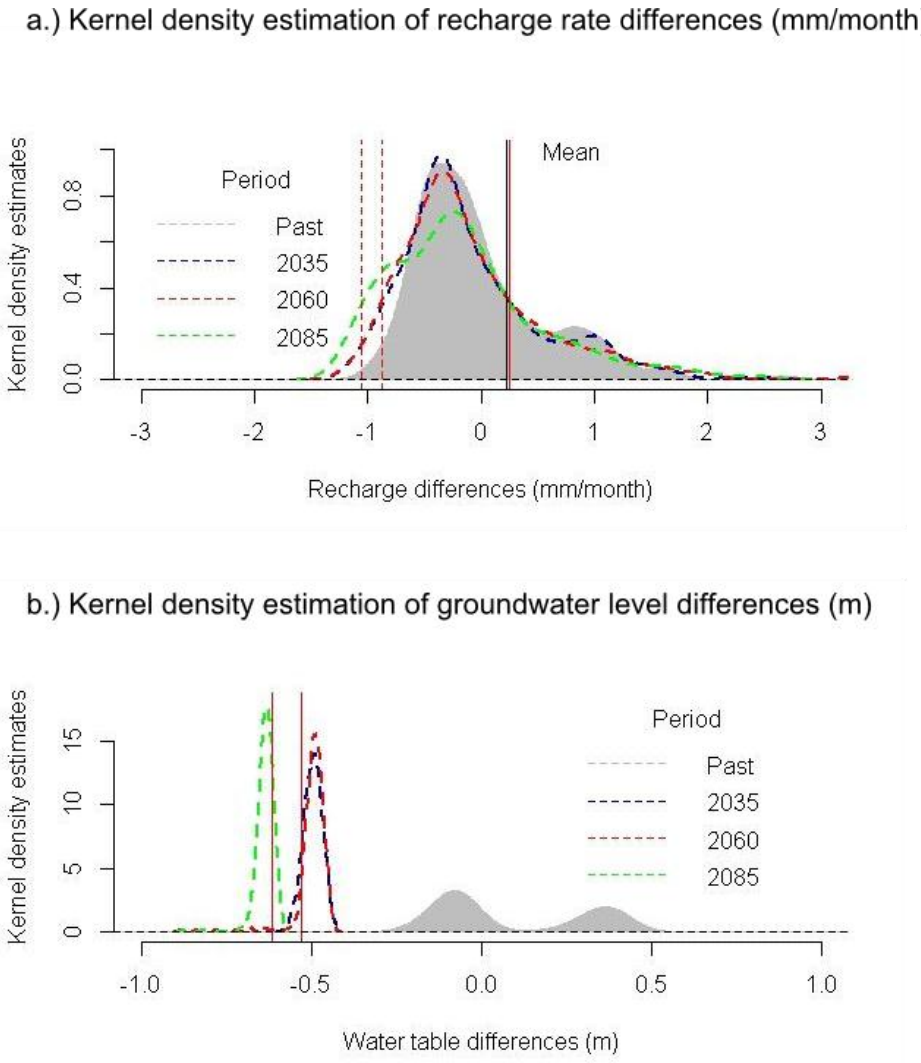

Figure 5. 20: a.) Probability density function (Kernel density estimates) of recharge differences (mm/month) for past period (grey area), Period 2035 (blue dashed line), Period 2060 (red dashed line) and Period 2085 (green dashed line). The red vertical lines correspond to the threshold values from the summer heatwave 2003. b.) Kernel density estimates of groundwater level differences (m). The Kernel density estimation is a non-parametric way to estimate the probability density function.

5.7 Summary and Conclusion

A physically based flow model is used to evaluate the impact of CC for a small scale aquifer in Northern Switzerland. The study was carried out by considering the soil-unsaturated zone-groundwater system as a whole using the physically-based model HGS. The model was calibrated using a combination of pilot points and mathematical regularization to obtain hydraulic conductivity values. For the applied scenarios, 10 different climate model chains were used in order to estimate the predictive uncertainty originated from variability among different GCM-RCM combination for three future time periods.

Simulated mean past recharge is 352 mm, which lies in the same range as that obtained with a peak displacement method. Mean annual recharge rates altered only to a small percentage for the Period 2035 and 2060 under all model chains, but increase for the period 2085.

Changes in recharge rate seasonality shows that the strongest effect of CC occurs in autumn and not in mid-summer. One reason is that summer evapotranspiration exceeds precipitation and hence an increase in the evapotranspiration rates in this period does not have much effect on recharge. Another reason is an elongation of the "summer" period into autumn which is induced by a change in the climatic forcing functions due to CC (delta change signals). The high temperature values from the summer period are still present in autumn. Therefore, the higher temperature and less precipitation in autumn can be considered as an elongation of the summer period. Another effect is the soil moisture memory, which is effect by hotter and drier summers. A stronger drying out of the soil leads to less recharge. As a result of the depleted unsaturated zone with less soil moisture, a larger amount of precipitation is required in autumn until considerable recharge occurs compared to the past conditions. However, although the climate model chains show a large predictive uncertainty for annual recharge rates, they have similar changes in the seasonality. Apart from the uncertainty in the absolute values the trend in the seasonality is equal and indicate that the potential for water shortage will increase not only in summer but also in autumn.

Similar to recharge rates, the simulated groundwater levels show uncertainty for all time periods related to the climate model chain variability. Increasing as well as decreasing trends can be observed within small bounds of a few centimeters. However, the mean calculated groundwater levels, based on the 10 model chains, show quite a similar performance as that simulated for the past. For the seasonal variation quite similar changes are predicted as observed for recharge, although the variations in groundwater levels are small. The seasonal change in groundwater levels is consistent with the recharge. Strong variations in groundwater levels are most likely buffered by a delayed inflow from the borders due to low hydraulic conductivity. Also possible is inhibiting discharge of the aquifer to the river, which lead to the smooth groundwater levels. Although, these are only assumptions to explain the small

seasonal variation and magnitude of groundwater levels, the small variations are also observed in the field data.

Estimation of drought frequency for a "worst-case" scenario indicates an increase in frequency and intensity under CC. Until the end of the century the drought frequency increases by a factor of five for recharge rate based on the applied threshold approach. Also for future groundwater levels, an increasing drought frequency and intensity are observed. However, with the chosen threshold level, an extreme case, only the upper bound of drought frequency increase is considered. The potential of "unsevere" drought is clearly higher. Therefore, water shortage will most likely more frequently occur, especially in summer and autumn, whereas for all other seasons no water stress is predicted. However, the uncertainty in all simulations carried out in this study is large originated from variability among different model chains. Large differences in the downscaled output of the 10 climate model chains are observed, especially for precipitation, and lead to high predictive uncertainty.

Acknowledgements

The authors gratefully acknowledge the financial assistance provided by the Swiss National Science Foundation, Project NFP 61, Sustainable Water Management. The CH2011 data were obtained from the Center for Climate Systems Modeling (C2SM).

5.8 Reference:

Allen, R. G., Pereira, L. S., Smith, M., Raes, D., and Wright, J. L.: FAO-56 dual crop coefficient method for estimating evaporation from soil and application extensions, Journal of Irrigation and Drainage Engineering-Asce, 131, 2-13, 10.1061/(asce)0733-9437(2005)131:1(2), 2005.

Ashby, S. F. and Falgout R. D.: A parallel multigrid preconditioned conjugate gradient algorithm for groundwater flow simulations, Nuclear Science and Engineering, 124(1), 145-159 pp., 1996.

Bosshard, T., Kotlarski, S., Ewen, T., and Schaer, C.: Spectral representation of the annual cycle in the climate change signal, Hydrol. Earth Syst. Sci., 15, 2777-2788, 10.5194/hess-15-2777-2011, 2011.

Brouyere, S., G. Carabin: "Climate change impacts on groundwater resources: modelled deficits in a chalky aquifer, Geer basin, Belgium." Hydrogeology Journal 12(2): 123-134., 2004.

Brunner, P., and Simmons, C. T.: HydroGeoSphere: A Fully Integrated, Physically Based Hydrological Model, Ground Water, 50, 170-176, 10.1111/j.1745-6584.2011.00882., 2012.

CH2011 (2011), Swiss Climate Change Scenarios 2011, published by C2SM, MeteoSwiss, ETH, NCCR Climate, and OcCC, Zurich, Switzerland, 88pp. ISBN: 978-3-033-03065-7"

Doherty, J.: Ground Water Model Calibration Using Pilot Points and Regularization, Ground Water, 41, 170-177, 10.1111/j.1745-6584.2003.tb02580.x, 2003.

Doherty, J.: PEST- Model-Independent Parameter Estimation. Watermark Numerical Computing. peshomepage.org. 2010

Fischer, E. M., Seneviratne, S. I., Lüthi, D., and Schär, C.: Contribution of land-atmosphere coupling to recent European summer heat waves, Geophysical Research Letters, 34, L06707, 10.1029/2006GL029068, 2007.

Goderniaux, P., Brouyere, S., Fowler, H. J., Blenkinsop, S., Therrien, R., Orban, P., and Dassargues, A.: Large scale surface-subsurface hydrological model to assess climate change impacts on groundwater reserves, Journal of Hydrology, 373, 122-138, 10.1016/j.jhydrol.2009.04.017, 2009.

Goderniaux, P., Brouyere, S., Blenkinsop, S., Burton, A., Fowler, H. J., Orban, P., and Dassargues, A.: Modeling climate change impacts on groundwater resources using transient stochastic climatic scenarios, Water Resour. Res., 47, W1251610.1029/2010wr010082, 2011.

Harbaugh, A.W.: MODFLOW-2005—The U.S. Geological Survey modular ground-water model—The ground-water flow process: U.S. Geological Survey Techniques and Methods book 6, chap. A-16, 2005.

Kristensen, K.J. and S.E. Jensen: A model for estimating actual evapotranspiration from potential evapotranspiration. Nordic Hydrol., 6:170-88., 1975.

Nakicenovic, N. (2000). "Greenhouse gas emissions scenarios." Technological Forecasting and Social Change 65(2): 149-166.

Peters, E., van Lanen, H. A. J., Torfs, P. J. J. F., and Bier, G.: Drought in groundwater—drought distribution and performance indicators, Journal of Hydrology, 306, 302-317, http://dx.doi.org/10.1016/j.jhydrol.2004.09.014, 2005.

Refsgaard, J. C., and B. Storm, MIKE SHE, in Computer Models of Watershed Hydrology, edited by V. J. Singh, pp. 809–846, Water Resour. Publ., Littleton, Colo., 1995.

Schaap, M. G., Leij, F. J., and van Genuchten, M. T.: ROSETTA: a computer program for estimating soil hydraulic parameters with hierarchical pedotransfer functions, Journal of Hydrology, 251, 163-176, 10.1016/s0022-1694(01)00466-8, 2001.

Schär, C. and G. Jendritzky: Climate change: Hot news from summer 2003. Nature 432(7017): 559-560., 2004.

Seneviratne, S. I., Lehner, I., Gurtz, J., Teuling, A. J., Lang, H., Moser, U., Grebner, D., Menzel, L., Schroff, K., Vitvar, T., and Zappa, M.: Swiss prealpine Rietholzbach research catchment and lysimeter: 32 year time series and 2003 drought event, Water Resour. Res., 48, W06526 10.1029/2011wr011749, 2012.

Stoll, S., Franssen, H. J. H., Butts, M., and Kinzelbach, W.: Analysis of the impact of climate change on groundwater related hydrological fluxes: a multi-model approach including different downscaling methods, Hydrol. Earth Syst. Sci., 15, 21-38, 10.5194/hess-15-21-2011, 2011.

Sulis, M., Paniconi, C., Rivard, C., Harvey, R., and Chaumont, D.: Assessment of climate change impacts at the catchment scale with a detailed hydrological model of surface-subsurface interactions and comparison with a land surface model, Water Resour. Res., 47, W01513, 10.1029/2010WR009167, 2011.

Therrien, R. McLaren, R.G., Sudicky, E.A.: HydroGeoSphre-a three dimensional numerical model describing fully integrated subsurface and surface flow and solute transport, Groundwater Simulations Group, University of Waterloo, 2007.

van Dam, J.C. R.A. Feddes.Numerical simulation of infiltration, evaporation and shallow groundwater levels with the Richards' equation J. Hydrol., 233 2000, pp. 72–85

van Roosmalen, L., Christensen, B. S. B., and Sonnenborg, T. O.: Regional differences in climate change impacts on groundwater and stream discharge in Denmark, Vadose Zone Journal, 6, 554-571, 10.2136/vzj2006.0093, 2007.

van Roosmalen, L., Sonnenborg, T. O., and Jensen, K. H.: Impact of climate and land use change on the hydrology of a large-scale agricultural catchment, Water Resour. Res., 45, W00A15, 10.1029/2007wr006760, 2009.

van Roosmalen, L., Christensen, J. H., Butts, M. B., Jensen, K. H., and Refsgaard, J. C.: An intercomparison of regional climate model data for hydrological impact studies in Denmark, Journal of Hydrology, 380, 406-419, 10.1016/j.jhydrol.2009.11.014, 2010.

van Roosmalen, L., Sonnenborg, T. O., Jensen, K. H., and Christensen, J. H.: Comparison of Hydrological Simulations of Climate Change Using Perturbation of Observations and Distribution-Based Scaling, Vadose Zone Journal, 10, 136-150, 10.2136/vzj2010.0112, 2011.

vanGenuchten: A Closed-form Equation for Predicting the Hydraulic Conductivity of Unsaturated Soils, 1980.

Woldeamlak, S. T., Batelaan, O., and De Smedt, F.: Effects of climate change on the groundwater system in the Grote-Nete catchment, Belgium, Hydrogeology Journal, 15, 891-901, 10.1007/s10040-006-0145-x, 2007.

5.9 Supporting information

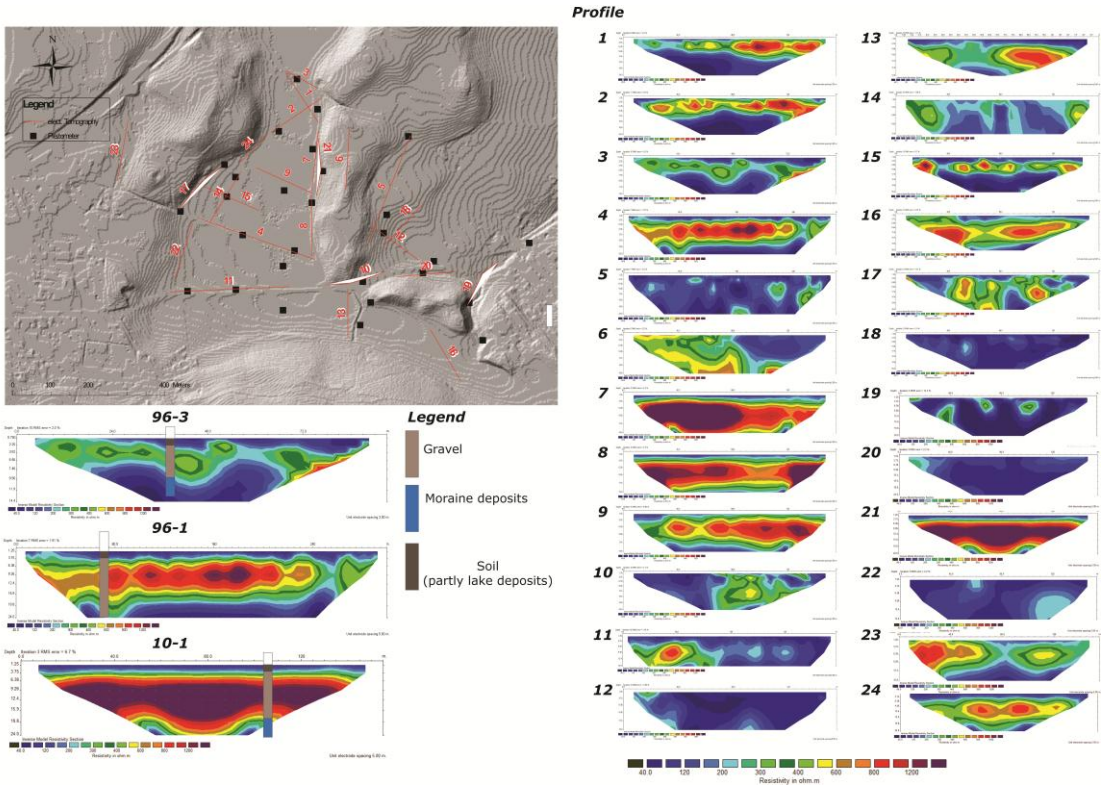

Figure A5. 6: 24 electrical resistivity profiles in the study area, where dark red colors relates to sand-gravel and blue colors to loam to loamy sand material In the upper panel the location of the 2D sections in the catchment are indicated.

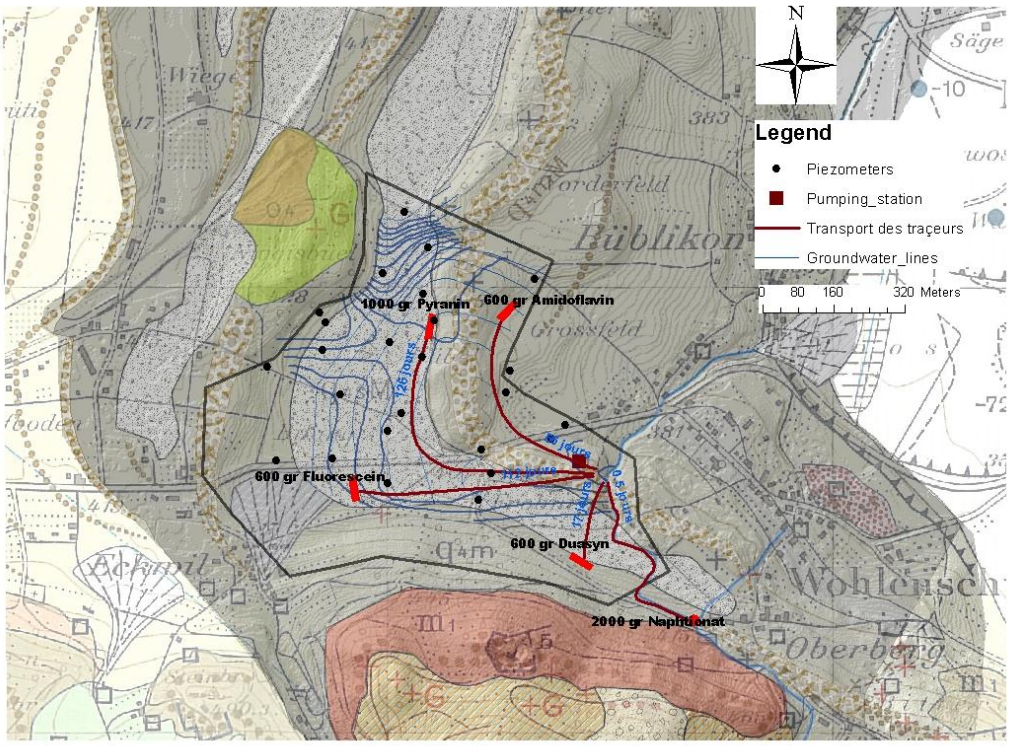

Figure A5. 7: Tracer trasnport times, injected mass and assumped flow direction in the catchement are shown.

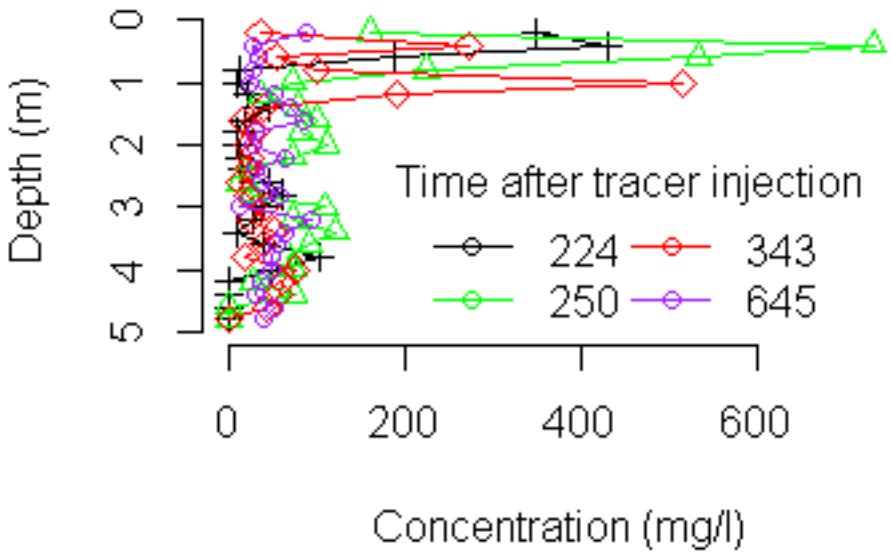

Figure A5. 8: NaCl tracer concentration over depth used to calculate the drainage rate with the peak displacement method.

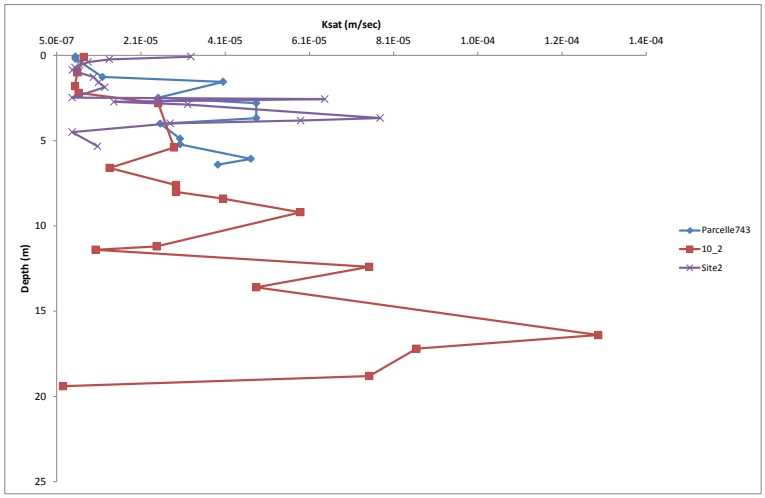

Figure A5. 9: Calculated hydraulic conductivity over depth for three locations in the catchment based on Rosetta, a pedo-transfer model, which used the obtained grain size data.

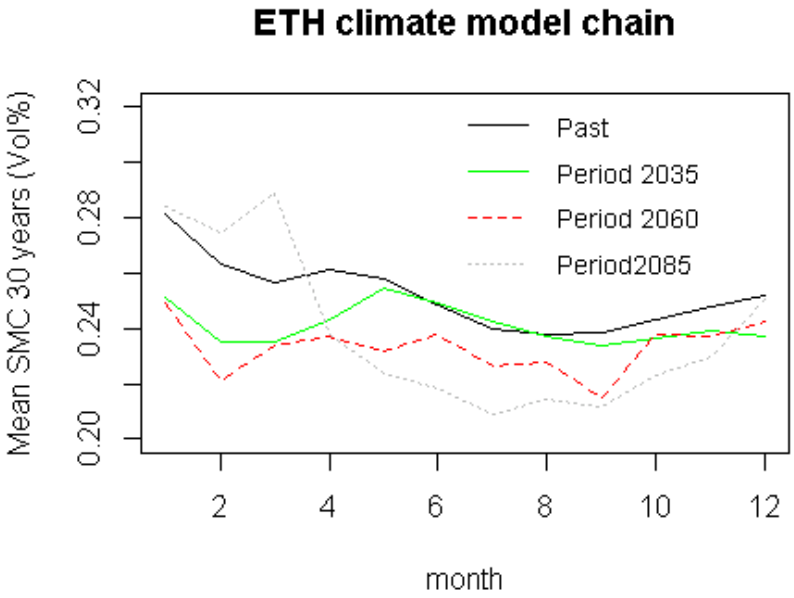

Figure A5. 10: Seasonality of soil moisture content (SMC) in 44cm depth for past conditions and under the ETH climate model chain for period 2035, 2060 and 2085.

Chapter 6

6. Conclusion and Perspectives

This PhD consists of a series of three studies, two of them dedicated to the topic of groundwater recharge, and a third one to the CC response of an aquifer. These studies have been set in response to the gap of knowledge in CC impact studies, where recharge and groundwater modeling was carried out. They respond also to the question to what extent model simplification influence the groundwater recharge predictions. A brief summary of the obtained results is given (see Chapter 6.1). Subsequently an evaluation of the different sources of uncertainty within CC impact studies is presented (see Chapter 6.2). Finally, perspectives are drawn to indicate still missing knowledge and gaps in CC impact studies and to indicate possible future research fields (see Chapter 6.3).

6.1 Modeling Recharge rates and Groundwater levels

To quantify the influence of CC, models with different levels of complexity are use in numerous CC impact studies (see Chapter 2.5). However, although different models to simulate groundwater recharge have been used before, it was not clear yet whether models of different complexity give similar recharge predictions for a given climate scenario. Therefore, five different approaches to simulate groundwater recharge were compared in this PhD (see Chapter 3).

The best model performance in reproducing future recharge rates taken from the complex 2D references model was archived by the physically based numerical model. Although, a homogenous model parameterisation was applied, the model still performed better than the semi-mechanistic and soil water balance models. More extreme weather conditions increased the model bias in the recharge predictions. Infiltration and evapotranspiration processes are solved differently in the five different model structures to simulate recharge. The potential for model predictive bias increases with the difference between the climatic forcing function and the calibration period. This is a quite important outcome because many large scale impact studies use different kinds of soil water balance model approaches to simulate future recharge rates under CC (Chapter 2.5). Thus CC impact results from these studies need to be interpreted with caution. Comparison of both uncertainties, CC and model simplification, indicate that the highest uncertainty is related to CC, but model simplification can also introduce a significant predictive error. Therefore the applied model in CC impact studies should be always carefully considered to avoid misinterpretation. If computational time is still acceptable physically based models should be used to archived robust CC impact results. If this is not possible then at

least lumped models where model parameters and relationship emulate physical processes of infiltration and evapotranspiration should be used.

How different crops and crop rotations influence CC effect on groundwater recharge was explored with a numerical exercise using data from lysimeters. It is well known that evapotranspiration can strongly vary among crops and therefore CC effect on recharge might be crop dependent (see Chapter 4).
The obtained results indicate differences in recharge rates around 10% between the available three soils. This is the least significant factor compared to climate and vegetation in this study. Comparing, the effect of CC on recharge rates under different crops indicate that for most crops a decreasing trend occurs (between -5 to -60%) during their specific vegetation period. Differences in crop parameters such as leaf area index and root depth between the different crops leads to diverse recharge rates. Recharge rates and changes are also strongly depending on the vegetation period. Recharge rates for crops which growth during summer lead to strong decreasing recharge, while recharge rates under crops in winter show just small changes. For catch crops such as Phacelia and Temporary grassland (small LAI and RD) an increasing recharge trend can be observed. Using these crops in a crop sequence buffered to a certain amount the decreasing trend on recharge rates under CC, but the amplitude depends also in the growing season where catch crops are used. Assuming a change in agriculture practice from the associated crops to a single crop Temporary grassland would mostly create an increase in recharge for the entire year. An analysis of the sensitivity of LAI and RD on recharge which was carried out indicates that simulated recharge is inversely related to LAI and RD, where recharge is more sensitive to a decrease in LAI than to RD. We can conclude that land use changes are quite important in CC impact studies and should be always also considered. Using different crops or crop sequences can have a influence on recharge rates like CC. However, in all simulations a high predictive uncertainty in results is given due to variability originated among GCM and RCM combinations and stochastic realisations of the future climatic conditions. This indicates that always a multi-climate-model approach should be the preferred method under CC impact studies simulation changes in the hydrological systems. Only with a considerable amount of climate model chains a robust estimation of predictive uncertainty due to the variability among the climate model chains can be realised.

How changes in groundwater recharge rates and seasonality influence groundwater levels was explored for a small aquifer used for water supply (see Chapter 5). The study was carried out by considering the soil-unsaturated zone-groundwater system as a whole using the physically-based model HGS.
Simulations of future recharge rates indicated that the seasonality is changing under CC. An elongation of the “summer” period into autumn can be observed which is induced in the first place by a change in the climatic forcing functions due to CC (delta change signals). The higher temperature and less precipitation in autumn can be considered as an elongation of the summer period. Another effect is the soil moisture

memory. A stronger drying out of the soil during hotter and drier summers leads to less recharge. As a result of the depleted soil moisture, in autumn a larger amount of precipitation is required until considerable recharge occurs compared to the past conditions. For the winter season recharge rates increase for almost all climate model chains and periods. The strong precipitation increase during these months is the controlling factor for increasing recharge, especially for the period 2085. However, although the climate model chains show a large predictive uncertainty for annual recharge rates, they lead to almost same changes in the seasonality. In summer and autumn temporal water stress can occur but the intensity depends on the chosen climate model chain. Estimation of recharge and groundwater drought frequency for a "worst-case" scenario based on a threshold approach indicates an increase in frequency and intensity with increasing time periods. The mean of recharge difference (monthly future recharge rates minus monthly mean past), however, does not change under the future time periods but the skewedness of the distribution does. Most recharge droughts in summer become extremer due to increasing temperature originated by CC. Also for future groundwater levels, an increasing drought frequency and intensity are observed. Similar to recharge rates, the simulated groundwater levels show uncertainty for all time periods related to the climate model chain variability. Increasing as well as decreasing trends can be observed within small bounds of a few centimeters. For the seasonal variation quite similar changes are predicted as observed for recharge, although the variations in groundwater levels are small. The seasonal change in groundwater levels is consistent with the recharge. Although the aquifer system is relatively small with a high transmissivity the groundwater table reacts not rapidly to seasonal variations in recharge. Strong variations in groundwater levels are most likely buffered by a delayed inflow from the borders due to low hydraulic conductivity. Also possible is inhibiting discharge of the aquifer to the river, which lead to the smooth groundwater levels. Although, these are only assumptions to explain the small seasonal variation and magnitude of groundwater levels, the small variations are also observed in the field data.

Although different types of models are used in this PhD, the majority of simulations are carried out with HydroGeoSphere. That is why in the following a summary about the attractiveness of choosing HydroGeoSphere (or any other fully coupled physically based model) is given. This summary attempts to illustrate again the advantage of these types of models for climate impact studies.

- The interconnected flow processes, such as groundwater recharge, are physical based represented.
- Compared to other models recharge is better characterized because all flow equations are simultaneously solved in all domains (surface, unsaturated and saturated zone). Changes in the water table during the simulation controls the unsaturated zone thickness and directly the adjoined the moisture content in the unsaturated zone. Therefore, groundwater recharge is also directly influenced. This illustrates the coupled behaviour of the model.

- Different types of plants can be described based on different model-plants parameters, which can be used to investigate land use changes.
- Due to the possibility to simulate coupled flow process a wide range of observations can be used to calibrate the model. Compared to just groundwater models, the implementation of e.g. actual ET or surface observations in the calibration enables to check the correctness of all components of the water balance. Therefore, bias induced by the calibration is easier to detect than using only groundwater levels to calibrate a model.

6.2 Uncertainty evaluation

The quantification of uncertainty is a major challenge and requirement within climate change impact studies. Strategies to evaluated the different uncertainties in this PhD are listed below:

- The uncertainty linked to variability among the GCM and RCM combinations was evaluated by using a multi-model ensemble approach (up to ten different GCM-RCM combinations; see Chapter 3-5).

- The uncertainty linked to the interannual variability of the climate was evaluated by using different equiprobable stochastic realisations of the climate conditions used as climatic forcing inputs for the hydrological models (see Chapter 4).

- The uncertainty linked to the downscaling approach was not studied.

- The uncertainty linked to the hydrological model structure was evaluated by using different types of recharge models (see Chapter 3).

- The uncertainty linked to the calibration of the simplified models was evaluated by calibrating the chosen simplified models against recharge outputs from 100 stochastic 2D references models (see Chapter 3). In this stochastic framework, hundred different realizations of hydraulic parameters of the references model were created.

- The uncertainty linked to the calibration of the lysimeter soil models was evaluated by comparing all simulated components of the water balance against the observation. The simulated coupled flow process enables to validate the correctness of all components of the water balance and to detect model bias induced by the calibration (see Chapter 4).

All studies demonstrated that the uncertainty surrounding projected recharge rates and groundwater levels are relatively large. Some model chains indicate decreasing

recharge and groundwater levels, while other show increasing trends. For instance for the Wohlenschwil aquifer a change in annual recharge between -16% and 12% was simulated, while the mean of all climate model chains indicate no changes. Therefore, it is quite difficult to state on the magnitude of the change with high confidence. However, not the mean is important, but rather the seasonality. Almost all climate model chains lead to almost same changes in the seasonality, although the magnitude is different. In addition, the uncertainty linked to the interannual variability of the climate is highly uncertain and can lead to strongly different results and conclusions depending on analyzed equiprobable stochastic realisations. However, the main uncertainty is linked to GCM-RCM combinations. This uncertainty is followed by the uncertainty originated by natural variability of the climate and model simplification. The calibration of the hydrological model is a further uncertainty, but could be reduced by improving the model calibration, if needed. A good strategy in the context of CC would be to test if different calibration leads to same conclusion, although the absolute values of e.g. recharge changed a bit.

6.3 Perspectives

Growing periods of plants will probably adapt to changing weather distribution. Changes in plants parameter due to changing soil water availability are possible. In this PhD (see Chapter 4) already a modeling strategy was applied to represent the plants-soil water interaction. However, still this approach has some limitation. It is assumed that the growing period will be constant in time also under CC. However, one of the most fundamental conceptual aspects is the vegetation dynamic. Representing crops growth with increasing accurateness and using methodologies to couple vegetation and soil moisture content more strongly will provide more robust future recharge rates estimations.

Also a more complex representation of the soil structure can lead probably to changes in the result. Although the modeling strategy for the soils exceed common approach for CC impact studies (see Chapter 2.5) and the models are already spatial distributed and fully coupled physically based, the modeled soil structure is still simplified in this PhD. For instance macropores, which likely occur increasingly in the future due to more drought periods with drying-out cracks can have a significant influence on recharge rates. In this PhD, the direct (preferential) recharge rates play under actual weather conditions only a minor role, but can become increasingly important in future which is not taken into account.

This mentioned two-way coupling could also transferred to a high number of other variables (e.g. snow and ice), which should interact between hydrological model and climate. Although it is already done or in process in models like HGS there is still a lot of physical processes, which are not adequate (in a fully physical way) described. However, the interaction can contribute to a better understanding of the linkages

between all variables and will create possibly more precise results in CC impact studies.

Another quite important source of uncertainty aside of using different GCM-RCM combinations is downscaling. Using the transient climate change scenario (see Chapter 4 and published also in Goderniaux et al., 2011) is a great way to create possible different realisations of future precipitation distribution and temperature values for each of the GCM-RCM combinations. This approach is more realistic at simulating climatic variability compared to the simple delta change downscaling approach. Furthermore, the possibility to analysis in detail when an expected change in recharge rates occur can help to developed sustainably water resource management. However, restrictions of this approach are still the highly uncertain probability of extremes in the future. The prediction of frequency, duration and intensity of, for instance, heavy precipitation events and dry spells is still quite difficult although climate models become more reliable.

It was already shown that using models of varying complexity can lead to different recharge predictions. These differences in the predictions can lead to a completely different water resource management strategy. It would be interesting to extend this research and using different models on a catchment scale, which also include, for instance, surface water, surface runoff and snow melt processes.

Another quite important point, which was not covered in this study are socio-economic scenarios. Changes in water supply, such as increase pumping rates due to increasing populations can induce comparable changes in the water balance than CC. A scenario modeling approach, integrating both, CC and socio-economic changes would probably help to predict in a more efficient way changes in e.g. groundwater levels.

For the aquifer system Wohlenschwil a 3D integrated modeling approach was chosen (see Chapter 5). The physical-based representation of flow processes lead to extreme long computing times, especially for CC impact studies which require applying long time series of climatic forcing functions. This, however, prevents different applications, like an extensive uncertainty analysis (e.g. Monte Carlo approach to estimate model parameters with "Null-space" projection). Nevertheless, a lot of research is currently performed in the field of integrated modeling, and future new developments may help reducing these large computation times. Especially, the already powerful existing parallel version of HGS or PEST (BeoPEST) indicates necessary increasing code efficiency in terms of computational power. This is a reasonable approach to reduce computation effort for CC impact studies or any other numerical exercise.

Appendix

Pilot point calibration using PEST applied to HydroGeoSphere[4]

Abstract

Groundwater and surface model calibration has made great advances in last decades with practical and powerful calibration tools such as pilot points implemented into PEST. However, as opposed to many other hydrogeological models, this pre-existing type of calibration has so far not been applied to HydroGeoSphere (HGS), even though HGS is a widely used and one of the most powerful tools for simulating hydrological processes. Addressing this gap, we present a workflow and example that illustrates the application of pilot points in HGS using PEST. Additional post-processing analysis was carried out due to the danger of over-fitting because of over-parameterization of the inverse problem. Cross-validation (CV) and linear uncertainty analysis (LUA) is applied to identify the importance of observations to parameter estimates and prediction. Both, CV and LUA showing similar results and identify important location for observations, but the latter at much smaller computational cost. The detailed description of the example and source code of all developed programs is provided in the tutorial available in the appendix. In addition, we discuss how the provided methodology can be transferred to other numerical models, which do not provide GUI support for pilot point calibration.

Introduction

Groundwater model calibration methods have made great advances in the last two decades with powerful tools such as PEST (Fienen et al., 2009). Virtually every hydrogeological investigation requires an estimate of hydraulic conductivity (Butler, 2005) and spatial variations play an important role in controlling flow and solute movement in the subsurface (e.g. Sudicky and Huyakorn, 1991; Sudicky et al., 2010; Zheng and Gorelick, 2003). However, heterogeneity can typically not be investigated in all details. Nevertheless, model parameters must be provided to the employed models and therefore, calibration is required. The classical calibration approach is based on the principle of parsimony. It consists of subdividing the model domain into zones of piecewise constancy. Calibration software is subsequently applied to adjust the calibration parameters to obtain a good fit between model outputs and field measurements. The strengths and weaknesses of this approach have been described by Hill and Tiedeman (2006) and are subject to an ongoing debate in the scientific community (Doherty, 2009, 2010; Hill, 2010; Doherty and Hunt, 2009, Franssen et al., 2009).

Pilot points are an alternative to the zonation approach. Pilot points introduce great flexibility to calibrate heterogeneous systems without neglecting expert knowledge (Doherty, 2003).

[4] C. Moeck[1], P. Brunner[1], D. Hunkeler[1]

[1] Centre of Hydrogeology and Geothermics, University of Neuchâtel, Switzerland

Appendix

Renard (2007) illustrated a brief history of pilot point methods, which was proposed first by de Marsily (1978). The method was further developed by de Marsily et al. (1984), Lavenue et al. (1995) and Ramarao et al. (1995) and has been implemented into the automatic parameter estimation software PEST (Doherty, 2010).

Using the pilot point method, PEST has been combined with various numerical models of different conceptual complexity to simulate a wide range of environmental problems. For instance, Dausman et al. (2010) used SEAWAT (Langevin and Guo, 2006) to simulate the effect of variable density flow and transport and developed an optimization for data acquisition. MODFLOW (Harbaugh et al., 2005) was used for an investigation of the potential error in predictions made by highly parameterized models calibrated using regularized inversion (Tonkin et al., 2007). Herckenrath et al. (2011) used a "Null-Space-Monte-Carlo" approach to quantify predictive uncertainty for a saltwater intrusion problem. The impact of pilot points positions on inversions results was investigated by Kowalsky et al. (2012) and the importance of intraborehole flow in solute transport by Ma et al. (2011). All these studies are based on and used the pilot point approach.

Several technical challenges arise by using automatic calibration software, and pilot points in particular. The numerical model and the calibration software have to interact throughout the calibration process. Given that different numerical models are based on different input-output structures, employing a calibration tool such as PEST is often not straightforward. The challenges are even greater if pilot points are used, because pilot points have to be assigned to specific grid- locations and the interpolation between the pilot points have to be mapped to the model grid. The application of PEST using pilot points has been optimized for a number of codes by developing automatic and easy to use code specific utilities that facilitate the communication between the numerical model and PEST (e.g. MODFLOW (Harbaugh et al., 2005), MT3DMS (Zheng, 1990), SEAWAT (Langevin et al., 2008), FEFLOW (Diersch, 2009), MicroFEM (Hemker and de Boer, 2009), and RSM (South Florida Water Management District, 2005).

The above mentioned models are only a subset of available numerical codes. In the past few years, a range of integrated hydrological models like MIKE SHE (Refsgaard and Storm, 1995) and fully coupled, physically based models such as PARFLOW (Ashby and Falgout, 1996), InHM (Vanderkwaak and Loague, 2001) and HydroGeoSphere (Therrien et al., 2007) have been developed.

It is interesting to note that the pilot points capability of PEST has only been employed to numerical models where model specific utilities that facilitate the application of PEST are available. This suggests that the absence of tools that simplify the implementation of pilot points tends to exclude their application. We speculate that the reason for this lies in the absence of a GUI and the several, albeit minor technical challenges that come along with employing the pilot point method through PEST. No such tools exist for HGS, and to the best of our knowledge, pilot points have so far not been combined with this model.

Our intention is to make the pilot point approaches implemented in PEST easily accessible to the rapidly growing HGS community by presenting a workflow and provide the tools required to combine pilot point calibration of PEST with HGS. Additionally to the implementation, we

demonstrate two post-processing methods to validate alternative calibrated hydraulic conductivity fields to identify the importance of observations to parameter estimates and prediction. This is needed due to the possibility of over-parameterisation of the inverse problem and resulting over-fitting. Cross-validation (CV) and linear uncertainty analysis (LUA) is applied.

HGS is a powerful state of the art tool used to reproduce many environmental physical processes such as the investigation of climate change effects on water resources (Goderniaux et al., 2009), water flow in mountain regions (Gleeson and Manning, 2008), effect of heterogeneous streambeds (Irvine et al., 2012), comparison between automated baseflow separation against simulated baseflow from surface water-groundwater model (Partington et al., 2012) hydrologic response in a large-scale watershed (Li et al., 2008) and influence of soil heterogeneity on catchment water balances (Sciuto and Diekkrueger, 2010) are only a few study examples.

Our paper is organized as follows: In section 2, an overview on how pilot points can be used in HGS is given. We also indicate how this methodology can be transferred to other model types. In section 2 the theory of CV and LUA is addressed additionally. In section 3 an example is presented. Results and conclusions of both, pilot point calibration and CV as well as LUA are presented in section 4 and 5. The appendix contains a detailed step by step tutorial to reproduce the example.

Methodology

Implementation of pilot points in HydroGeoSphere using PEST

Calibration of a model using pilot points involves the following steps. Firstly, pilot points are distributed over the model flow domain, the mesh network emulating the study site. Note that any model parameter can be associated with various pilot points. Once the pilot points have been defined, PEST interpolates the values between the pilot points based on a user defined method (e.g. Kriging). Note that PEST offers the option to define multiple geostatistical models that can be assigned to predefined zones in the model domain. The model is then run with the given parameter field, and an objective function is calculated by comparing measured and simulated observations. In the subsequent calibration, pilot points values are varied and the corresponding objective functions calculated. PEST modifies the pilot points values to minimize the objective function. All options of PEST to minimize the objective function can be used for this task, including mathematical regularisation approaches (e.g. Tikhonov regularization and/or Singular value decomposition (SVD)). An extensive description of the pilot point theory can be found in (Christensen and Doherty, 2008; Doherty, 2009, 2011; Doherty, 2003).

The application of pilot points requires coordinate transformations between the model and PEST. In the “PEST domain” values for pilot points are estimated through the inverse process and the interpolation between them are carried out through “ppk2facg” and “fac2g”. These two programs are part of the PEST suite (Doherty 2010). A re-transformation into the model

specific file structure has to be carried out previous to the model run. Figure App1.1 illustrates this workflow for HGS.

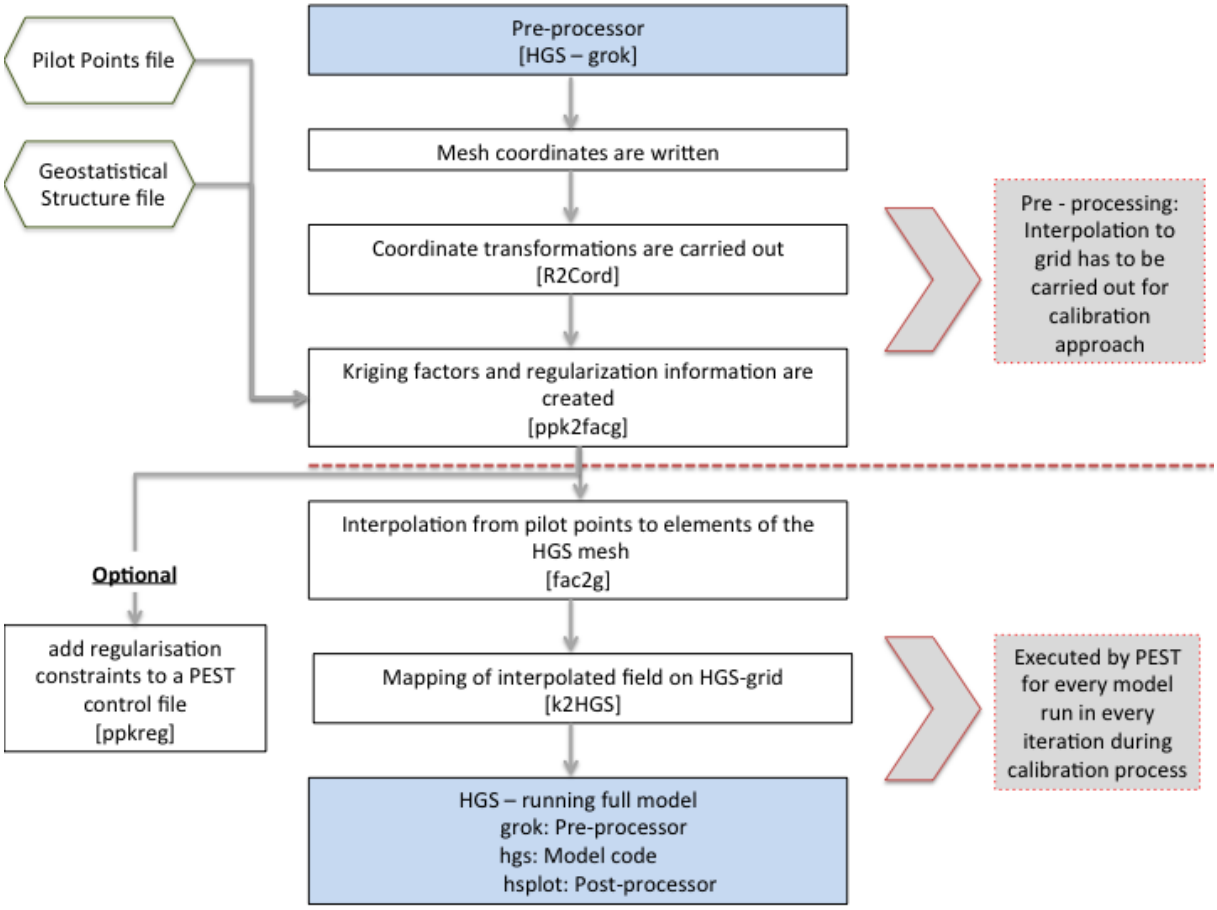

Figure App1. 8: Flowchart of the methodology to combine pilot point calibration using PEST with HGS. In the top panel, the pre-processing and the preparation of the input files are shown. The lower panel illustrates the calibration procedure.

[1] In a first step, the HGS mesh must be written to a file by using the HGS command "Mesh to Tecplot", which causes the pre-processor of HGS (grok) to write all available mesh information. [2] The program "R2Cord" (available as supplementary material) makes this information readable to the PEST program "ppk2facg" (Doherty, 2010). [3] Then, executing "ppk2facg" generates a set of kriging factors through which the interpolation can take place from a set of pilot points. To run "ppk2facg", two additional files are required. The first file (Pilot Points file) provides name, easting and northing of every pilot point as well as the predefined zone and the assigned value. These values are used for the spatial interpolation to the elements of the model grid. The second file contains the geostatistical structure defined through a variogram. This information is required for kriging between the pilot points. In addition to generating a set of kriging factors, "ppk2facg" writes regularization information, which can optionally be used by "ppkreg" to add prior information to the PEST control file.

Prior information used for regularization can help to avoid overfitting and numerical instability caused by the heterogeneity of the generated model parameters. All tasks outlined in this paragraph have to be carried out only once for a pilot point calibration approach (see top panel of Figure App1.1).

[4] After completing the preparation of the input files, the program "fac2g" (Doherty, 2010) undertakes the interpolation from pilot points to elements of the HGS mesh. This interpolation tends to generate smoothed projections of the true hydraulic conductivity. If the number of pilot points or observations is too small, the true extent of heterogeneity is likely to be underestimated.

[5] The interpolated field is mapped on the elements of the HGS- grid by using the program "K2HGS" (available as supplement). The pre-processor of HGS (grok) is then initialized by PEST, followed by the model run itself. After achieving the predefined convergence criteria, HGS generates all model specific output data. [6] PEST reads these data and calculates the objective function. Based on the updated objective function, PEST generates a new set of values for the pilot points. This procedure is repeated until PEST aborts the calibration process following the predefined convergence criteria. The sequential calling of the executable as described above must be defined in a batch file.

Implementation of pilot points for physical based models

The provided workflow can be applied to other physically based models by changing two steps. Firstly, coordinates of each mesh element must be provided in a text file. Secondly, the "R2Cord" program must be modified to ensure that mesh structure can be imported by PEST. From this point on, the steps of section 2.1 are carried out until the execution of "K2HGS". "K2HGS" has to be modified (source code available as supplement) to import and create a file readable by the numerical model.

Cross-Validation and Linear Uncertainty analysis

Using pilot point calibration can produce the possibility of over-fitting due to over-parameterisation of the inverse problem, although mathematical regularisation is applied. Therefore, additional post-processing analysis is needed where alternative calibrated hydraulic conductivity fields are validated to identify the importance of observations to parameter estimates and prediction. Here, cross-validation (CV) and linear uncertainty analysis (LUA) is applied and compared with each other.

The target of CV and LUA is to identify the dependence of the model fit and estimated parameter values on each observation (Foglia et al, 2007, Hill and Tiedeman, 2007). We apply CV by omitting one observation or group and re-calibrate the model. Subsequently, we apply different types of statistics to rate how much the estimated parameter and the simulated values vary during the calibration when observations are omitted. CV is a computational demanding method, which accounts for model nonlinearity due to the model re-calibration. However, due to the rapid calibration time of our example this computationally demanding method is still applicable. Two different types of statistics (described by Cook and Weisberg

(1982)) are applied subsequently after the re-calibration. The influences of each observation on the pilot point values and on model predictions are calculated.
Using LUA, parameter identifability of each parameter depending on the information content of the available observations can be calculated. The contribution to the pre- and post-calibration error variance and uncertainty made by different parameters can be computed as well as the worth of different observations in lowering the error variance and uncertainty by selectively removing observations. In our example we use the PEST utility "genlinpred" (Doherty, 2010), a batch program running other PEST utilities used for the linear uncertainty analysis. A quite important factor, which demonstrates the attractiveness of the present linear uncertainty analysis, is that, actual parameter or observation values are not needed. Only parameter and observation sensitivities are involved. Therefore, this analysis can be already applied albeit the model is not yet calibrated.
A detail description about the two concepts can be found in the tutorial or in the listed references (e.g. Foglia et al, 2007, Hill and Tiedeman, 2007, James et al., 2009, Moore and Doherty, 2005 and 2006, Brunner et al., 2012).

Example

In this example, the hydraulic conductivity field of a finite element 2-D model will be calibrated with pilot points using regularization. The example shown here can be reproduced by the step-by step instructions provided in the tutorial.

Reference Model

A synthetic fully saturated unconfined porous aquifer is created. The 2-D steady state model has a stationary spatially variable hydraulic conductivity field throughout the whole model domain and is described by a log exponential variogram with a range of 200 m and a sill of 0.29. The mean hydraulic conductivity is $5.8E^{-4}$ m sec^{-1} (Figure App1.2).

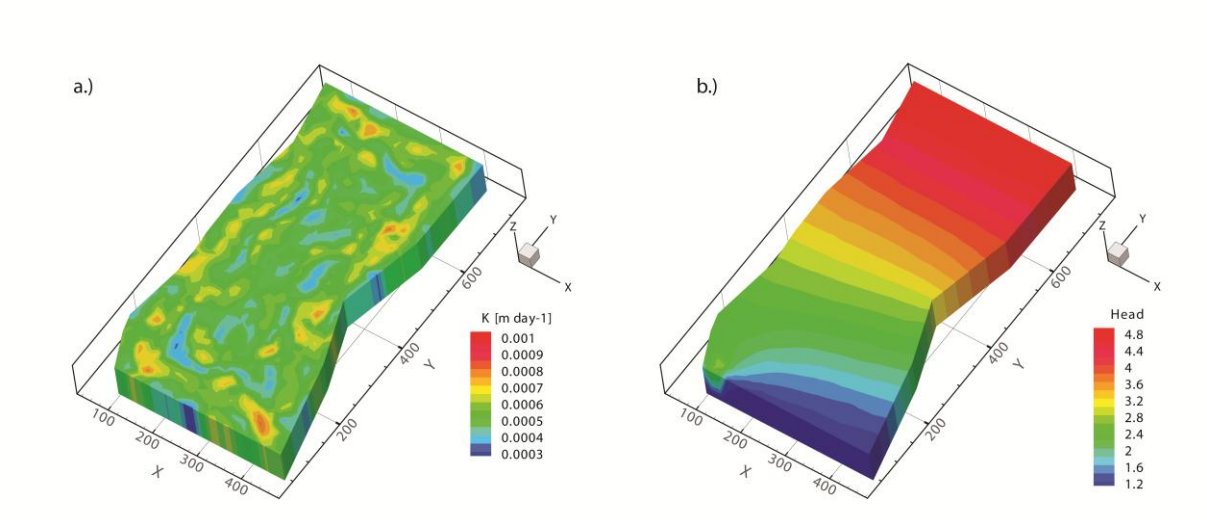

Figure App1. 9: (a) Distribution of reference hydraulic conductivity [m day^{-1}] within the finite element model domain. (b) Simulated heads within the model domain.

Steady state groundwater flow is induced with constant head boundaries of 1 m at the southern border and 5 m at the northern border. "No flow" boundaries are imposed on the remaining borders. A total of 12 observation wells for head measurements are distributed in the model domain (Figure App1.3). No random noise was added to the head observations in order to simplify the data estimation.

Model Calibration

130 pilot points were regularly spaced distributed in the model domain. Observations of hydraulic head of the reference wells are used for the calibration (Figure App1.3).

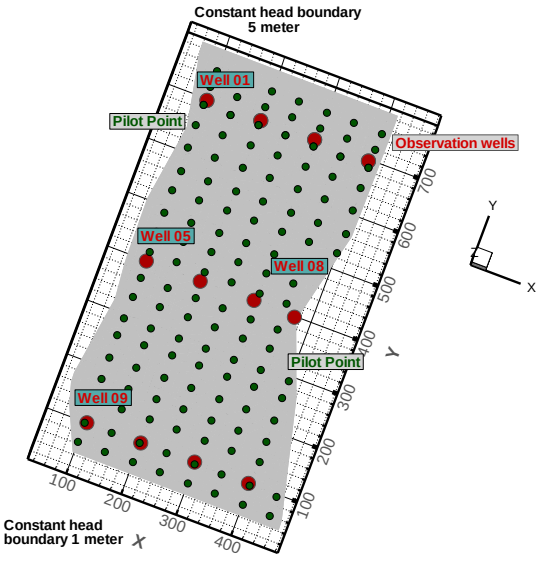

Figure App1. 10: Model domain with locations of 12 observation wells (red points), uniformly distributed 130 pilot points (small green points) and constant head boundary conditions.

In the calibration process, initial log transferred hydraulic conductivity of $1.4E^{-5}$ m sec^{-1} are assigning to all pilot points as well as the lower and upper bounds of $1.0E^{-10}$ and $1.0E^{10}$ m sec^{-1}. This large parameter range was chosen to demonstrate how well PEST estimates realistic parameter values using mathematical regularization. Log transferred hydraulic conductivity was chosen because it has the advantage that variability is expressed in terms of factors and not in absolute values. Equal weights are applied to all observations and singular value decomposition (SVD) as well as Tikhonov regularization is applied in the calibration process. Because of no random noise in the reference head observations the target objective function is set to 0.0.

Results and Conclusions

Model Calibration

A perfect fit was obtained between model output heads and head observations from the synthetic reference model through 6 iteration steps in the calibration process (Figure App1.4).

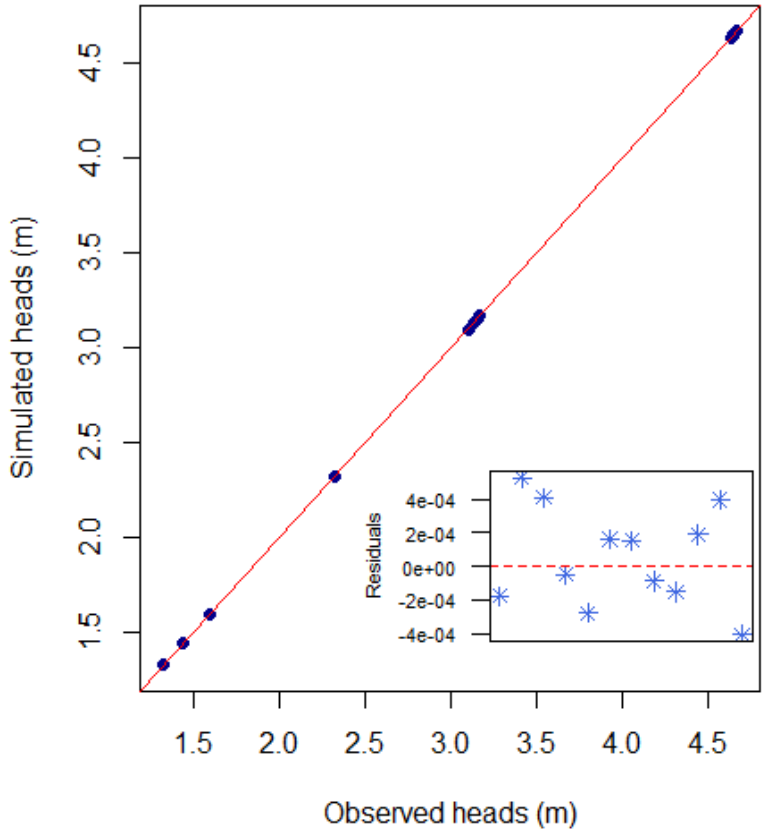

Figure App1. 11: Simulated versus observed heads. Residuals of all observation wells are displayed in the small rectangle.

Comparing the hydraulic conductivity fields between reference and calibrated model shows large differences in its structure (Figure App1.5), even though a perfect fit has been obtained between calculated and observed hydraulic heads.

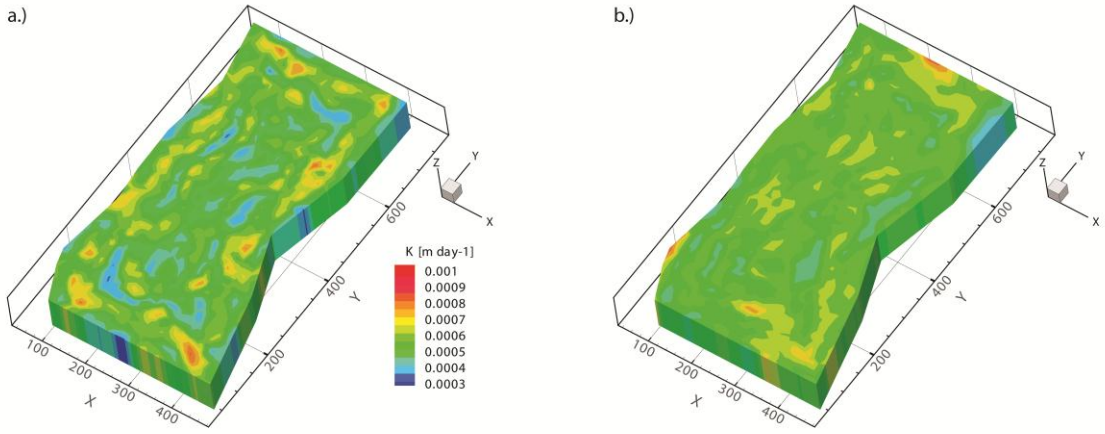

Figure App1. 12: (a) Reference and (b) calibrated hydraulic conductivity [m day^{-1}] field within the model domain.

The calibrated hydraulic conductivity field shows only a fraction of the real heterogeneity of the reference model. Note that PEST has the capability to quantify data worth of observations, and to determine the additional observation types as well as their measurement location to reduce the parametric uncertainty in the most efficient way (see next chapter and see for instance examples of Gallagher and Doherty (2007) and Brunner et al. (2012)).

Cross-Validation and Linear Uncertainty analysis

Using CV to calculate the influence of observations on predictions show that the head observations close to the southern border (well 9 to 12) contain the highest information content in all observations (Figure App1.6, left panel). In this particular area the head change (gradient) is highest compared to all other model areas. Especially if the information content from observation well 9 is omitting, a good reproducing of the piezometric head field during the calibration is difficult. Omitting an observation in the northern part of the model domain (see for instance piezometric head in figure App1.2) has none or only a small effect for the predictions. The horizontal head differences are small between the observation wells in that line (e.g. the 4 wells close to the northern border) and can be reproduce also just with 3 observations if one is omitted. Similar results can be obtained with the linear uncertainty analysis (Figure App1.6, right panel), although the results between CV and uncertainty variance can not be compared in terms of absolute values. Omitting observation well 9 and to a smaller part observation well 10 in the calibration would increase the predictive uncertainty variance for reproducing the "reference" piezometric head field. Omitting any other observations has only a small effect for the predictions based on the LUA. Although both methods indicate similarity in the results, the computation time is different. For CV a re-calibration is needed for each omitted parameter whereas for the LUA actual parameter or observation values are not needed. Only parameter and observation sensitivities are involved. Therefore, this

analysis can be already applied albeit the model is not yet calibrated. However, it should be note that CV shows in contrast to linear uncertainty analysis the actual effect of omitted observations for the calibration.

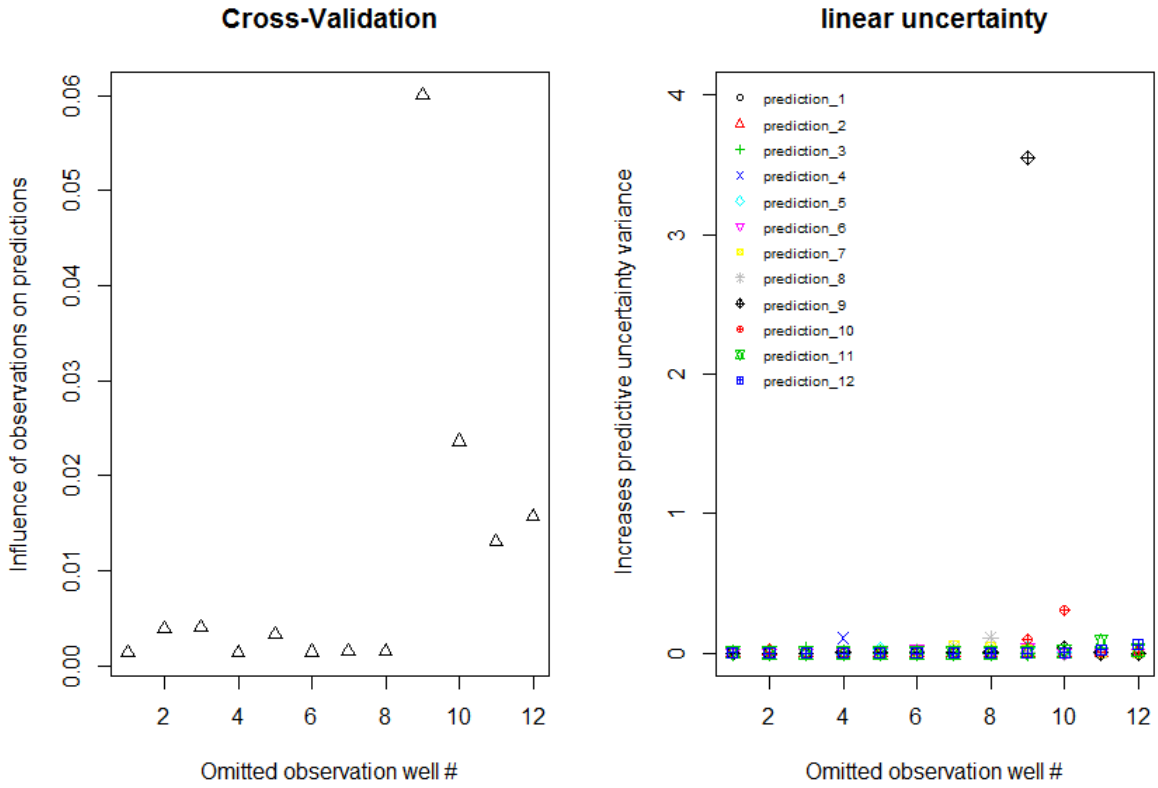

Figure App1. 13: Left panel: Influence of observations on predictions (equation 2, see tutorial) by CV. On the x-axis the omitted observation is shown. The predictions, which takes subsequently place are the simulated head produced with parameter values estimated when the chosen observation is omitted. Right panel: The increase of predictive uncertainty variance for each head due to the loss of observation is shown (equation 1, see tutorial).

The influence of each omitted observation for the pilot point hydraulic conductivity values obtained by CV are shown in figure App1.7 (Equation 21, see tutorial). For most omitted observations only a small change in the parameter values can be observed (white to light yellow colours). Only for the omitted observation well 9 and observation group down, which includes observation well 9, the biggest change in pilot point values can be observed (dark yellow to red colours). This is of particular interest because it is known that observed differences between the "real" and the calibrated hydraulic conductivity field can result in considerable uncertainties of predictions, as demonstrated by Moore and Doherty (2006, 2005) using an example of contaminate transport.

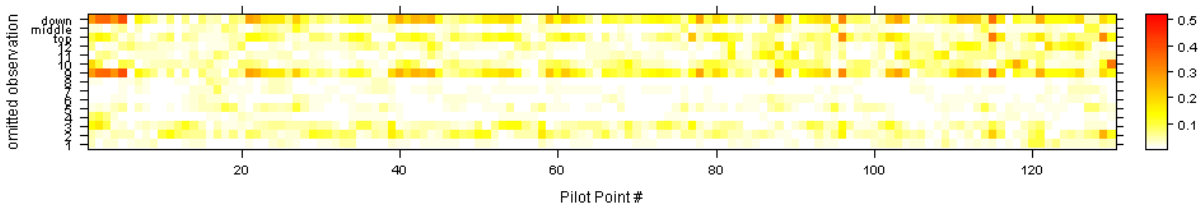

Figure App1. 14: Parameter influence statistics (Equation 1, see tutorial) from the CV experiment. Omitted parameters are labels as observation 1 to 12 as well as observation group top (the 4 observations close to the northern border), down (the 4 observations close to the southern border) and middle (the 4 observations between down and top). All 130 pilot points used in the calibration are displayed at the x-axis. The statistic shows the differences between a calibration with all observation and the re-calibration with omitted observation(s) for the pilot point hydraulic conductivity values.

We can conclude that observation well 9 contains the highest information content for the calibration of the hydraulic conductivity field. Calculating the parameter identifability (figure App2.9 given in the tutorial) based on the available observations, show not values larger than 0.22 for each pilot point hydraulic conductivity. That indicates that the data worth of the hydraulic heads are insufficient to constrain the hydraulic conductivity field. To increase the parameter identifability different types of observations, such as groundwater plume concentration measured at the observation wells, must be used additionally. However, methodologies to explore this predictive uncertainty have been developed in last recent years (e.g. Moore and Doherty, 2006, 2005; Christensen and Doherty, 2008; Dausman et al., 2010; Tonkin et al., 2007; Herckenrath et al., 2011; Doherty and Christensen, 2011; Gallagher and Doherty, 2007). These approaches are readily applicable to models calibrated through pilot point methods. For instance, the contribution of the parameter null space can be investigated by using pilot points (Hunt et al., 2007) and/or in combination with stochastic field generation to apply a Monte Carlo analysis (Tonkin and Doherty, 2009). A more detailed investigation and description of predictive uncertainty can be found in the aforementioned papers.

Summary

A workflow to combine pilot point calibration using the program PEST in combination with the physically based finite element model HGS is presented. We provided two executables that are required to use PEST with HGS, and illustrated the workflow with a comprehensive tutorial. The program “R2Cord” (source code available as supplement) transfers mesh coordinates and makes the information readable for further steps using the PEST programs. The mapping of the undertaken interpolation from pilot points to elements of the HGS mesh is done by the program “K2HGS” (source code available as supplement). The provided workflow and tutorial can be easily applied to any other numerical models by adjusting the two executables

(as discussed in the previous chapters). The provided workflow and tutorial help to overcome the technical challenges associated with employing the pilot point method using PEST. Although, the pilot point method is an attractive tool in model calibration often only a fraction of the real heterogeneity can be represented and the possibility of over-fitting due to over-parameterisation of the inverse problem exist. Therefore, it is recommended to apply post-processing analysis to identify the importance of observations to parameter estimates and prediction. Here, CV and LUA was used and compared with each other. Both, CV and LUA showing similar results and identify important location for observations but the latter at much smaller computational cost. Therefore LUA is very attractive to identify important observations and locations and can help to developing a highly efficient fieldwork and modelling strategy. Furthermore, the pilot point method combined with e.g. stochastic field generators gives the possibility to generate many different stochastic realizations of, for instance hydraulic conductivity fields, all with a quite similar value for the objective function. Subsequently running the model on all generated fields can give a wide range of different results for predictions and therefore a more detail insight about predictive uncertainty. All these methods equipped modellers with a powerful tool to explore uncertainty within satisfying stochastic, field measurements and calibration constrains.

Acknowledgements

The authors gratefully acknowledge the financial assistance provided by the Swiss National Science Foundation, Project NFP 61, Sustainable Water Management. The authors thank Maria Herold and Mehdi Ghasemizade for testing the tutorial and providing valuable feedback.

Linear uncertainty theory

A complex and high level of model parameterization in complex environmental problems does not automatically ensure that the model will make correct predictions (Hunt et al. (2007) and Moore and Doherty (2006)). However, what can be expected are the confidence intervals, conditioned on the available calibration data set.
Methods to quantify the uncertainty in ill-posed problems are briefly discussed following. Ill posed-problems mean that more parameters are used in the model than are capable of unique estimation on the basis of the available dataset. In the used example 130 pilot points values are calibrated against only 12 observations.
A brief overview about the theory of linear uncertainty analysis is presented. Parameter and predictive error are explained as well as Parameter identifability. The concept of predictive error variance and uncertainty variance are given. However, for more detail information about linear uncertainty, see for example Moore and Doherty (2005).

Appendix

Parameter and predictive error

The action of a model on the model parameter p (vector) can be represent as a matrix X. The outcome of the interplay between X and p will be the vector h represent observations of the system state. The vector h comprise the calibration dataset which are effected by the measurement noise ε:

$$\boldsymbol{h = Xp + \epsilon} \qquad (4)$$

The objective ϕ, which calculates the differences between observed and simulated data can be described as:

$$\boldsymbol{\phi = (Xp - h)^t Q(Xp - h)} \qquad (5)$$

where Q is a weight matrix. Weights are normally given by the inverse of the covariance matrix of measurement noise C(ε). The superscript t indicates matrix transpose.

$$\boldsymbol{Q = \sigma_r^2 C^{-1}(\epsilon)} \qquad (6)$$

where $\boldsymbol{\sigma_r^2}$ is a reference variance.

If the number of parameters to estimate for the vector p is small enough for a unique estimation based on the current calibration dataset the minimization of the objective ϕ leads to an estimated model parameter set p'. This well posed problem can be described as:

$$\boldsymbol{p' = (X^t Q X)^{-1} X^t Q h} \qquad (7)$$

However, for most model application as used also in our example more model parameter (elements) in p exist than can be uniquely estimated on the basis of the current calibration set. Supposing in addition that a low ϕ can be obtained on the model parameters of vector p' calculated from h, the vector can be described as follows:

$$\boldsymbol{p' = Gh} \qquad (8)$$

(G will be derived in the section singular value decompastion).
If now equation 4 is substituted into Equation 8, we get:

$$\boldsymbol{p = GXp + G\epsilon = Rp + G\epsilon}$$

(9)

where the resolution matrix is described as R = GX. Assuming no measurement noise, the "i"th row of R provides the averaging function through which an estimated parameter p_i (the "i"th element of p) is related to the unknown real-world hydraulic properties encapsulated in p.
Based on equation 9, the resulting parameter error can be calculated as:

$$\boldsymbol{p' - p = -(I - R)p + G\epsilon} \qquad (10)$$

The covariance matrix of parameter error C(p' − p) can computed as:

$$\boldsymbol{C(p' - p) = (I - R)C(p)(I - R)^t + GC(\epsilon)G^t} \qquad (11)$$

where C(p) contains prior and expert knowledge about variability of hydraulic parameters and uncertainty in the study site. After Moore and Doherty (2006), nonzero diagonal elements in C(p) describes the geologic uncertainty whereas geologic knowledge is expressed through nonzero off- diagonal elements (prior knowledge of the spatial correlation of e.g. hydraulic conductivity) and finite diagonal elements (indicating that there are bounds on geological uncertainty).

If a prediction s is now given, it depends on sensitivity on parameters in vector p. The sensitivities are recorded in the vector y.

$$\boldsymbol{s = y^t p} \qquad (12)$$

The model prediction, s' in contrast depends on the model parameters p' as:

$$\boldsymbol{s' = y^t p'} \qquad (13)$$

so that predictive error is:

$$\boldsymbol{(s' - s) = y^t(p' - p)} \qquad (14)$$

The predictive error now depends on the true parameters of p and the model parameter of p'. It is obviously that predictive error can never be known because of lacking knowledge about the true parameters p of the system.
But using Equation 11, predictive error variance $\boldsymbol{\sigma^2_{s'-s}}$ can be calculated:

$$\boldsymbol{\sigma^2_{s'-s} = y^t C(p' - p)y = y^t(I - R)C(p)(I - R)^t y + y^t GC(\epsilon)G^t y} \qquad (15)$$

A demonstration using the derivate equations and predictive error variance in groundwater model can be found in Gallagher and Doherty (2006).

Appendix

Singular Value Decomposition

In case that more parameters that can be estimated uniquely based on the current calibration dataset are sought, p' cannot be calculated due to the not invertible conditions of $\boldsymbol{X^tQX}$. However, to calculate p' modifications are need. This is done by singular value decomposition (SVD) of $\boldsymbol{X^tQX}$ and creates two matrices S and V:

$$\boldsymbol{X^tQX = VSV^t} \quad (16)$$

which is equivalent to (after partitioning)

$$\boldsymbol{X^tQX} = [\boldsymbol{V_1} \quad \boldsymbol{V_2}] \begin{bmatrix} \boldsymbol{S_1} & \boldsymbol{0} \\ \boldsymbol{0} & \boldsymbol{S_2} \end{bmatrix} \begin{bmatrix} \boldsymbol{V_1^t} \\ \boldsymbol{V_2^t} \end{bmatrix} = \boldsymbol{V_1 S_1 V_1^t + V_2 S_2 V_2^t} \quad (17)$$

where V is a m by m matrix of orthogonal unit vector ,V^t is the conjugated transpose of V and S is a m by n rectangular diagonal matrix spanning parameter space. In equation 17 the right hand side separates the solution space (subscript 1) from the null space (subscript 2). The orthogonal unit vectors spanning the solution space comprise the columns of V1. In contrast, the orthogonal unit vectors comprising the null space comprise the columns of V2. These two spaces are orthogonal to each other. The problem of the null space is that singular values of zero or very small and are appearing in the S_2 matrix, creating non-uniqueness of the inverse problem of model calibration. However, using truncated SVD solved this problem by elimination of them. The ill posed inverse problem of estimating p' can subsequently solved.

Using truncated SVD to solve for solution of the ill-posed inverse problem of estimating p', then G and R of Equations 8 and 9 become:

$$\boldsymbol{G = \left(V_1 S_1^{-1} V_1^t\right) X^t Q} \quad (18)$$

$$\boldsymbol{R = V_1 V_1^t} \quad (19)$$

Using truncated SVD the objective target function ϕ (equation 5) is minimized by referring only zero, or values close to zero, singular values to S_2. As mentioned by Moore and Doherty (2005) it is most efficient to truncate non-zero singular values, with a truncation level depending on the noise amount ε related to h. Using non-zero singular values avoids over-fitting in the calibration and directly lower the effect of measurement noise to parameter and predictive error.

It comes apart from equation 15 that two contributors to parameter and predictive error variance $\boldsymbol{\sigma^2_{s'-s}}$ exist. The first term includes the null space, which contributed to predictive error variance. This is due to parameter simplification, which is needed to

achieve a unique solution in the calibration. The whole complexity of the unknown hydraulic properties cannot represent by the calibrated model parameters. The solution space of equation 15 (second term) contributes to parameter and predictive error variance due to the measurement noise ε, which is related to h. All estimations are based on the dataset h, which contains also a certain contribution of measurement noise and therefore the estimations are potentially in error.

However, if the C(p) matrix is diagonal, parameters are normalized and noise ε is zero, then truncated SVD leads to a minimum norm solution for p'. In other words, calibrating a model with truncated SVD where truncation is such that S_2 is 0 the maximum likelihood solution for p' is obtained.

Parameter Identifiability

Demonstrated by Doherty and Hunt (2009) the diagonal elements of R (equation 16) can be used to estimate parameter identiability. Each diagonal element of R builds angle between a vector in the direction of the corresponding parameter and its projection onto the solution space. This cosine of the angle ranges from 0 to 1, where zero indicates that the parameter cannot be identified during the calibration (un-identifiable). In contrast, an angle of 1 indicates that the parameter can completely identified. The identifiability (f_i) of parameter i can be calculated as:

$$\boldsymbol{f_i} = (\boldsymbol{V_1 V_1^t})_{\boldsymbol{ii}} = \boldsymbol{i^t}(\boldsymbol{V_1 V_1^t})\boldsymbol{i} \qquad (20)$$

where i is a unit vector in the direction of the parameter. However, a value of one means not directly that the parameter can be estimated without error. That's due to the fact that measurement noise are still in the measurement dataset h.
By replacing y with $p_i i^{'}$, where pi is the "i"th element of p in equation 18 computation of the error in each estimated parameter can be carried out. The relative error reduction e_i is given by:

$$e_i = 1 - \sqrt{\frac{\sigma_i^2}{[\sigma_i^2]_0}} \qquad (21)$$

where $[\sigma_i^2]_0$ is the precalibration variance of the parameter.
The relative error reduction lie normally between zero and one, where one shows that the full solution space is used. However, e_i can research sometime negative values. Incorrect truncation can increase the potential for error in some parameters.

Predictive Uncertainty and Predictive Error Variance

Assuming that p and ε are normally distributed, the variance of uncertainty of any predictions s based on the calibrated dataset h can be estimated by (Christensen and

Appendix

Doherty 2008):

$$\sigma_s^2 = y^t C(p) y - y^t C(p) X^t [X C(p) X^t + C(\epsilon)]^{-1} X C(p) y \quad (22)$$

The pre-calibration uncertainty term $y^t C(p) y$ is a function of C(p) (innate parameter variability) and the prediction sensitivity y to model parameters. The term $-y^t C(p) X^t [X C(p) X^t + C(\epsilon)]^{-1} X C(p) y$ represents the reduction in predictive uncertainty variance due to calibration. The contribution of different parameter types for predictive uncertainty can be calculated using equation 22. Furthermore, the relative reduction in uncertainty by already existing ore potential new observations can be calculated. Using equation 18, the relative uncertainty reduction of any individual parameter used in the calibration can be computed. In that case σ_i^2 in equation 21 is calculated from equation 22 by replacing y with $pi^{i.}$ A quite important factor, which demonstrates the attractiveness of the present linear uncertainty analysis, is that, neither equation 15 (predictive error variance $\sigma_{s\prime-s}^2$), or equation 22 (predictive uncertainty varianceσ_s^2) contains actual parameter or observation values. Only parameter and observation sensitivities are involved. Therefore, this analysis can be already applied albeit the model is not yet calibrated.

References:

Ashby, S. F. and Falgout R. D.: A parallel multigrid preconditioned conjugate gradient algorithm for groundwater flow simulations, Nuclear Science and Engineering, 124(1), 145-159 pp., 1996.

Brunner, P., Doherty, J., and Simmons, C. T.: Uncertainty assessment and implications for data acquisition in support of integrated hydrologic models, Water Resour. Res., 48, n/a-n/a, 10.1029/2011wr011342, 2012.

Butler, J. J.: Hydrogeological Methods for Estimation of Spatial Variations in Hydraulic Conductivity Hydrogeophysics, in, edited by: Rubin, Y., and Hubbard, S. S., Water Science and Technology Library, Springer Netherlands, 23-58, 2005.

Christensen, S., and Doherty, J.: Predictive error dependencies when using pilot points and singular value decomposition in groundwater model calibration, Advances in Water Resources, 31, 674-700, 10.1016/j.advwatres.2008.01.003, 2008.

Dausman, A. M., Doherty, J., Langevin, C. D., and Sukop, M. C.: Quantifying Data Worth Toward Reducing Predictive Uncertainty, Ground Water, 48, 729-740, 10.1111/j.1745-6584.2010.00679, 2010.

de Marsily, G.: De l'identification des systemes hydrogeologiques. Doctorat d'etat thesis, Ecole des Mines de Paris, Centre d'Informatique Geologique, Paris, 1978

de Marsily, G., F. Delay, J. Gonc*x*alve`s, P. Renard, V. Teles, and S. Violette.: Dealing with spatial heterogeneity. Hydrogeology Journal 13, no. 1: 161–183, 1978

de Marsily, G., C. Lavedan, M. Boucher, and G. Fasanino.: Interpretation of interference tests in a well field using geostatistical techniques to fit the permeability distribution in a reservoir model. In Geostatistics for Natural Resources Characterization. NATO ASI Ser. C, 182, ed. G. Verly, M. David, A.G. Journel, and A. Marechal, 831–849. Dordrecht, The Netherlands: D. Reidel Publishing Co, 1984

Diersch, H.-J. G.: FEFLOW Version 5.4, Finite element subsurface flow and transport simulation system: Berlin, Germany, DHI-WASY GmbH, 202 p., 2009

Doherty: Two statistics for evaluating parameter identifiability and error reduction, 2009. Journal of Hydrology, 366(1), 119-127.

Doherty: Response to Comment on ‘‘Two statistics for evaluating parameter identifiability and error reduction”, 2010. Journal of Hydrology, 380(3), 489-496.

Doherty, J.: Ground Water Model Calibration Using Pilot Points and Regularization, Ground Water, 41, 170-177, 10.1111/j.1745-6584.2003.tb02580.x, 2003.

Doherty, J., and Hunt, R. J.: Two statistics for evaluating parameter identifiability and error reduction, Journal of Hydrology, 366, 119-127, 10.1016/j.jhydrol.2008.12.018, 2009.

Doherty, J., and Christensen, S.: Use of paired simple and complex models to reduce predictive bias and quantify uncertainty, Water Resour. Res., 47, W1253410.1029/2011wr010763, 2011.

Doherty, J. 2010. PEST- Model-Independent Parameter Estimation. Watermark Numerical Computing. peshomepage.org.

Doherty, J.E., Fienen, M.N., and Hunt, R.J.: Approaches to highly parameterized inversion: Pilot-point theory, guidelines, and research directions: U.S. Geological Survey Scientific Investigations Report 2010–5168, 36 p., 2010

Franssen HJ, Alcolea A, Riva M, Bakr M, van der Wiel N, Stauffer F, et al. A comparison of seven methods for the inverse modelling of groundwater flow. Application to the characterisation of well catchments. Adv Water Resour ,32(6):851–72, 2009

Fienen, M. N., Muffels, C. T., and Hunt, R. J.: On Constraining Pilot Point Calibration with Regularization in PEST, Ground Water, 47, 835-844, 10.1111/j.1745-6584.2009.00579.x, 2009.

Gallagher, M., and Doherty, J.: Parameter estimation and uncertainty analysis for a watershed model, Environmental Modelling & Software, 22, 1000-1020, 10.1016/j.envsoft.2006.06.007, 2007.

Gleeson, T., and Manning, A. H.: Regional groundwater flow in mountainous terrain: Three-dimensional simulations of topographic and hydrogeologic controls, Water Resour. Res., 44, W1040310.1029/2008wr006848, 2008.

Goderniaux, P., Brouyere, S., Fowler, H. J., Blenkinsop, S., Therrien, R., Orban, P., and Dassargues, A.: Large scale surface-subsurface hydrological model to assess climate change impacts on groundwater reserves, Journal of Hydrology, 373, 122-138, 10.1016/j.jhydrol.2009.04.017, 2009.

Harbaugh, A.W.: MODFLOW-2005—The U.S. Geological Survey modular ground-water model—The ground-water flow process: U.S. Geological Survey Techniques and Methods book 6, chap. A-16, 2005.

Hemker, C.J., and de Boer, R.G.: MicroFEM User's Guide: Amsterdam, The Netherlands, Dr. C.J. (Kick) Hemker, 25 p., 2009.

Herckenrath, D., Langevin, C. D., and Doherty, J.: Predictive uncertainty analysis of a saltwater intrusion model using null-space Monte Carlo, Water Resour. Res., 47, W0550410.1029/2010wr009342, 2011.

Hill: Comment on ''Two statistics for evaluating parameter identifiability and error reduction" by John Doherty and Randall J. Hunt, 2010.

Hunt, R. J., Doherty, J., and Tonkin, M. J.: Are models too simple? Arguments for increased parameterization, Ground Water, 45, 254-262, 10.1111/j.1745-6584.2007.00316.x, 2007.

Irvine, D. J., Brunner, P., Franssen, H. J. H., and Simmons, C. T.: Heterogeneous or homogeneous? Implications of simplifying heterogeneous streambeds in models of losing streams, Journal of Hydrology, 424, 16-23, 10.1016/j.jhydrol.2011.11.051, 2012.

James, S. C., Doherty, J. E., and Eddebbarh, A. A.: Practical Postcalibration Uncertainty Analysis: Yucca Mountain, Nevada, Ground Water, 47, 851-869, 10.1111/j.1745-6584.2009.00626.x, 2009.

Kowalsky, M. B., Finsterle, S., Williams, K. H., Murray, C., Commer, M., Newcomer, D., Englert, A., Steefel, C. I., and Hubbard, S. S.: On parameterization of the inverse problem for estimating aquifer properties using tracer data, Water Resour. Res., 48, W06535, 10.1029/2011wr011203, 2012.

Langevin, C. D., and Guo, W.: MODFLOW/MT3DMS–Based Simulation of Variable-Density Ground Water Flow and Transport, Ground Water, 44, 339-351, 10.1111/j.1745-6584.2005.00156.x, 2006.

Langevin, C.D., Thorne, D.T., Dausman, A.M., Sukop, M.C., and Guo, W.: SEAWAT Version 4—A computer code for simulation of multi-species solute and heat transport: U.S. Geological Survey Techniques and Methods, book 6, chap. A-22, 39 p., 2008.

Lavenue, A. M., Ramarao, B. S., Demarsily, G., and Marietta, M. G.: Pilot Point Methodology for Automated Calibration of an Ensemble of Conditionally Simulated Transmissivity Fields. 1. – Theory and Computational Experiments, Water Resour. Res., 31, 495-516, 10.1029/94wr02259, 1995.

Li, Q., Unger, A. J. A., Sudicky, E. A., Kassenaar, D., Wexler, E. J., and Shikaze, S.: Simulating the multi-seasonal response of a large-scale watershed with a 3D physically-based hydrologic model, Journal of Hydrology, 357, 317-336, 10.1016/j.jhydrol.2008.05.024, 2008.

Ma, R., Zheng, C. M., Tonkin, M., and Zachara, J. M.: Importance of considering intraborehole flow in solute transport modeling under highly dynamic flow conditions, J. Contam. Hydrol., 123, 11-19, 10.1016/j.jconhyd.2010.12.001, 2011.

Moore, C., and Doherty, J.: Role of the calibration process in reducing model predictive error, Water Resour. Res., 41, W0502010.1029/2004wr003501, 2005.

Moore, C., and Doherty, J.: The cost of uniqueness in groundwater model calibration, Advances in Water Resources, 29, 605-623, 10.1016/j.advwatres.2005.07.003, 2006.

Partington, D., Brunner, P., Simmons, C. T., Werner, A. D., Therrien, R., Maier, H. R., and Dandy, G. C.: Evaluation of outputs from automated baseflow separation methods against simulated baseflow from a physically based, surface water-groundwater flow model, Journal of Hydrology, 458–459, 28-39, http://dx.doi.org/10.1016/j.jhydrol.2012.06.029, 2012.

Ramarao, B. S., Lavenue, A. M., Demarsily, G., and Marietta, M. G.: Pilot Point Methodology for Automated Calibration of an Ensemble of Conditionally Simulated Transmissivity Fields. 1. – Theory and Computational Experiments, Water Resour. Res., 31, 475-493, 10.1029/94wr02258, 1995.

Refsgaard, J. C., and B. Storm, MIKE SHE, in Computer Models of Watershed Hydrology, edited by V. J. Singh, pp. 809–846, Water Resour. Publ., Littleton, Colo., 1995.

Renard, P.: Stochastic hydrogeology: What professionals really need?, Ground Water, 45, 531-541, 10.1111/j.1745-6584.2007.00340.x, 2007.

South Florida Water Management District (SFWMD): Theory manual—Regional Simulation Model (RSM): West Palm Beach, Fla., SFWMD, Office of Modeling, 308 p., 2005.

Sciuto, G., and Diekkrueger, B.: Influence of Soil Heterogeneity and Spatial Discretization on Catchment Water Balance Modeling, Vadose Zone Journal, 9, 955-969, 10.2136/vzj2009.0166, 2010.

Sudicky, E. A., and Huyakorn, P. S.: Contaminat Migration in Imperfectlz known Heterogeneous Groundwater Systems, Reviews of geophysics, 29, 240-253, 1991.

Sudicky, E. A., Illman, W. A., Goltz, I. K., Adams, J. J., and McLaren, R. G.: Heterogeneity in hydraulic conductivity and its role on the macroscale transport of a solute plume: From measurements to a practical application of stochastic flow and transport theory, Water Resour. Res., 46, W01508, 10.1029/2008wr007558, 2010.

Therrien, R. McLaren, R.G., Sudicky, E.A.: HydroGeoSphre-a three dimensional numerical model describing fully integrated subsurface and surface flow and solute transport, Groundwater Simulations Group, University of Waterloo, 2007.

Tikhonov, A.N.: Solution of incorrectly formulated problems and the regularization method: Soviet Mathematics Doklady, v. 4, p. 1035–1038, 1963a.

Tikhonov, A.N.: Regularization of incorrectly posed problems: Soviet Mathematics Doklady, v. 4, p. 1624–1637, 1963b.

Tikhonov, A.N., and Arsenin, V.Y.: Solutions of ill-posed problems: New York, Halstead Press-Wiley, 258 p, 1977.

Tonkin, M., Doherty, J., and Moore, C.: Efficient nonlinear predictive error variance for highly parameterized models, Water Resour. Res., 43, W0742910.1029/2006wr005348, 2007.

Tonkin, M., and Doherty, J.: Calibration-constrained Monte Carlo analysis of highly parameterized models using subspace techniques, Water Resour. Res., 45, W00b1010.1029/2007wr006678, 2009.

Zheng, C. M., and Gorelick, S. M.: Analysis of solute transport in flow fields influenced by preferential flowpaths at the decimeter scale, Ground Water, 41, 142-155, 10.1111/j.1745-6584.2003.tb02578.x, 2003.

Zheng, C.: MT3D—A modular three-dimensional model for simulation of advection, dispersion, and reactions of contaminants in groundwater systems: Ada, Okla., U.S. Environmental Protection Agency, 170 p., 1990.